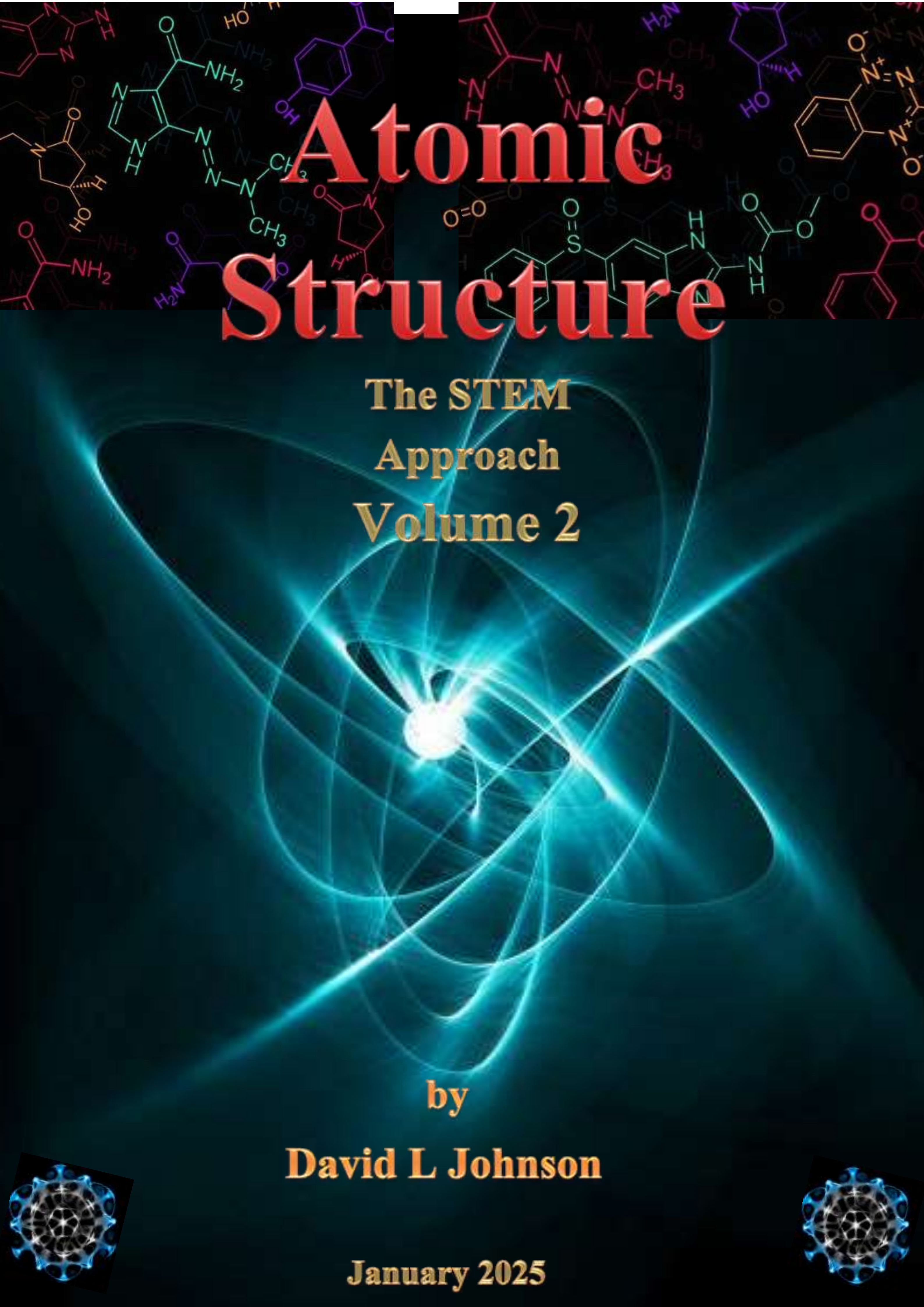

Atomic Structure

The STEM Approach

Volume 2

by

David L Johnson

January 2025

Table of Contents

Prologue

Central to conventional Science's model for the atom is the **Orbital Nuclear Atomic Model** (**ONAM**). To maintain electrical neutrality, an ONAM atom has an equal number of protons and electrons, with protons and neutrons strongly bound together to form a strong atomic nucleus that is encapsulated by electrons (or their wave-like equivalents) in orbitals that are mathematically-defined by the wave functions of **Quantum Mechanics** (QM).

Whereas ONAM represents nucleons as spheres which are tightly bonded together as an amorphous mass to form a spherical atomic nucleus, the **Spin Torus Energy Model** (**STEM**) represents atomic nuclei as polygonal structures. STEM contends that the geometry of the nucleus dictates many of the unique physical unique characteristics (e.g. polymorphic and allotropic forms, hardness, crystalline form or lack thereof etc.) of the various elements in the Periodic Table, as well as their observed bonding preferences and geometries formed with other elements and compounds.

STEM is an **energy-centric** approach that is based upon the hypothesis there is only **one type of energy-generating material** (**energen**), with fundamental particles having an energy core consisting of a toroidal concentration of energen and having electromagnetic fields consisting of less concentrated energen. The proposed **STEM** structure for up and down-quarks is used to model nucleons; and the nucleons used to generate a polygonal lattice-like structure for nuclei with atomic numbers 2 and above. STEM also provides a feasible explanation for **nucleon-type conversion**, as evidenced by **electron capture** and **beta decay**.

The STEM treatment of atomic structure is significantly different to that of ONAM and, as such, will challenge many long-held beliefs about electromagnetism and atomic theory. It provides feasible explanations for many phenomena that are poorly or not addressed at all by the conventional Science approach, and the multi-layered atom structures and geometries developed are more compatible with the bonding geometries of chemical compounds.

This is the STEM Volume 2 paper. Volume 1 covers Electricity and the Duplicit Electron and Volume 3 covers the Nature of Light.

Preons and Concentrated Energen Sources (CES)

According to the Standard Model (SM), nucleons consist of up and down quarks, and nucleons build into and the atoms of ordinary matter. Although some consider that up/down quarks to be indivisible **fundamental particles**, others consider that they are **composite particles** consisting of smaller fundamental particles called preons. Should quarks not be a fundamental particle, then what is a fundamental particle, and do all fundamental particles have a common structure?

In his 2009 book 'Aethro-Kinematics' (a 3.2 Mb pdf file), Steven Rado claimed that fundamental particles has a '**donut-vortex**' form and consist of an ideal fluid called **aether** (or **ether**). In Greek mythology, aether was thought to be the pure essence that the gods breathed and, according to the theories of Descartes, Huygens, Leibnitz, Euler and many others, aether was considered to be the conveyer of light-waves and the possible cause of gravitational force. The concept of aether as an ever-present material that pervades the whole of Space has been variously accepted and rejected by scientists throughout the history of modern Science: at various stages Einstein embraced and distanced himself from the concept, finally declaring '*that the Special Theory of Relativity does not compel us to deny ether*'.

Rado is one of the most recent supporters of the aether concept, and has extended its function to the creation of fundamental particles and matter itself. In the Aethro-Kinematics book he treats aether as a material with properties akin to those of an ideal fluid, which means that it is totally **frictionless**. Assuming that aether consists of hypothetical particles (**aethrons**) analogous to atoms or molecules within a 'normal' fluid, Rado uses **Bernoulli's Principle** (which is states that the total energy components of a moving fluid remains constant) to show how aether has a propensity to form or concentrate into **donut vortices** (see figure 1a). Furthermore, he suggests that donut vortices by '*a natural, evolutionary condensation of kinetic energy form into ponderable matter*'.

On page 200 of his book, Rado states that '*evidently, the continuous re-generation of the same flow-patterns in the frictionless environment of the aether, the conservation of the shape and substance of the systems and their inherent ability to connect with one another implies that the **donut vortex** could represent a potential kinematical description of a permanent **elementary building block of matter**.*' Furthermore, he considers that **all fundamental particles** have the donut vortex form; and this includes preons and electrons. The implication of this process is that all matter and related phenomena such as electricity, electromagnetic fields and characteristics, EMR (inclusive of light) and gravitational force are associated with various forms and concentrations of aether.

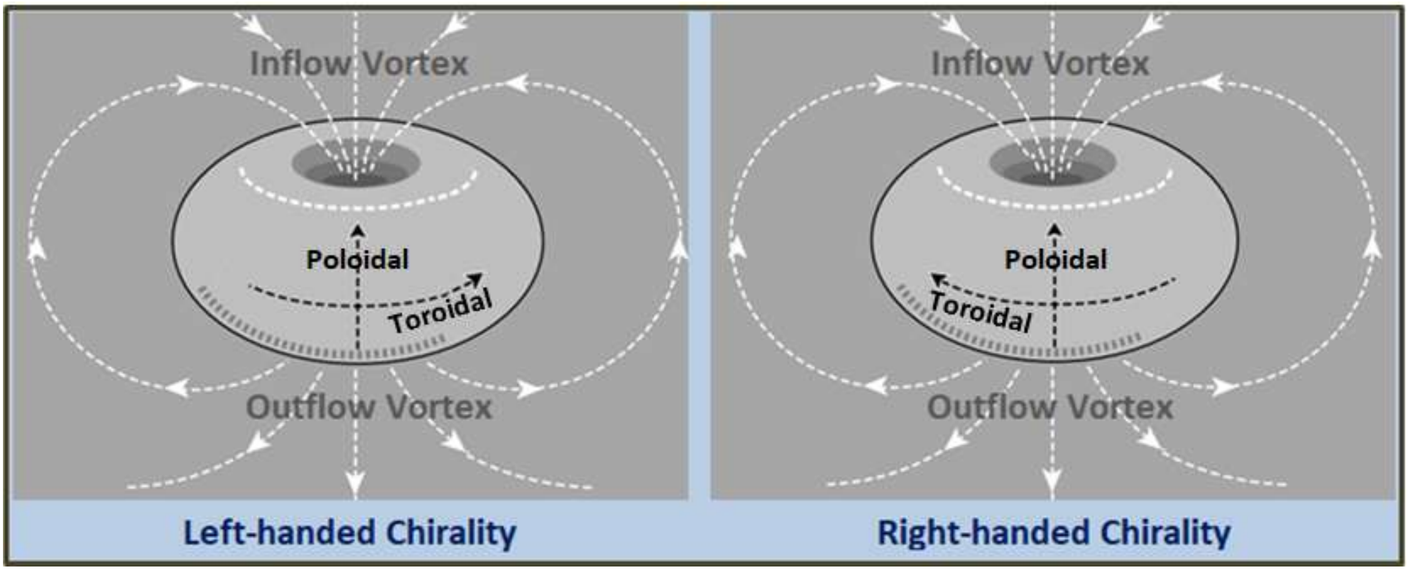

Figure 1a: Aether-based Rado 'Donut Vortices'

Another approach is the Spin Torus Energy Model (**STEM**), which forms the main subject of this paper. STEM is an energy-centric approach first developed to model the electron, as detailed in the paper titled 'Electricity and the Duplicit Electron'. Whereas Rado's Aethro-Kinematics model involves aether, STEM is predicated upon the hypothesis that there is only one form of **energy-generating material** that has been called **energen**. STEM contends that an **electron** consists of a **torus-shaped concentration** of energen flowing (or spinning) in a **toroidal** path at close to the **speed of light** to form an **energy-core** that is enveloped by **field-energy**. The field energy forms an outer torus of less concentrated energen, and is responsible for the electron's electromagnetic characteristics and the ways it interacts with other energen-based matter.

As described in detail in 'the Duplicit Electron' paper, due to the **poloidal** and **toroidal** flow components of its field-energy, an electron is **chiral**. By definition, the **left-handed** chiral form of an electron is considered to represent a

negative charge carrier (a **cetron electron**, with field energy blue left in figure 1b); and the **right-handed** chiral form representing a **positive charge carrier** (an **aptron electron**, with field energy red left in figure 1b).

To avoid confusion between it and other definitions or models for the preon (including Rado's 'donut vortices'), the STEM version of the **preon** is called a **Concentrated Energen Source** (**CES**). The **CES** has an almost identical physical structure as an electron but, with a rest mass of 52.5 MeV/c^2, it contains about 100 times more energen than an electron, which has a rest mass of 0.511 MeV/c^2. And, interestingly, a muon, which is created by the high-energy collision of cosmic rays with matter (see the Plasma and Cosmic Radiation chapter), has a mass of 105 MeV/c^2, which corresponds to the mass of a CES pair.

To avoid confusion within diagrams, **CES** have a yellow **energy-core torus**, whereas **electrons** have a green energy-core torus, as shown in figure 1b (which is not to scale; figure 15 provides a true relative-scale representation of an electron and a CES). As for an electron, the **field energy** of a CES has **chirality**: an **e-CES** has **left-handed chirality** (corresponding to a **cetron** electron), and a **p-CES** has **right-handed chirality** (corresponding to an **aptron** electron).

Both electrons and CES have a **structure** similar to that of a spheromak , which is a specific form of compact torus. Experimentally, spheromak quite readily form within plasma, and have balanced magnetohydrodynamic forces that provide them with stability. Thus the CES concept is directly relatable to the observable phenomena of **compact tori**.

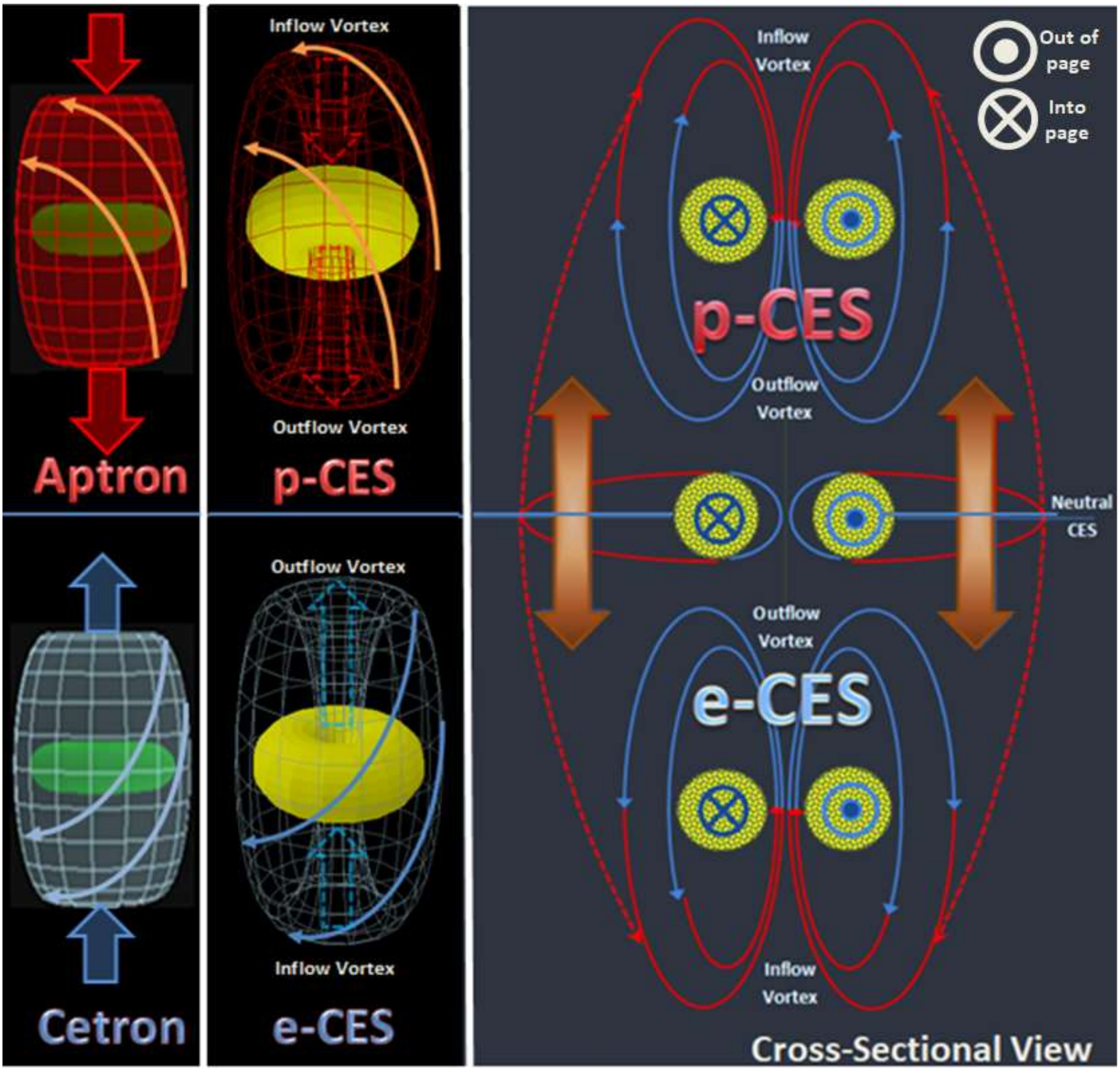

Figure 1b: Comparison between Electron (Cetron and Aptron) and CES (e-CES and p-CES) Structures

The rightmost in figure 1b is a **cross-sectional view** of a hypothetical **neutral CES** (the centre torus in the graphic that has no chirality). An **e-CES** is created when that field- is directed downwards (in figure 1b) parallel to the toroidal spin axis. A **p-CES** is created when the field-energy is directed in the other direction (i.e. upwards as shown).

This 'polarisation' process is described in more detail in the 'Duplicit Electron' paper and, **most importantly**, the chirality of a CES (and of an electron) can be **reversed** by the impact of a high energy collision with another particle (e.g. a kinetically energised electron), as explained in the Nucleon Type Conversion chapter.

With STEM's energen seemingly being the equivalent of Rado's ideal fluid form of aether, there are close similarities between of the Rado and STEM model for **fundamental particles**: both approaches consider fundamental particles to be the spheromak-like **torus-shaped particles**. Such similarities are quite amazing because the two approaches have been developed completely independently of each other, and have been derived from completely different perspectives. The author only became aware of Rado's book and associated articles in 2022, to be included for the first time in the October 2022 update of this position paper; and Rado's book was published in 2009, well before the development of STEM or the release of papers related to it.

However, despite the similarities, there are **significant differences** between the Rado and STEM approaches. For instance, Rado does not factor in the chiral nature of the field-energy of fundamental particles; nor does he indicate how 'donut vortices' combine to create quarks, nucleons or atoms. Also, STEM does not assume or require that (Outer-)Space be full of 'neutral' aether to sustain the propogation of light through an empty void or to generate gravitational force. As discussed in the Force of Gravity chapter, STEM contends that energen accumulates around all matter and is reponsible for the creation of gravitational force rather than being related to univeral aether.

As for an electron, the toroidal (circular) spin of a CES can be determined using the **modified version of Maxwell Right-Hand Grip Rule** shown as figure 2. By pointing the **thumb** of the left hand for an e-CES (or the right hand for a p-CES) in the direction of the field-energy's **outflow vortex**, the direction of the fingers indicates the direction of the toroidal spin (or flow) of the core-energy, and of the toroidal component of field-energy flow.

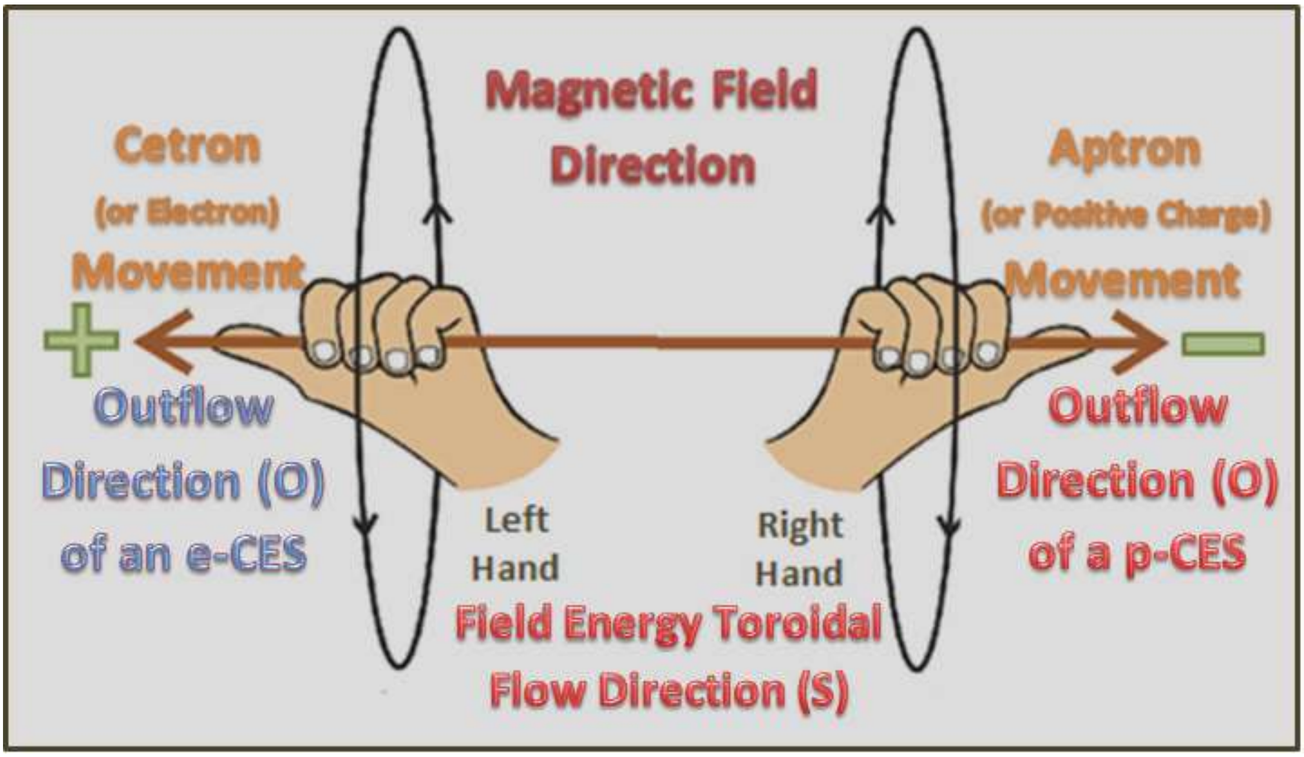

Figure 2: The Modified Maxwell's Right-Hand Grip Rule

Quarks are **fermions** (spin-½ particles), and many types of quarks have been identified (up, down, top, bottom, charm and strange). Of these varieties of quark, only **up** and **down-quarks** are considered to be involved in the structure of nucleons. The other four types of quark may have a purpose, although to date none has been identified; or they may simply be fragments of atoms and compounds after the high impact collision of atomic particles (e.g. as part of particle accelerator research) or transient high temperature/pressure plasma-related derivatives. At this stage, STEM contends that they are not needed or associated with the building or maintenance of the structure of an atomic nucleus.

In the next chapter, a structure will be developed for up and down-quarks, which will then be used build **nucleons** (protons and neutrons), and then to develop the basic **structural elements** involved in the building of an atomic nucleus in the Nucleons and Strong Force Bonding chapter. For subsequent chapters, topics such as **nucleon type conversion**, **Beta decay**, **electron capture**, inter-atom **bonding** and the basic statistics of the sub-atomic particles will be discussed before the structure of the nucleus for specific elements will be addressed in the 'Atomic Structure' chapters. The last three chapters address the cosmologic **macro-scale implications** of the STEM atomic structure.

Quarks

A quark is an elementary particle that can combine to form composite particles called hadrons; and the most stable hadrons are the **nucleons** (i.e. protons and neutrons), which combine to form atomic nuclei.

The main current preon-based model for quarks is the Rishon (or Harari–Shupe) model**,** as first proposed by H Harari in 1979. It defines two types of preons (**V** and **T**), with up and down quarks consisting of three preons each. Similarly, STEM defines two types of preon (**the e-CES** and the **p-CES**), but postulates that each up and down quark consists of a three-dimensional array of 6 CES, or 3 muon-like CES pairs (which corresponds to the 3 rishons of the Rishon model), held in a **regular octahedron** form by their respective electromagnetic fields, as represented by the stick connectors in figure 3.

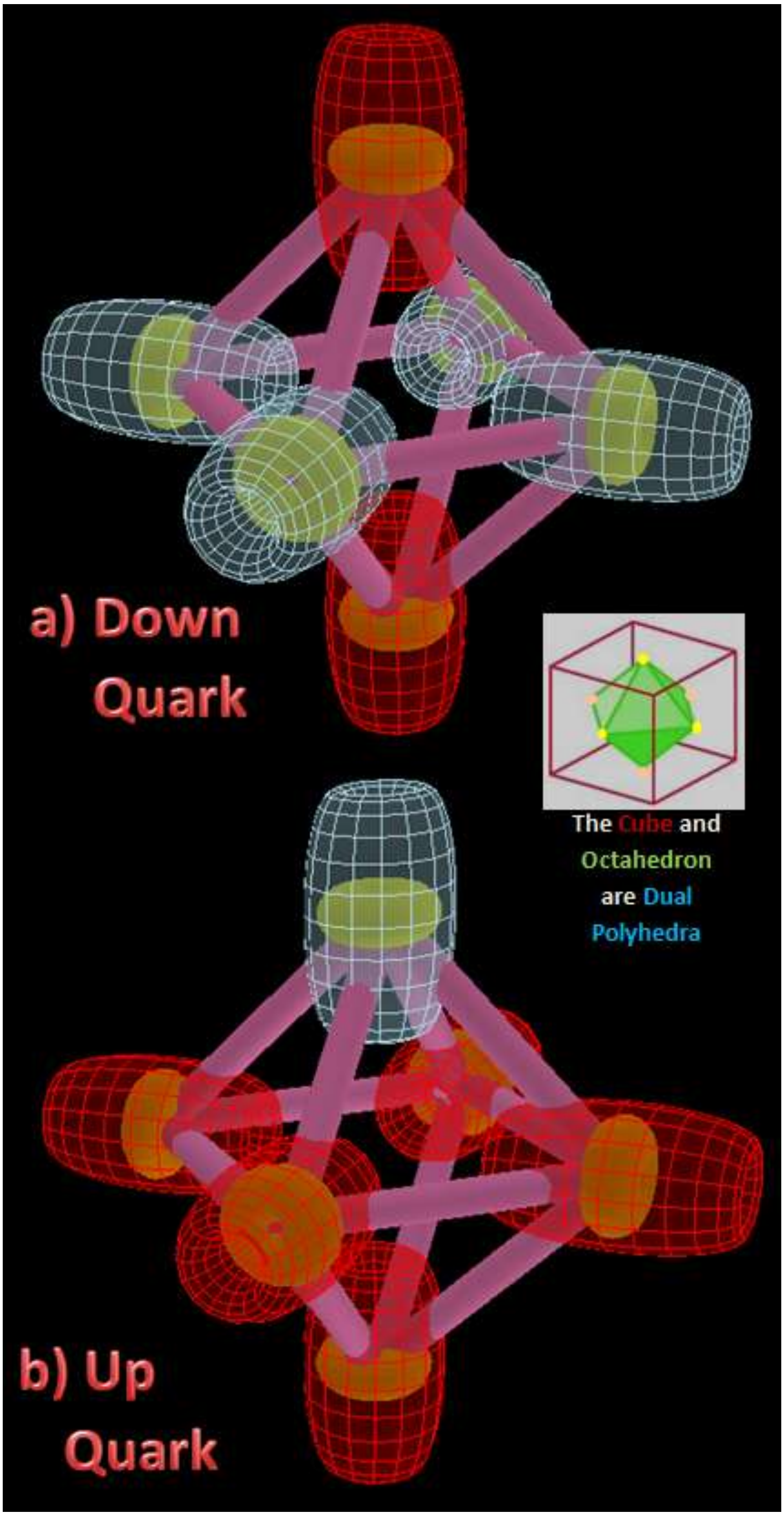

Figure 3: Ball and Stick Model of Down and Up Quarks

As can be seen in the figure 3 insert, the cube and regular octahedron are equivalent geometrical forms, and represent dual polyhedra. Thus, rather than using **ball and stick models** which require 12 sticks as well as the 6 CES per quark for the internal bonding, up and down quarks can be represented by their simpler equivalent **cubic model**, with the one CES energy-core shown central to each face of the cube as shown in figures 4a and 4b.

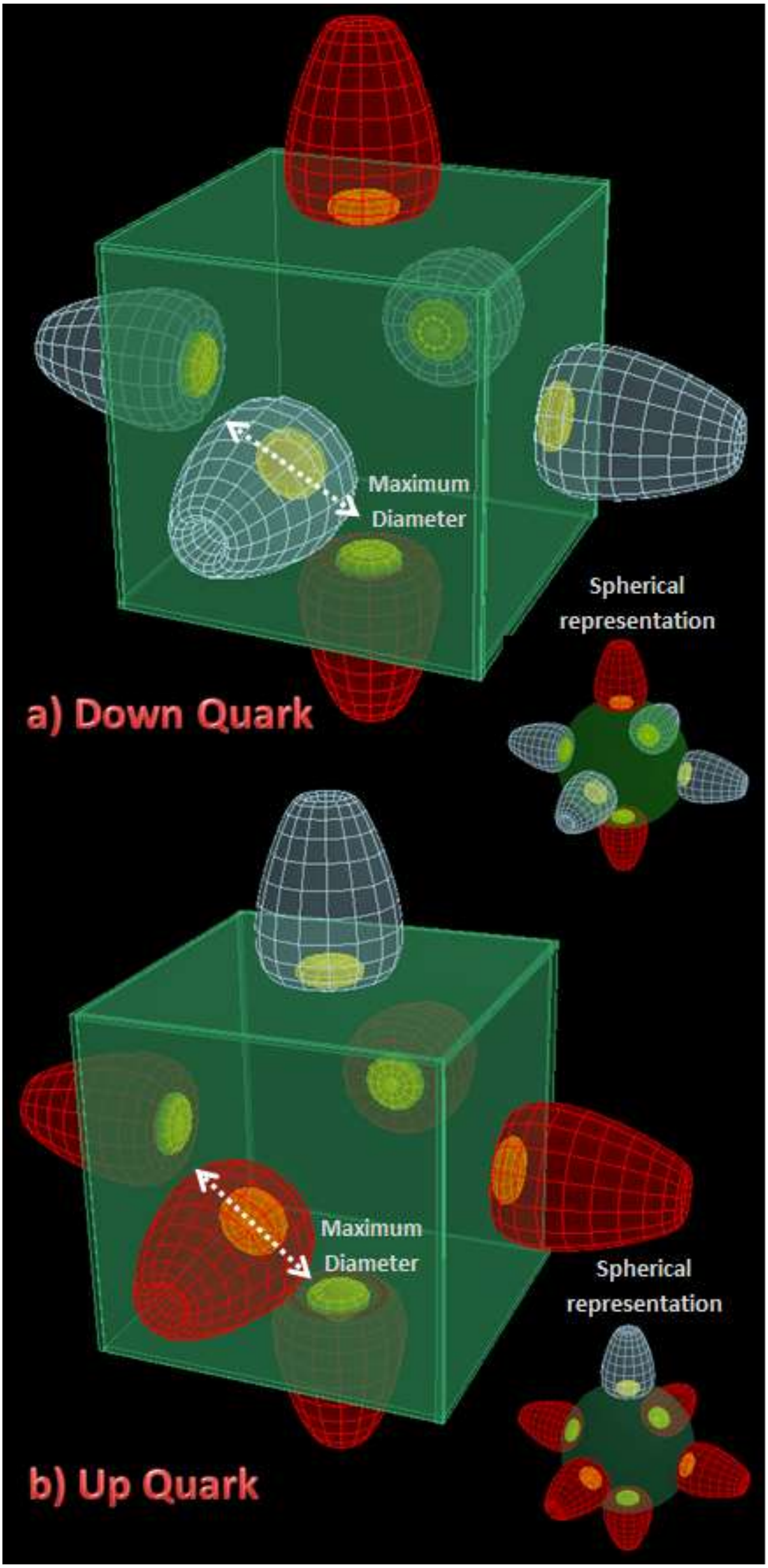

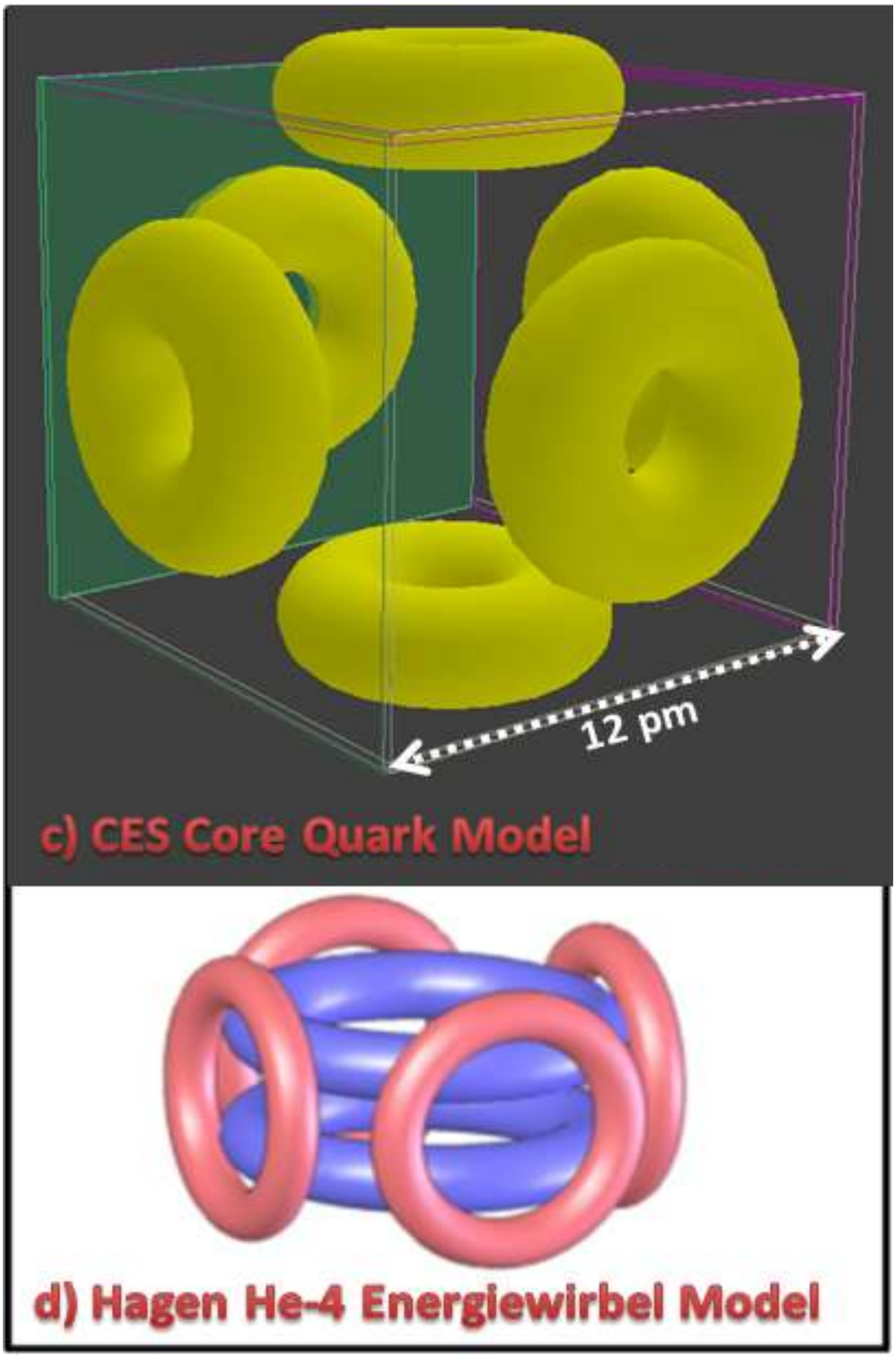

Figure 4: Cubic Form of an Array of Six Spin Torus Energy Concentrations

In cubic form, up/down quarks have a side width of 12 pm[1] (see figure 4c), based upon STEM's fundamental particle sizes as provided in the table of figure 15. Although more aesthetically pleasing represented as a spherical form, such as shown in the figure 4a and 4b inserts, use of the spherical representation for modelling purposes tends to obscure the geometry and structure of atomic nuclei. The price of clarity of atom nuclear geometry is the cubic approach which unfortunately makes models of atoms look quite bland and brick-like.

For STEM 3D quark models of atoms and molecules, the size of quarks used will be true-scale but, to increase the clarity of diagrams, the included CES energy-cores and the extent of their energy-fields will be somewhat reduced from that expected to be the case, and will thus not be true-scale.

Interestingly, the Energiewirbel Model (**EM**), an atomic model developed by W. Hagen, contends that the helium-4 atom consists of six energiewirbels (which are CES-like toroidal concentrations of electromagnetic energy) that are firmly held together to form a cubic structure as shown in figure 4d. The red toroidal structures in Hagen's EM helium-4 structure represent protons and the blue ones represent electrons, with a neutron being considered to be a

---

[1] Note that a 12pm quark size leads to a larger nucleon size than current electron-deflection estimates suggest, but the larger nucleon size still produces molecular bond lengths consistent with those measured. Also see comments about nucleon size.

bound electron and proton pair. Although Hagen's EM for an atomic nucleus is quite different to that of STEM, both approaches claim that compatible toroidal concentrations of an energy-generation substance can bind together to form a strong cubic array structure.

Nucleons are considered to consist of different combinations of up quarks (**U**) and down (**D**) quarks, with a neutron being a **DUD** combination and a proton being a **UDU** combination. The ONAM-determined electric charge estimates for up and down quarks are +2/3 e (where **e** = the elementary electric charge) and -1/3 e respectively, which means that neutrons and protons have a net electric charge of 0 e (calculated as 2*-1/3 +1*+2/3) and +1 e (calculated as 2*+2/3 + 1*-1/3) respectively.

STEM allocates a nominal charge of +1/6 e to a p-CES and -1/6 e to an e-CES (the rationale behind this charge allocation can be found in Electrons and Atomic Bonding chapter). Thus, with an up quark (U) consisting of five **p-CES** and one **e-CES** (see figures 3 and 4), its effective electric charge is +2/3 e (calculated as 5*+ 1/6 + 1*-1/6). Similarly, a down quark consisting of two **p-CES** and four **e-CES**, carries an effective electric charge of -1/3 e (as calculated as 2*+1/6 + 4*-1/6), which corresponds to the ONAM determined up/down nominal quark charge values.

For atoms to be considered electrically neutral, ONAM requires the electric charge of a **proton** to be +1 e, with each proton being matched with the same number of **orbital electrons**; and for **neutrons** to have no net electric charge (this requirement conflicts with the fact that neutrons have magnetic moment of $-9.6623653(23)\times10^{-27}$ J·T^{-1}). However, unlike ONAM, STEM is not particularly concerned about the electric field strength of protons and neutrons, with protons and neutrons each having magnetic moment values that do not need to be considered 'intrinsic'.

With STEM, the **strong force bonds** (see the next chapter) that bind the quarks within nucleons and the nucleons within an atomic nucleus are key issues, with the nominal charge allocated to quarks not being greatly important in nuclear structure.

And, once again, it must be emphasised that the **green** **cubic geometry**, as used to depict up and down quarks within quark models, simply defines the 3D space containing the quark's octagonal array of six CES. The quark is definitely not, and should not be considered to be, a brick-like cubic structure. Quark geometry could very well be represented as a **sphere** that indicates the extent of its external field energy. Although a sphere is generally considered to be more aesthetically pleasing in comparison to a cube for representing atomic structure, a spherical representation produces diagrams in which nuclear structure is less evident and, quite often, becomes obscured when clarity is required.

Nucleons and Strong Force Bonding

According to the **Standard Model** (**SM**), nucleons consist of three up/down quarks confined by strong-force interactions between each other as mediated by gluons. Putting aside the colour charge dynamics required to prevent an infringement of the Pauli Exclusion Principle, the net effect of such interactions is the equivalent of three equal strong-force bonds between each of the quarks as shown in figure 5a for the conventional Science model, with the three quarks being held in an equilateral-triangular pattern.

This SM nucleon model assumes that strong-force interactions exist equally between **like-charge quarks** (U-U and D-D bonds), which would otherwise be expected to repel and thus avoid each other, and **unlike-charge quarks**, which would attract each other. Although electrical attraction is not the basis for strong-force interactions, it would seem likely that mutual attraction would reduce opposite-charge quark separation and facilitate strong-force interaction between them; and that the reverse effect would apply to like-charge quarks.

The simple act of removing the strong-force bonds between like-charge quarks (the '*unlikely strong-force bonds*' of figure 5a), results in a nucleon consisting of a **central** positive or negative quark bonded to a pair of opposite-charge quarks. This results in a proton consisting of a central down quark and a pair of up quarks; and a neutron consisting of a central up quark and a pair of attached down quarks.

As shown in figure 5b, nucleons with two strong-force bonds would have either a **linear** or a **right-angled triangular** geometry, which are referred to **as I-form** and **L-form** nucleons respectively. Purely on the basis of geometry, with there being 6 possible strong-bond formation points due to the face-centred-cubic CES structure of up/down quarks, there is an 80% probability that a nucleon would be L-form, and a corresponding 20% probability of it being I-form.

As covered in more detail in the Fission, Fusion and the Creation of the Elements chapter, the element creation environments would most likely have been violent, chaotic, energised fusion environments. In such hostile environments, I-form nucleons, which have limited flexibility, would be quite susceptible to being broken down and re-cycled. On the other hand, L-form nucleons present less of an impact target, and their arms can rotate or swivel so that they are more flexible: they would, thus tend to roll or tumble with the blows rather than break up. With L-form nucleons being more robust than their I-form equivalent, it is reasoned that their percentage availability for nucleus-building purposes would increase markedly from the 80% mark (due to geometry) to well over the 90% mark.

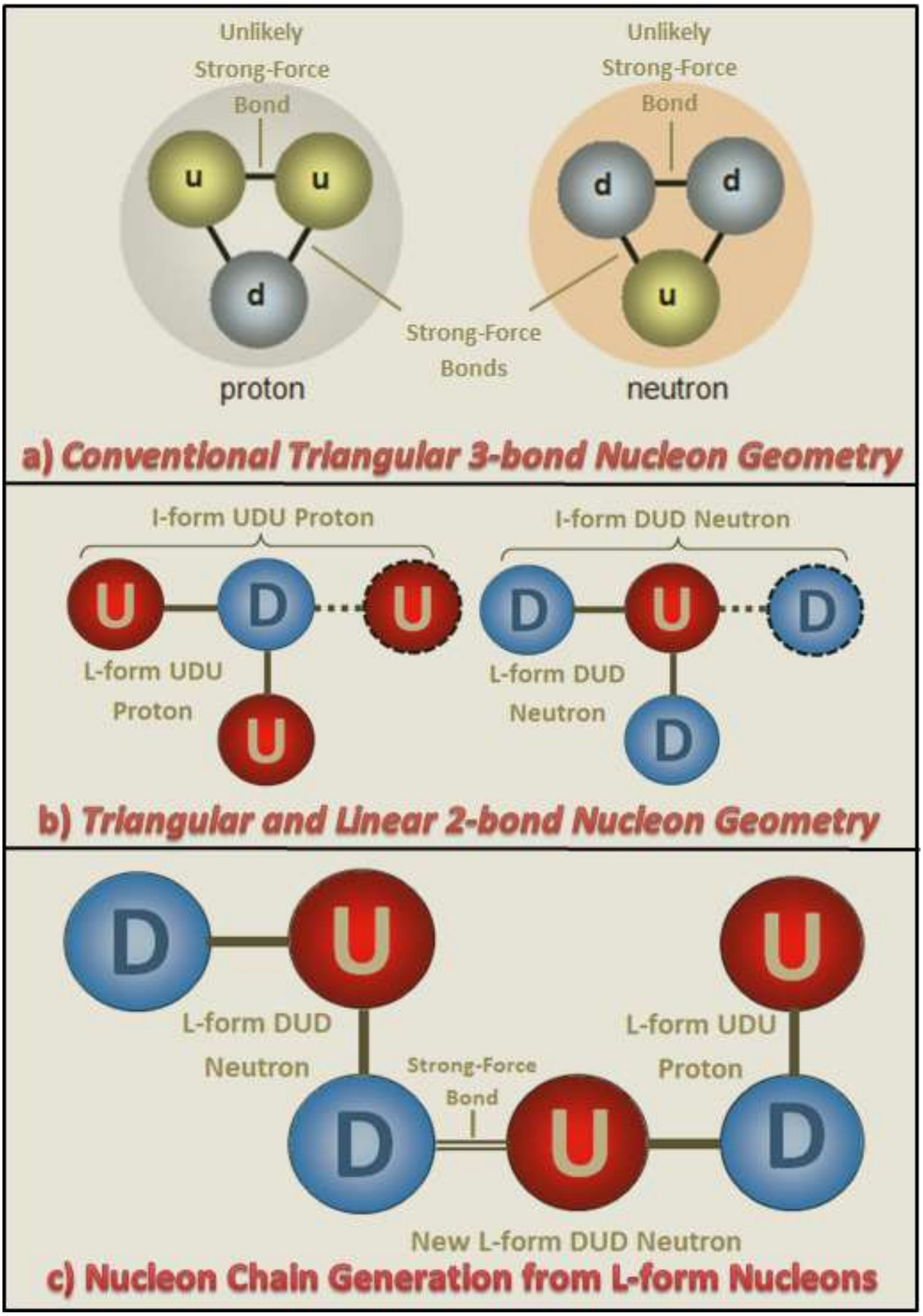

Figure 5: Strong-Force Bonds, Nucleon Structure and Nucleon Chain Structure

With well in excess of 90% of free nucleons being L-form rather than I-form, it would seem highly likely that the bulk of the nucleus building blocks would be in terms of L-form nucleons. L-form protons would strong-force bond to L-form neutrons, or vice versa, to create nucleon chains of alternating protons and neutrons such as represented in figure 5c. Note that a nucleon chain built from L-form nucleons results in the apparent formation of I-form nucleons such as the one labelled 'New I-form DUD Neutron' in figure 5c.

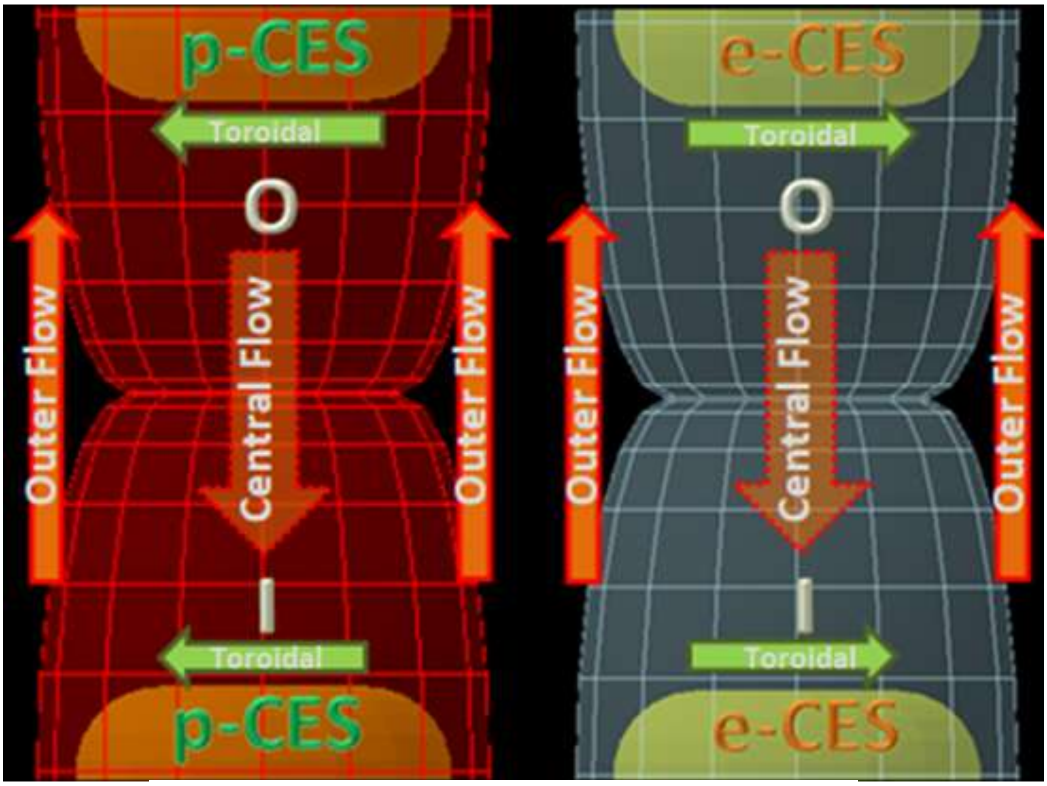

Figure 6: Strong-Force Inter-Quark Bond Formation

The strong-force interactions that bond up and down quarks within nucleons and between nucleons to form nucleon chains are called **inter-quark bonds**. These strong-force bonds are created when the outflow (**O**) vortex of one CES is forcefully brought into close contact with the inflow (**I**) vortex of the same-type CES, as shown in figure 6 for a pair of p-CES and a pair of e-CES. The strong binding effect of inter-quark bonds is considered to be due to the two-way flow of field-energy between the CES pair, with figure 7b showing typical two-way energen flows for the inter-quark bonds between quarks within L-form nucleons.

Another aspect is that the **nucleon-chain** building process, and ultimately the entire atomic nuclei building process, may simply be an extension of a simpler **quark-chain** building process that does not actually require or need the prior building of nucleons. The simplest quark-chain would then be a meson-like bonded positive and negative quark pair, which would be very short-lived before acquiring another quark to become a nucleon. The newly formed nucleon can then grow with the addition of more individual quarks that bond to the available appropriate latch point, and/or by the addition of other quark-chains. On this basis, nucleons would simply represent the shortest quark chain that is relatively stable within the element-creation fusion environment.

Referring to figure 7a, inter-quark bonds allow any unrestrained outer (or end) quarks to freely spin as indicated by the blue circular arrows. End-quark spin, which would be quite rapid, helps provide nucleons with a reasonably evenly distributed surround electric charge: positive for protons and a (slightly-negative to) neutral charge for neutrons. However, in terms of net electric field strengths, the two up quarks of a proton contribute +2/3 e and the one down quark -1/3 e, resulting in a net electric charge of +1e. The contributions of a neutron's two down quarks and one up quark result in a net electric charge of 0 e (i.e.is electrically neutral). However, this is not particularly important to the STEM model.

As noted in the footnote of page 7, a 12pm quark size leads to a larger nucleon size than current electron-deflection estimates: currently nucleon diameters are considered to be 1.7 x 10^{-15} metres (or 0.0017pm). However, as can be seen in the three planar cross-sections of the STEM nucleon of figure 7c, the STEM nucleon consists of a quite sparse three-dimensional array of CES, which is not factored into the statistical simulation estimates used to interpret electron-deflection experiments. Thus with less deflection than expected and assuming that nucleons are solid spheres, the statistical analysis is bound to result in a far smaller size estimate for nucleons.

Note also that, for visual clarity, the figure 7c is not to scale, with CES being considered to be far thinner than shown. Also, the CODATA **electron diameter** estimate is 5.6 x10^{-15} metres, which is over three times their size estimate for a nucleon despite having an energy mass that is 1/2000 smaller, which is quite incongruous, and suggests such CODATA size estimates may well be too low by a factor of about 1000.

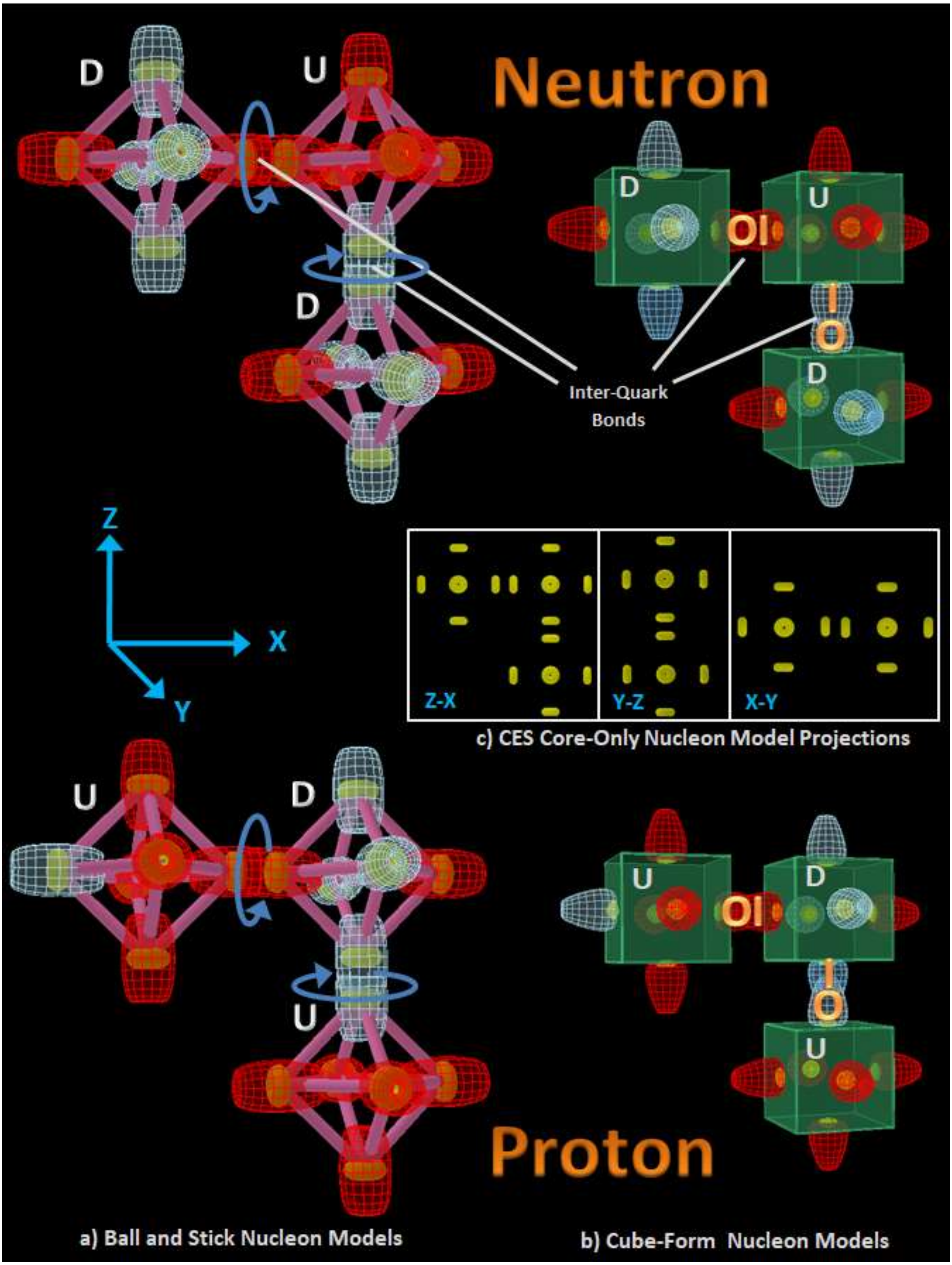

Figure 7: L-form Proton and Neutron Structure

The Fundamental Particle Statistics chapter provides a more detailed discussion related to the dimensions and energy mass characteristics of electrons, CES and nucleons.

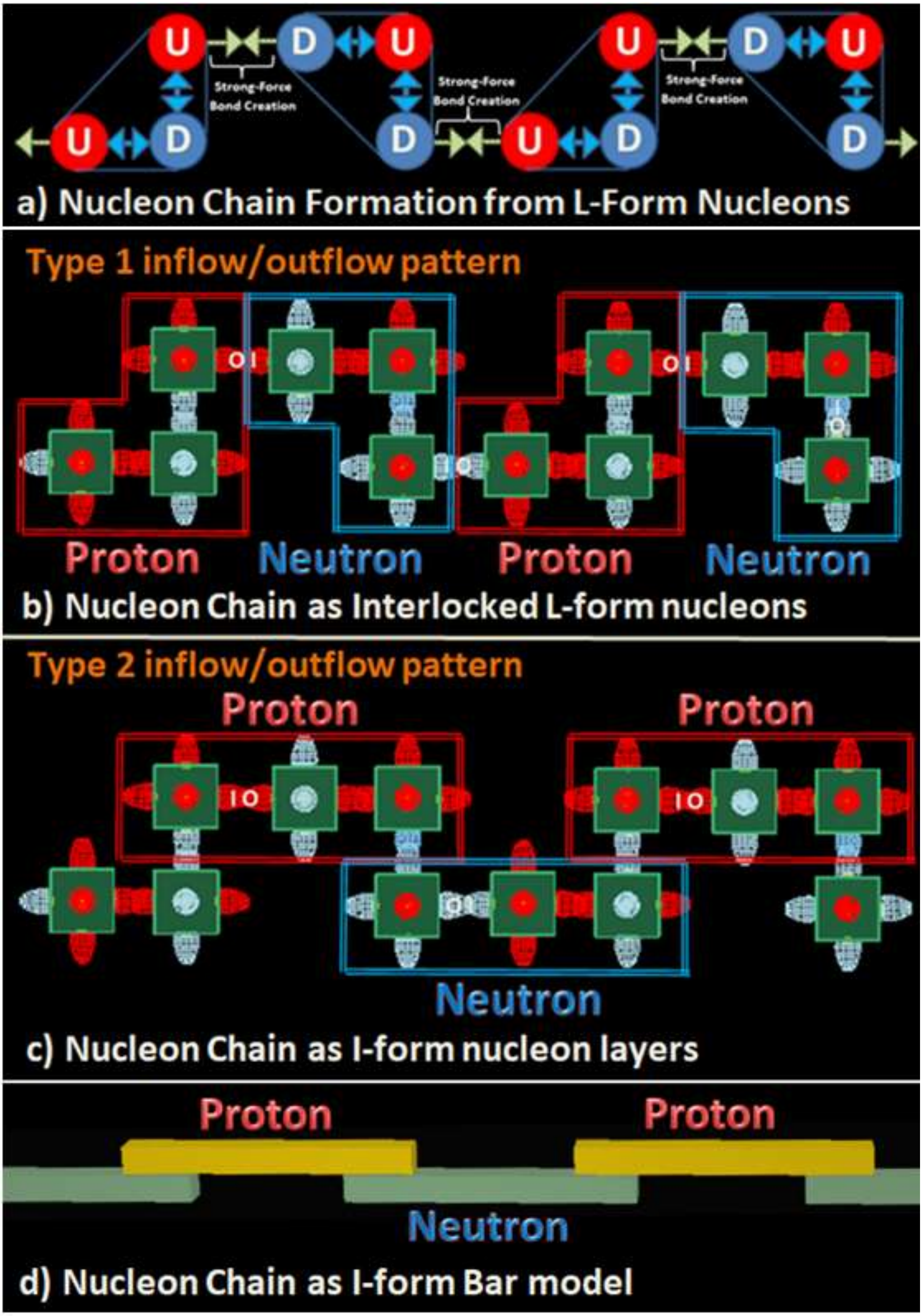

Figure 8: Interlocked L-form Nucleons Forming Nucleon Chains with I-Form Nucleon Layers

Extending the simple 2-nucleon chain example of figure 5c to a 4-nucleon chain, figure 8a shows the L-form nucleon join pattern; figure 8b shows the STEM quark model equivalent; and figure 8c highlights the development of I-form **nucleon layer** patterns although the chains are generated from L-form nucleons. The I-form nucleon layers allow overlapping bars to be used as in figure 8d, with **I-form protons** represented by **gold bars** and **I-form neutrons** by light **green bars**, which is most useful for nucleus model building. However, although such **bar models** highlight the polygonal structure of nuclei, they can look somewhat like matchstick models and are not true to scale, which can somewhat distort the height-to-width ratio of the atomic nucleus.

Each nucleon chain consists of a pair of I-form nucleon layers: one a neutron layer and the other a proton layer. Nucleon chains can extend vertically, developing as co-joined sets of nucleon chains to create multiple pairs of I-form nucleon layers as shown labelled 1 to 8 in figure 9. In order to allow multiple co-joined nucleon chains to build, two subtly different types of L-form nucleon, called **Type 1** and **Type 2**, are required, wherein the inflow/outflow direction of **all CES** within Type 1 nucleons (P1 protons and N1 neutrons) are the reverse of that for Type 2 nucleons (P2 protons and N2 neutrons).

Each extra nucleon chain added vertically adds another proton (P) and neutron (N) pair to generate an I-form nucleon layer pattern NPPNNP... or PNNPPN... An even number of such nucleon layer pairs has either a neutron layer top-and-bottom (e.g. layers 1 to 4 in figure 9), or a proton layer top-and-bottom (e.g. layers 3 to 6), whereas an odd number of pairs has a proton layer on one side (top or bottom) and a neutron layer on the other side (e.g. layers 1 to 6, which span 3 nucleon layer pairs). Such patterns become important when considering the electromagnetic characteristics of elements that are related to their bonding patterns and ionic orbital potential.

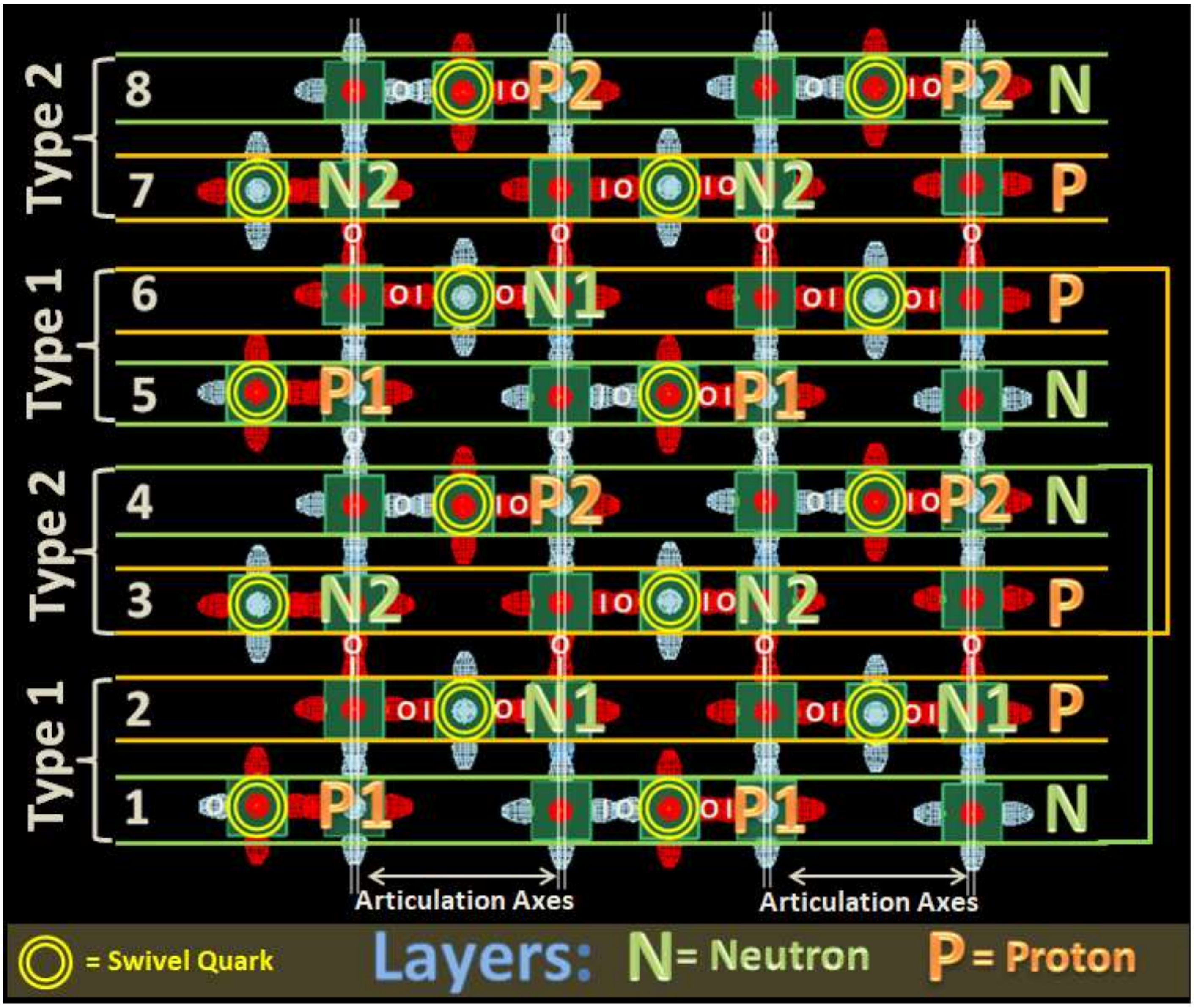

Figure 9: Nucleon Type and Nucleon Layer Patterns within Vertically-Joined Nucleon Chains

The join points of co-joined nucleon chains define a vertical articulation axis (the light double lines in figure 9) that act as hinge lines to allow the end-quarks of each chain to meet and become inter-quark bonded to convert it into a stronger, more stable lattice-like polygonal structure, so transforming the chain into an atomic nucleus or part thereof.

The inter-quark bonds within nucleons and those bonding nucleon chains together are identical in strength. According to STEM, all the elements in the Periodic Table, with the exception of the single proton hydrogen atom, consist of a robust polygonal nucleus created from inter-locked multi-level L-form nucleon chains which present with distinct I-form proton and neutron layering. As well as strongly bonding quarks together to create L-form nucleons, and bonding L-form nucleons to create nucleon chains and nucleon layers, inter-quark bonds provide an internal two-way field-energy exchange and balancing mechanism. Within the polygonal form of an atomic nucleus, this facility supports energy sharing and balancing between all parts of the nucleus.

Of particular interest are those quarks highlighted by **yellow double circles** in figure 9 which, unrestrained, spin or swivel in the direction of the toroidal flow direction of the pair of inter-quark bonds that support them. Rapidly spinning, these quarks are called **swivel quark**, and they radiate the energy-fields of 4 same-charge CES, so generating an external electromagnetic field of strength approximately 4 times that of the other fixed quarks (which only expose 1 CES to the outside world). As addressed in subsequent chapters, swivel quarks are important for chemical reactions and the formation of molecules and chemical compounds.

The electromagnetic field close to an atomic nucleus is dominated by the strong electromagnetic field of swivel quarks. As can be ascertained from figures 8 and 9, when closed to form a polygonal structure, every nucleon chain would contain an equal number of outwards facing e-CES and p-CES, which results an approximately **neutral** electromagnetic field close to atomic nuclei (i.e. the net **near-field** is neutral). However, due to the influence of the swivel quarks, because there is approximately an equal number of up quarks (with a net field strength of +2/3 e) and down quarks (with a net field strength of only -1/3 e), the net **far-field** of atomic nuclei is **positive**.

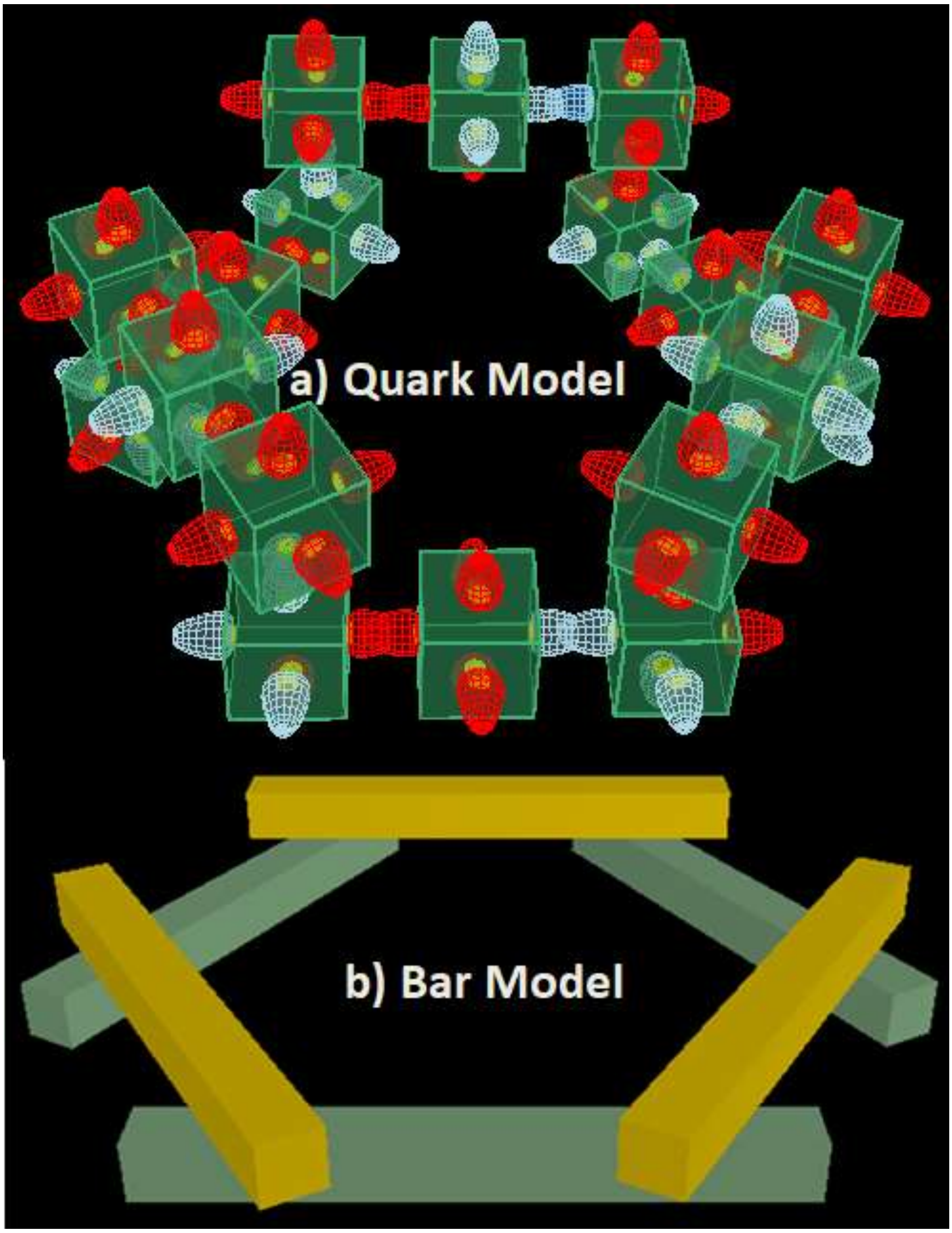

Figure 10: Single-Chain Hexagonal Polygonal Structure

Figure 10 shows a single chain consisting of 3 neutrons and 3 protons per layer, end-joined to create a hexagonal structure. As can be seen, the geometry and I-form nucleon structure is clearer in the bar model than the quark model and allows for faster nuclear modelling. The original nucleon chain may be a type-1 or type-2 type chain, with increased **polygonal nucleon layers** providing the nucleus with increased strength and resilience.

It would seem highly unlikely that a pair of Type-1 and Type-2 nucleon chains would come together so as to join via strong-force inter-quark bonds to produce chains, and thus nuclei, that are 4 or more nucleon layers in height. It is far more likely that the creation (and re-cycling) of atomic nuclei evolves from the simple **quark-chain building process** described earlier (page 10) rather than a nucleon chain build-and-join process.

Currently, the gluon mediation theory of Quantum ChromoDynamics (**QCD**) provides the most strongly supported explanation for strong-force interactions within and between hadrons. The QCD explanation is heavily reliant upon the gluon, a mathematically defined massless, but as yet unconfirmed, theoretical vector boson that is considered to be the elementary particle that mediates strong interactions between quarks. STEM, on the other hand, is far more specific about the nature of strong force bonds and the manner in which the nucleons inter-connect to form an atomic nucleus

A distinct point of difference is that the ONAM approach considers the nucleus to consist of an amorphous group of nucleons held together by mysterious strong forces, whereas STEM contends that atomic nuclei have a lattice-like structure, the polygonal geometry of which correspond to the observed characteristics of the elements and their interaction with other elements and compounds.

In this chapter, the inflow/outflow patterns of CES involved in the formation of inter-quark bonds between nucleons have been emphasised. The CES inflow/outflow patterns must be consistent with the flows indicated in figure 6 to create a strong-force inter-quark bond. In the next chapter, the inflow/outflow patterns of all CES within L-form nucleons will be considered, and it will be shown how a forced change of flow pattern of certain CES can cause an instantaneous change of nucleon type, with a neutron becoming a proton, and vice versa.

Nucleon Type Conversion

An element in the Periodic Table is identified by the number of protons that it contains, which is its **atomic number**. Different **isotopic forms** of the same element contain a different number of neutrons, meaning that the **atomic mass**, which is the total number of protons and neutrons within an atom, may be different.

Conventional Science deems that when the atomic number changes, you have a different element. However, neutrons can dynamically convert into protons and, vice versa, as evidenced by beta decay and electron capture. This means that the atomic number can randomly dynamically change, which implies that the atom, purely defined upon its atomic number, can transform from one element into another over time. Consequently, for certain specific elements, the maintenance of a sample of 100% purity over time can be a problem.

The ability for a proton to change into a neutron and vice versa is due to the ability of an e-CES to be converted into a p-CES, or vice versa, by simply reversing the CES's inflow and outflow vortex flow directions. This conversion process, called **CES flipping**, can be caused by the compression of the field-energy by a high-impact.

The right-side of figure 11 (similar to figure 1b) shows the 'polarisation' of a hypothetical neutral CES: when its energy-field is polarised by pushing it upwards (large red arrows), a p-CES is created, and when it is pushed downwards (large blue arrows) an e-CES is created. The neutral CES is hypothetical, because in Nature the energy-field of a CES is always polarised, but with the impact of a direct hit by a fast-moving particle (such as an electron) can cause the CES's energy-field to 'flip', wherein the outflow vortex is pushed to the other side of the CES's energy-core, so converting (or flipping) an e-CES into a p-CES, or vice versa.

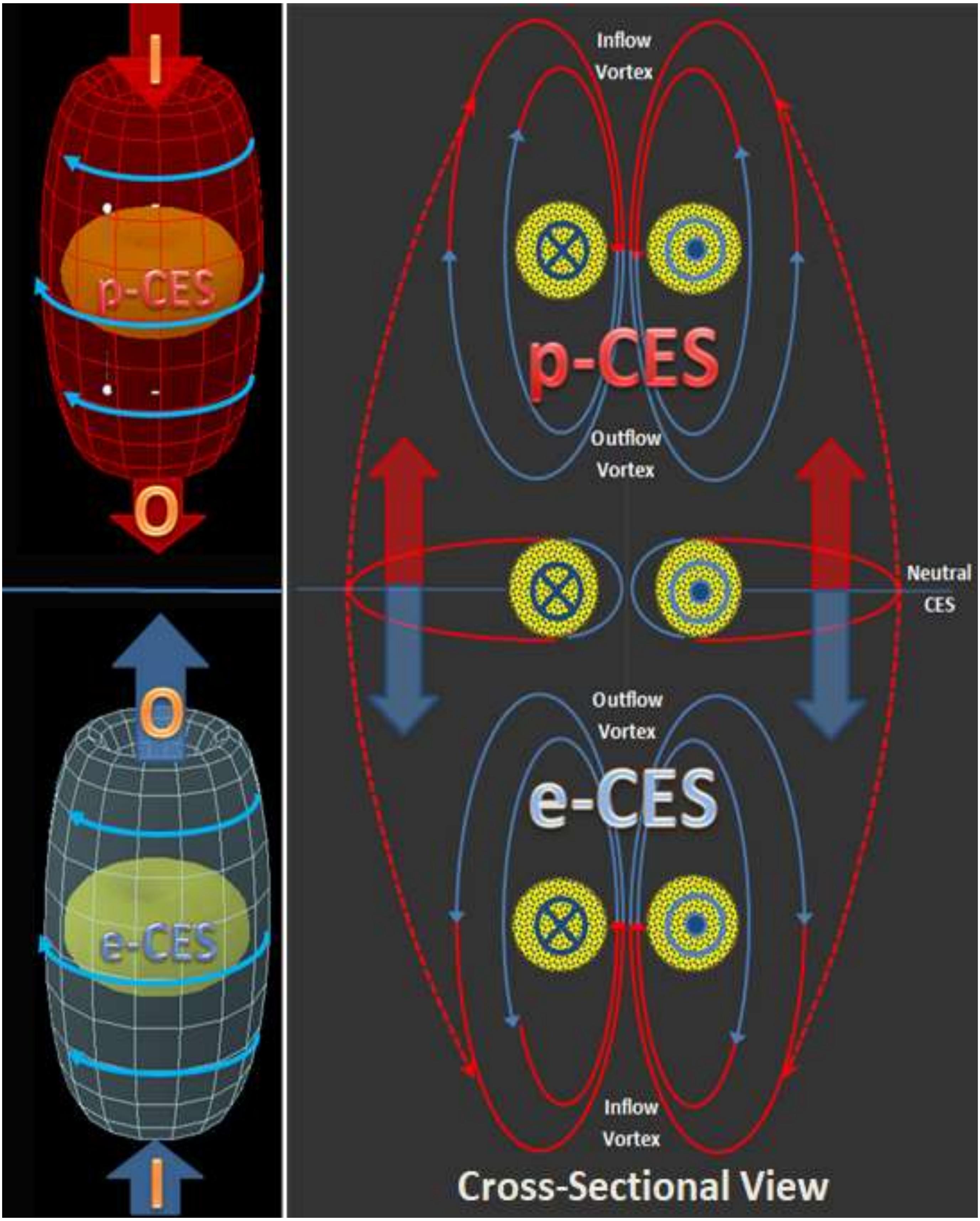

Figure 11: An e-CES flip into a p-CES

Up and down quarks each contains six CES, all of which can be flipped except for the one p-CES, which is labelled as the **Invariant p-CES** in figure 12a. Note that, although the **toroidal direction** of energen flow within energy core of each CES remains the same for both the down and up quark shown, the **poloidal flow** direction of their field energy, as indicated by the central arrow, has been reversed (i.e. flipped) except for the uppermost p-CES (the invariant CES).

Nucleon conversion, wherein a neutron is converted into a proton, and vice versa, occurs when all the up quarks convert into down quarks, and vice versa, with the exception of each quark's invariant p-CES, which remain intact. Interestingly, each nucleon has two spinner arms (i.e. the quark arms can potentially spin around the inter-quark bond attaching them to the central quark), but it is the one not containing the invariant CES (the horizontal arm in figure 12b) that becomes the up and down **swivel quarks** within the nucleon layers of the nucleus.

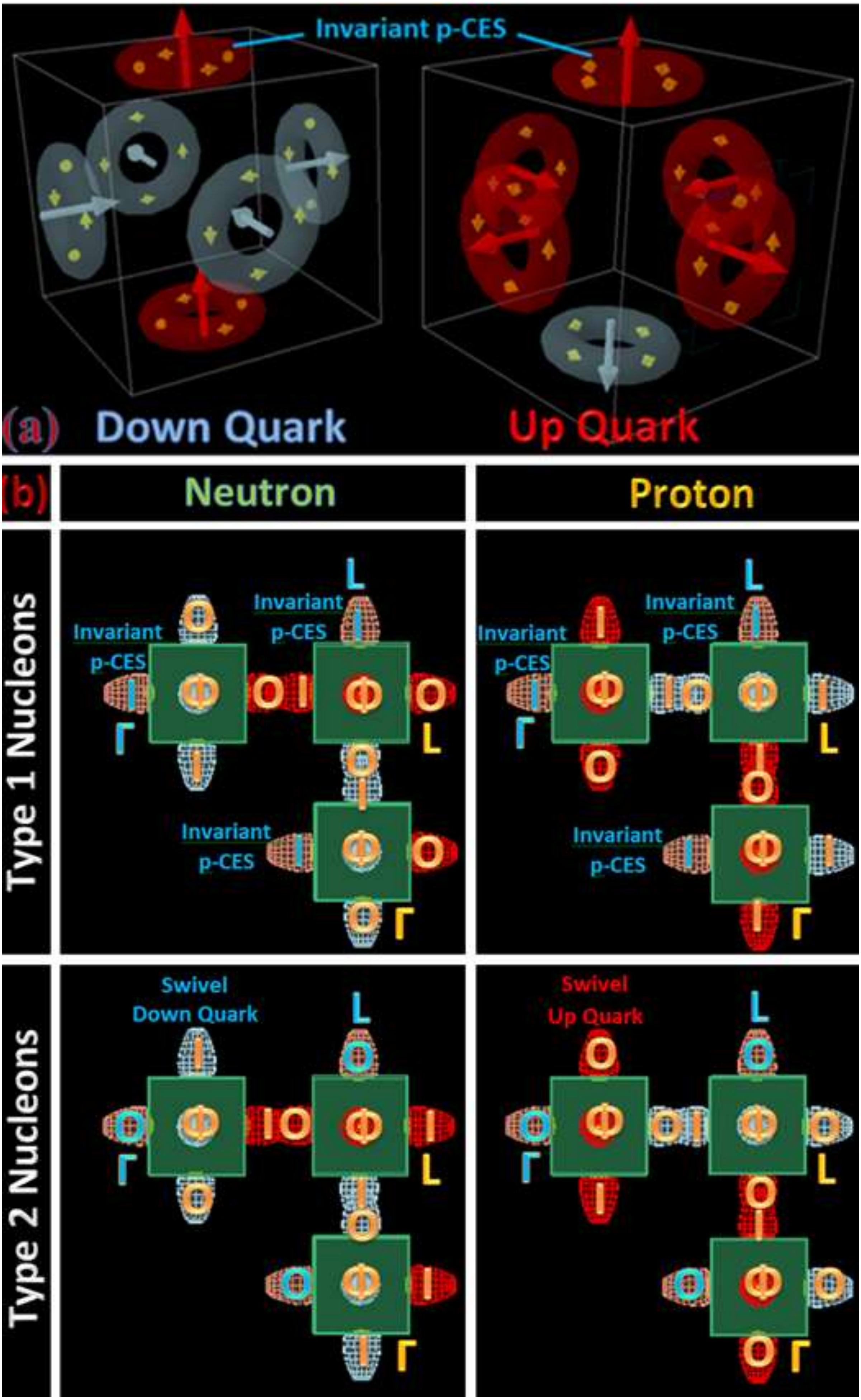

Figure 12: Down/Up Quark and Nucleon Conversion

Within an L-form nucleon, it would seem that when one flippable CES is flipped, it acts as a **trigger** to the flipping of all other CES within the structure, with the exception of the three invariant p-CES. It would seem that the reversal of the flow direction within the inter-quark bonds between a nucleon's quarks to trigger the flipping of all amenable CES in the other two quarks.

The most likely and common cause of the nucleon type conversion process is impact by another energised particle (e.g. a fast-moving electron or alpha particle), as explained in the Beta Decay and Electron Capture chapter. The CES trigger for the process is most likely a flippable outflow CES. Hopefully future modelling will reveal the physics behind such orchestrated dynamics but, in the meantime, the CES-flipping process of all flippable quarks within the nucleon provides a feasible and reasonably simple explanation of how a **neutron** within an atomic nucleus can be instantaneously transformed into a **proton**, and vice versa; which is something ONAM can only describe.

An important aspect of nucleon-type conversion process is that it can only proceed should **all** the flippable CES within the nucleon remain **unrestrained**. This means that should **any one** of the flippable CES be restrained by being inter-quark bonded to another nucleon, then none of the flippable CES can be flipped. Thus, because most nucleons within a **complete nucleon layer** have at least one of their flippable CES bonded (see the small yellow circled inter-quark joins in figure 13), they cannot be flipped.

In figure 13, the notation **P(→N)** indicates that the nucleon that started as a proton can be possibly type converted into a neutron, but not very often; and similarly **N(→P)** indicates a neutron that can be converted into a proton, but not very often. The notation **(P→)N** indicates a nucleon that started as a proton, but very likely to be converted into a neutron. An isolated **P** notation indicates a proton that cannot be type converted into a neutron, and an isolated **N** indicates a neutron that cannot be type converted into a proton.

Figure 13 shows a proton and a neutron layer which, when end-joined to form a polygon, would contain four I-form nucleons in each layer. It shows all possible attachment orientations of L-form nucleons to the outer proton and neutron layer using the foot-in anchor points (┘ in figure 12) and foot-out (┐ in figure 12) anchor points. Within the complete nucleon layers there is one L-form proton that could possibly be type-converted into a neutron, as highlighted with the **P(→N)** annotation: however, for the right inter-quark join of its upper (as shown) up quark, there is only a 33% (1 in 3) probability that the p-CES involved would be invariant to make such conversion possible.

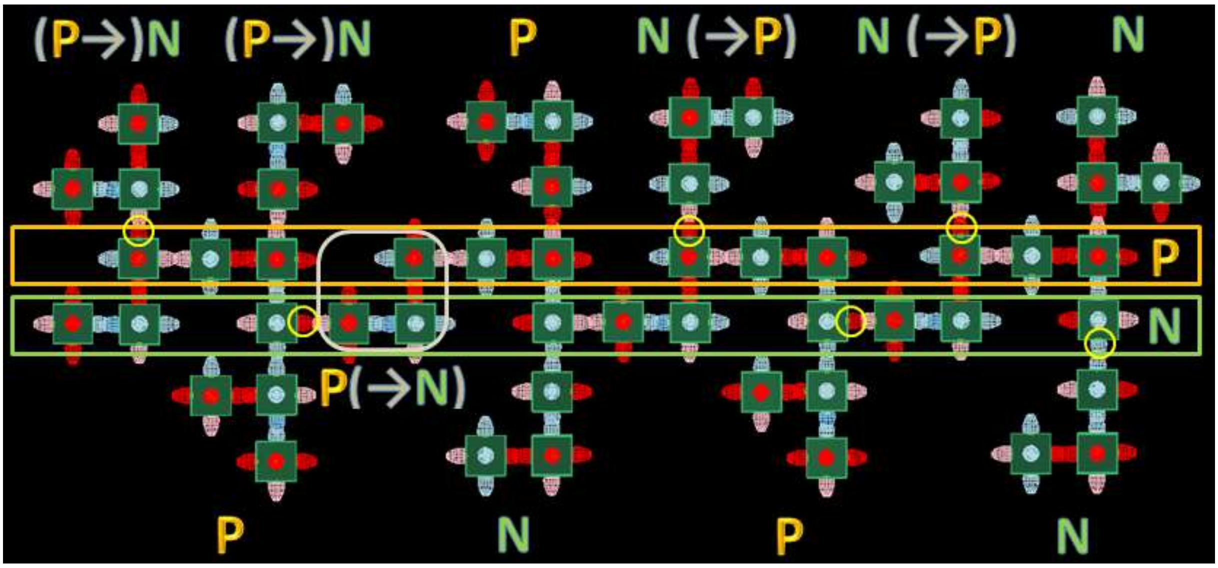

Figure 13: Attachment of L-form Nucleons to Outer Nucleon Layers

As apparent in figure 13, a lot of variability in neutron-to-proton ratios could be expected within atoms, as evident in the ration plot across the element of the Periodic table, as plotted in the graph of figure 14. Apart from a quite rare nucleon type-conversion within an upper or lower full nucleon layer, the bulk of the variability in the neutron-to-proton ratio would seem to be attributable to variation in the composition of the partial nucleon layers principally consisting of L-form nucleons inter-quark (strong force) connected to the outer surfaces of the full nucleon layers.

For most elements, the last stage of their evolution involved the formation of chemical bonds with other elements, molecules and compounds, quite often in high pressure and temperature environments. In such environments, kinetically energised electrons would abound that would facilitate proton-to-neutron via **Beta**$^{+}$ **decay** and **electron capture** processes (for more detail, see the Beta Decay and Electron Capture chapter), which would mean that most protons attached to an outer proton layer and annotated **(P→)N** in figure 13 would be converted into neutrons. However, it is most likely that **positrons** generated by the conversion process would only travel a short distance before undergoing electron-positron annihilation and being destroyed, and thus not being able to **Beta**$^{-}$ convert another neutron into a proton.

It is likely that amenable L-form protons attached to an outer proton layer would become type converted into neutrons by energised electrons, with most attached **(P→)N** nucleons becoming neutrons. However, with insufficient energised positrons, few **N(→P)** neutrons would be converted into protons. The net effect is more neutrons than protons within the nucleus and, assuming that each of the 8 orientations of attached L-form nucleons of figure 13 has an equal probability of occurring, summing them up in their most likely form (neutron Vs proton), there are 7 neutrons (5 attached to proton layer and 2 to neutron layer) and 3 protons. With 4 nucleons within each full nucleon layer, there would be 11 neutrons and 8 protons, which corresponds to the equation **N = 1.375 * Z**, where **Z** = number of protons.

This estimate is not far removed from the **best-fit** trend line **N = 1.5 * Z** for elements observed in Nature, as represented by figure 14. With a reduced gradient apparent in the **Z<30 range** of the figure 14 graph, a **1.375** gradient (shown as the **light orange** **Z<30** line) can be considered to be a good estimate. Also, due to the variability of the nucleon type conversion processes as discussed above, computer simulation using STEM atomic structures would likely generate Z:N ratios reflecting the **spread** of **isotopic forms** apparent in the plotted ratios of figure 14.

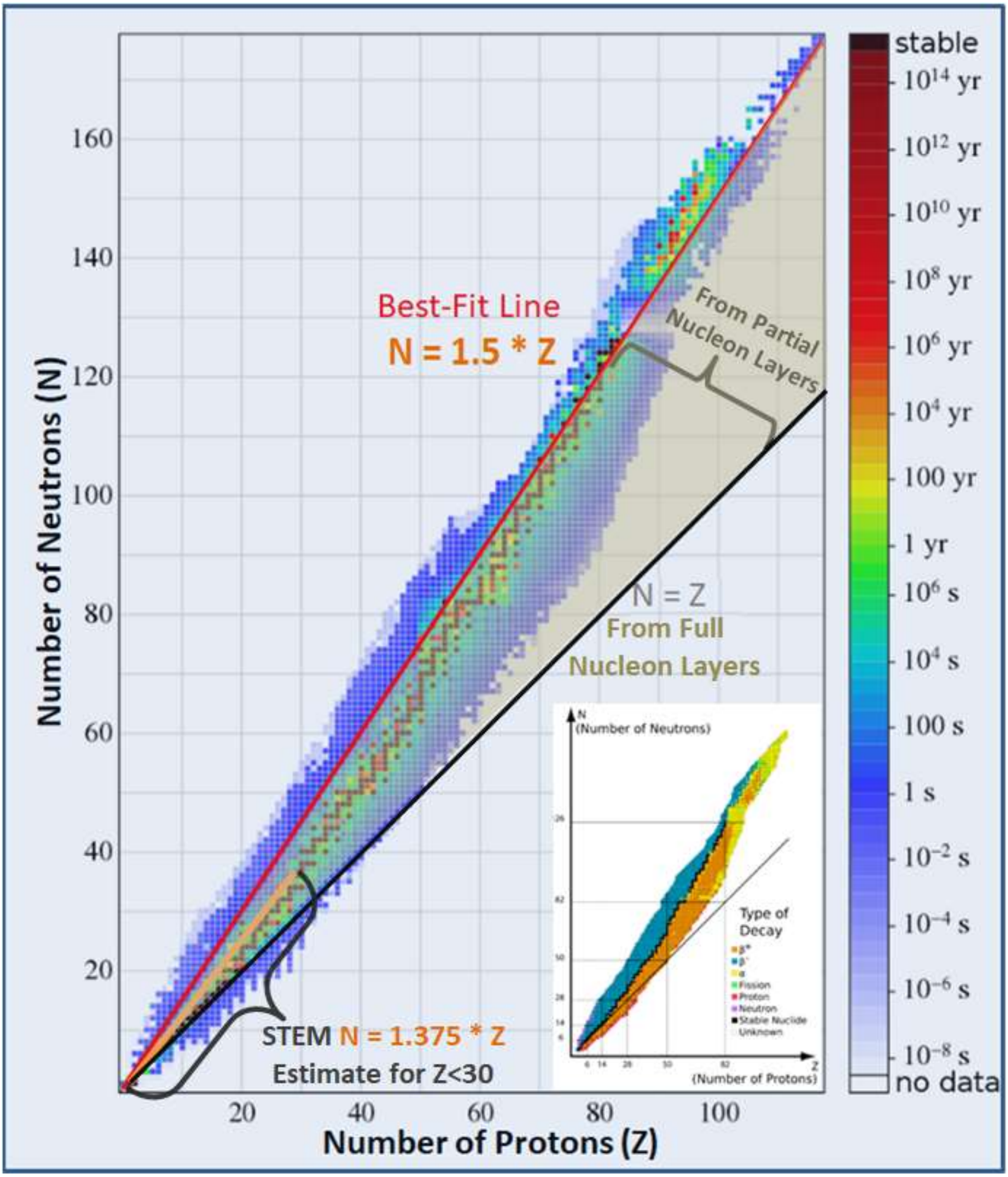

Figure 14: Proton-to-Neutron Ratio and Decay Half-life Spread by Atomic Number (Z)

STEM contends that the polygonal nuclear structure is the main factor that determines the physical characteristics of each element, and that the full polygonal layers of an atom provide the 'base' count of protons and neutrons, as reflected by the **N = Z** graph. Also, as apparent in the figure 14 graphs, a definition of an element purely in terms its contained proton count (Z) is inappropriate, and bound to fail, with the **stochastic nuclear signature** approach, as detailed towards the end of the ‘Atomic Structure: Period 3 and Onwards’ chapter, representing a more realistic and preferable way to identify elements, their isotopic forms and their decay-related transitions.

Fundamental Particle Statistics

The CODATA radius of the electron, which represents “classical electron radius", is $2.82\ \times 10^{-15}$ m, and the corresponding CODATA value for the proton’s radius is 0.877×10^{-15} m. The latest available estimate of the **proton’s radius** was made in 2010 using pulsed laser spectroscopy to measure a muonic hydrogen atom (a proton orbited by a negative muon, with a muon being considered to be a ‘heavy’ short-lived energised electron): with Lamb shift adjustment, its radius was estimated to be 0.842×10^{-15} m.

Such estimates suggest an amazingly small size proton radius that is about 1/3rd that of the CODATA electron radius. The possibility of (relatively) large electrons whizzing around the diminutive nucleus of an atom creates a huge dilemma for an ONAM-based Physics world. A possible reason for such a small estimate of proton size is the assumption that a proton to be a single spherical particle, when, according to STEM, it consists of an array of 18 much smaller torus shaped CES particles as in figure 5c. The scattering observed, thus reflects a greatly reduced probability of making a direct hit of a sparse targets provided by CES within a free proton.

.

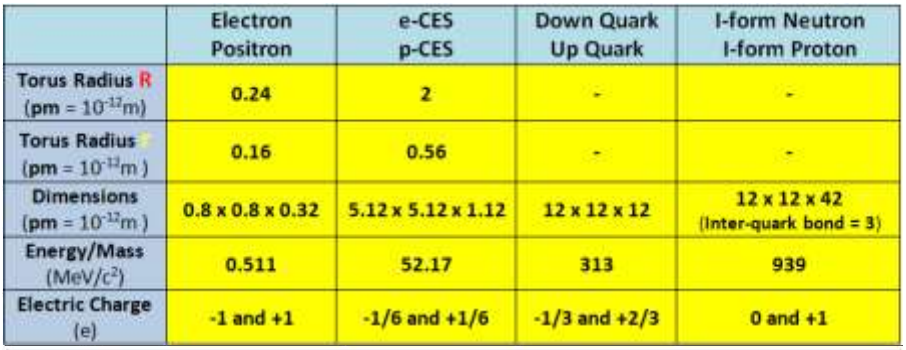

	Electron Positron	e-CES p-CES	Down Quark Up Quark	I-form Neutron I-form Proton
Torus Radius R (pm = 10^{-12}m)	0.24	2	-	-
Torus Radius r (pm = 10^{-12}m)	0.16	0.56	-	-
Dimensions (pm = 10^{-12}m)	0.8 x 0.8 x 0.32	5.12 x 5.12 x 1.12	12 x 12 x 12	12 x 12 x 42 (Inter-quark bond = 3)
Energy/Mass (MeV/c^2)	0.511	52.17	313	939
Electric Charge (e)	-1 and +1	-1/6 and +1/6	-1/3 and +2/3	0 and +1

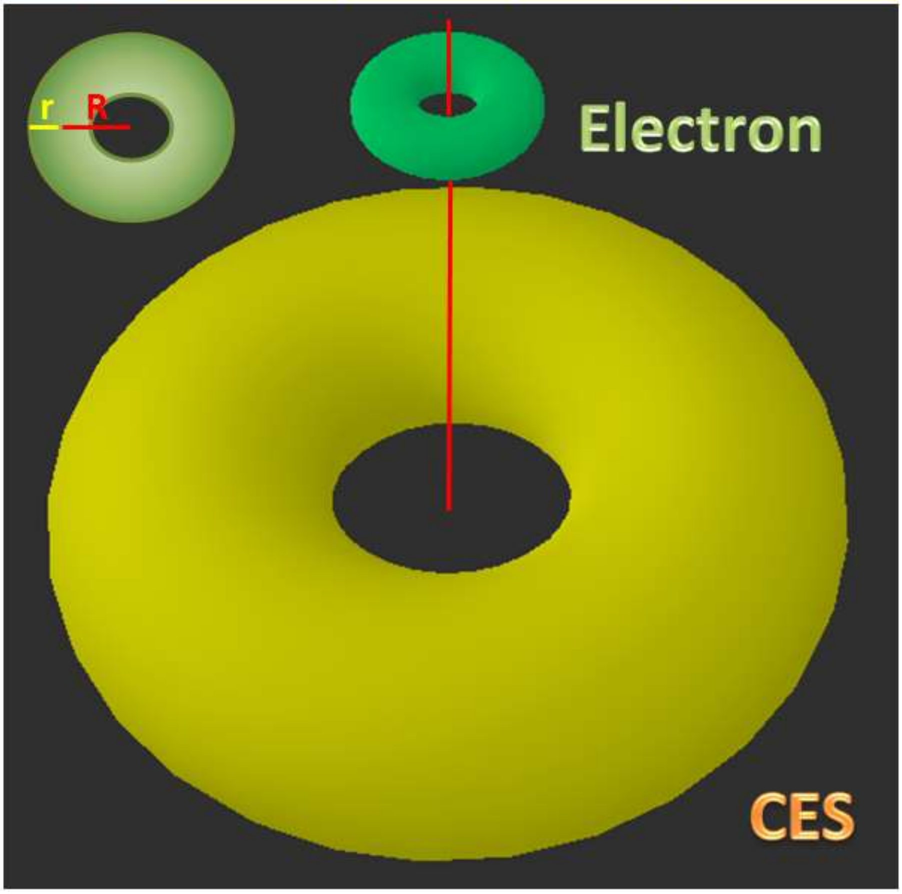

Figure 15: Electron, CES, Up/Down Quark and Nucleon Statistics

Earlier estimates by M MacGregor (‘The Enigmatic Electron’: Klurer Academic, 1992) placed the radius of an electron in the range 4 x 10^{-13} to 7 x 10^{-13} m, which is compatible with the 2015 Bowen and Mulkern estimate of 3.86 x 10^{-13} m. These estimates are about 100 times larger than the classical CODATA electron radius, and some 200 times larger than the classical proton radius, making the classical proton radius estimate even more difficult to accept

Bowen and Mulkern consider an electron to be a photon that has closed on itself (i.e. a head-to-tail wrap-around) to form a torus loop, and that its photon-like charge rotates around the torus loop at the speed of light. This is quite similar to STEM’s electron model and, in their 2015 paper ‘An Electron Model Consistent with Electron-Positron Pair Production from High Energy Photons’, the radius of a toroidal electron has been calculated to be 3.86 x 10^{-13} m.

The large radius (R) of the STEM electron is 0.24 pm (2.4 x 10^{-13} m) and the small radius (r) is 0.16 pm (see the table of figure 15). With an outer equatorial radius of 4 x 10^{-13} m (i.e. R + r), the STEM electron radial size corresponds pretty close to that of Bowen and Mulkern. At 25.6 x 10^{-13} m, the outer equatorial radius of a CES core-energy torus is about 6.4 times that of an electron which, as will be explained in the next chapter, is important to an explanation of why a CES has a nominal charge of only ±1/6 e.

Although there is considerable variability in the size estimates for electrons and nucleons, it would appear that their mass equivalence estimates are well researched and quite well established. However, the mass equivalences of their composite particles appear to be anomalous or, in the very least, inconsistent. For example, the claimed mass equivalence of up(**U**)/down(**D**) quarks is in the 1.8 to 5.8 MeV/c^2 range, but the mass equivalence of protons (UDU) and neutrons (DUD) is 938.3 MeV/c^2 and 939.6 MeV/c^2 respectively, which simply does not add up.

In need of more precise estimates, STEM has assumed an average mass equivalence value of 939 MeV/c^2 for nucleons, with the mass equivalence of CES and up/down quarks (each consisting of 6 CES) being 52.17 and 313 MeV/c^2 respectively, as determined on a pro-rata distribution of a nucleon’s 939 MeV/c^2. These estimates may be more precise (i.e. specific) and less anomalous than the wide range of ONAM-based estimates, but they are not necessarily more accurate. Independently verified accurate and anomaly-free estimates are needed further down the track so that the appropriate adjustments can be made to the STEM model.

In the meantime, the current STEM size and mass equivalence estimates provide ball-park figures that can be applied so as to allow the building of a physical atomic structure. The result is an atomic model that provides true-to-scale physical structures for the elements of the Periodic Table; and helps to help explain the physical and chemical characteristics of elements, including the common/ bonding patterns observed between atoms, molecules and chemical compounds.

STEM atomic nuclei models have been generated from I-form nucleons based upon a 12 pm cubic quark plus a 3pm inter-quark (or strong) bond length. The nuclear structures generated are lattice-like and polygonal in cross-section. However, the resulting nuclei sizes are somewhat larger than the nuclear sizes suggested by conventional Science. The resulting nuclear sizes most likely represent upper-limit estimates, but the bond lengths associated with multi-atom molecules and compounds do correspond very well to those as determined experimentally, which is re-assuring.

It is worth noting that the radial size of the CES was determined assuming that energen in its energy core (52.17 MeV/c^2) has the same density as that of an electron’s energy core. However, as discussed in the next chapter, although having the toroidal structure of a fundamental particle, electrons and positrons are most likely to be particles derived from the field energy of CES. Thus the energy core energen of CES could be considerably denser than that of an electron, which would mean that the outer radial size of CES could be considerably less than 2.56 pm, and consequentially the 12 pm up/down quark radial size could be as much smaller and the size of atomic nuclei would be much smaller. However, it was decided to err on the larger size that seemed to be the more conservative option.

Also, with a mass equivalence estimate of 52.17 MeV/c^2, the energen contained in the core-energy torus of a CES is more than 100 times that of an electron, and yet its allocated electric charge (±1/6 e) is a sixth that of an electron (±1 e), which seems incongruous. An explanation of this apparent miss-match between mass equivalence and electric charge value will be provided in the next chapter.

And interestingly, in energen terms and allowing for energen loss due to the creation process, the rest mass of a CES-pair (104.3 MeV/c^2) approximates to that of a muon (105.7 MeV/c^2) and, allowing for even more energen loss, strange quarks (with an approximate mass of 96 MeV/c^2). Also, three CES (156.5 MeV/c^2) could approximate to a pion (139.6 MeV/c^2). This would be consistent with the contention that pion and muon (and possibly strange quarks) result from the high-energy bombardment of ordinary matter which causes up/down quarks within nucleons to split or fragment, rather than being special fundamental particles as suggested by ONAM. Also, ONAM has no feasible explanation for electron spin or for neutron magnetic moment, with these properties being deemed to be ‘intrinsic’, and there is considerable variation of ONAM’s physical size estimates for electrons and nucleons plus inexplicable discrepancies related to their mass equivalence estimates.

Electrons and Atomic Bonding

With the conventional Science approach (ONAM), protons are considered to be discrete positively charged particles that can be expected to forcibly repel each other whenever in close proximity such as within an atom's nucleus. To counter the possibility of the nucleus spontaneously disintegrating, a range of strong-force carriers/enablers called gluons have been proposed by the **Standard Model** and **Quantum Chromo-Dynamics** (QCD), the existence of which, as mentioned earlier, has not been proven.

The early Rutherford/Bohr models considered that electrons assumed planet-like orbitals around the nucleus: for planets, gravitational pull keeps them in orbits around the Sun, whereas electric field attraction was considered to keep negatively charged electrons in orbit around a positively charged nucleus. Since the advent of Quantum Mechanics, although 'spdf' orbitals derived from wave equations are less planet-like in geometry, the planet-like sentiment remains, particularly in Chemistry texts. However, whereas our Solar has only eight planets in orbit around the Sun, large nuclei have many, many more electrons buzzing around an atomic nucleus: for example, according to ONAM, each gold atom has 79 electrons in orbit, uranium 92, and copernicium 112. Considering the speed of the electrons and the confined space, this is a miraculous and mid-boggling proposition that beggars belief.

Unlike ONAM, STEM does not support or require the concept of inner shell (or inner 'spdf') electron orbitals, or the need for the number of electrons to equal the number of protons for an element to be considered electrically neutral. However, as discussed in the Ionisation and Redox chapter, STEM supports **ionic orbital electrons** which, although functionally these are similar to ONAM's conduction band electrons, have **planar orbitals** rather than orbitals that fully envelope the nucleus as for the 'spdf' and Bohr-like electron shell orbitals. As well as supporting the **ionisation** of elements, ionic electrons can form **covalent bonds** (fig 16b), but without the electrons having to pass between nuclei of the bonded pair as for the ONAM approach (fig 16a), which requires really tricky navigation and timing.

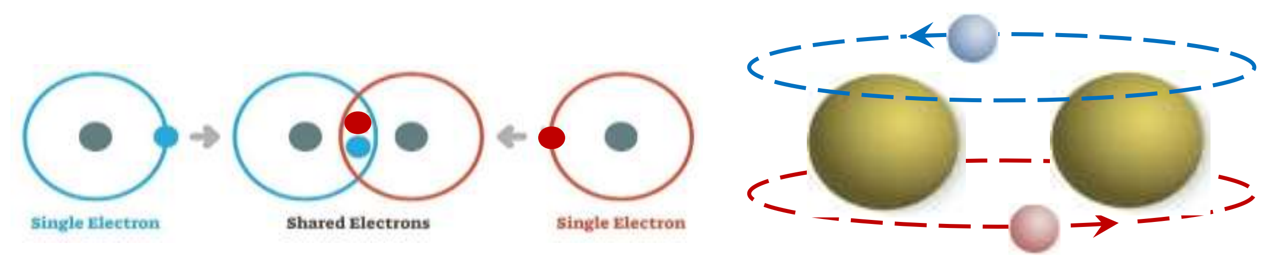

a) Simple Conventional Covalent Bond

b) Simple Planar Orbital Covalent Bond

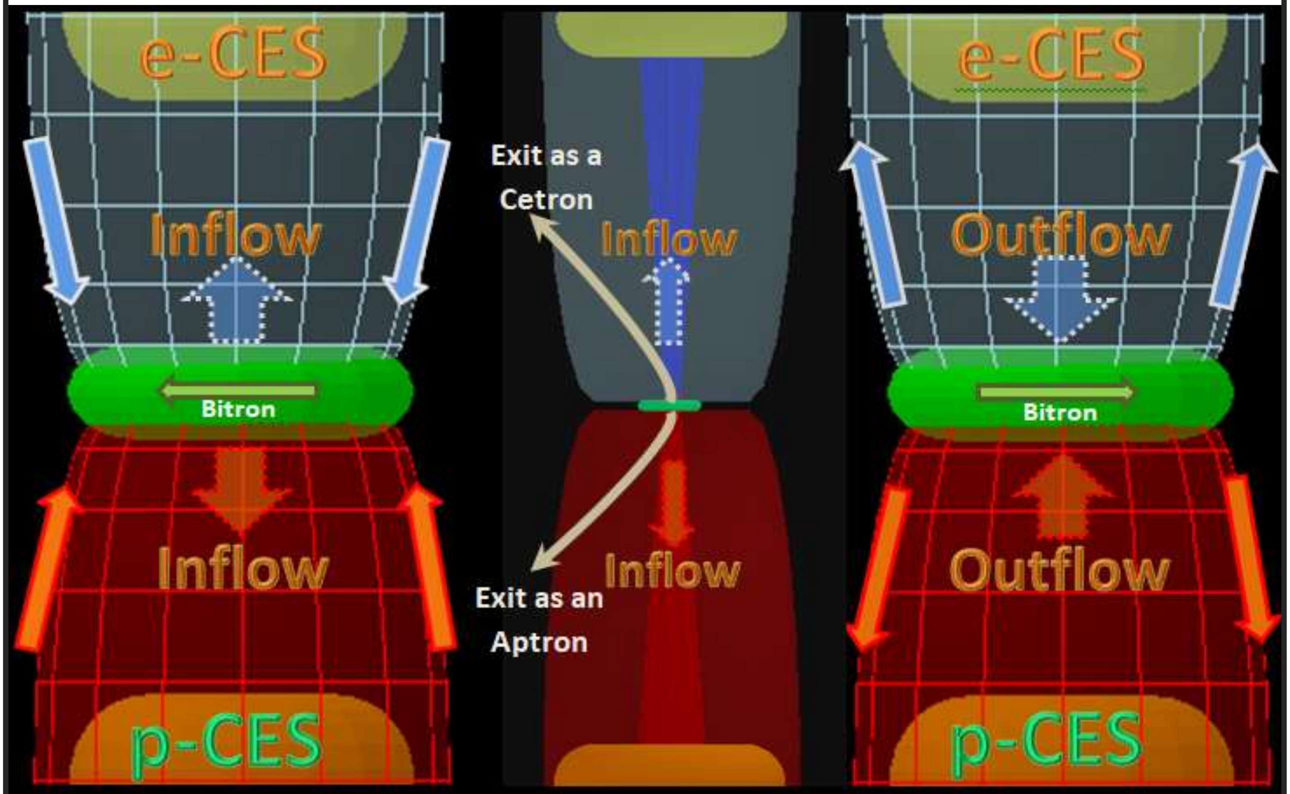

c) Opposing Inflow CESs

d) Close to Scale

e) Opposing Outflow CESs

Figure 16: Covalent and Bitron Bonds

STEM also introduces a new type of bond, the **bitron-bond** (or **b-bond**). A b-bond can be created when a pair of inflow vortices (or a pair of outflow vortices) of opposite chirality CES face each other in close proximity as shown in figures 16c to 16e. When the vortices are both inflow vortices, because the inner inflow vortex flow rates are significantly stronger than the outer outflow rates, the CES pair strongly attracts each other and the b-bond binds them together. For outflow vortices, the CES repel each other, and thus can only form a b-bond when they are forcedly held in close proximity, such as might occur by the formation of some crystalline substances.

B-bonds involve a pair of opposite-charge CES that are 45 to 100 pm apart. With such separation there is an overlap and concentration of their energy-fields and, as both energy-fields have the same circular spin direction, their **toroidal flow components** combine and strengthen, whereas their **poloidal flow components** are in opposite directions and so cancel each other out. The net result is that a toroidal ring of **concentrated field-energy** quickly develops, which is called a **bitron**. A bitron is a toroidal ring quantised (i.e. becomes stable) at 0.511 MeV/c2, and is the equivalent of the **energy-core** of an electron.

B-bonds are far weaker and longer in length than inter-quark bonds that hold the up/down quarks together to form nucleons and to hold the nucleons together within the structure of an atomic nucleus. A **bitron** is equivalent to the energy core of an electron and represents a **pre-cursor** to electron generation: it only becomes an electron, either a **cetron electron** (a negative charge carrier) or an **aptron electron** (a positron or positive charge carrier), upon its release from the b-bond.

A **bitron** can be bump-released by the impact of an excited free electron, or from EMR photon or radioactive particle bombardment, or from direct mechanical force. A bitron can become either a cetron or an aptron electron depending upon which side of the bond it passes through upon release, as shown in figure 16d (which, like figure 15, are close-to true-scale for a bitron relative to CES size, whereas figures 16c and 16e are not to scale). Although some newly released electrons may be captured internally and become ionic orbital electrons, most would seem to be surplus-to-needs and have sufficient energy to escape as **free electrons**, as evidenced by electron emission from electron gun elements and from solar cell collector plates via the photoelectric effect.

Should a CES pair remain in close proximity after release of their bitron as a cetron or aptron electron, another bitron rapidly forms, which means that electrons are in effect a **derived fundamental particle** and a **renewable resource**, with b-bonds being considered to be **electron breeders**. With the abundant supply of electrons within Nature (and electric conductors in particular), and with electron-positron annihilation able to remove electrons, it makes logical sense for atoms to be able to dynamically generate bitrons and thus electrons. And there are many implications related to electrons being a derived fundamental particle and a renewable resource.

One implication of electrons being a renewable resource is that they can be derived from atom-bonding processes rather than being mysteriously generated en-masse (in numbers well in excess of the number of atoms in existence) by processes unknown, and then having to find candidate atoms to which they can become attached as orbital electrons.

Another implication is an explanation as to why a CES has a nominal charge of approximately ±1/6 e. For the STEM electron, with an energy core radius $R = 2.4 \times 10^{-13}$ m (or 0.24 pm), the tangential velocity of an electron's field energy can be calculated as:

$\mathbf{v_e} = S / (m_e{*}\ R) = 5.27\times10^{-35} / (9.1\times10^{-31} \times 2.4\times10^{-13}) = 2.4\times10^{8}$ m/s, which is close to the speed of light
where $m_e = 9.1\times10^{-31}$ (the mass of an electron),
and $\mathbf{S} = 5.27\times10^{-35}$ Js. (the QM estimate of intrinsic spin which is based upon the Bohr electron).

The angular velocity (ω_e) of the electron's energy core is $v_e/R = 2.4\times10^{8} / 2.4\times10^{-13} = 10^{21}$ radians/sec.

Assuming the tangential velocity (v_c) of a CES to approximately be the speed of light (3×10^{8} m/sec), its angular velocity (ω_c) = $v_c/R = 3.0\times10^{8} / 20 \times 10^{-13} = 1.5\times10^{20}$ radians/sec = $1/6.7 \times \omega_e$. With the electric field of a fundamental particle being defined by the circular (toroidal) flow component of its energy field, its field strength is directly proportional to the angular velocity (ω) of that field energy. Thus, because ω_e generates a field strength that defines an electric charge of 1 e, it is reasonable to assume that ω_c (= $1/6.7 \times \omega_e$) defines an electric charge of 1/6.7 e. Consequently, the electric charge associated with a CES can be expected to be in the range 1/6 e to 1/7 e.

Another implication is that in material with very few charge carriers (i.e. free electrons), such a silicon wafer used in semiconductors, additional electrons can be dynamically generated and released by EMR photon bombardment to support the generation of an electric current. This is the basis for the operation of photovoltaic cells and photodiodes.

Bitron generation within b-bonds, and subsequent release as electrons, represents an important part of an atom's energy balancing repertoire, allowing more significant amounts of energy to be released or absorbed than can be achieved via electromagnetic radiation (EMR) alone. Bitron bonds and the electron generation process also have big implications for ionisation processes and the operation of Redox reactions (see the Ionisation and Redox chapter).

Being formed by interaction between a pair of inflow CES, b-bonds cause mutual attraction between the CES pair. When a bond is formed by a pair of outflow CES, no bitron forms and the CES pair mutually repel each other, and are called **offset bonds**. Bitron-style bonds that are over 100 pm wide have insufficient field-energy overlap to generate a bitron (i.e. they are bitron-less), and being analogous to polar bonds, are referred to as **p-bonds**.

Swivel quarks are the central CES of I-form nucleons: an up-quark for I-form neutrons and a down-quark for I-form protons (see figure 17). Swivel quarks in the upper and lower nucleon layers of an atomic nucleus align with their energy fields combining to generate the electromagnetic field that supports ionic orbitals above and below an atom.

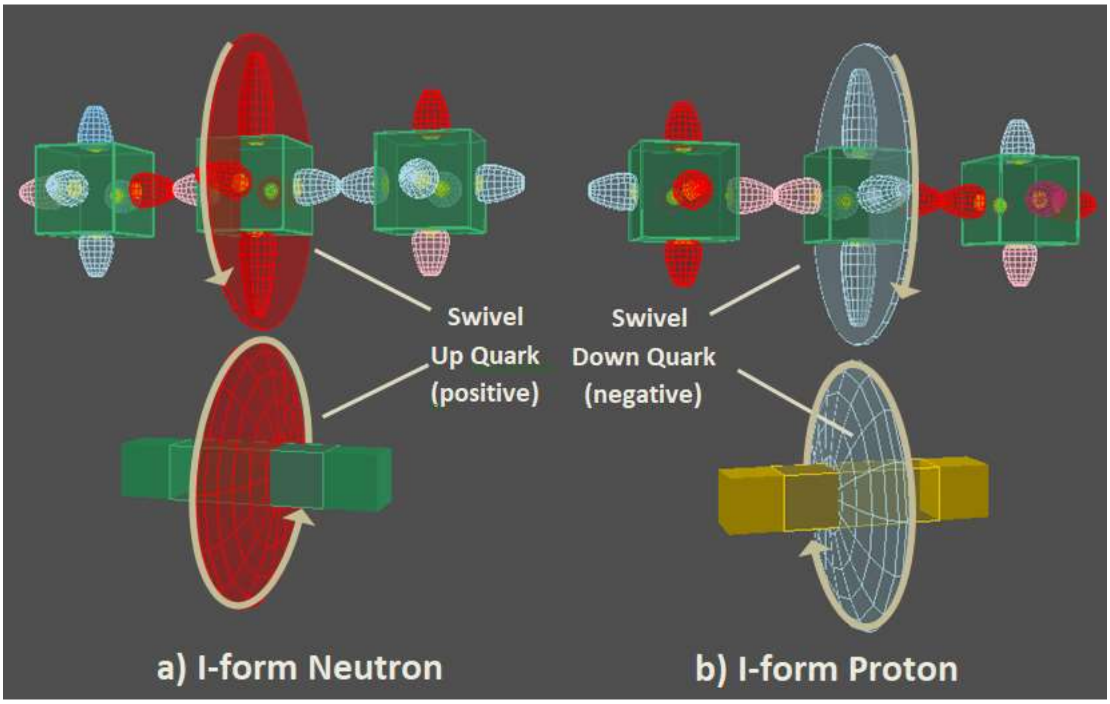

Figure 17: Quark and Bar Models of Swivel Quarks within I-form Nucleons

An atom’s connection to the outside world is via the energy-fields radiating from its outwards-facing CES. When unconstrained by participation in ionic orbital support or a b-bond, swivel-quarks have electromagnetic fields that are about four times as powerful as a single restrained CES, and they have orientation flexibility. Unconstrained swivel-quarks spin rapidly and their powerful electromagnetic fields behave as thruster-like jets that help align an atom appropriately with adjacent atoms and/or compound complexes, making them key players in the external chemical bonding processes, with all external b-bonds being between matching pairs of swivel quarks.

Both STEM and conventional Science’s ONAM approach consider that the chemical behaviour of atoms is related to quite small numbers of electrons, with conventional Science only being concerned with the outer couple of orbital shell valence electrons and ignoring the larger number of similar electrons in lower shells. For STEM, orbital electrons are not essential for atomic structure, and when electron orbits do occur (e.g. for electrical conductors), they are planar and supported by the combined electromagnetic fields of swivel quarks in the top and/or bottom nucleon layer. STEM contends that it is the geometry of the atom, the orientation of the swivel-quarks and the availability of ionic electron orbitals that dictate the chemical behaviour of atoms and their bond geometries, with the b-bonds formed between pairs of swivel-quarks providing additional electron-equivalents to an atom’s electron count.

Beta Decay and Electron Capture

Beta decay (**β decay**) is a type of ‘weak reaction’ radioactive decay in which a **beta ray** and a neutrino are emitted from an atomic nucleus. Beta decay is quite prevalent across elements of the Periodic Table (see figure 14).

Beta decay only affects nucleons that have no constrained flip CES: this includes any **L-form nucleon** attached to an outer nucleon layer of an atom by one of its invariant CES and some similarly unconstrained nucleons in a partial (or incomplete) nucleon layer.

Beta plus (β^+) decay (**orange** colour in figure 14 insert graph) can occur when an unconstrained L-form proton type-converts into a neutron, so decreasing the atom's atomic number (Z) by 1, and

Beta minus (β^-) decay (**dark aqua** colour in figure 14insert graph) can occur when an unconstrained L-form neutron type-converts into a proton, so increasing the atom's atomic number by 1.

Alpha (**α**) decay (**yellow** colour in figure 14 insert graph) occurs when an alpha particle (a helium nucleus) is emitted from an unstable high atomic number isotope, or from neutron on proton bombardment of susceptible elements. It results in the number of nucleons decreasing by 4 (2 protons and 2 neutrons). The radioactive series and alpha decay process are covered briefly in the Fission, Fusion and the Creation of the Elements chapter.

β^+ decay is triggered when a fast moving free **cetron electron** (a conventional electron) collides with an outflow flip p-CES on one of a proton's rapidly spinning up-quarks, as shown in figure 18a for a foot-in type 2 proton that is attached to a proton layer via an invariant inflow p-CES.

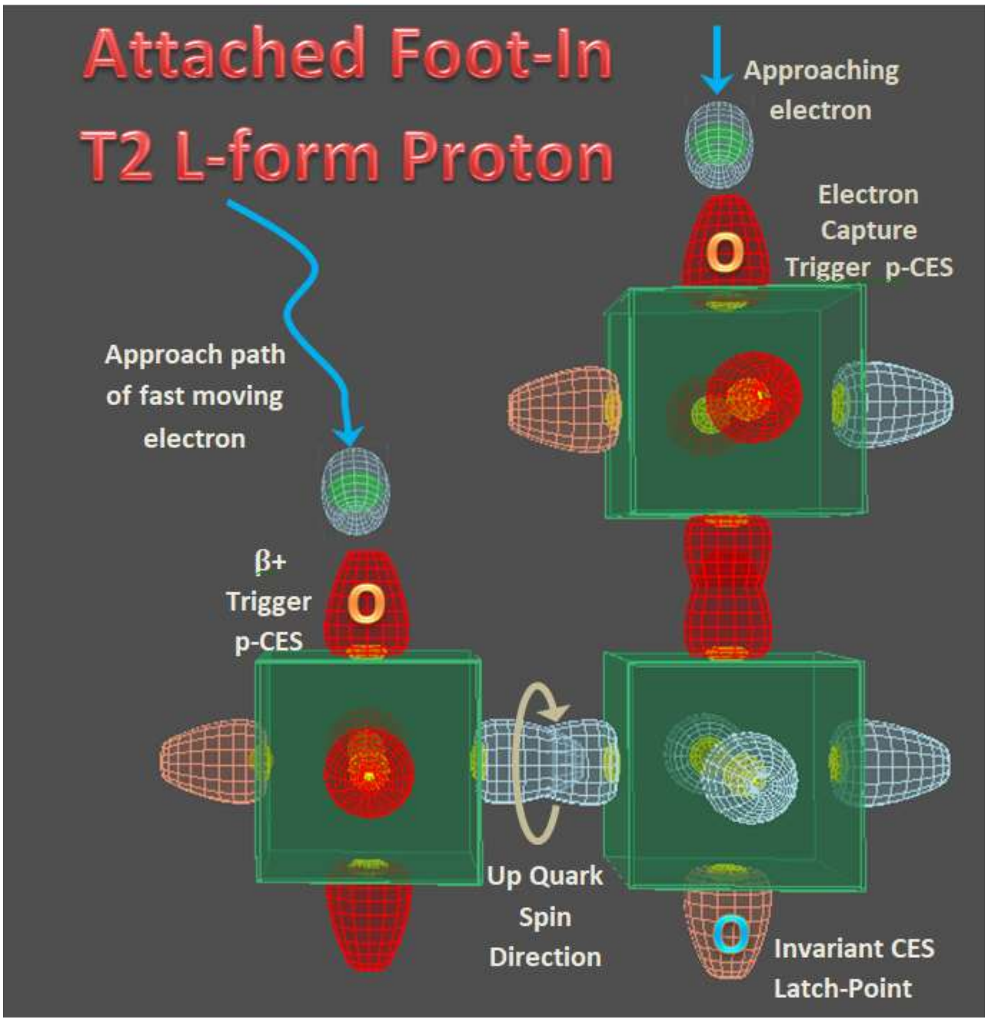

Figure 18a: Proton to Neutron Conversion via β^+ Decay

Figures 18b provides the detail of what happens at the moment a fast-moving cetron electron collides head-on with a fast spinning outflow flip p-CES. As the cetron approaches, the toroidal spin direction of the energy-fields of both particles is the same, which could possibly help to align the approaching cetron electron towards the centre of the rapidly spinning p-CES. Their poloidal energy-field flows oppose each other so as to cause an instantaneous concentration of field-energy, bitron-like, into a toroidal ring of concentrated field-energy (the small **brown ring** of figure 18b).

The compression between the cetron and p-CES outflow fields causes the rebound of the cetron and the instantaneous flipping of the energy-fields of both. The cetron electron thus becomes an aptron electron (i.e. a positron) and the p-CES becomes an e-CES. The newly created positron gains momentum from the head-on collision and explosively rebound as shown in figure 18b, with sufficient kinetic energy to allow it to escape at speed from the host medium.

The flipping of the p-CES to create an e-CES triggers the 5 flippable CES in each of the proton's 3 quarks to flip in unison, instantaneously converting the proton into a neutron in one simple, magical transformation.

The field-energy compression ring (the small brown ring in figure 18b) has the same toroidal spin as the CES and flipped cetron, ending up with the same poloidal spin as the CES and being ejected as an **electron neutrino**. With a half-life of approximately 10 minutes, its energen is far less concentrated than the energy-core torus of an electron but far more than that of a **field-energy-ring** (**FER**) within a photon of light or related EMR.

Side Note: *a FER represents the basic energy-form of EMR (see the STEM position paper 'The Nature of Light Based upon a Physical Model for EMR'). It consists of a very small amount of field-energy (possibly in the range 8 x*10^{-6} *to 25 x*10^{-6} *eV) in comparison with that of an electron neutrino (approximately 0.12 eV), or of an electron (0.511 MeV). The scale of difference between the contained energen of each of these three energen forms is in the order of* 10^{6}.

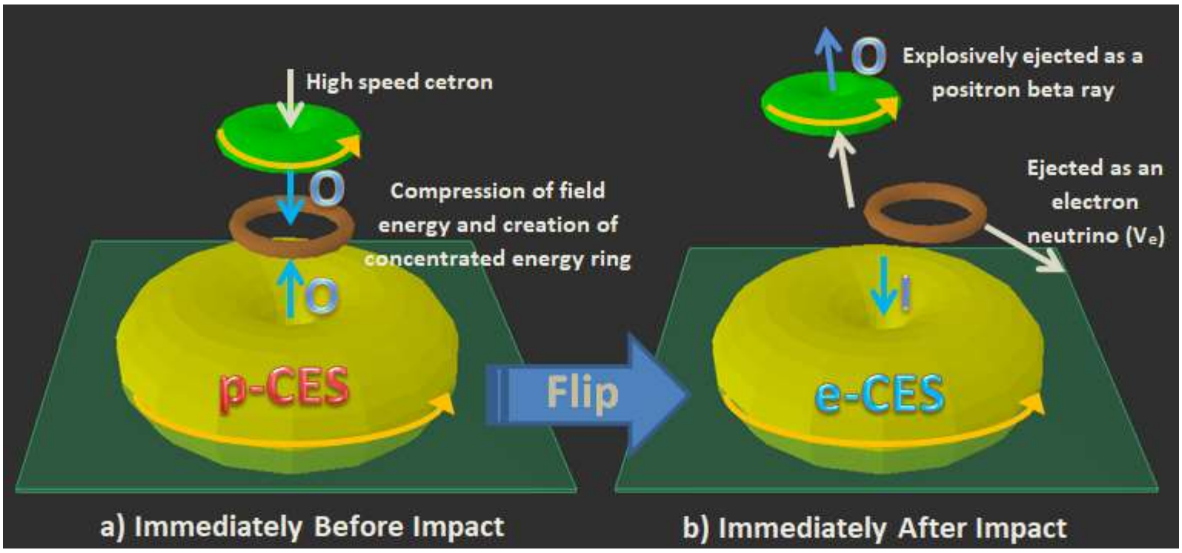

Figure 18b: Details of the β^{+} Decay Process

The bi-products of the β^{+} decay process are a neutron, an energised e^{+} beta ray (which is the cetron electron flipped into an aptron electron), and an electron neutrino (ν_e). The STEM equation for β^{+} decay is shown below (***Note*** *that STEM uses the symbol » for processes that involve* ***nucleon-type conversion****, such as β decay or electron capture, reserving the → symbol for equations related to* ***proton/neutron acquisition*** *and* ***chemical reactions***).

$$P + e^{-} \text{ » } N + e^{+} + v_{e}$$

Conventional Science considers that protons are inheritably unstable, with β^{+} decay occurring spontaneously: apart from stating that colour charge changes are involved, no explanation of the phenomenon is provided. The Conventional Science equation for β^{+} decay is:

$$P \text{ » } N + e^{+} + v_{e}$$

Electrons generated by an **electron gun** or by the **Photoelectric Effect** are exclusively cetron electrons. This is because the **motor force** associated with the circular magnetic field generated by the electron orbitals of adjacent atoms pushes them towards the outer surface of the metal host medium, whereas aptron electrons are pushed in the opposite direction to remain confined within the metal (see pages 14 to 15 of STEM's Nature of Light position paper referenced above for more detail). However, **positrons** (i.e. aptron electrons) generated by β^{+} decay are kinetically energised, so providing them with sufficient momentum to allow them to escape the host medium.

However, should a fast moving free cetron collide with a stationary outflow flippable p-CES that is not part of a fast-spinning up quark (e.g. the end of the foot-in arm in figure 18a), the collision impact is far less, but is still sufficient to trigger the conversion of the proton into a neutron; the electron into an aptron electron; and the generation of a mini bitron-like neutrino from field-energy compression. However, the lower impact of the collision compared to that of β^{+} decay means the aptron electron acquires insufficient kinetic energy to allow it to escape from of its host medium, and it remains thus entrapped within the host medium. This **low-impact** version of β+ decay is called **electron capture**.

Whereas β+ decay is caused by the spinning up quark of a foot-in L-form type 1 or type 2 proton attached to a proton layer, electron capture is restricted to the one outflow flip p-CES only within a type 2 proton as shown in figure 18: it cannot occur for a type 1 proton. Electron capture thus occurs significantly less frequently than β+ decay, and cannot take place with type 1 protons at all.

As shown below, the STEM electron capture equation is identical to that for β^{+} decay except that the newly generated aptron is bracketed to indicate that it has insufficient kinetic energy to enable it to escape from its host medium:

$$P + e^{-} \text{ » } N\,(+\,e^{+}) + v_{e}$$

Because no positron is observed to leave the host medium, conventional Science omits it from the electron capture equation as shown below, which suggests that most of the electron's energy is absorbed by the conversion process:

$$\mathbf{P + e^- \gg N + v_e}$$

A well-documented example of both β^+ decay and electron capture relates to synthetic C-11 which has a half-life 20 minutes. It mainly β^+ decays to Boron (B-11), with only 0.2% of it decaying via electron capture to B-11. The low percentage of electron capture sits well with the STEM explanation of electron capture relying upon the one and only potential trigger, a p-CES that is not well exposed within an unconstrained type-2 proton. The STEM equations for β^+ decay and electron capture, complete with experimentally determined **residual energies**, are shown below.

β+ decay → $^{11}C + e^- \gg {}^{11}B + e^+ + v_e + 0.96\text{ MeV}$

Electron Capture → $^{11}C + e^- \gg {}^{11}B\ (+ e^+) + v_e + 1.98\text{ MeV}$

For the β^+ decay case, the new aptron acquires most of the collision's impact energy (at least 1.2 MeV/c^2, but more usually in a 2 to 3 MeV/c^2 range), allowing it to escape from the host medium as a highly energised positive beta ray.

Should electron capture simply be a form of β^+ decay as STEM contends, it would be reasonable to assume that the resultant **residual energy** for each ^{11}C decay to ^{11}B interaction would be the same (i.e. 0.96 MeV/c^2), and that the any energy difference associated with the processes would relate to the amount of kinetic energy imparted to the aptron. Thus, the energy acquired by the aptron resulting from the electron capture process would be 1.02 MeV/c^2 (i.e. 1.98 - 0.96 MeV/c^2), which is well short of the minimum 1.2 MeV/c^2 kinetic energy required to escape its host as a positron. Hence neither the aptron nor its kinetic energy escapes from the host, as reflected in the higher residual energy for electron capture.

β^- decay is essentially the reverse of β^+ decay, being triggered when a fast-moving aptron electron (a conventional **positron**) collides head-on with an outflow flip e-CES within a fast-spinning down-quark of an unconstrained nuclear neutron. The impact of the collision causes the trigger e-CES to flip, turning the neutron into a proton, with the release of an **electron beta ray** and an **anti-neutrino** ($\tilde{V}_e$), as:

$$\mathbf{N + e^+ \gg P + e^- + \tilde{V}_e}$$

Some examples of all three types of decay are provided in the table right.

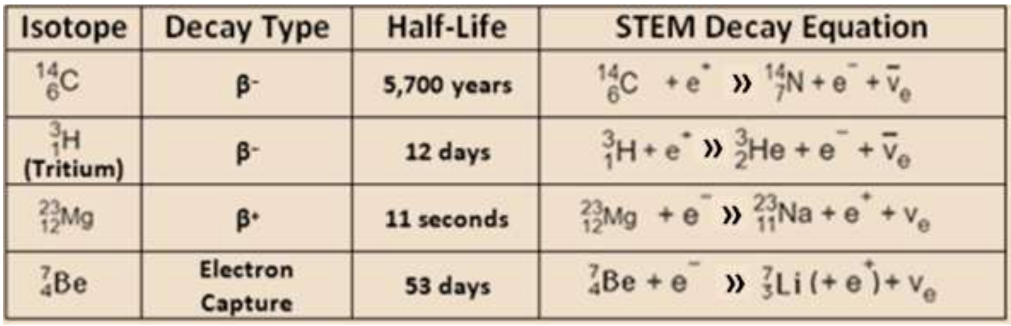

Isotope	Decay Type	Half-Life	STEM Decay Equation
$^{14}_{6}C$	β-	5,700 years	$^{14}_{6}C + e^+ \gg {}^{14}_{7}N + e^- + \bar{v}_e$
$^{3}_{1}H$ (Tritium)	β-	12 days	$^{3}_{1}H + e^+ \gg {}^{3}_{2}He + e^- + \bar{v}_e$
$^{23}_{12}Mg$	β+	11 seconds	$^{23}_{12}Mg + e^- \gg {}^{23}_{11}Na + e^+ + v_e$
$^{7}_{4}Be$	Electron Capture	53 days	$^{7}_{4}Be + e^- \gg {}^{7}_{3}Li\,(+ e^+) + v_e$

Also, free neutrons β^- decay into protons automatically within about 15 minutes of their release. STEM suggests that the reason for this is that the free neutrons are mostly I-form nucleons that have been knocked from a nucleus via alpha radiation (as opposed to free protons that are L-form nucleons retrieved from hydrogen gas). As can be seen in figure 13, only one of the end down-quarks of an I-form DUD neutron can be type-converted into an up-quark to produce an I-form DUU proton, which is subtly different.to an I-form or L-form UDU proton. STEM contends that no aptron electron is required for this type-conversion because the rapid spin of the end quarks of other I-form neutrons (and newly created I-form protons) do the trick, with the release of energy from the conversion process meaning that conversion back into an I-form neutron would be highly unlikely. Another aspect of this auto-decay process is the neutron lifetime puzzle: **bottle-contained** free neutrons are less constrained than **beam-contained** free neutrons, with Brownian motion creating more random collisions which in turn results in the overall β^- decay time being about 10 seconds less for bottle-contained neutron situation.

Interestingly, as for beta decay, **muon decay** produces electron and neutrino by-products, although a different decay process is involved. As mentioned earlier, STEM considers muons to be a **CES-pair** (with **μ^-** and **μ^+** being an e-CES and a p-CES pair respectively) that, with a half-life of 2.2 µs, are quite unstable, disintegrating into cetron electrons (for **μ^-**) or aptron electrons (for **μ^+**). The cause of this instability is attributed to the strong force attraction between the 2 CES once they are released from an up or down quark, which forces the energy cores to come close together and then to instantly rebound, resulting in a rapid vibrational effect that generates multiple neutrinos, EMR (possibly in the ɣ ray frequency range), with the final-stage CES residual being an electron. The conventional Science equations for muon decay, as shown right, are quite similar to the STEM interpretation, although the neutrino mix is conjectural.

$$\mu^- \rightarrow e^- + \bar{\nu}_e + \nu_\mu$$

$$\mu^+ \rightarrow e^+ + \nu_e + \bar{\nu}_\mu$$

Positron Production

Low level concentrations of positrons can also be sourced from **Beta+ decay**, as described in the previous chapter. The β^+ decay process provides positron sources commonly used for medical probes and scanners, and possibly represents one of the few 'natural' ways in which positrons can be produced commercially. Electron capture generates positrons but they remain trapped within the host medium because they have insufficient kinetic energy to overcome the associated **work function**.

As explained in pages 12 to 15 of the STEM position paper related to the Nature of Light, the **photoelectric effect** is a low energy process that can generate photoelectrons but not positrons. Similarly, devices such as **electron guns** and **cathode ray tubes**, which represent mid-range energy phenomena for which Compton and Raleigh scattering are dominant, do not generate positrons. To eject of aptron electrons as positrons, an energy-range above 1MeV is required: this includes phenomena such as gamma ray bombardment, pair production, and photofission.

To produce **significant quantities** of positrons, high-energy brute-force techniques such as the 200 MeV high-energy Large-Scale Collider at CERN were once required. Fortunately for Science research, positron-generation techniques continue to improve with the development of more affordable and compact high-power benchtop lasers. Petawatt (1015W) lasers have been available since 2012, and the power has continued to increase ever since. Figure 19a has been sourced from the 2013 article by Sarri et. al., which describes the laser setup used to generate a positron stream and provides a detailed discussion of the results.

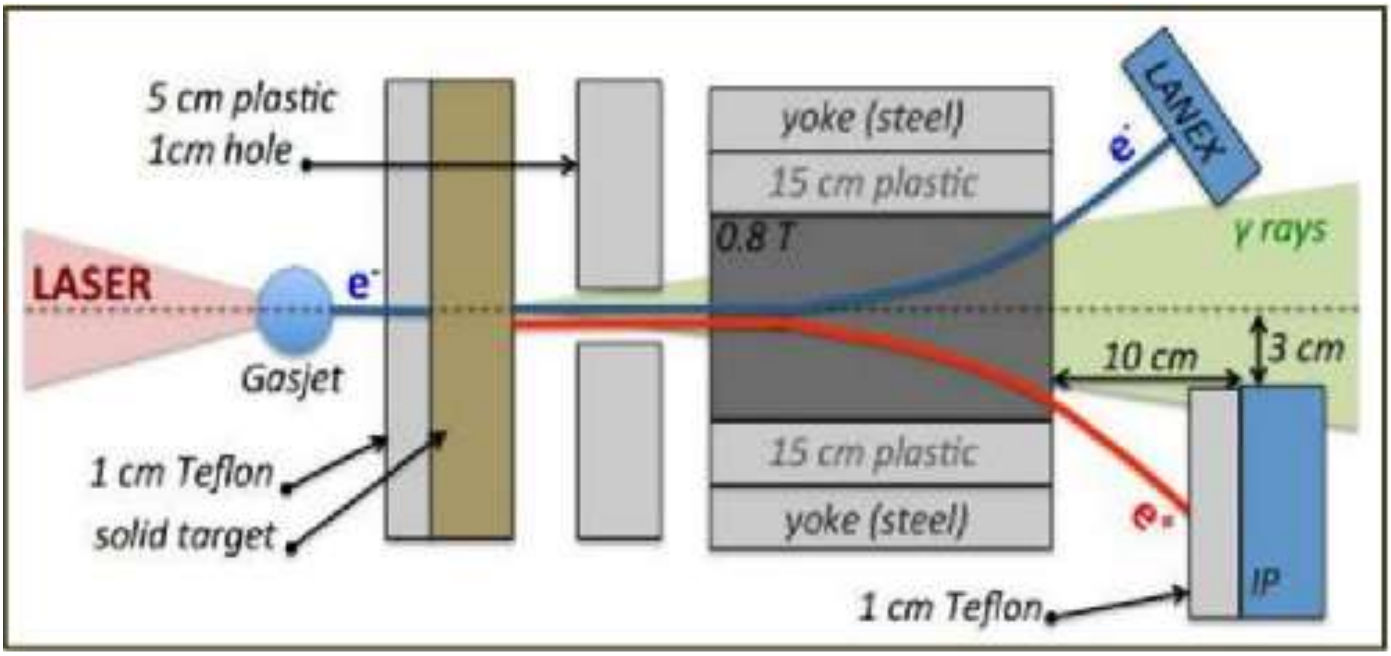

Figure 19a: Benchtop Laser Setup for Electron and Positron Generation

The laser approach to positron generation involves bursts of light energy to bombard a solid target to produce an electron stream of energy in the 80-200 MeV range. The conventional Science view, as described in the Sarri et.al article, is that **gamma photons** are generated by Bremsstrahlung, which is caused by the slowing down of the incident electrons. Bremsstrahlung is more effective for target atoms with a high Z number (atomic number) and packing density. The resulting gamma photons are considered to spontaneously create or transform into an electron and positron pair in a process called Pair Production. These newly-created energised electrons and positrons escape from the host material and separated to generate separate electron and positron streams.

Figure 19b shows a typical cross-sectional plot of Copper for photons in the 10 keV to 100 GeV range. It reflects the complex nature of such a high-energy environment that involves a mix of multiple interactions between atoms (and their atomic bonding), electrons and photons for varying photon energy levels. It variously involves energy transfer via elastic Thompson scattering (the photoelectric effect) and inelastic Raleigh and Compton scattering of electrons by photons, as well as nuclear and electron based pair production. It represents a very complex energy transfer environment with multiple processes occurring simultaneously.

The energy band of the incident electron beam (the input energy) in the Sarri setup has been highlighted by the vertical maroon band in figure 19b: it can be expected that emitted electrons would display a range of energy levels below the lower end of this range (i.e. less than 80 MeV), and thus, although the target material was not Copper, quasi-deutron disintegration and Pion production would most likely not be involved.

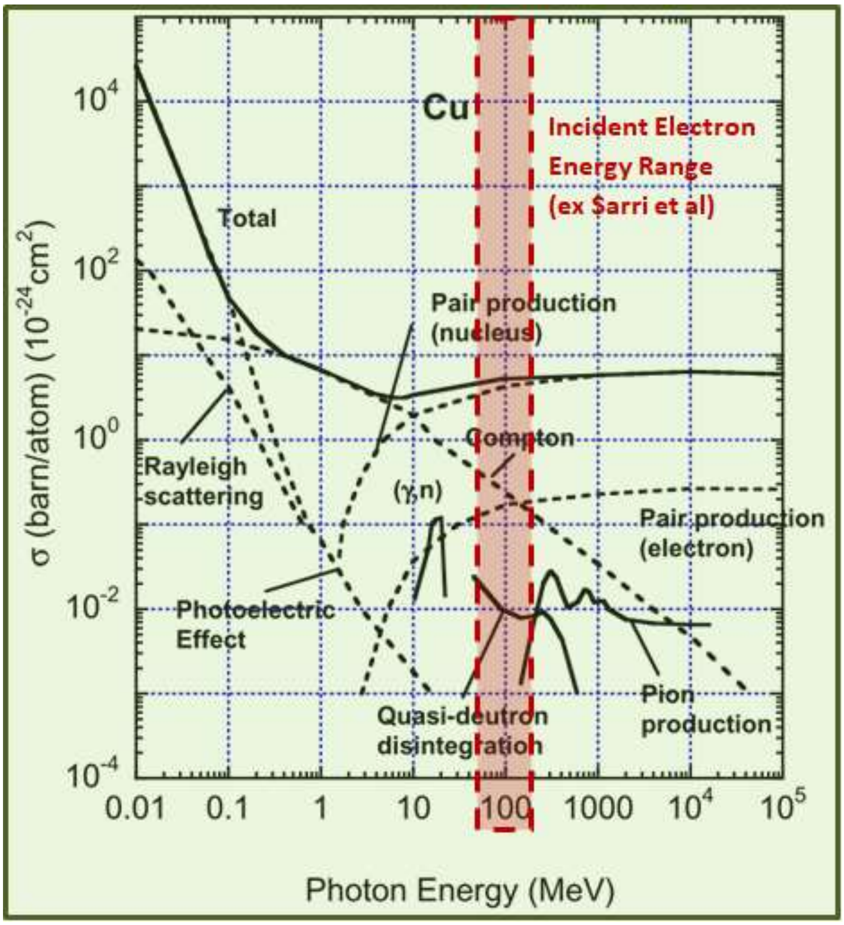

Figure 19b: Cross-Sectional Plot of Copper for 10keV to 100 GeV Photons

Breit–Wheeler pair production is the process by which a positron–electron pair is created near an atomic nucleus from the collision of two photons in the gamma frequency range. The gamma rays need an energy level greater than 1.02 MeV to produce two particles each having a minimum net energy of 0.511 MeV (the rest mass of an electron). The conventional Science equation for pair production is:

$\gamma + \gamma \rightarrow e^{-} + e^{+}$ (spontaneous simultaneous electron/positron creation)

The Breit–Wheeler process has never been observed in practice because of the difficulty in preparing colliding gamma ray beams and the very weak probability of such collisions. It is now widely interpreted as the possible splitting of one photon of energy greater than 1.022 MeV. Certainly, the actual pair production mechanism is speculative, and far from being well established.

STEM considers that pair production may have several causes. One such cause is that the pair production process is a high-energy version of the photoelectric effect, with 0.511 MeV gamma ray energy needed to knock an aptron electron (i.e. a positron) from its ionic orbital with sufficient kinetic energy to overcome its high work function and exit its host medium. Although cetron electrons do not need such high-energy rays, they are also knocked out of their ionic orbitals by the gamma rays in approximate equal numbers.

A second possible cause is that the gamma rays force the ejection of a bitron from a b-bond, which then has an equal probability of becoming a cetron or aptron electron: the high energy rays are simply needed to provide the newly created aptron electrons with sufficient kinetic energy to allow them to exit its host medium.

A third possible cause involves high impact electron-to-electron or electron-to-nucleus collisions, which is analogous to CES type-conversion discussed earlier. In this scenario, the gamma rays energise free electrons, resulting in high-speed head-on collision of a pair of free electrons or of a free electron and an ionic electron. The high-speed impact would result in the instantaneous compression of the electron's outflow vortices which would cause a **reversal of the poloidal flow direction** of the field energy of one or both electrons, which would instantly reverse their chirality. The result instantaneous type-conversion of one or both electrons would into a positron. In case of Sari's desktop positron generation setup, Bremsstrahlung-generated gamma rays would not even be required because the laser-energised electrons would have sufficient energy to cause electron type-conversion.

With the STEM approach, gamma rays don't magically convert themselves into an electron-positron pair. Instead, there are thus several feasible explanations for positron generation based upon the high energy particle interactions.

Atomic Structure: Hydrogen to Boron

Hydrogen, the first element in the Periodic Table, has three naturally occurring isotopes, denoted ^{1}H, ^{2}H (or D) and ^{3}H (or T). The first two, **Protium** and **Deuterium**, are stable, while **Tritium** beta decays. The conventional Science (ONAM) representation for the trio is shown in figure 20 which, in their diatomic molecular forms, are considered to covalently share each other's electron.

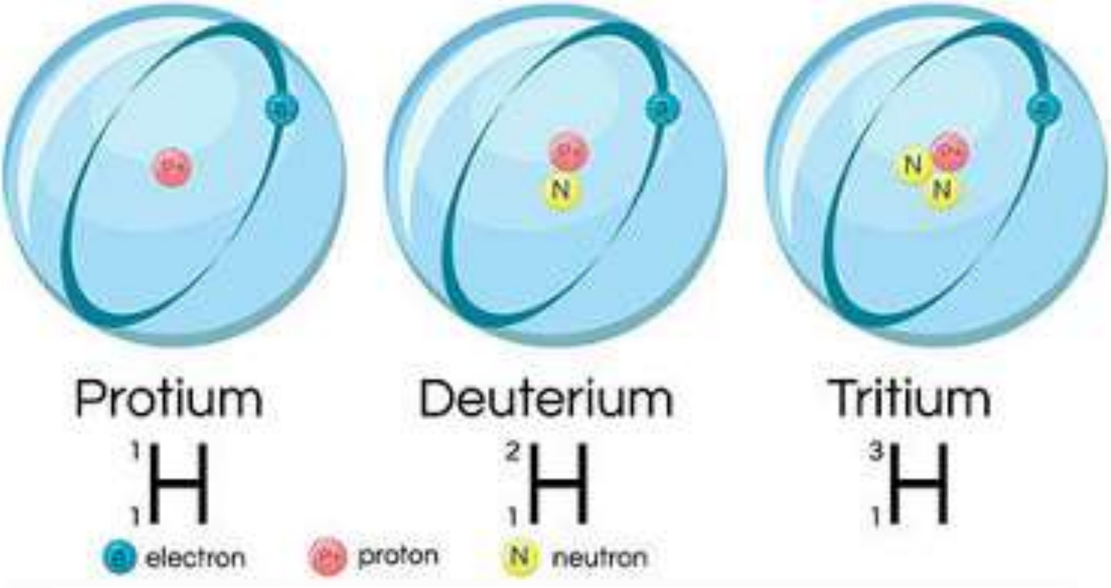

Figure 20: Conventional Science Models of Protium, Deuterium and Tritium

Protium is the most prevalent hydrogen isotope, and is considered to consist of a single proton. Rather than presenting in a monoatomic form, protium is found in a diatomic molecular form (H_2) or variously bonded to other elements.

The STEM H_2 (or $^{1}H_2$) molecule consists of two protons held together by a b-bond. However, as shown in figure 21, there are two forms of the H_2 molecule: **ortho-hydrogen** and **para-hydrogen**, distinguished by having different orientation (or spin state) of the magnetic field of their protium atoms. For ortho-hydrogen the spin state of each protium atom is in the same direction as shown in figure 21a, whereas for para-hydrogen the spin states are in opposite direction as in figure 21b.

Both ortho-hydrogen and para-hydrogen molecules have a measured centre-to-centre H-H bond length of 74.1 pm, which corresponds to a b-bond length of 47.1 pm as indicated in the true-scale quark diagram of figure 21. The H-H bond represents one of the shortest and strongest single-bond between atoms, having a strength of 435 kJ per mole.

Ortho-hydrogen and para-hydrogen molecules each consist of a type 1 and type 2 proton pair, with ortho-hydrogen having two possible bonding patterns (figure 21a) and para hydrogen having only the one pattern. Assuming that each bonding pattern between a type 1 and type 2 proton pair to have equal probability of being formed, an ortho to para ratio of 4:2, or a mix containing 66.7% ortho-hydrogen molecules, could be expected. However, it would seem that the pre-disposition for a free type 1 and type 2 proton pair to assume a particular pattern is **temperature dependent**.

At **STP** (i.e. standard or 'normal' room temperature), hydrogen gas is found to contain 75% ortho-hydrogen and 25% para-hydrogen, which remains steady for greater temperatures. When cooled to **77^{O}K**, the mix consists of 50% of each molecular type, with a mix containing 66.7% ortho-hydrogen, corresponding to the scenario of the STEM bonding patterns having equal probability of occurring, falling somewhere in between. As **0^{O}K** is approached there is no mix; just 100% para-hydrogen. And the process is reversible by simply warming up the sample.

A possible explanation for the temperature-dependent change of para and ortho hydrogen mix is that the para-hydrogen molecules represent the lower energy option. In the higher temperature gaseous and liquid states, molecular impact and the damaging effect of the spinning arms of the hydrogen molecules around their long axis cause the protium atoms (type 1 and type 2 protons) to separate. Within the mix, newly released protons would combine to form ortho or para hydrogen molecules dependent upon the temperature and pressure of the mix. As the temperature reduces and the mix starts to solidify, the para-hydrogen re-combinations tend to become more prominent, until as **0^{O}K** is approached there is no ortho-hydrogen.

The other aspect of the hydrogen molecule is that, consisting of only two protons, it only can support two ionic electrons and the covalent bonding effect of those orbits is less in the ortho-hydrogen configuration than the para-hydrogen. This, combined with the better symmetry and compactness of the para-hydrogen molecule, may contribute to it being the preferred molecular form in low temperature, low energy environments.

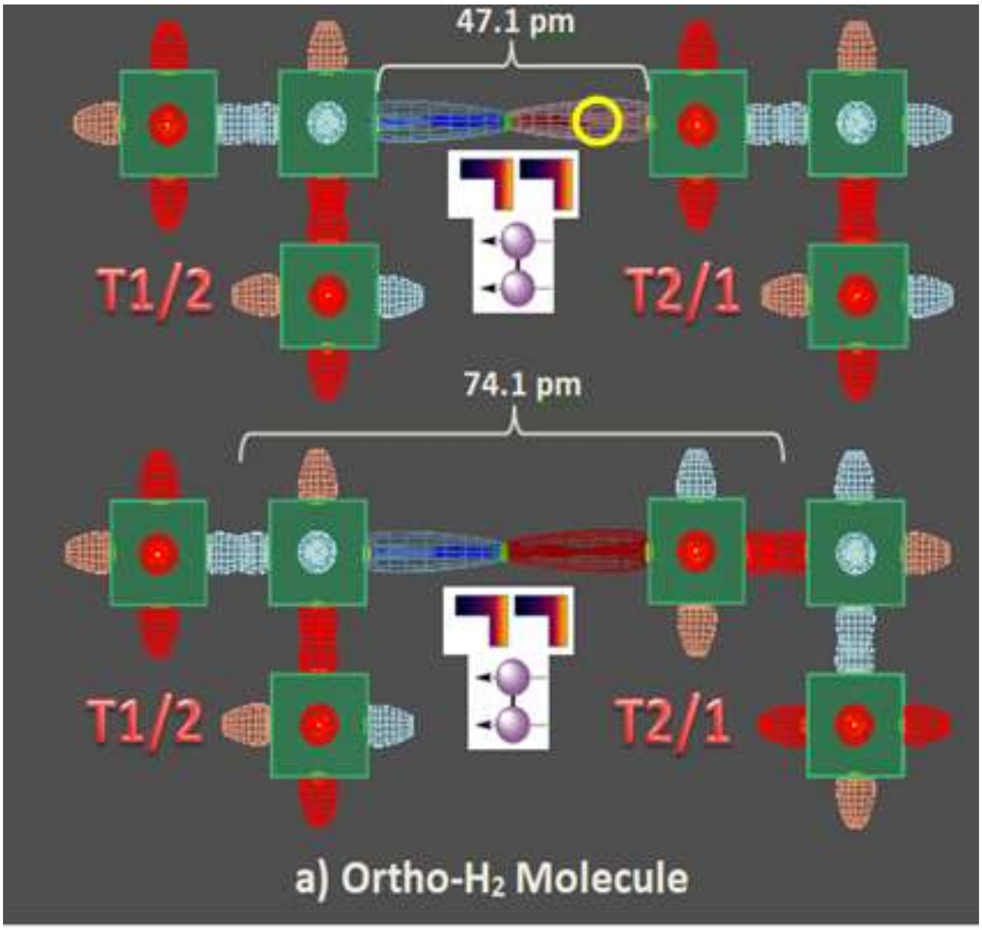

a) Ortho-H_2 Molecule

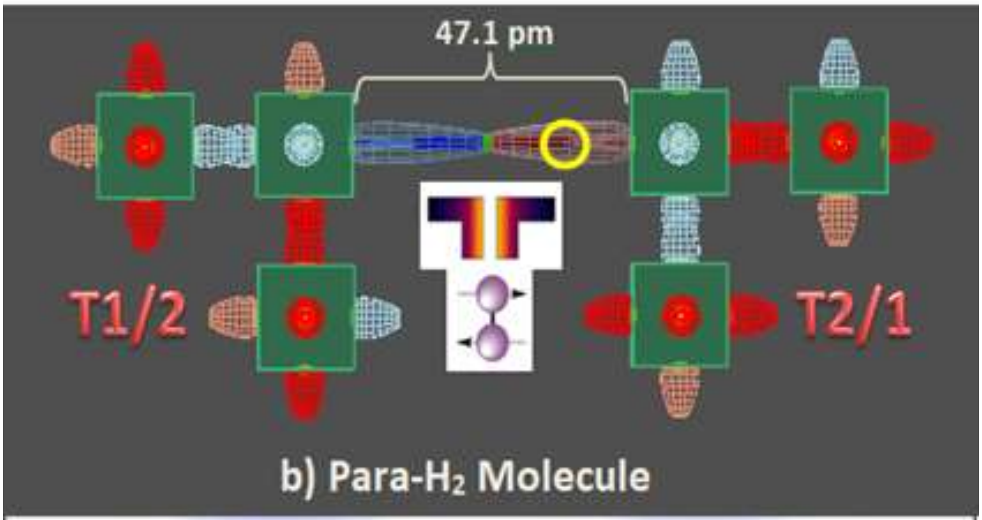

b) Para-H_2 Molecule

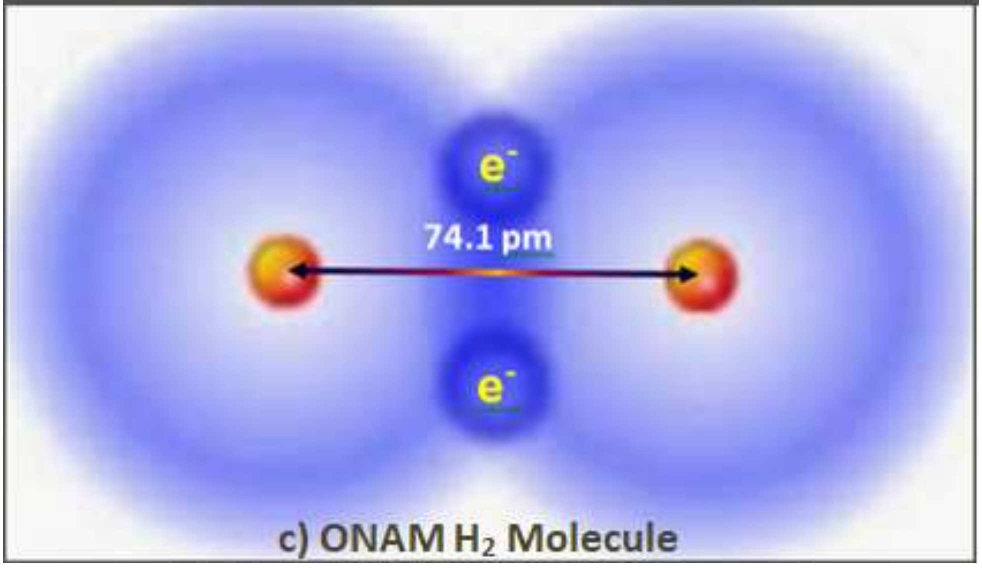

c) ONAM H_2 Molecule

Figure 21: Ortho-Hydrogen and Para-Hydrogen Molecular Structures

Both STEM and the ONAM approaches consider that the protons of both para-hydrogen and ortho-hydrogen molecules are covalently bonded, but STEM considers that a bitron bond between the pair of protons is the main means of bonding. Figure 21c shows the typical ONAM representation, but ONAM provides no feasible explanation for the 2 molecular forms of the hydrogen molecule, their respective magnetic field orientations nor the para-ortho ratio-change phenomenon.

Of the 3 possible structures of the hydrogen atom, only 1 of the 2 ortho-hydrogen molecule patterns and the para-hydrogen pattern contain an invariant p-CES (highlighted by yellow circles) within their b-bond. The invariant p-CES within these b-bonds means that one of the protons (the rightmost ones in figure 21) can be type converted into a neutron to create a **deuterium molecule** (**$^2H_1$**).

A deuterium molecule has the same notational formula as a **deuterium atom** (figure 22), but the molecular form is held together by a b-bond whereas the deuterium atom is held together by a strong force inter-quark bond. It is quite likely that the creation of deuterium molecules is **mistakenly interpreted** as the creation of deuterium atoms by **low energy nuclear reaction** (LENR and Cold Fusion) research groups.

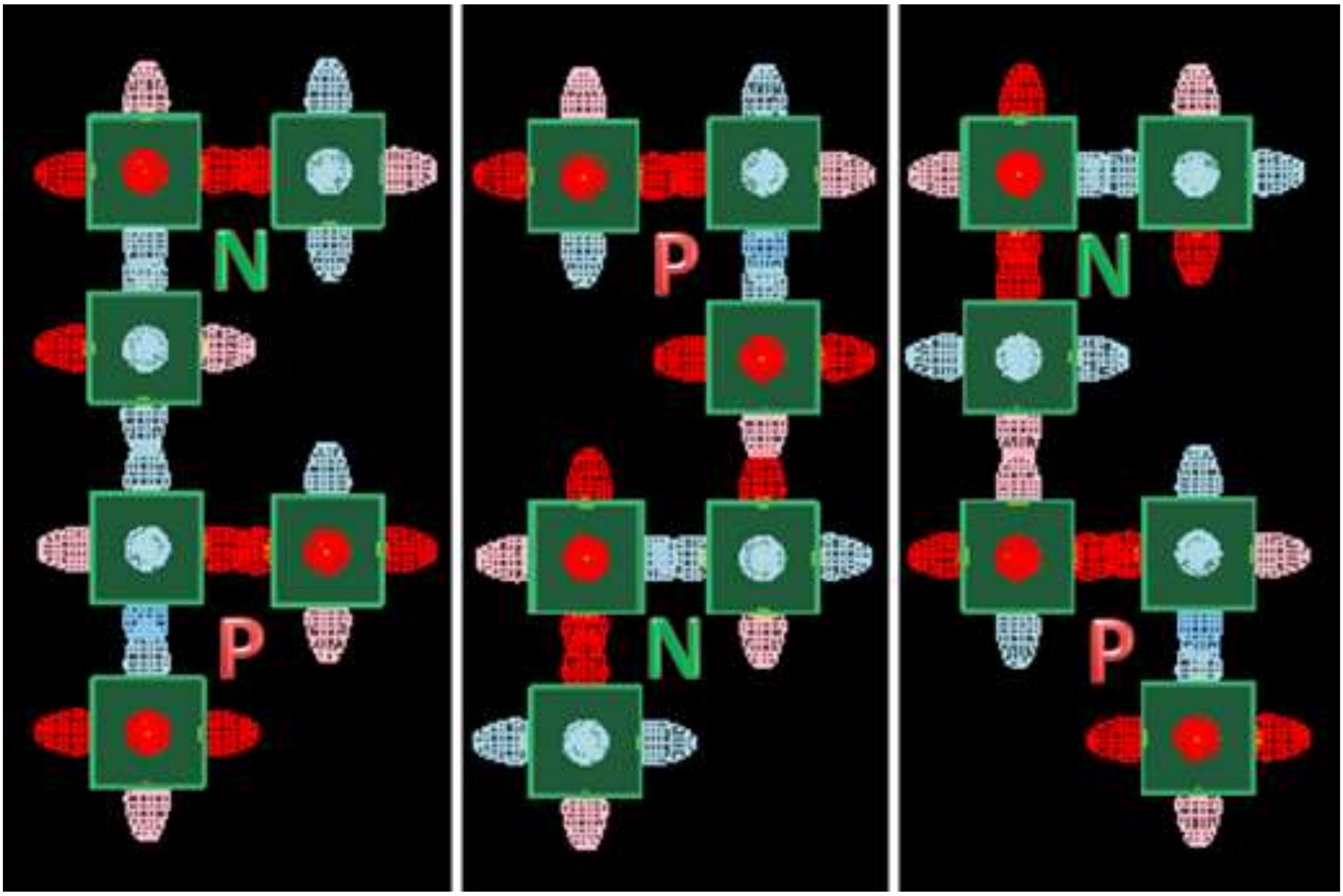

Figure 22: $^2H_1$ Deuterium Atom

A **deuterium atom** (**$^2H_1$**), often represented by the letter **D,** is variously termed **deuteron** or **deutron**. Deuteron consists of an **inter-quark bonded** proton and neutron, such as represented in figure 22, with atom's nucleus having the form of an open 2-nucleon quark chain. Whereas the rarer b-bonded deuterium molecule can be produced in less energised environments, deuterium atoms result from **nuclear fission**.

Deuterium atoms readily substitute with hydrogen atoms within **light water** (**H_2O**) molecules to produce **semi-heavy water** (**HDO**) molecules. HDO occurs naturally on Earth in regular water at a proportion of 1 part in 3200, and may be separated from regular water by distillation, electrolysis or by various chemical exchange processes. When both hydrogen atoms of a water molecule have been replaced with deuterium, **heavy water** (**D_2O**) molecules are created. D_2O is present naturally in water at a proportion of less than 1 part in 5,000.

Tritium (**$^3H_1$** or **T**), is a radioactive isotope of hydrogen consisting of one proton and two neutrons that are inter-quark bonded as shown in figure 23. Neither of the deuteron or tritium nucleon chains is of sufficient length to join end-to-end so as to generate a polygon.

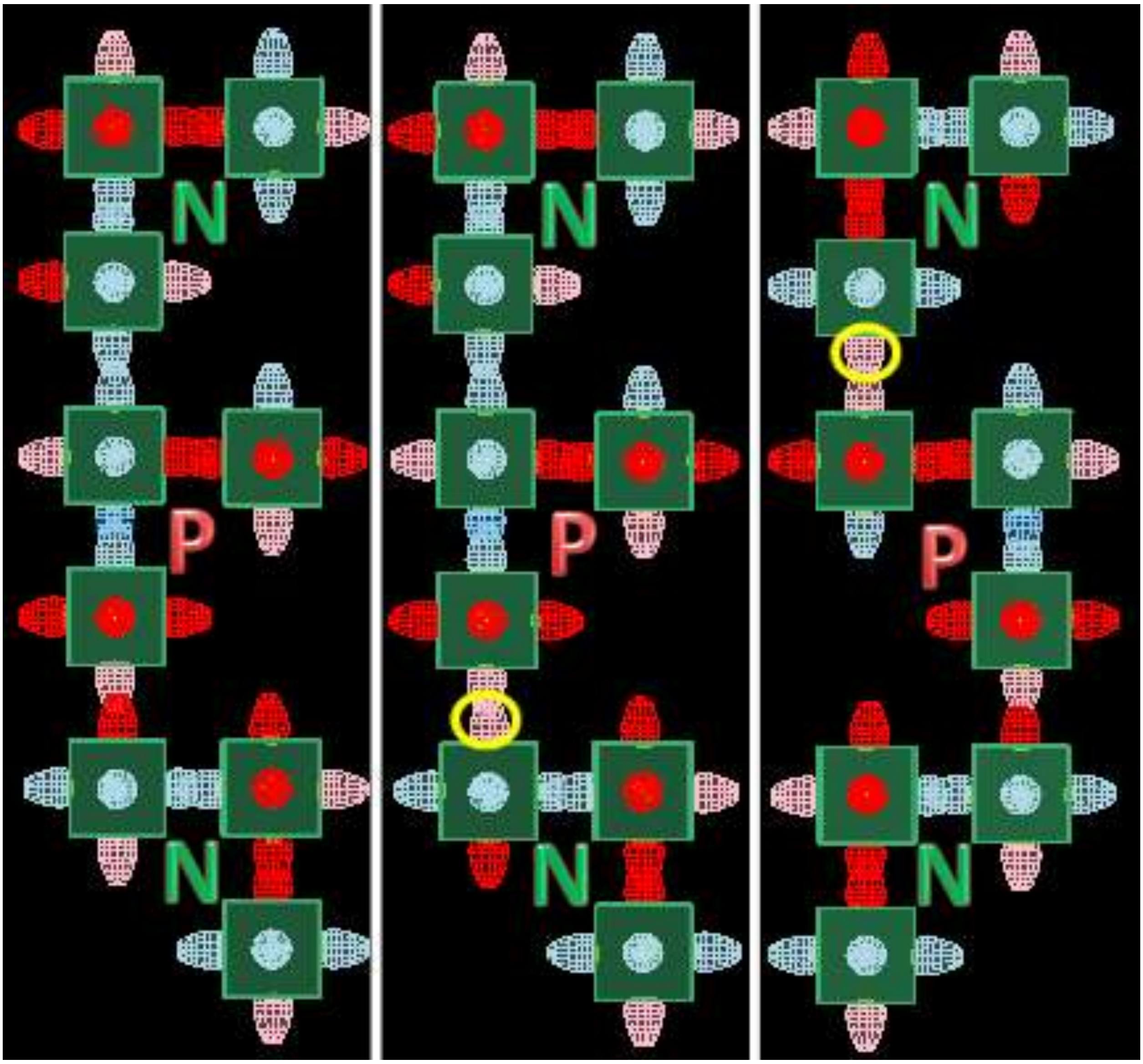

Figure 23: $^3H_1$ Tritium Atom

As a **radioactive isotope** of hydrogen, tritium can β^- decay into Helium (**^{3}He)**, as shown below. It has a half-life of about 12 years.

$$^3H_1 + e^+ \gg {}^3He + e^- + \tilde{\nu}_e$$

However, not all tritium atoms can beta decay, as apparent in the leftmost example of figure 23: the p-CES latch point is a flippable CES that needs to be unconstrained to allow the neutron to be type converted. The latch points of the other 2 examples involve invariant CES (highlighted by yellow circles), which allows these neutrons to be type-converted into protons.

In nuclear reactors, tritium is most often produced by **neutron activation** of **lithium**, which causes a lithium atom to split into a helium atom and a deuterium atom, with the latter quickly acquiring a neutron to create a tritium atom, as shown below (which corresponds to equation 1 in the section on lithium):

$$^6Li\ (+\ n) \rightarrow {}^4He + {}^2H_1;\ {}^2H_1 + n \rightarrow {}^3H_1$$

Similarly, high-energy neutron irradiation of **boron** (**^{10}B**) will also occasionally produce tritium (although, a more common end-product is ^{7}Li and ^{4}He as shown in equation 4 of the section on boron), as shown below:

$$^{10}B\ (+\ n) \rightarrow 2\ {}^4He + {}^2H_1;\ {}^2H_1 + n \rightarrow {}^3H_1$$

Although the hydrogen atom has a simple structure (just 1 proton), its molecular structure, as discussed in this section, is quite complex. Adding to the complexity, hydrogen has 2 other natural isotopes and 4 synthetic isotopes. And as the atomic number of elements in the Periodic Table increase, so does the structural complexity and variation possible.

Note *that, from figure 24 onwards, the* **CES colours** *used in* **quark diagrams** *will be different to those used so far in this paper. They reflect an earlier colour scheme that will be updated when time resources allow. The colour differences in no way invalidate the explanations provided or the structures presented.*

Helium

The **second element** in the Periodic Table is helium (**^{4}He or He-4**), which is the first in the **Noble Gas group** in the Periodic Table. He-4 consists of two L-form proton and neutron pairs inter-locked to form a proton and neutron layer consisting of two I-form members each so as to create a double-U profile as shown in figure 24a. It is the first fully closed nucleon chain and first element to display a sandwich-like neutron and proton layering. As a monatomic gas, He-4 is compact in size and the inter-quark bonds provide it with a high binding energy (see the graph of figure 24d) compared with other low atomic number elements.

When kinetically energised as **alpha radiation**, helium-4 nuclei can be quite damaging to other matter over short distances. Also, in spite of being a strong structure with square rectangular prism form, the articulation axes within its nucleon chain mean that can easily be distorted (as shown in figure 24c) so as to present with a hexagonal close-packed (HCP) crystal form.

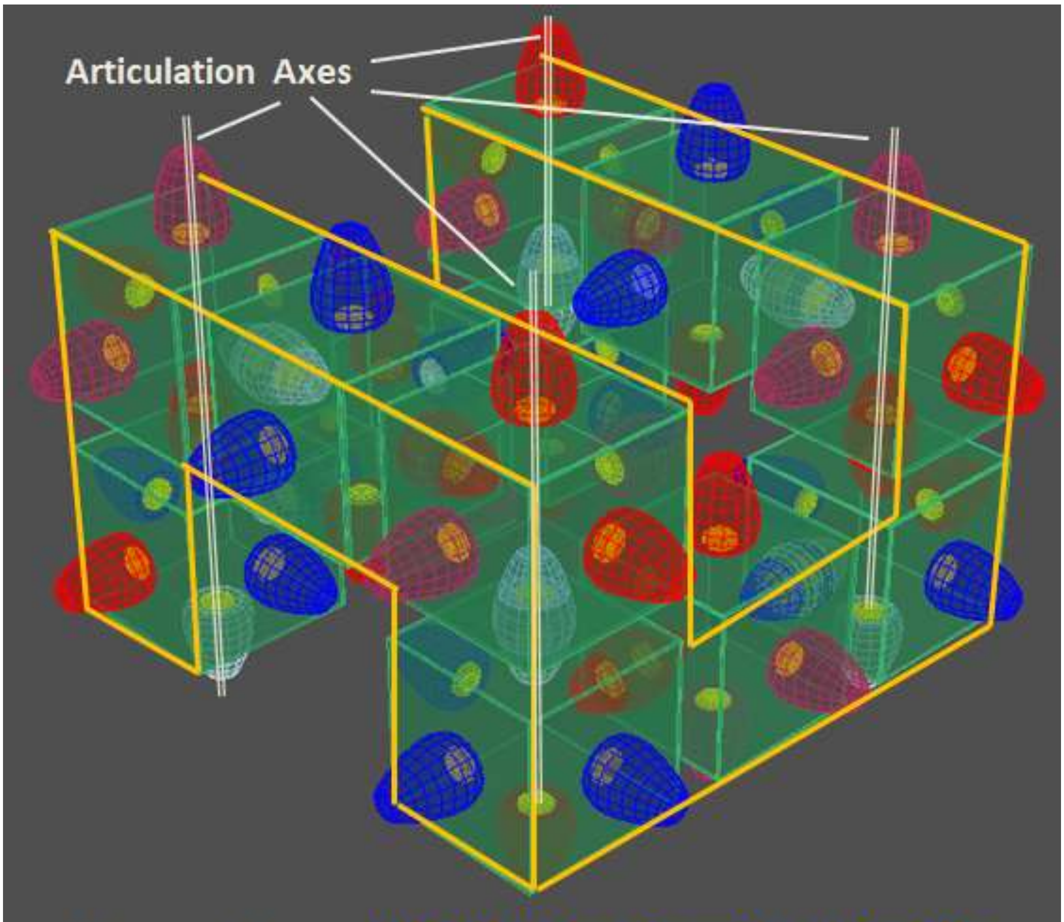

a) Quark Model Highlighting Double-U Profile

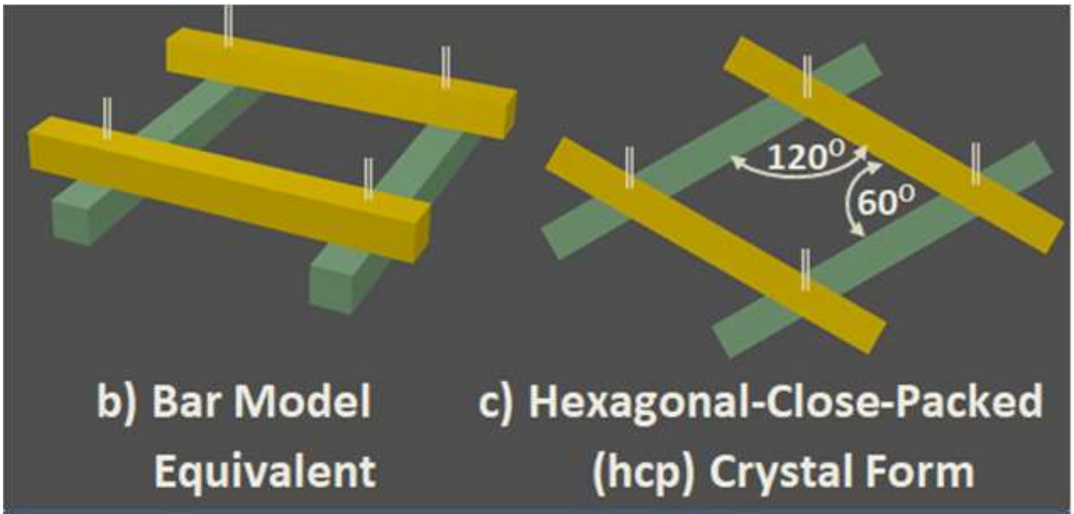

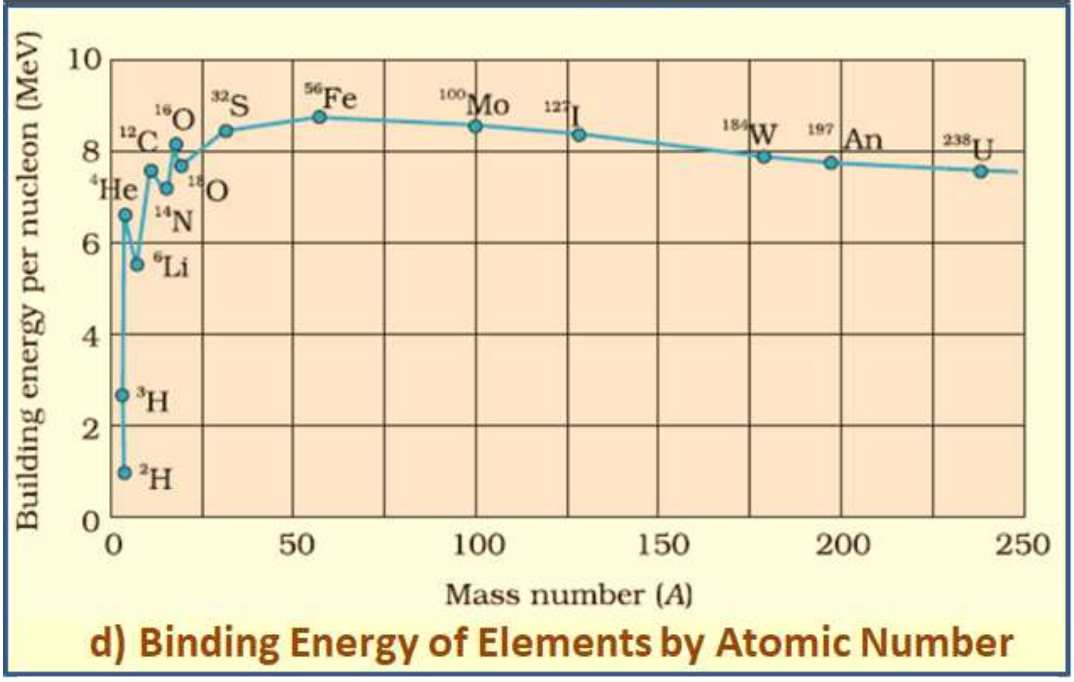

Figure 24: The Helium-4 Atom and Binding Energy by Atomic Number Graph

Assuming that, in the chaotic environment in which atom building and re-structuring occurs, should a He-4 atom have one of its corners, which consists of an L-form nucleon, forcedly removed, then a He-3 or tritium atom would result. For neutron removal, 3 scenarios are possible. For the first scenario, the removed neutron is one of the chain-building L-form neutrons, such as highlighted in yellow in figure 25a to produce the He-3 atom of figure 25b. Alternatively, such a partial layer could result from the nucleon chain building process itself. Regardless of origin, the inter-quark links of the 2 protons are flip-CES, so that none of the 3 nucleons can be type-converted to create tritium.

For the second scenario, the removed neutron is a pseudo L-form neutron (i.e. is not one of the chain-building neutrons), such as that highlighted in red in figure 25a, to produce the He-3 atom of figure 25d. Because the inter-quark bonds between the L-form 2 remaining protons and the neutron are invariant CES, they can be type-converted to create a $^3H_1$ tritium atom.

For the third scenario, the removed neutron of an I-form neutron, such as highlighted in blue in figure 25a, produces a He-3 atom such as that of figure 25c. As the inter-quark bonds between the I-form 2 protons and the neutron are invariant CES, they can also be type-converted to create a tritium atom.

Should it be a proton that is forcedly removed from a He-4 atom, the 3 scenarios paralleling neutron removal apply, but results in the creation of a tritium atom rather than a helium-3 atom. And similarly to neutron removal, 2 of the 3 scenarios allow the tritium atom to be converted back into He-3, which corresponds to the tritium → He-3 β-decay conversion described in the previous chapter. In summary, should a chain-building L-form proton or neutron be removed from a helium-4 atom, then subsequent tritium → helium-3 conversion (or vice versa) cannot take place.

Hydrogen and helium are the earliest of elements derived directly from pre-existing nucleons via nucleosynthesis initiated by the **Big Bang**, which resulted in the universe containing approximately 75% hydrogen and 24% helium by mass, and traces of other elements such as lithium and the hydrogen isotope deuterium. Star formation and destruction produced the bulk of heavier elements, all of which have been derived, albeit indirectly, from hydrogen and helium.

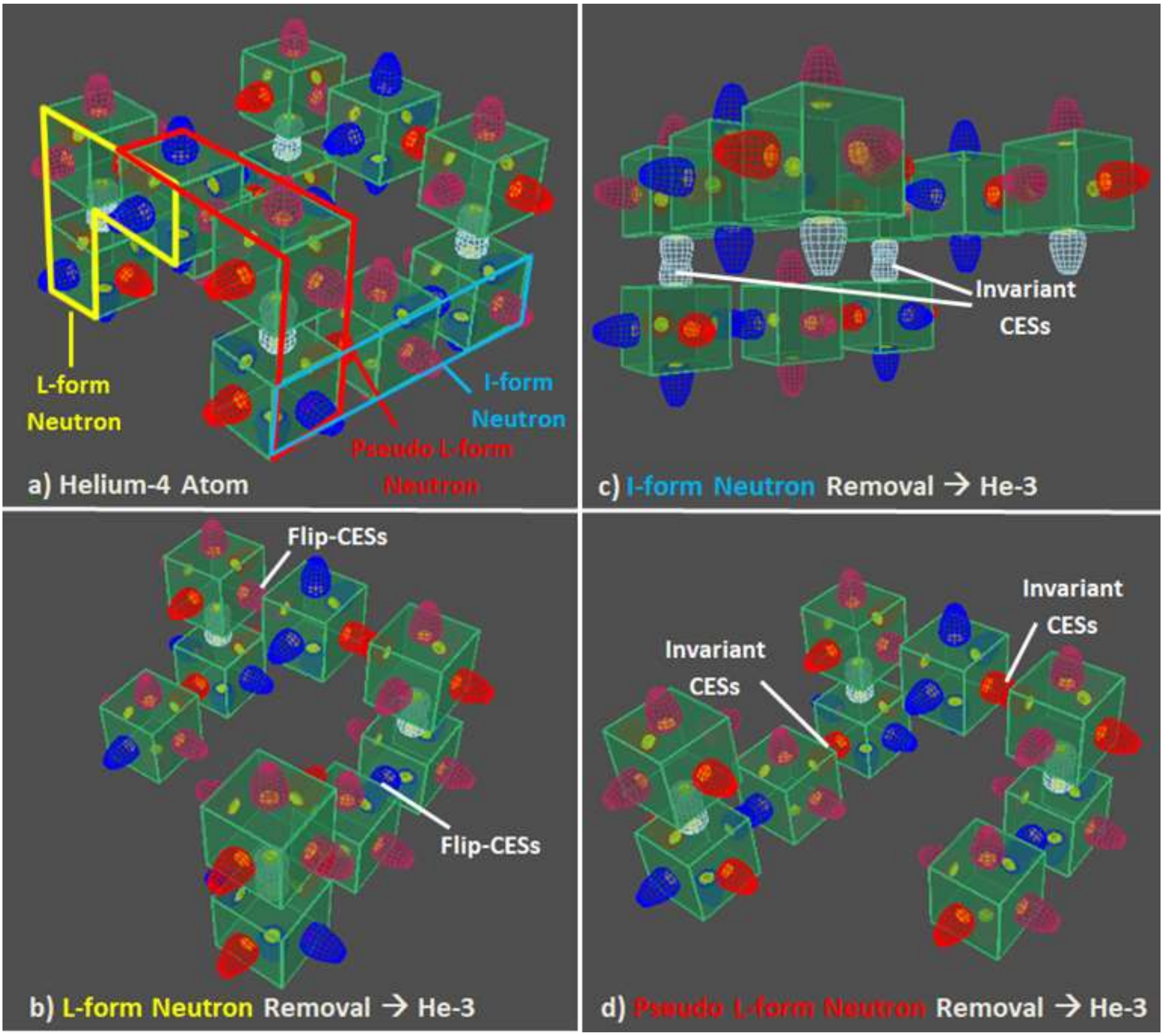

Figure 25: He-4 to He-3 Conversion

***Note** that the 3 pm inter-quark bond length makes it difficult to see the bond detail (such as e-CES versus p-CES, or invariant versus flip CES) within to-scale quark models. Thus, purely for diagrammatic purposes, from figure 24 onwards inter-quark bond lengths within quark model, are shown as being about 12 pm long, which is close the width of a quark. However, for all estimates of atom nucleus size, bond-length and density, an inter-quark bond width of 3 pm has been used.*

Lithium

The **third element** in the Periodic Table is Lithium, which has two isotopes: **Li-6** (or ^{6}**Li**) with an abundance of 7.6% and **Li-7** (or ^{7}**Li**) with an abundance of 92.4%. Lithium is the lightest solid element and the lightest metal. As an alkali metal, lithium is highly reactive and flammable, and when cut, it exhibits a metallic lustre with but moist air quickly corroding it to a dull silvery grey and then more slowly into a black tarnish.

It is quite apparent in the figure 26 model of the Lithium isotopes have a relatively fragile partial chain superstructure and the articulation axes mean that it is quite pliable: hence, in metallic form, it is soft and malleable. Also, lithium has unconstrained swivel quarks (circled yellow in figure 26a and 26c), that can meander within a 270^{O} arc while swivelling (i.e. spinning fast), which possibly contributes to the highly volatile chemical reactions of lithium metal.

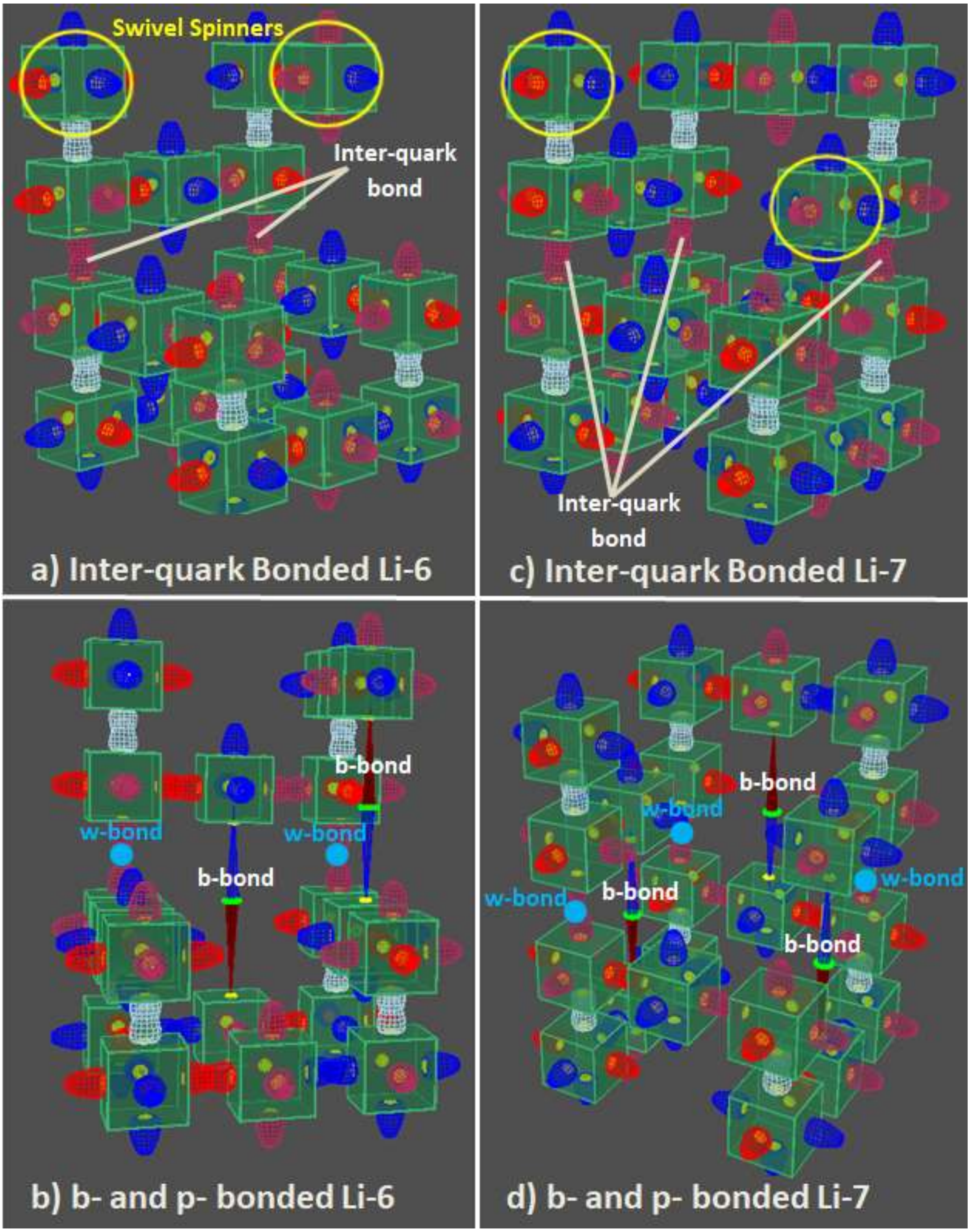

Figure 26: Quark models of Lithium Isotopes

Should Li-6 be bombarded by neutrons, it can split into a He-4 and a deuterium atom, which in turn can combine with a neutron to create a tritium atom, providing a useful source of **tritium**:

$$^{6}\mathrm{Li}\ (+\ \mathrm{n}) \rightarrow {}^{4}\mathrm{He} + {}^{2}\mathrm{H}; \quad {}^{2}\mathrm{H} + \mathrm{n} \rightarrow {}^{3}\mathrm{H} \qquad ①$$

Similarly, should Li-6 be bombarded with protons, it can acquire one to become a beryllium-7 atom. Should 1 of the Be-7 protons then be type-converted, it becomes lithium-7, which in turn can acquire another proton to become Be-8, which readily splits into 2 He-4 atoms. This rather complex sequence provides a useful **alpha radiation** source, with the schematic equation below highlighting problems related to defining elements simply by their proton count.

$$^{6}\mathrm{Li} + \mathrm{p} \rightarrow {}^{7}\mathrm{Be} \gg {}^{7}\mathrm{Li} + \mathrm{p} \rightarrow {}^{8}\mathrm{Be} \rightarrow 2\ {}^{4}\mathrm{He} \qquad ②$$

Two versions of Li-6 and Li-7 are shown in the quark models figure 26. Each isotope has 2 complete nucleon layers (1 chain) and a partial layer that is strongly (inter-quark) bonded to a full layer, or moderate-strength bonded via a combination of b- and w-bonds.

Should the partial layers of Li-6 or Li-7 be inter-quark connected as in figure 26a and 26c, the bond strength between and within all their L-form and I-form nucleons would be the same and, with such bonding uniformity, it would be unlikely that the atoms would consistently split at the full-layer interface so as to release He-4 atoms when bombarded with nucleons. Instead, various patterns of nucleon groups could be expected to split off such as those shown in figure 25 related to the splitting of a He-4 atom.

To release helium atoms when bombarded by nucleons, it would seem far more likely that adjacent chains (part or full nucleon chains) would be joined by lower strength bonds, such as the combination of **b-bonds** and **w-bonds** as shown in figures 26b and 26d, rather than by strong inter-quark bonds of figures 26a and 26c. As is discussed in the 'Bond Types and Strengths' chapter, w-bonds are **weak-bonds** that reflect Van der Waals attractive force associated with a pair of CES that can potentially form an inter-quark bond, but are too far separated (by 15 pm or more). A b- and w-bond combination would be marginally stronger than a simple chemical b-bond, but is significantly weaker than a corresponding inter-quark bond. Between the helium structure and the part-layer of the Li-6 and Li-7 atoms, it is highly likely that this weak bond combination provides a **cleavage plane** between the two layers, which can readily give way to allow separation of the 2 parts (at least 1 He-4 atom) when bombarded by energised nucleons.

Before an inter-quark bond can form, a work function barrier called the Coulomb Barrier must first be overcome. It is quite feasible that when the energy available is insufficient to create inter-quark bonds, helium and/or its various isotopes could initially join via a combination of b- and w-bonds, a process that, in many cases, represents a pre-cursor to inter-quark bond formation. In a high temperature, high pressure post-formation environment, such as a collapsing star, or even a less intense environment such as that of a **kimberlite pipe** for diamonds formation, the helium structures can subsequently be squeezed closer together, overcoming the Coulomb barrier and so converting p-bonds into inter-quark bonds and possibly breaking the b-bonds, so releasing electrons and positrons in the process.

Many elements, including lithium to cubic diamond C-12 within the period 2 range, can contain helium sub-structures that can be released as helium and/or its derivatives. The proportion of atoms with each type of bonding would also vary within mineral concentrations, which would be a reflection of the environment in which it was created and the subsequent concentration processes it underwent. For atoms of a particular element, their chemical characteristics and atom size would be very similar, if not identical, regardless of whether the helium structures are strongly (inter-quark bonds) or moderately (b- and w-bonds) bonded. However, their physical strength, susceptibility to alpha decay, and possibly even their associated half-life, would be different.

Another aspect is that if b-bonds can exist between chains that are not inter-quark bonded, it is most likely they would also exist where inter-quark bonding exists between nucleon chains or parts thereof. Should this be the case, the b-bonds between adjacent pairs of up and down swivel quarks would restrict their ability to swivel freely. Should additional bitrons be present between inter-quark bonded layers, then more electrons would be present within the atom than shown in the atomic model diagrams provided in this paper. It would also mean that the number of electrons (albeit in bitron form) associated with elements would be approximately the same as that claimed by ONAM; although for elements in the higher atomic number range the ONAM electron count would still far exceed that of STEM.

Adding to the speculation regarding helium, referring to figures 25c and 25d, both the end-protons of these He-3 chains can be type-converted into neutrons. Should this happen, a relatively-stable electromagnetically-neutral three-neutron particle would result, which would have characteristics that are possibly compatible with those of dark matter.

In summary, there would seem to be 3 main ways in which atoms consisting of 4-sided (cubic) polygonal nucleon layers, such as those from helium to carbon-12 diamond, can form. The first way is via the building and subsequent joining of nucleon chains (a minimum of 4 nucleons required): all quarks within these structures are inter-quark bonded, with some nucleons in outer partial nucleon layers subject to β decay. Then there are atoms built wholly or partially from variations of helium structures. In lower temperate/pressure environments, the helium structures attach to each other and/or other structures via a combination of b- and w-bonds: these atoms can be readily split by nucleon bombardment. In high temperature/pressure environments, existing b- and w-bond combinations can be transformed into inter-quark bonds; and possibly some helium structures become inter-quark bonded directly (the third way). Atoms in which all quarks are inter-quark connected are more resistant to nucleon bombardment: however, they can fail by high-energy impact with other particles which can cause the random loss of I-form and/or L-form nucleons.

As can be seen from these deliberations many variations and possibilities exist for the formation and modification of elements, including alpha and beta decay. STEM certainly does not have all the answers related to atom structure, formation or modification, with further targeted research and modelling being required to prove (or disprove) and expand upon STEM's processes. However, with its current modelling it would seem that the role and range of natural variation at the atomic level far exceeds what is currently acknowledged by conventional Science. At this stage STEM can only suggest a range of feasible possibilities that follow directly from its basic hypotheses and associated modelling, which will doubtlessly be refined over time as more research ensues.

Beryllium

The **fourth element** in the Periodic Table is Beryllium, which is a divalent element only occurring naturally in combination with other elements within minerals. As a free element it is a steel-grey, strong, lightweight and brittle alkaline earth metal.

Be-8 (it can be created by the decay of Li-6 as in **equation 2** above) has a half-life of only 10^{-16} seconds, decaying into alpha rays. It most likely consists of 2 helium atoms b- and w-bonded together as in figure 27c.

Be-9 is the only one stable isotope of Beryllium, and thus it can be considered to be monoisotopic. It is believed that most of Be-9 in the universe was originally created in the interstellar medium when cosmic rays induced fission in heavier elements found in interstellar gas and dust. As a primordial fission product, its 2 helium atom structures are most likely inter-quark bonded together, with the extra neutron being an I-form or an L-form (as shown as figure 27a and 27b respectively) impact residual from the partial destruction a larger atom.

As for the He-4, the Be-9 atom is quite strong structurally, and it is used as a strengthening agent for metallic alloys.

The reason why a more stable version of Be-8 does not exist could be due to the inter-quark bonded version of Be-8 does readily acquire a third helium atom to be transformed into a C-12 diamond atom, whereas the attached neutron of Be-9 prevents the acquisition of a third helium atom unless the extra neutron is first removed. Support for this argument can be found in the conversion of Be-9 to a C-12 diamond atom by energetic alpha particle bombardment: soon after the impact removal of the attached neutron to create a temporary Be-8 atom to which a helium atom soon attaches, as in equation 3, to eventually create a C-12 diamond atom.

$$^{9}\text{Be}\ (+\ ^{4}\text{He}) \rightarrow\ ^{8}\text{Be} + \text{n};\quad ^{8}\text{Be} +\ ^{4}\text{He} \rightarrow\ ^{12}\text{C} \qquad ③$$

.

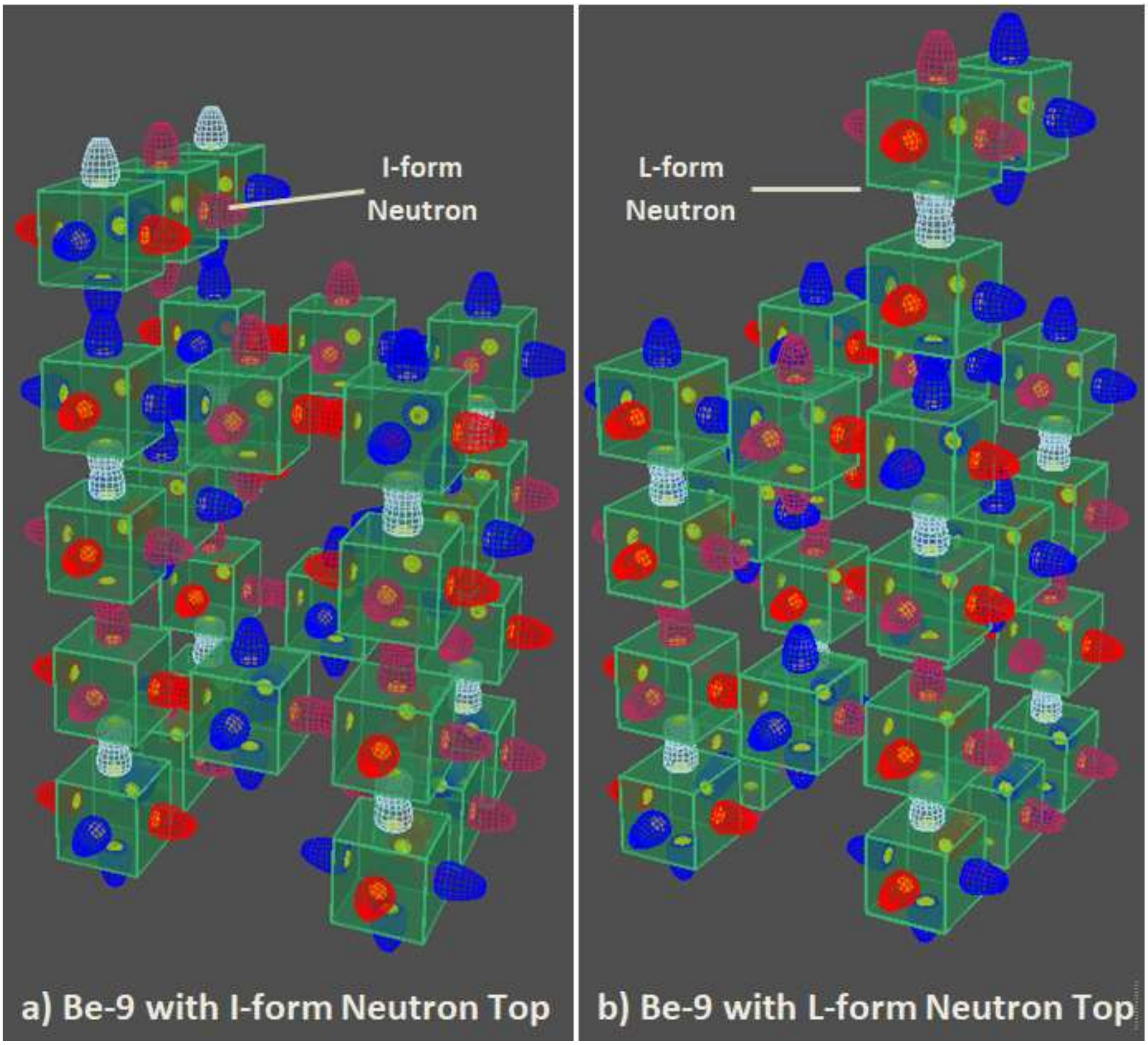

a) Be-9 with I-form Neutron Top

b) Be-9 with L-form Neutron Top

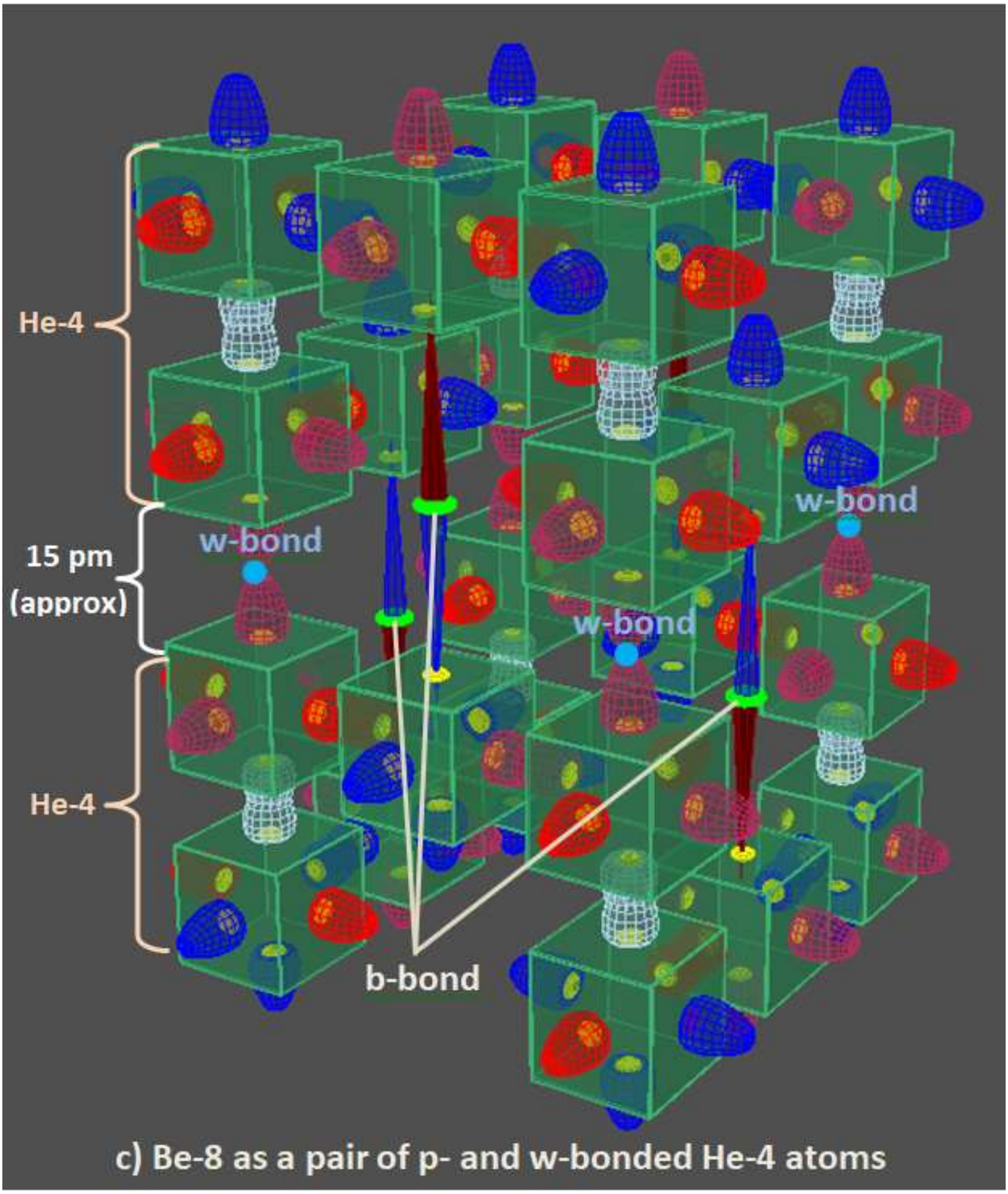

Figure 27: Quark Models of Beryllium Isotopes

Boron

The **fifth element** in the Periodic Table is Boron. Boron has two naturally occurring stable isotopes, with 19.9% being ^{10}B (or B-10) and 80.1% being ^{11}B (or B-11). Elemental boron is a metalloid that is found in small amounts only in meteoroids but is not otherwise found naturally on Earth in an un-combined state. Boron is concentrated by water-solubility of its more common naturally occurring compounds, the borate minerals. These are mined industrially as evaporites, such as borax and kernite.

Crystalline boron is silvery to black, extremely hard (about 9.5 on the Mohs scale), which is not unexpected as it has a structure quite similar to beryllium and He-4 atoms. However, the crystalline structure of B-11, the majority isotope, has a monoclinic form. This is possibly because that under shear pressure (as shown in figures 28b) associated with the crystallisation environment, its partial-layer superstructure causes oblique slippage resulting in its rhombohedral crystal form. The superstructure of B-10 is on one side, and results in monoclinic crystal form (figure 28b).

B-10 has a number of uses as a neutron-capture agent. Enriched B-10 is also used for both radiation shielding and as the primary nuclide for **Boron Neutron Capture Therapy** (**BNCT**). A B-10 compound administered to the patient is selectively taken up by a malignant tumour and tissues near it. The patient is then treated with low concentration neutron radiation that triggers energetic, short-range alpha particles that destroy cells within the tumour. The nuclear reaction for this process is:

$$^{10}B + n \rightarrow {}^{11}B \rightarrow {}^{4}He + {}^{7}Li + 2.31\ MeV \tag{④}$$

As well as producing ^{7}Li and ^{4}He (equation 4), high-energy neutron irradiation of **boron** (**^{10}B**) will occasionally produce tritium, as in equation 5:

$$^{10}B + n \rightarrow 2\ {}^{4}He + {}^{3}H_1 \tag{⑤}$$

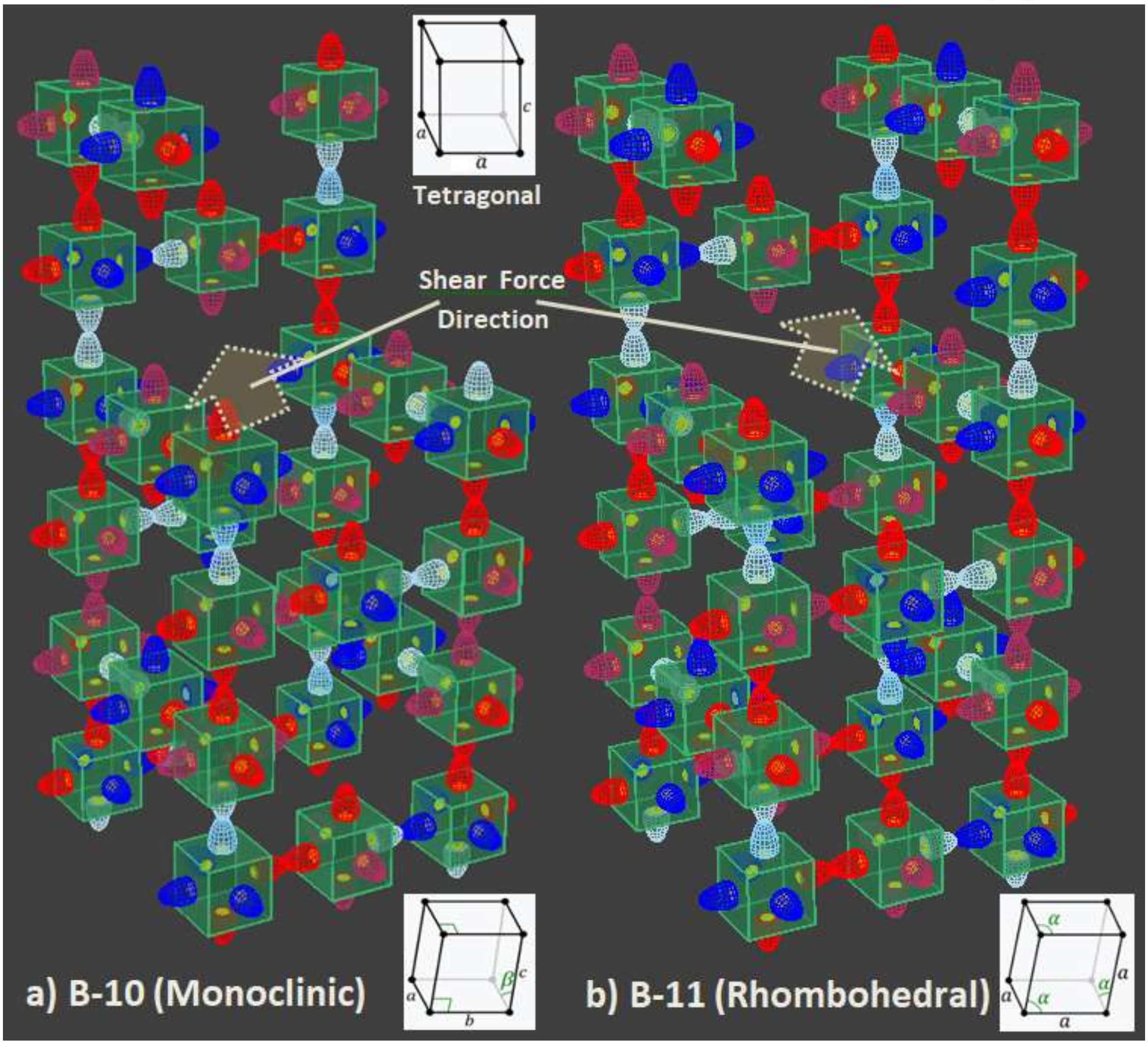

Figure 28: Quark Models of Boron Isotopes

Alpha radiation is a by-product of the atomic break-down of boron-10 and boron-11 as demonstrated by equations 4 and 5.This suggests that, in some of boron atoms at least, their base structure consists of a pair of loosely coupled He-4 atoms held together by a combination of b- and w-bonds would be a **diatomic He-4 pseudo-molecule** such as shown as figure 27c. The 4 b-bonds would be 25 to 30pm long, which is far shorter and stronger than external b-bonds associated with molecules and chemical compounds. The w-bonds would be about 15 pm long, far wider than the 2-3 pm of an inter-quark bond.

The production of helium-like by-products due to weakly bonded helium-like structures is a common theme for the elements with a tetrahedral 4-gon structure such as the elements lithium through to boron. Such elements can be de-stabilised by low-level neutron bombardment, which causes the b- and w-bonds to break, resulting in the release of low-level alpha rays as in equations 2 to 5. The energy associated with these low-level nuclear reactions is more in keeping with ‘normal’ chemical reactions involving the breaking of external b-bonds: should they have involved the breaking of inter-quark bonds, the energy released would be significantly higher. Alpha radiation associated with the unstable heavy atoms within the radioactive series is most certainly due to such He-4 atoms and diatomic He-4 pseudo-molecules embedded within those elements, but held by even shorter (less than 20 pm) and thus stronger b-bonds, as addressed in the Polymorphism, Embedding and Natural Variation chapter.

Due to its compatibility with silicon atoms, a small amount of ultrapure boron is used as a **dopant** in **semiconductor substrates**. There is the distinct possibility that b-bonds within diatomic He-4 pseudo-molecule base of boron atoms would provide an ongoing source of electrons (cetrons and aptrons) in the low-electron insulator-like environment of a semiconductor silicon wafer: thus a low emf, as generated across a diode, would be sufficient to release bitrons as negative charge carriers (cetrons) and positive charge carriers (aptrons) to support the flow of an electric current across the diode's depletion zone, with more bitrons being re-generated by the b-bond's CES pair to keep the process going.

The Role of Electrons within Atoms

Although the net charge of a proton is +1e and a neutron is electrically neutral, with many CES energy-fields being inwardly directed or participating in inter-quark bonds, the net charge of an atomic nucleus is not simply the atomic number (i.e. the number of protons) times +1e. Because there are approximately equal numbers of outward facing e-CES and p-CES, the nett close-field electric charge of an atomic nucleus is close to zero but possibly marginally positive. The minor positive charge of atoms and molecules within any medium (i.e. solid, liquid or gaseous) combines to produce a distinct positive far-field effect. Also, the net field-energy held internally by inter-quark connected quarks is considered to create an **energy capacitance** for each nucleon and nucleon layer within an atom.

The energy-field of **swivel quarks** is more concentrated and directional than that of fixed corner quarks. As addressed in the Chemical Bonds and Compounds chapter, bond geometries are influenced by the outer polygonal shape and size of the atoms and complexes involved; the field-energy capacitances of each nucleon layer of atoms, including any embedded structures; the distribution, availability, polarity and energisation-level of swivel quarks; the ionic electron configuration; and environmental factors (ionisation levels, gas/water molecular activity, catalyst etc.).

For instance, the He-4 atom contains 2 unrestrained swivel up-quarks and down-quarks, with the spin of the swivel quarks dominating its electrical characteristics so that it presents to the outside world as being electrically neutral to slightly positive due to there being more outfacing p-CES than e-CES. So, although the conventional Science model would consider that a He-4 atom would need 2 orbital electrons are needed to offset the positive charge of the 2 nuclear protons, this is not the case for the STEM approach.

Similarly, the diatomic He-4 pseudo-molecules of Be-8, as shown in figure 27c, contain 4 bitrons that restrain the 4 swivel quarks within the structure. The Be-8 atom is also electrically neutral and contains 4 bitrons, which are electron pre-cursors. However, it is just fortuitous that Be-8 contains 4 bitrons, which are electron equivalents and thus make it somewhat compatible with the 4 orbital electrons of conventional Science's Be-8 model.

With STEM, only some atoms contain bitrons (or pre-electrons), but they are not necessary to ensure electrical neutrality of an atom. As discussed in the Ionisation and Redox chapter, STEM supports **ionic orbital electrons** (often referred to as conduction band electrons), but does not support or require the concept of inner shell (or inner 'spdf') electron orbitals of an equal number to the number of protons in the nucleus: this difference represents a major point of difference between proponents of the conventional Science approach (ONAM) and STEM.

However, STEM is not alone in suggesting a restricted or non-orbital atomic model. In chapter 10 of the 2003 version of the Foundations of Physchemistry of Micro World, Professor P M Kanarev claims that 'the formation of the spectra of the atoms and the ions proves the lack of orbital motion of the electrons in the atom'.

Kanarev's published research and deliberations regarding the inappropriateness of the orbital model are, however, quite different to that of STEM in terms of the size and number of electrons, and the structure of nucleons and the atomic nucleus, as is apparent in the Kanarev diagram shown right of an electron and proton.

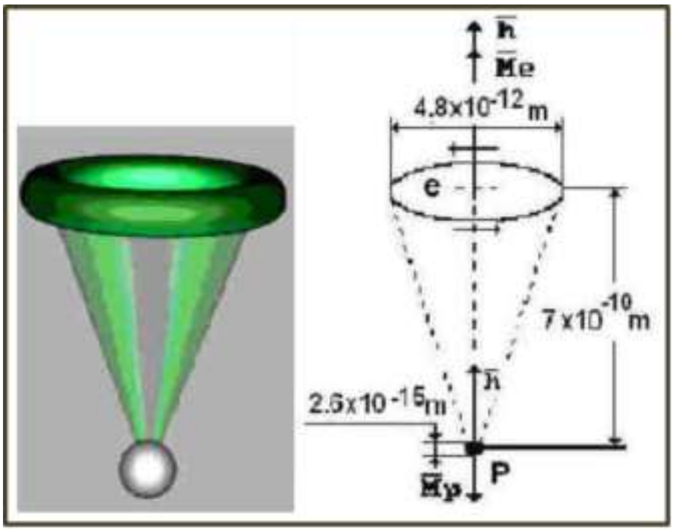

Atomic Structure: Carbon and Nitrogen

As the atomic number of elements increases from helium, the number of nucleon layers increases extending the height of atoms from helium’s cubic/tetragonal form. By **carbon-12**, the sixth element in the Periodic Table and is the 15th most abundant element in the Earth's crust, and the 4th most abundant element in the universe by mass after hydrogen, helium, and oxygen. C-12 consists of 6 protons and 6 neutrons, and has two allotropic forms: **diamond** and **graphite**.

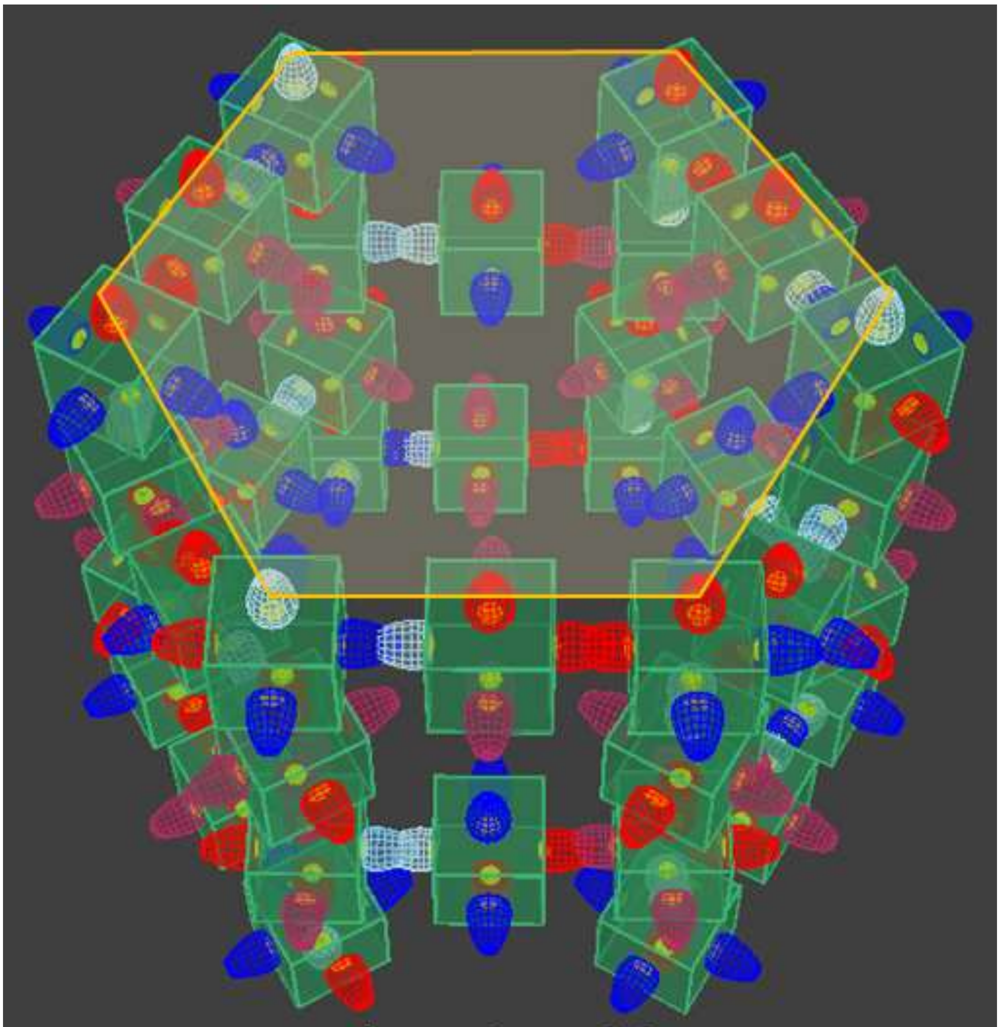

a) Quark Model

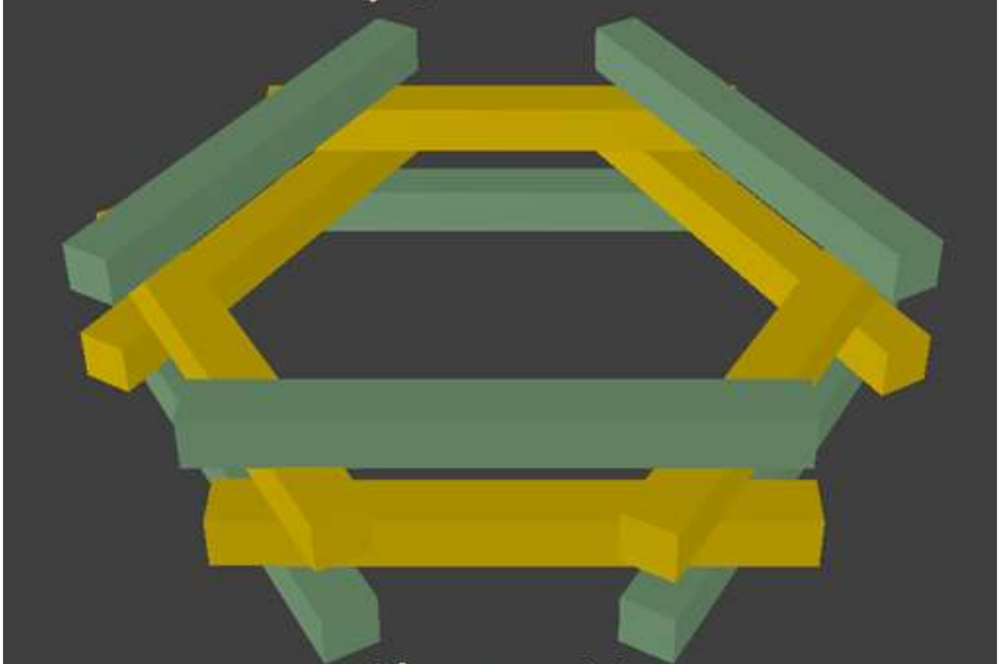

b) Bar Model

Figure 29: Quark and Bar Models of the C-12 Graphite Atom

Although they have the same nucleon count, the contrast between the physical characteristics of the two allotropic forms of C-12 is extreme in terms of looks and strength. **Graphite** is a layered, grey material that is soft, whereas **diamond** is clear, semi-transparent and sparkly, and is hard enough to cut glass: it represents the hardest natural substance known, with only artificially compressed wurtzite boron nitride (w-BN) being harder than diamond.

Graphite C-12 atoms have a **hexagonal** polygonal form and consist of 4 nucleon-layers, with each layer containing 3 nucleons, as shown in figure 29. Having an even number of complete neutron/proton layer pairs, the top and bottom layers are both either neutron layers (corresponding to layers 1 to 4 of figure 8), or proton layers (corresponding to layers 3 to 6 of figure 8), with each form being present in approximately equal numbers. A hexagonal C-12 atom has an outer side width of 42 pm, a side-to-side diameter of 72.75 pm and a height of 57 pm.

The 3 top and bottom swivel quarks of a C-12 graphite atom can each support up to 2 ionic orbital (or **conduction band**) electrons: aptron electrons for those with a pair of outer neutron layers and cetron electrons for those with outer proton layers. The ready availability of ionic electrons means that graphite is a good conductor of electricity.

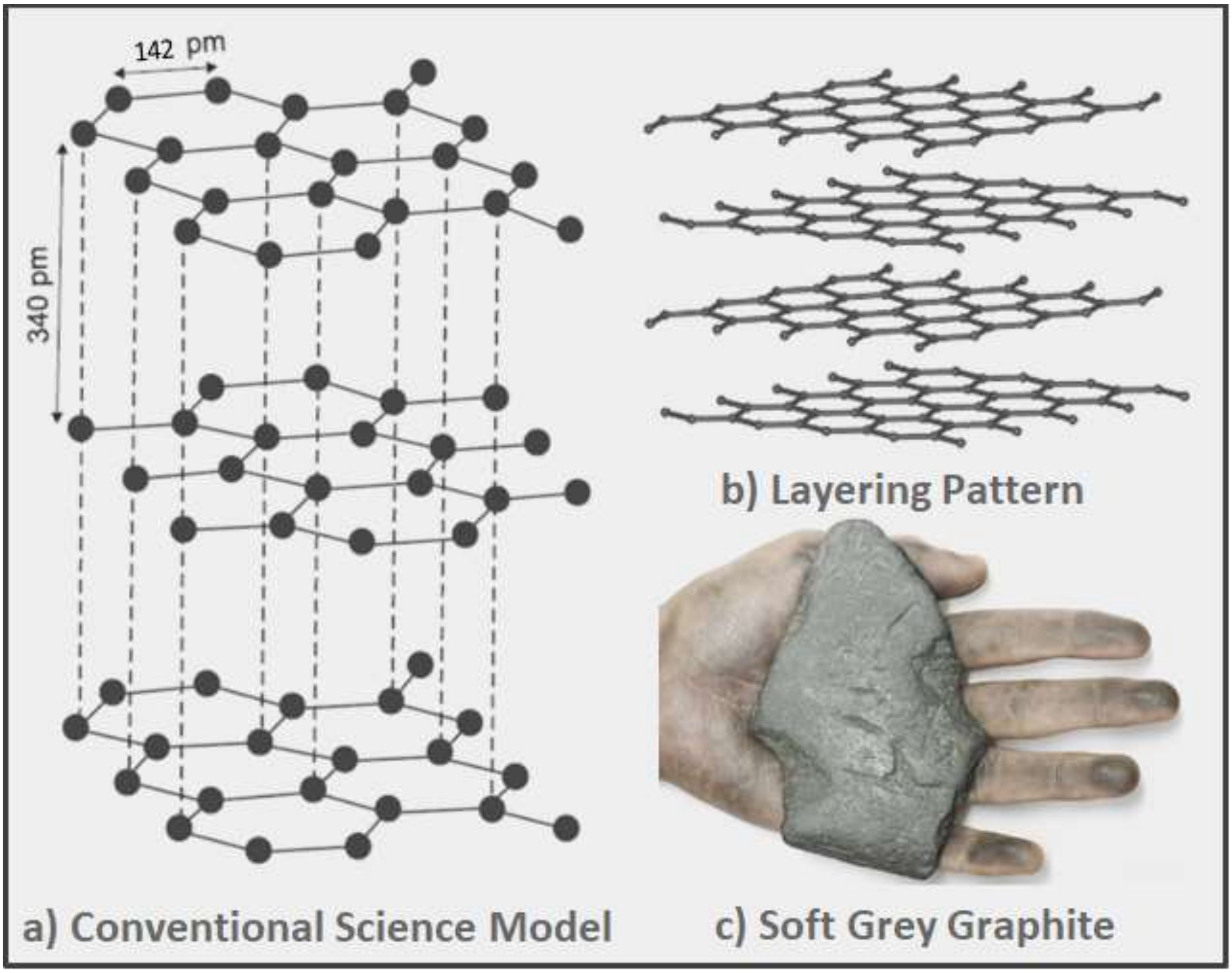

Figure 30: C-12 Graphite

The layering evident in graphite results from flakes and sheets formed by a hexagonal mesh of **bitron-bonded** hexagonal C-12 atoms as shown in figure 30a, with each C-12 atom (except for the peripheral atoms of a sheet) being bound to 3 other adjacent C-12 atoms by a pair of b-bonds.

The bond length between each connected C-12 atom is 142 pm, which corresponds to a b-bond length of 69 pm. Figure 31 provides a true-scale bar model of the hexagonal graphite mesh, although the bitrons have had to be enlarged to make them more visible, and are thus not to scale. Also, the field-energy of the swivel-quarks have been shown as disk-like zones to highlight the b-bond pattern between adjacent atoms.

The three unrestrained swivel quarks of each hexagonal C-12 atom are considered to generate an electromagnetic field above and below each atom which can acquire and hold **ionic orbital** (or conduction **band**) electrons (a topic covered in pages 73-74 of the Ionisation and Redox chapter). Thus, graphite has a ready supply of ionic orbital electrons that can easily be mobilised by an applied emf to generate an electric current that means it has high conductivity, a characteristic that makes it useful in electronic products such as electrodes, batteries, and solar panels.

In spite of its soft layered crystalline form, graphite is the most stable form of carbon under standard conditions. However, under high pressures and temperatures, it can be converted into the hexagonal diamond form. Due to its soft form and grey colour, graphite is used in pencils and as a lubricant. It is also a good conductor of heat and electricity.

Viewed from above, as in the figure 31, a single graphite sheet appears to be a uniform hexagonal mesh that might suggest a smooth surface, but its undulating surface causes granulation when rubbed as individual offset atoms and parts of the mesh become detached and rolled together. The surfaces themselves are separated by a minimum of 340 pm centre-to-centre, with a varying gap averaging about 190 pm between their effective outer surfaces. The separation gap is maintained by the p-bonds that form between the nucleons in the atoms' top and bottom nucleon layers that face each other.

Assuming that the average energy of each nucleon is 939 MeV/c^2, and using a conversion factor that 1 MeV/c^2 of energy equates to 1.79 x 10^{-27} grams, produces an energy-mass of 2.017 x 10^{-23} g for each 12 nucleon C-12 atom. Each graphite unit cell, consisting of one 142pm hexagonal mesh cell, encapsulates the equivalent of two hexagonal C-12 atoms which, at a minimum sheet separation of 340 pm, produces a calculated density of graphite of 2.265 g/cc. Allowing for natural variation (contamination and the occasional missing atom), this agrees well with the published measured density of graphite that is 2.26 g/cc.

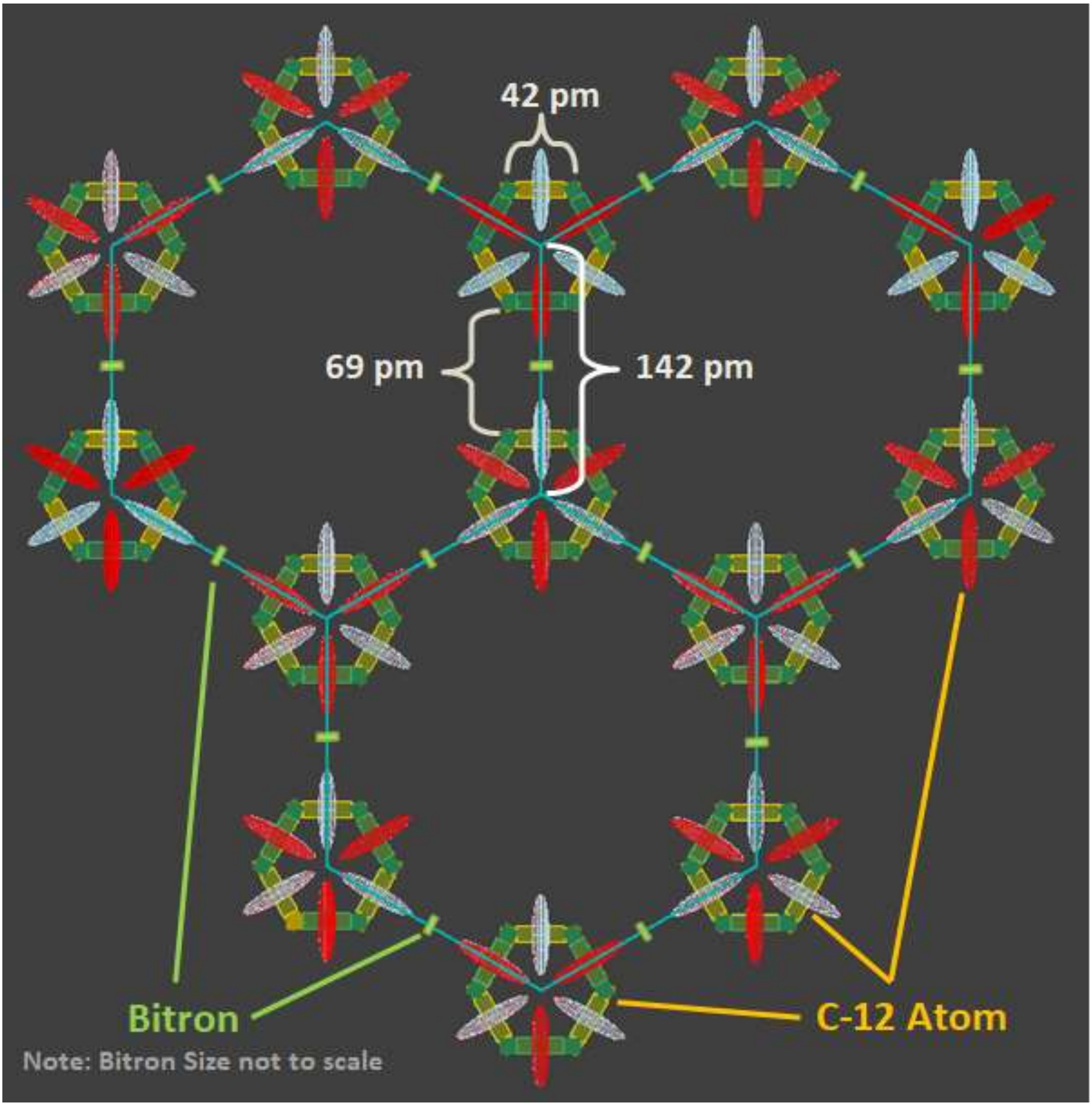

Figure 31: Modified Bar Model of the C-12 Graphite Sheet Structure

The height of a C-12 graphite atom is 57pm. However when, as in figure 32, the outer layers of adjacent atoms are the same, the b-bonds formed between them are offset, resulting in a nett height of 72 pm. In some instances, atoms will may be loosely bonded to each adjacent atom by only one b-bond, which can result in an even larger offset height of about 102 pm. With these offsets randomly occurring upwards or downwards from a graphite sheet's mid-plane, a wavy sheet surface with an effective nett thickness of 147 pm results, which is more than double the C-12 atom height. These offsets are made worse by sharing causing parts of graphite layers sharing off and being rolled up to create even further separation, with the average inter-sheet separation within crystalline graphite being 335 pm.

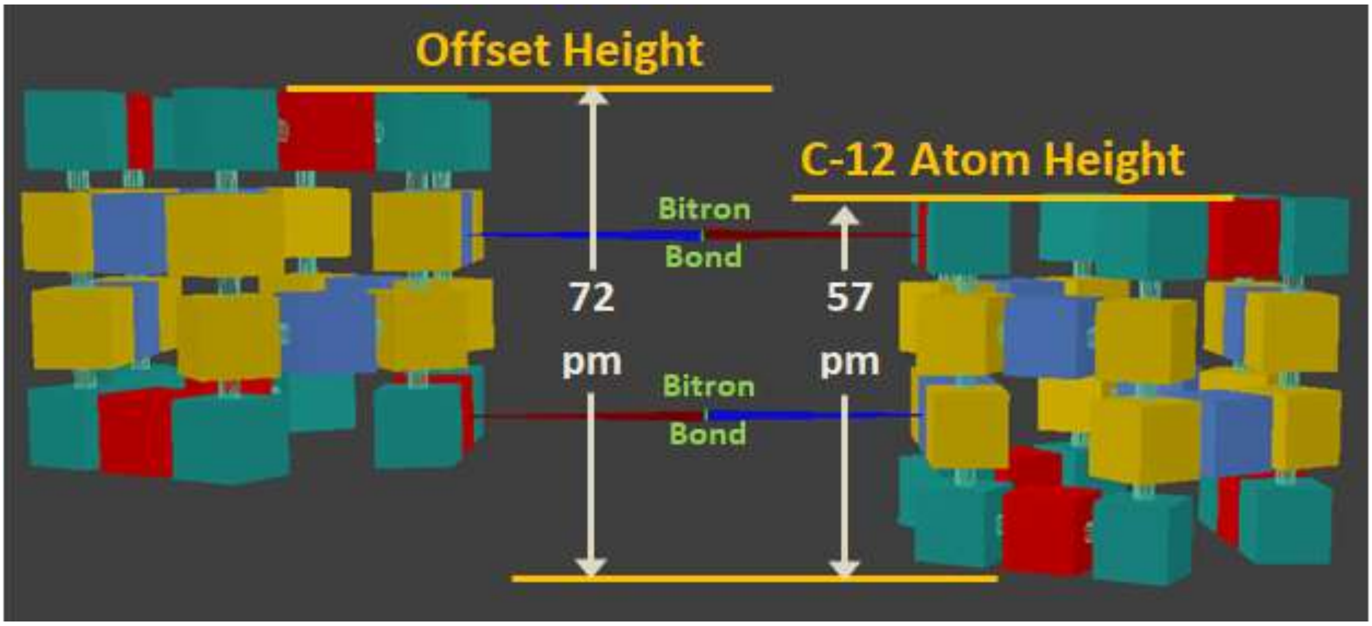

Figure 32: Adjacent C-12 Graphite Atom Offsets

Should graphite be subjected to intense pressure and elevated temperature, its crystal structure can be re-organised into a diamond-like structure. The process can be visualised by considering 3 adjacent bonded C-12 graphite atoms such as A, B, C and D in figure 33b. Rather than significantly shortening the b-bonds, the applied external pressure causes the swivel-quark b-bonds to swivel, pushing the central atom D upwards (side view in figure 33) or downwards into the inter-sheet gap. The net effect of the atoms moving into the inter-sheet gap on either side, is that the b-bond lengths stretch to about 154pm, creating a more compact triangular prism form that becomes part of a compressed hexagonal mesh pattern.

Upper atom **D** bonds with another atom (E say, which is not shown in figure 33), which would have been pushed downwards from the sheet above, to bond with tetrahedral structure **ABCD**. The end-product of the **high pressure, high temperature** (**HPHT**) process is **hexagonal diamond**, which is subtly different to the fcc (face-centred cubic) structure of natural diamond, both of which are shown as ball-and-stick models in figure 34.

When clarity and appearance are not paramount, HPHT hexagonal diamond provide a relatively cost-effective means for producing industrial diamond for diamond drill tips and a range of machining applications.

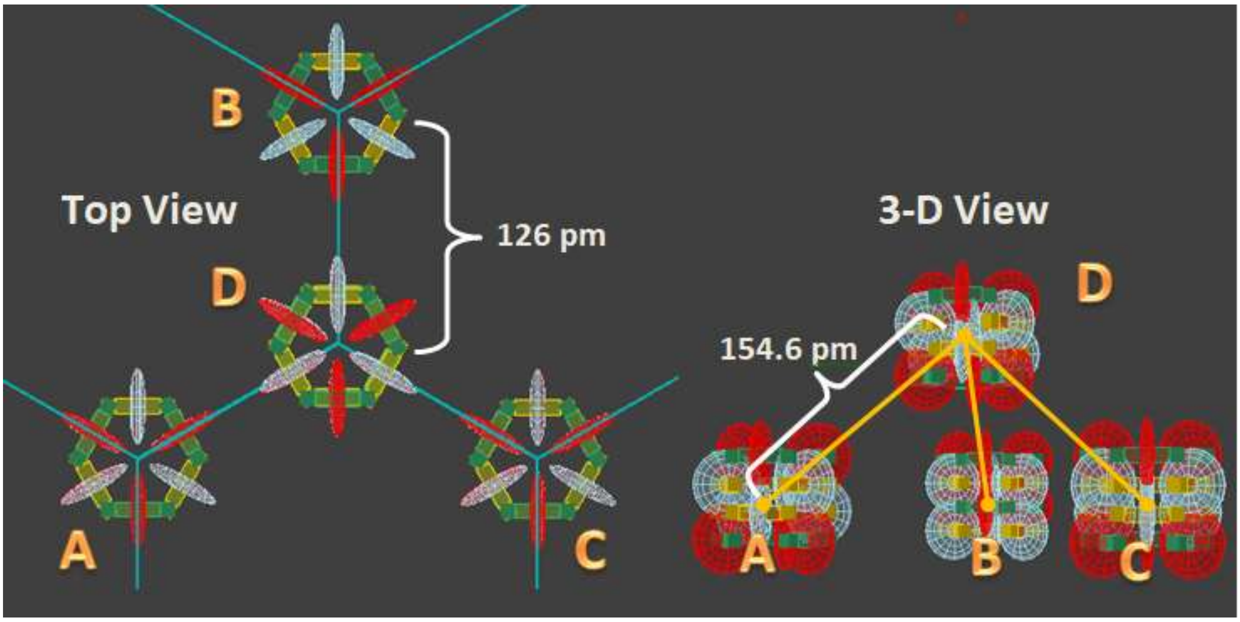

Figure 33: Transformation of Graphite C-12 Atom Groups into the Hexagonal Diamond Form

Hexagonal diamond occurs naturally as **lonsdaleite**, or synthetically by applying various high pressure, shear force and temperature combinations to graphite as described above for the HPHT process. Lonsdaleite was first found in nature in meteorite debris: when meteors containing graphite strike the Earth, great heat is generated and the impact creates shear stress that converts graphite's hexagonal crystal lattice into hexagonal diamond. Due to manufacturing controls, HPHT produced synthetic hexagonal diamond is much purer and higher grade than lonsdaleite, with X-ray crystallography required to distinguish it from high grade natural cubic diamond.

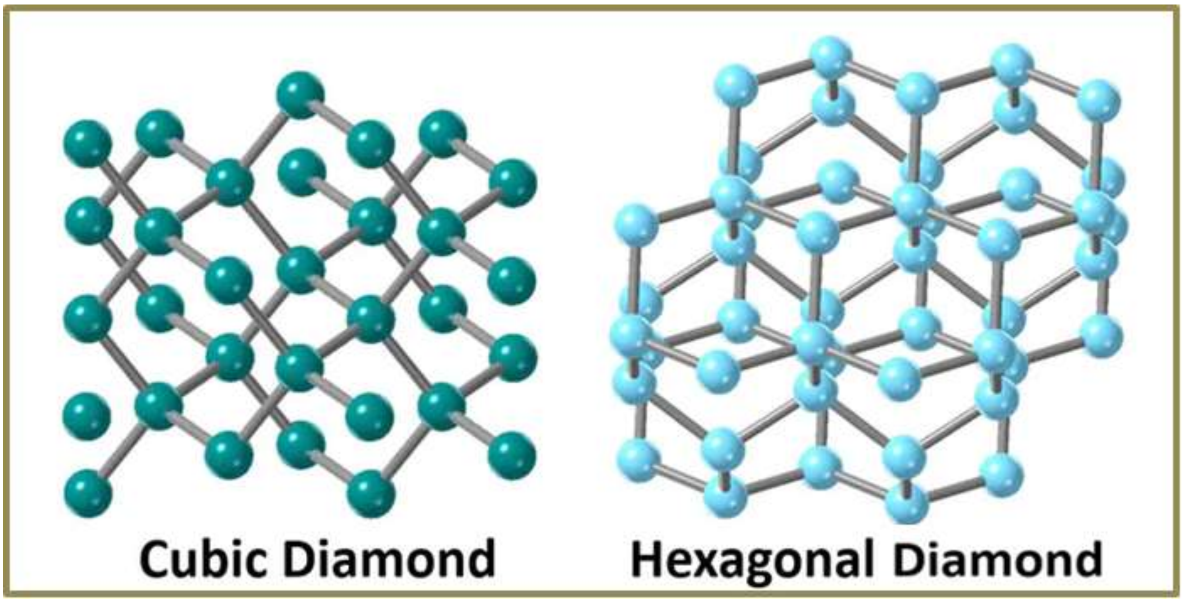

Figure 34: Cubic and Hexagonal Diamond Structures

Authenticated **natural diamonds**, and some synthetic diamonds produced by **chemical vapour deposition** (**CVD**), are referred to as **cubic diamond**. STEM contends that cubic diamond is subtly different to **hexagonal diamond** because they consist of different polymorphic forms (tetragonal and the hexagonal) of the C-12 atom.

Tetragonal C-12 atoms are predominantly created in the core of giant or supergiant stars via the triple-alpha process. Helium accumulates in the cores of stars as a result of the proton–proton chain reaction and the carbon–nitrogen–oxygen cycle. The triple-alpha process is a set of nuclear fusion reactions which involves three helium-4 nuclei (alpha particles) being fused together to create a tetragonal C-12 atom via Be-8, as reflected by the nuclear fusion sequence:

$$^{4}\mathrm{He} + {}^{4}\mathrm{He} \rightarrow {}^{8}\mathrm{Be} + {}^{4}\mathrm{He} \rightarrow {}^{12}\mathrm{C} + \gamma$$

Another way in which tetragonal C-12 atoms can be produced is by bombarding Be-9 with energetic alpha particles, which readily releases a neutron in the 2-part nuclear reaction (the same as equation 3 in the beryllium section):

$$^{9}\mathrm{Be}\ (+\ {}^{4}\mathrm{He}) \rightarrow {}^{8}\mathrm{Be} + n;\ \ {}^{8}\mathrm{Be} + {}^{4}\mathrm{He} \rightarrow {}^{12}\mathrm{C}$$

Even should the Be-8 atoms initially have the structure of a diatomic He-4 pseudo-molecule (figure 27c), the extreme temperature and pressure within a star core would soon squeeze their 2 He-4 atoms and the 3rd. attached He-4 atom closer together, converting the w-bonds into inter-quark bonds to create C-12 cubic diamond atoms.

Although essentially consisting of hexagonal C-12 atoms, graphite also contains (or is contaminated by) quantities of tetragonal C-12 atoms. CVD is a process that requires catalysts; a suitable substrate; and works at lower pressure and temperature than HTHP. It involves the deposition of carbon plasma onto the chosen substrate (often a low quality HTHP seed-diamond), and uses methane (CH_4), which predominantly consists of tetragonal C-12 atoms. Hydrogen is also added to maintain a ratio of about 1:99 so as to selectively etch away the hexagonal C-12 graphite atoms. Tetragonal C-12 atoms extracted from the methane gas and the graphite residuals deposit on the substrate, and grow as synthetic cubic diamond. Volcanism is considered to produce a similar etching, concentration and crystallisation process within **kimberlite pipes** to create natural cubic diamonds.

Cubic diamond cannot be created from hexagonal C-12 atoms because that would involve splitting hexagonal C-12 atoms and rearranging their nucleons to form tetragonal C-12 atoms. Rather, both natural and CVD synthetic cubic diamond creation is considered to be a process that **concentrates and crystallises tetragonal C-12 atoms**.

A tetragonal C-12 atom consists of 6 nucleon layers each containing 2 nucleons (see figure 35): it has the same square-polygonal cross-sectional form as He-4, and has an outer side width of 42pm and height of 87pm.

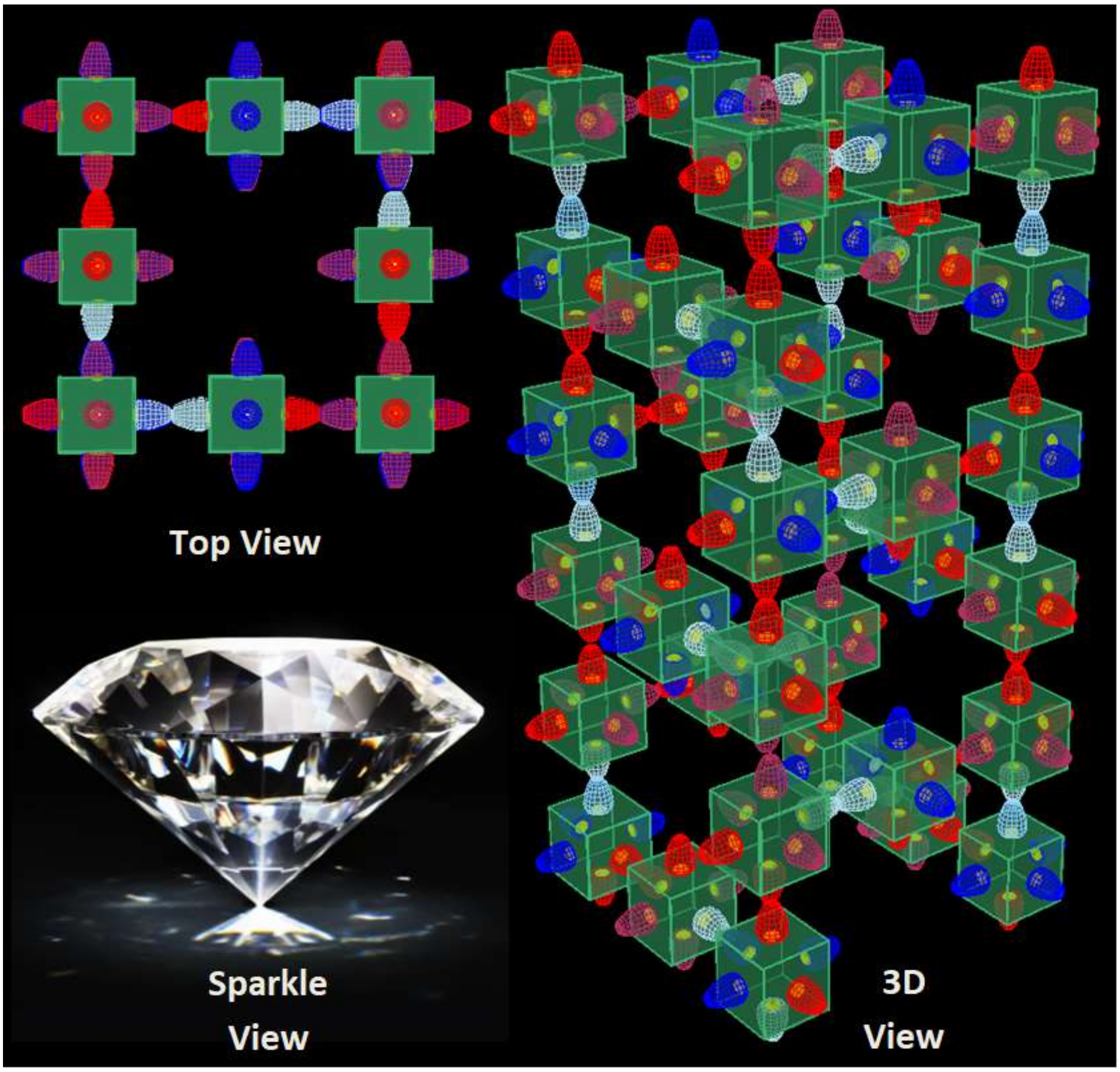

Figure 35: Quark Model of a C-12 Diamond Atom (and a Glittering Group Picture)

For cubic diamond is a face-centred cubic Bravais lattice in which each tetragonal C-12 atom is bonded with the 4 surrounding C-12 atoms, as shown in the ball-and-stick models of figure 36. Conventional Science considers the bonds to be covalent bonds, whereas STEM considers them to be polar-bonds (p-bonds or bitron-less b-bonds).

Figures 36 and 37 show the repeat-pattern **unit cube** for cubic diamond, with the unit-cube corner atoms being highlighted purple/mauve; centre-faced atoms in red; and fully internal atoms in orange. The unit cube side (a_O) is 357pm and each atom is equidistant at 154.6 pm centre-to-centre, with each 4-atom cluster subtending a tetrahedron (i.e. a triangular pyramid) shape.

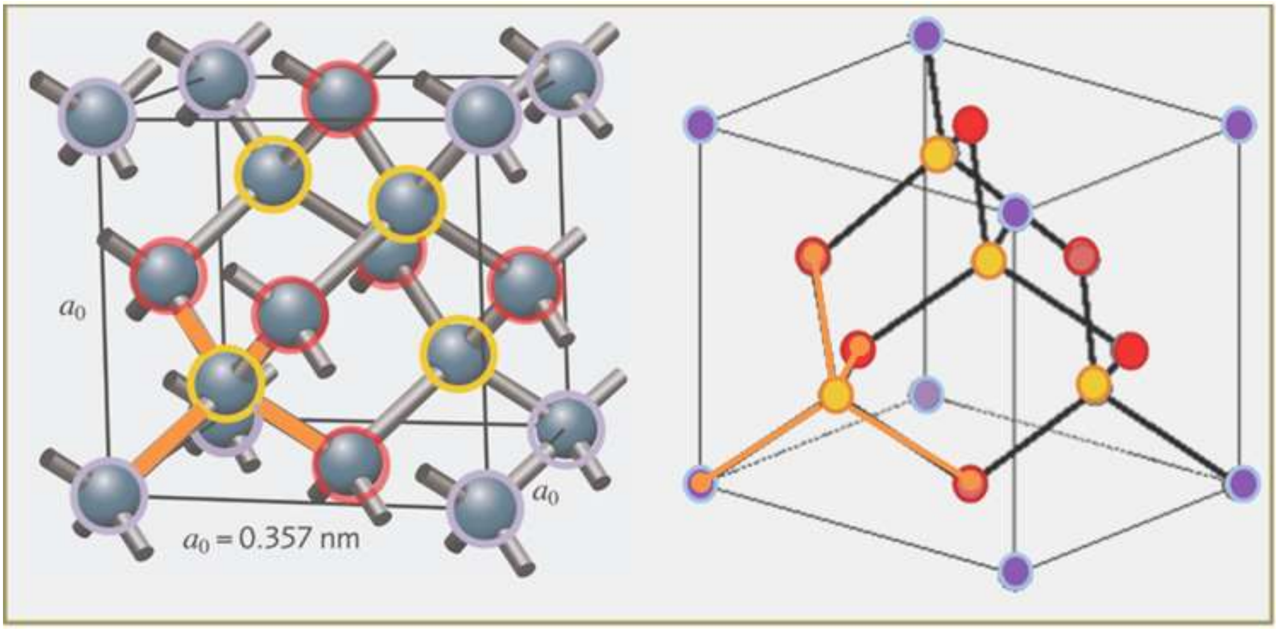

Figure 36: Cubic Diamond Unit Cell Structure

Figure 37 shows the STEM equivalent of the ball-and-stick models of figure 36. In plan-view, each tetragonal C-12 atom is rotated 45^O around the vertical (or z axis) and is bonded to each of its 4 closest neighbours. The centre-to-centre separation is 154.6 pm and the bond length is 110 pm. At 110 pm separation, it is most doubtful that the overlap of the swivel-quark pairs involved would be sufficient to generate a bitron, and thus the C-12 atoms are considered to be ‘bitron-less’ p-bonded, which accounts for why diamond is chemically unreactive. With only 2 swivel quarks per top and bottom layer, diamond atoms cannot support ionic electrons and thus acts as an excellent electrical insulator.

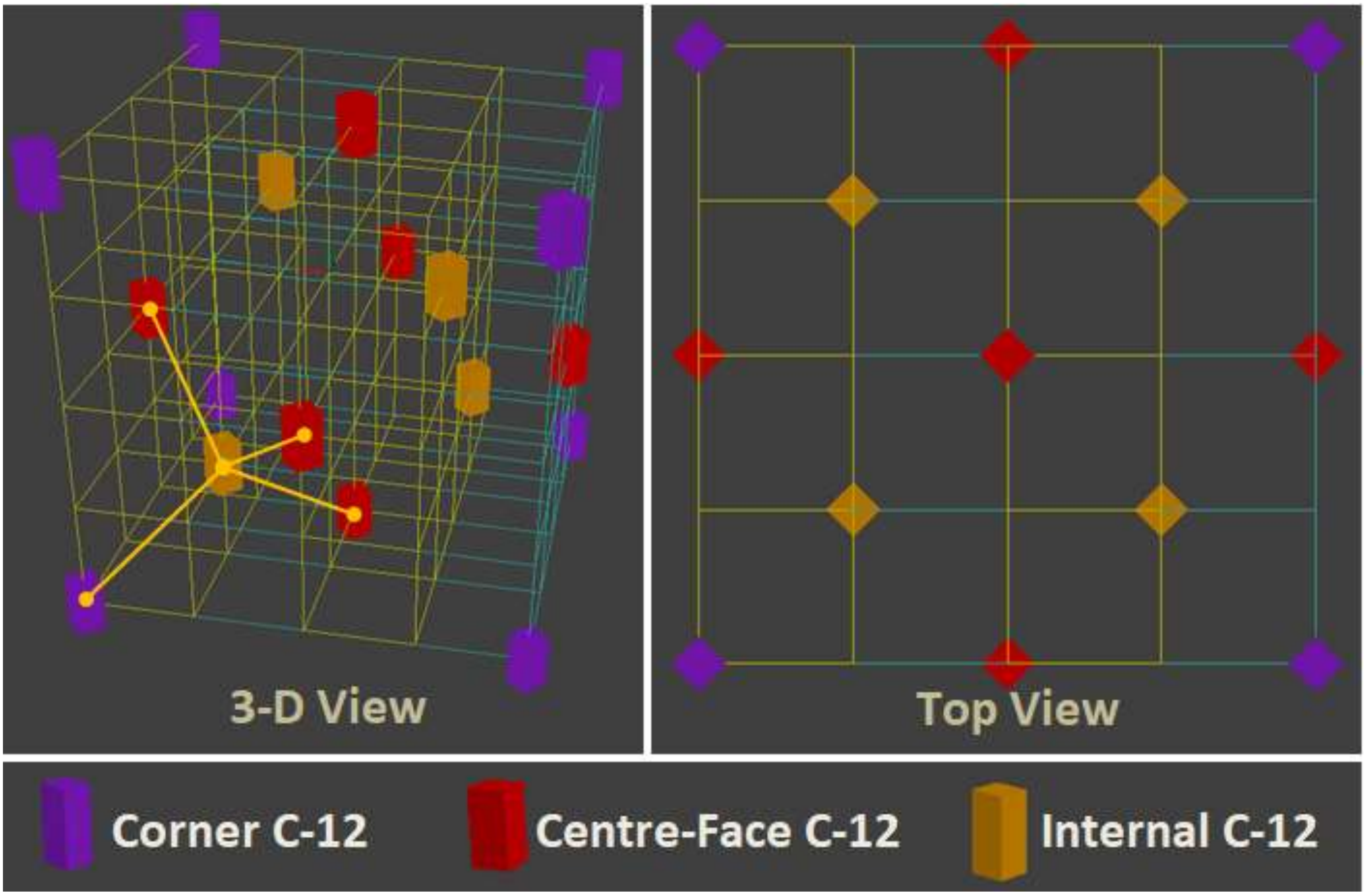

Figure 37: STEM Cubic Diamond Unit Cell Structure

Despite such wide bonds, the constraining characteristics of the tetrahedral symmetry mean that the atoms are held firmly in place by 4 pairs of p-bonds, totalling 8 p-bonds per C-12 atom. Also, the central swivel-quarks (in nucleon levels 3 and 4 if numbered 1 to 6) of each C-12 atom form p-bonds horizontally with immediate neighbours which are 210 pm away, with vertical bonding, at a vertical separation of 270 pm), are considered to have a minimal affect. The symmetry of the p-bonding makes cubic diamond one of the hardest natural substances known, although synthetic hexagonal diamond is marginally harder than cubic diamond.

The symmetry of cubic diamond crystal is an important aspect of its 3D consistency, with the pattern of the centre-points of each atom of the unit cube being identical when viewed in each of its x-y as in figure 37, and similarly in the x-z and y-z orthographic projections, regardless of how many unit cubes are included for ‘perfect’ cubic diamond.

Each unit cell for cubic diamond contains the equivalent of 8 C-12 atoms: 8 corner atoms shared by 8 unit cells, 6 centre-face atoms shared by 2, and 4 fully enclosed internal atoms. As calculated earlier, the energy-mass for a single C-12 atom is 2.017 x 10^{-23} g. For a unit cell of side length 357pm, this results in a calculated density of cubic diamond of 3.546 g/cc. Allowing for natural variation (contamination, flaws and vughs), this agrees well with the published measured density range for cubic diamond of 3.5 to 3.53 g/cc.

Both the conventional Science model and STEM are in agreement on the crystallographic structure of graphite, cubic diamond and hexagonal diamond. Apart from reference to the speculative science of hybrid orbitals (the concept that atomic orbitals can be mixed to create new hybrid orbitals), the ONAM approach provides no logical explanation for the different bond patterns involving exactly the same bond type (i.e. covalent bonding) and same C-12 atom type.

The STEM approach, on the other hand, is quite specific, providing two separate polymorphic structures for the C-12 atom that explain the different C-C bonds geometries. Furthermore, it claims that the structural differences between C-12 atom polymorphs mean that HPHT techniques alone (i.e. HTHP not involving the use of catalysts that lead to a concentration of tetrahedral C-12) do not and cannot produce synthetic cubic diamond.

The STEM model for graphite also explains the strength and flexibility of graphene, a single layer of graphite atoms that can be manufactured synthetically. Graphene consists of a two-dimensional hexagonal honeycomb lattice with 2 b-bonds per inter-atom link within the hexagonal mesh, with the swivel-quarks allowing extensive sheet bending and flexing, and allowing the formation of a range of different carbon structures such as those shown in figure 38a: graphite-like multi-layer groups; **carbon nanotubes** (graphene sheets rolled-up into tubes); and **spherical fullerenes**, with **buckyballs** being made from single-layer graphene (with some hexagonal rings replaced by pentagonal rings to achieve a ball-like shape), and **carbon onions** consisting of multiple nested buckyballs.

Graphene is the wonder-material of the nanoscience world and, with an intrinsic tensile strength of 130 GPa (1.9 x 10^7 psi) and a Young's modulus (stiffness) close to 1 TPa (1.5 x 10^8 psi), is the strongest material ever tested.

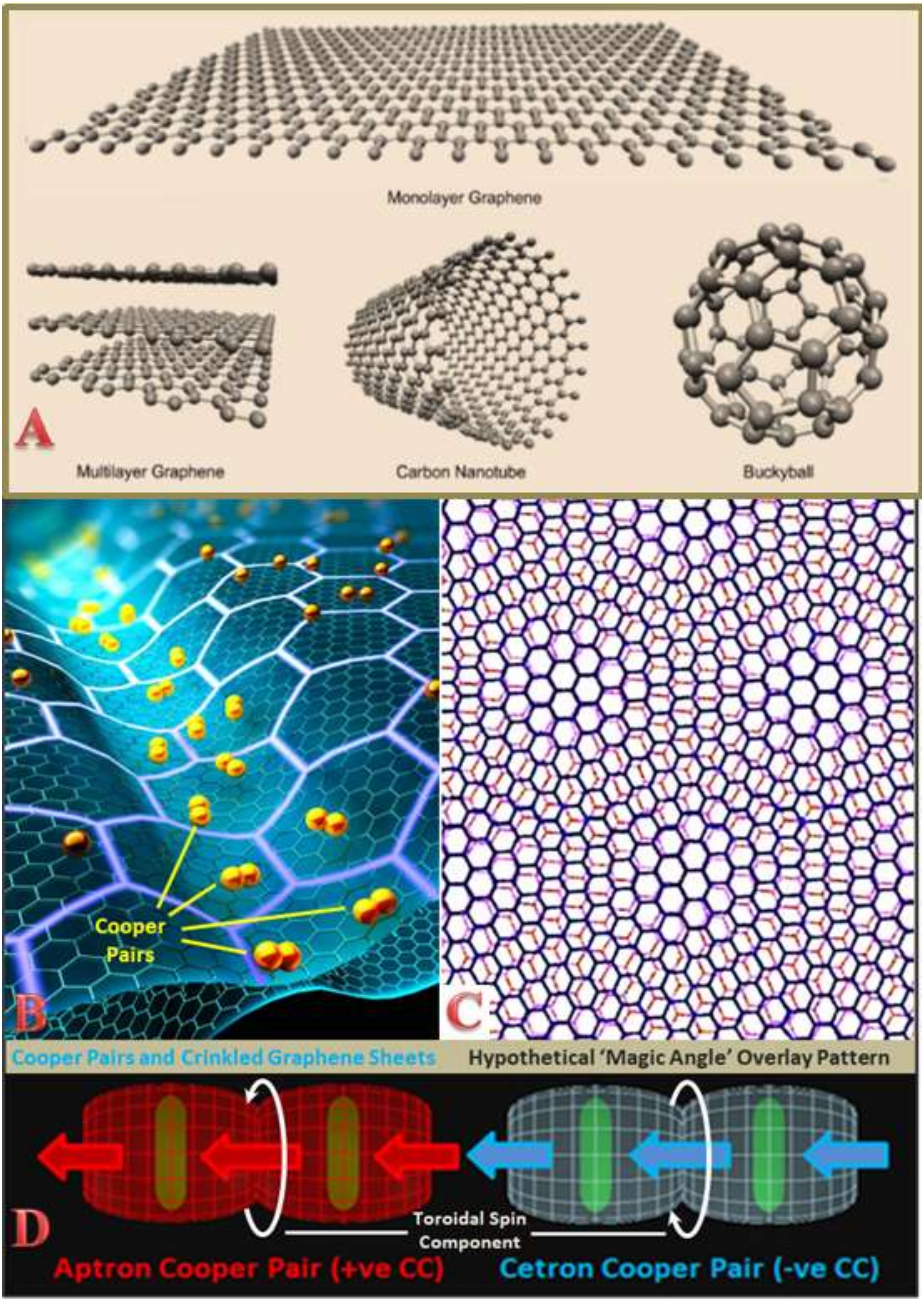

Figure 38: Graphene Shapes, Magic Angle Twisted Bilayer Graphene and Cooper Pairs

In 2018, the discovery of **M**agic **A**ngle **T**wisted **B**ilayer **G**raphene (**MATBG**), that could be **superconductive** or act as an electric **insulator**, was announced. MATBG consists of 2 overlaid single-layer graphene sheets, which normally act as an electric **insulator**, but when the sheets are rotated by the 'magic angle' (which is 1.1^{O}) to the other become **superconductive**. Since 2018, the 2-sheet MATBG version has been expanded to multi-layer versions and there have been many articles published discussing this intriguing phenomenon: of these, P Stepanov's 2021 article, titled 'Graphene with a Twist', covers the topic quite well.

Superconductivity is accompanied by the formation of Cooper pairs, which are bound electron pairs. Conventional Science struggles to provide a satisfactory explanation of how or why electrons, which should strongly repel each other, can become bound together as a Cooper pair. It is also unable to explain why, with minor re-orientation and/or confinement pressure changes, a pair of graphene sheets having electrical insulator characteristics can readily switch to having superconductor characteristics.

STEM suggests that when the upper and lower layers of the graphene sheets, which are quite flexible, are brought close together, they crinkle and flex against each other like 2 sheets of cling-wrap, as represented in figure 38b. Although there are many ionic electrons available, their ionic orbital planes are randomly orientated which is not conducive to orbital skipping in response to an externally applied emf or transient external magnetic field, and thus the sheets act an electrical insulator. This contrasts to crystalline graphite wherein the planar nature of graphite sheets result in the ionic orbital planes that are parallel to each other, which is supportive of good electricity conduction.

At the optimal 'magic angle', a combination of the atom overlap pattern and crinkle effect causes many ionic orbits to interfere with each other, resulting in many same-type ionic electrons to leave their orbitals and join together to form loosely coupled cetron and aptron Cooper pairs as shown in figure 38d. Because the individual graphene sheets contain equal numbers of cetron and aptron ionic electrons, approximately equal numbers of cetron and aptron Cooper pairs are generated, which can in turn act as negative and positive charge carriers to support an electric current. Possibly due to their combined mass, the Cooper pairs are not confined to an orbital and appear to be largely unaffected by the electromagnetic fields within the graphene sheets. It is the presence of such very mobile charge carriers (CCs) that is considered to provide MATBG with its superconductive characteristics.

Even slight departures from the 'magic angle' offset, or changes to the externally applied pressure, can drastically change the interface pattern of the graphene sheets. However, with Cooper pairs being quite loosely coupled, any such interface change can cause them to separate, with the individual electrons once again assuming ionic orbitals, which very quickly switches the graphite sheets from superconductive mode back into 'normal' electrical insulator mode.

The C-12 atom is associated with a wide range of **hydrocarbon compounds**. As discussed so far, although crystalline graphite can contain some tetragonal C-12 atoms, STEM contends that graphite and lonsdaleite (i.e. hexagonal diamond) consist of the hexagonal form of the C-12 atom, whereas cubic diamond consists of the tetragonal C-12 atom. The predilection for either tetragonal or hexagonal forms of C-12 extends to hydrocarbons, with tetragonal C-12 being prevalent in aliphatic hydrocarbons and hexagonal C-12 in aromatic hydrocarbons. Petroleum (crude oil) contains 49% cycloalkanes (naphthenes), 30% alkanes (paraffins) and 15% aromatic hydrocarbons (arenes), with the remainder concentrating as a tar-like cocktail (referred to as asphaltic) after the petroleum distillation process.

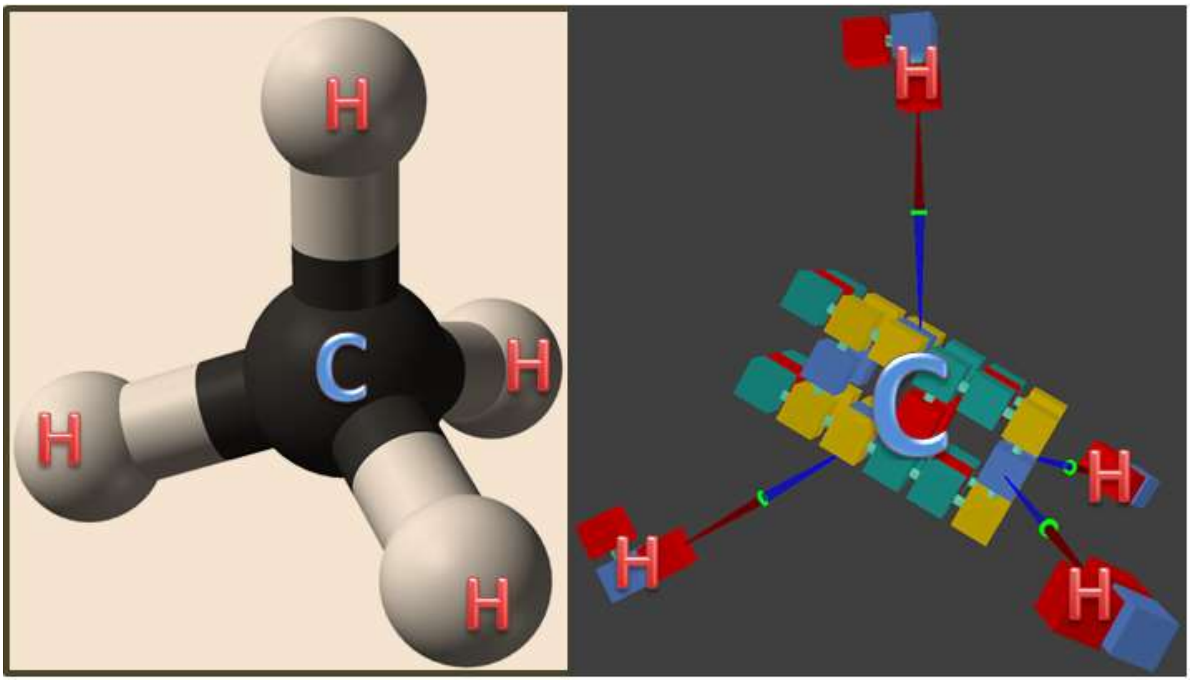

Figure 39: Methane (CH_4) Tetrahedral Structure

Methane (CH_4) is an **alkane** with a regular tetrahedron form around a central tetragonal C-12 atom: the H-C-H angle is 109.5^O and the H-C bonds are each 108.7 pm in length. At standard room temperature and pressure, methane is a colourless, odourless non-toxic gas that is extremely flammable when mixed with air: being denser than air, methane can act as an asphyxiant due to oxygen displacement. Figure 39 shows a ball-and-stick representation (not to scale) and the more detailed STEM bar model at the quark/nucleon level (true-scale except for bitron size).

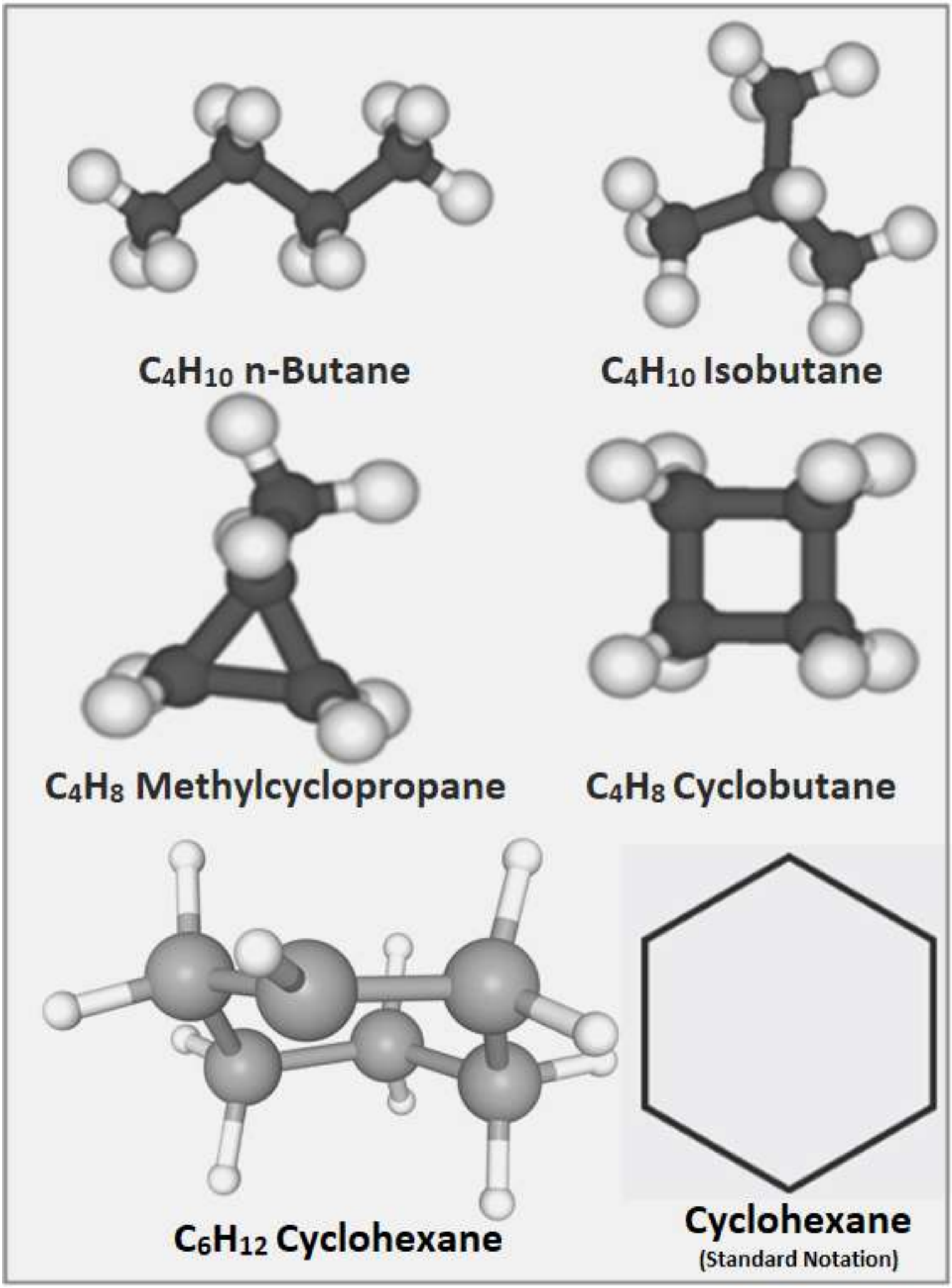

Figure 40: Aliphatic Hydrocarbon Structures

Alkanes are **saturated hydrocarbons** that have the general formula C_nH_{2n+2}. Alkane molecules present as a varied range of single chains, branched chains and polygonal (cycloalkane) forms, with each C-H module having the tetrahedral form of the methane molecule and each C-C bond can be represented by a single conventional Science covalent bond. Many molecules have several isomeric forms as shown in figure 40: this also shows the staggered form of chains and polygon shapes due to the tetrahedral C-H modules associated with tetragonal C-12 atoms.

Alkenes are **homologous hydrocarbons** that have the general formula C_nH_{2n}, and contain at least one carbon-carbon covalent double bond. Alkynes are **unsaturated hydrocarbons** have the general formula C_nH_{2n-2}, and contain at least one carbon-carbon triple covalent bond. As for alkanes, alkenes and alkynes have staggered physical form due to the tetrahedral form associated with tetragonal C-12 atoms.

The **methyl group** (CH_3) is an alkyl derived from methane: it contains one carbon atom bonded to three hydrogen atoms. The methyl group is a very stable group that occurs in many organic compounds, often multiple times (e.g. the end-members of the butane molecules of figure 40): in formulas it is often abbreviated **Me**. While the methyl group is usually part of a larger molecule, it can be also be found as a stand-alone anion, cation or radical form.

The distinction between alkenes, alkenes and alkynes would seem to be based upon the presence, or lack thereof, of double and triple covalent bonds that are due to the hybridization. A sp^3 **hybrid** (single **C-C** covalent bond) involves the combination of a carbon atom's *2s* and three *2p* orbitals form four identical orbitals. A sp^2 **hybrid** (double **C=C** covalent bond) involves the combination of a carbon atom's the *2s* orbital with two of the three available *2p* orbitals, forming a total of 3 sp^2 orbitals with one *p*-orbital remaining. A triple **C≡C** covalent bond is formed because a carbon atom is *sp* hybridised (2 pairs of linearly arranged electrons that can potentially form a π bond) and forms two π bonds and one σ bond (a hydrogen *1s* atomic orbital).

Hybridisation is a speculative theoretical rationalisation that selectively combines different electron orbitals so as to match observed bonding geometries, with aliphatic hydrocarbons defined in terms of single, double and triple hybrid carbon-to-carbon bonds and aromatic hydrocarbons in terms planar structures consisting of resonance and σ hybrid bonds. In contrast to ONAM's complex and enigmatic hybridisation explanation, the STEM approach is stunningly simple: carbon-to-carbon bonds consist of a pair of b-bonds and C-H bonds consist of only one b-bond, with aliphatic and aromatic hydrocarbon categories being dependent upon whether the carbon atom(s) have a tetrahedral or hexagonal structure.

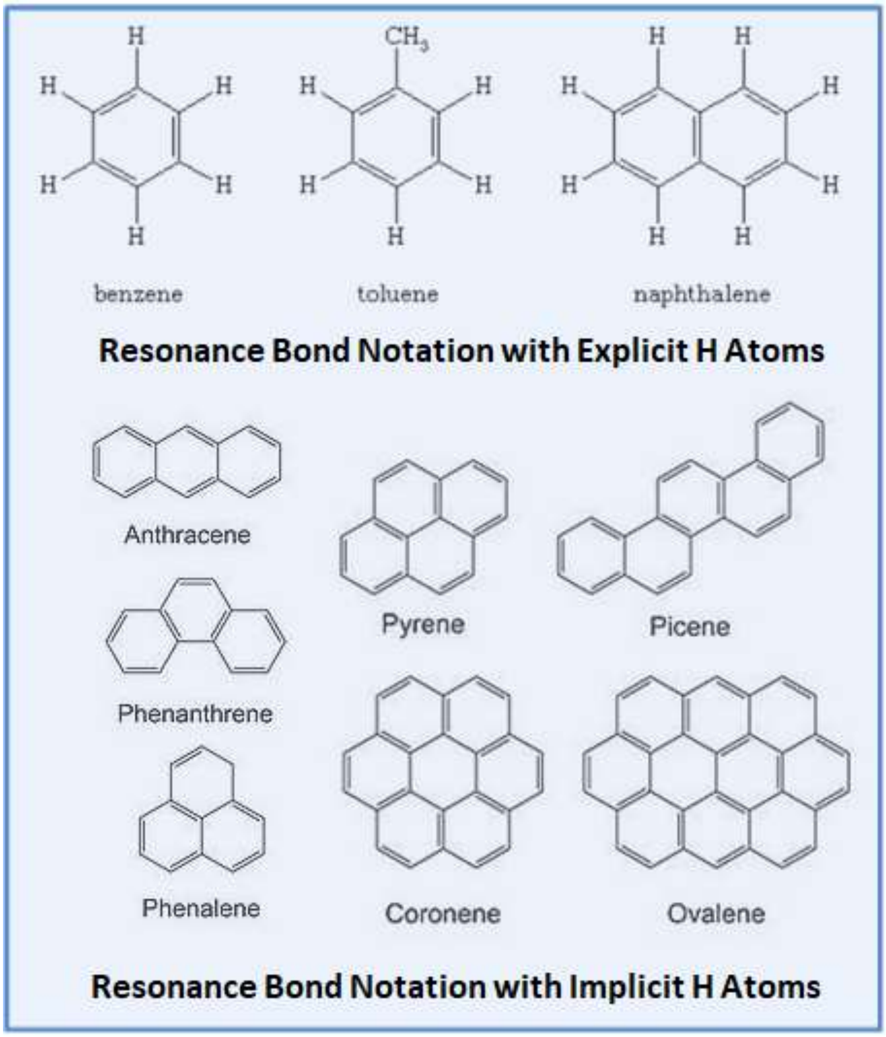

Figure 41: Monocyclic and Polycyclic Aromatic Hydrocarbon Structures

As can be seen in figure 41, aromatic hydrocarbons (or arenes) are ring-like (cyclic) structures based upon one or more hexagonal 'benzene rings'. Unlike cyclic aliphatic hydrocarbons, aromatic hydrocarbons have a planar structure reminiscent to that of graphite or graphene. Aromatics, so named for their fragrant aroma, are unsaturated hydrocarbon ring structures that exhibit unusual stability, are immiscible with water and are useful as solvents for many compounds.

The planar nature of the benzene ring, as apparent in figure 42 the quark/nucleon scale-model of the toluene molecule, is quite different to the kinked hexagonal aliphatic hydrocarbon benzene ring equivalent of cyclohexane in figure 40.

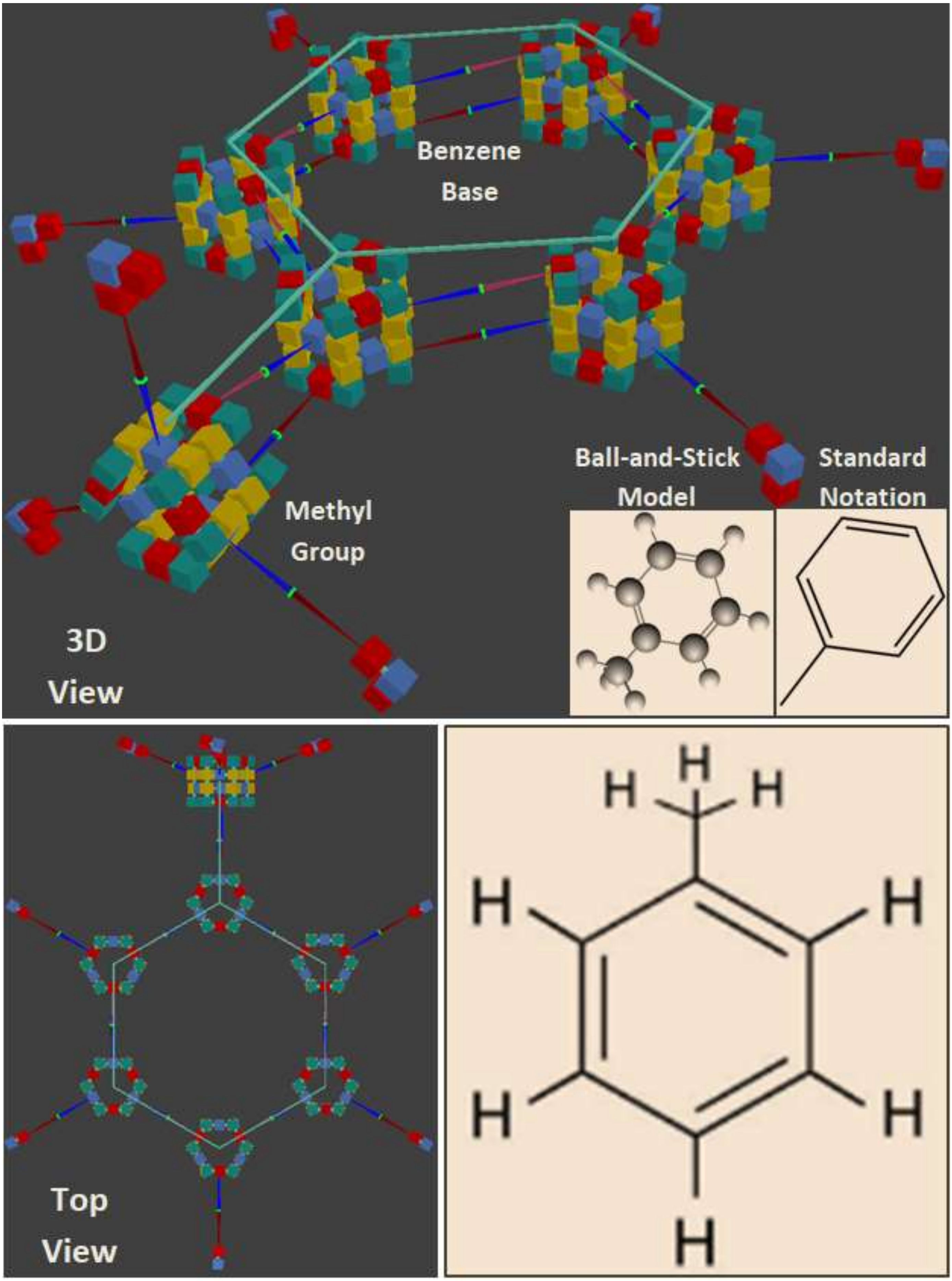

Figure 42: Toluene (C_7H_8) Structure

Although aliphatic and aromatic hydrocarbons are considered to consist of tetragonal and hexagonal C-12 atoms respectively, within the bounds of natural variation, either type of atom could randomly and occasionally be included within the structure of either hydrocarbon type. For instance, as can be seen in figure 42, the tetrahedral form of the methyl group (CH_3) can be based upon either a hexagonal or tetragonal C-12 atom (see figure 43). However, it would seem most likely that aliphatic hydrocarbons would develop in an environment where tetrahedral C-12 atoms are dominant and aromatics develop where hexagonal C-12 atoms are dominant: thus only the one form of C-12 is expected in most compounds.

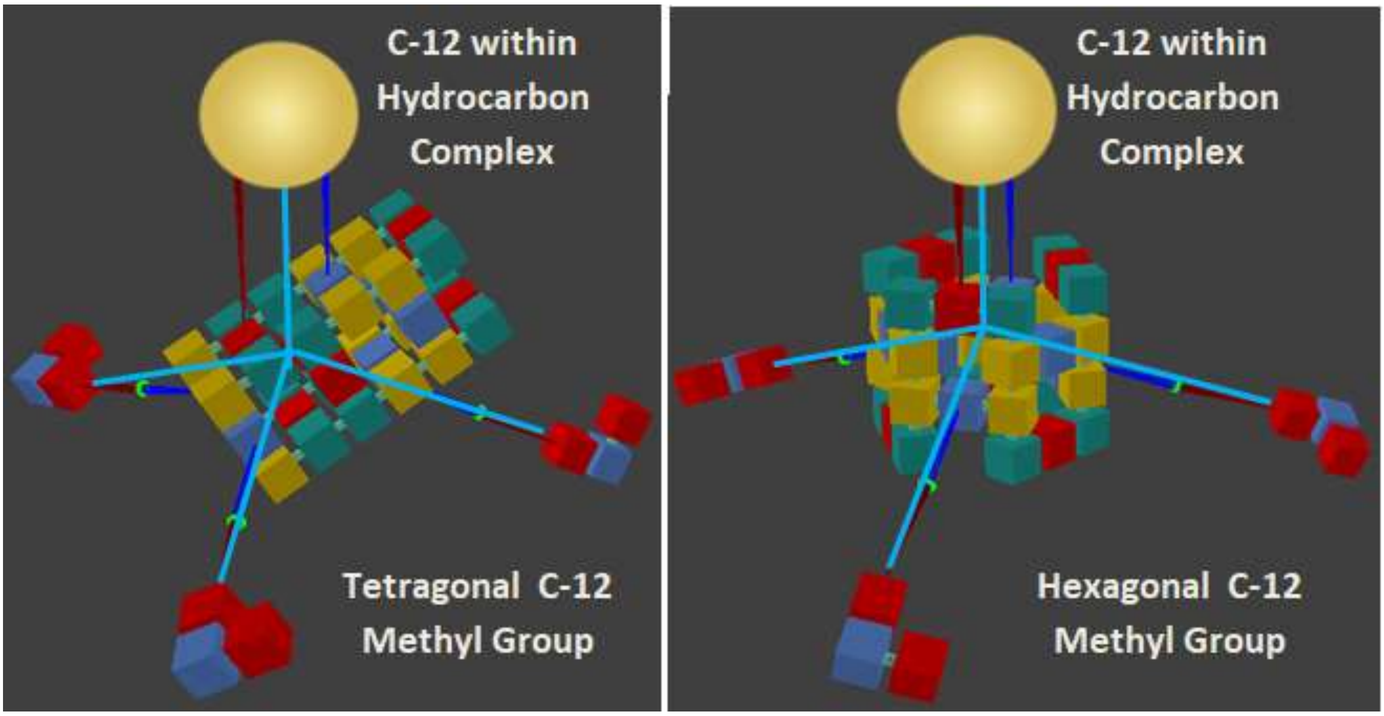

Figure 43: Tetragonal C-12 and Hexagonal C-12 Atom-Based Methyl Group (CH_3) Structure

Hydrocarbons represent an almost infinite range of combinations and conformations, being concentrations of carbon-based compounds based upon tetragonal C-12 atoms or hexagonal C-12 atoms, and sometimes a mix of each form. Also, by replacing some hydrogen atoms by a different element or functional group, many different hydrocarbon derivatives can be produced as exemplified by the benzene derivatives listed in figure 44 and complex polymer molecules.

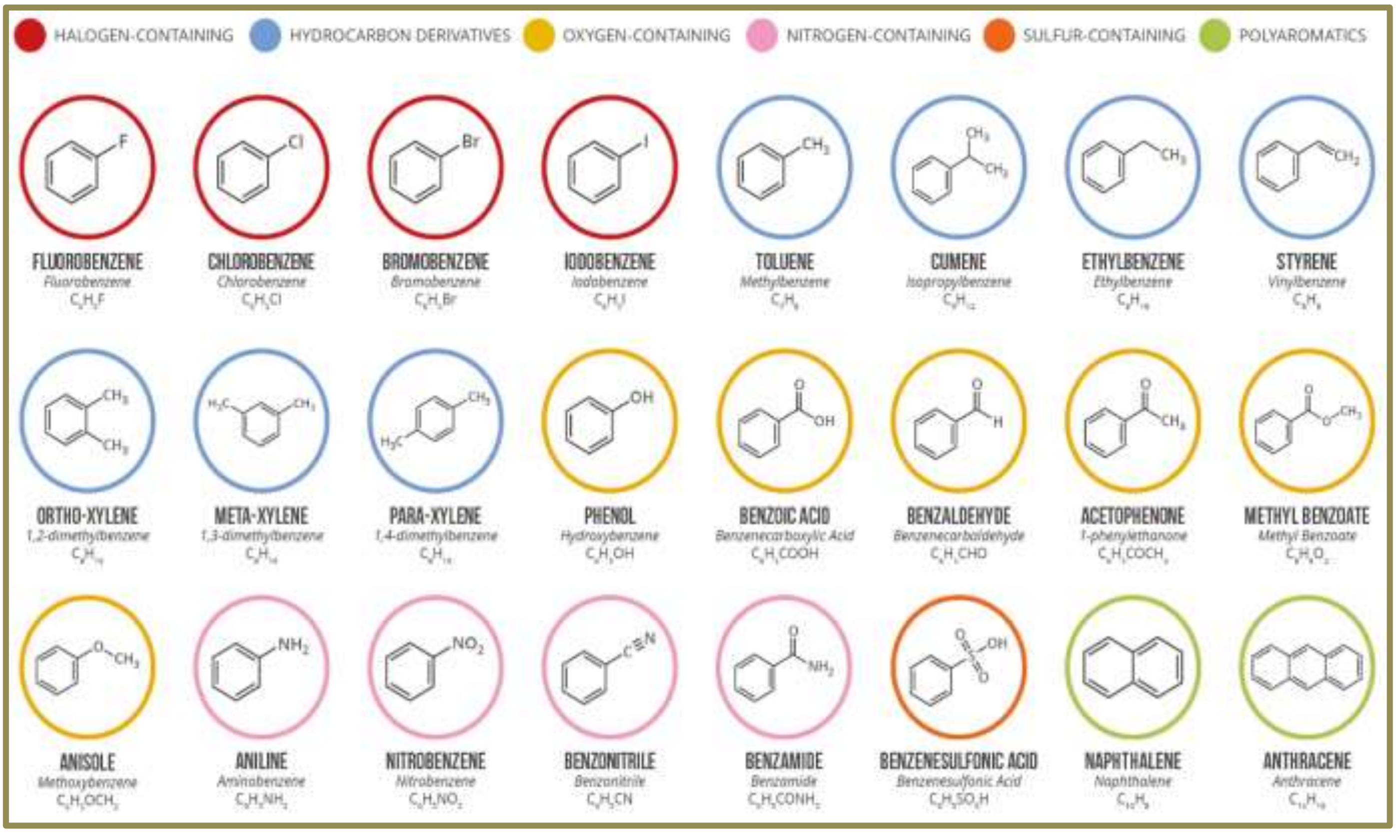

Figure 44: Examples of Aromatic Hydrocarbon (or Benzene-Based) Derivatives

Nitrogen

The **seventh element** of the Periodic Table is the **Nitrogen** atom which is an extension of the hexagonal C-12 atom, and thus has a hexagonal form with a top-most (or bottom-most) partial nucleonic layer. Nitrogen consists of 7 protons and 7 neutrons, and has the same cross-sectional diameter (72.7 pm) as the hexagonal C-12 atom, but with a height of 87 pm inclusive of the partial nucleon layer, it is 30 pm higher than C-12.

At standard temperature and pressure diatomic nitrogen (N_2) is a colourless and odourless diatomic gas that constitutes about 78% of Earth's atmosphere by volume (75.51 % by weight), making it the most abundant un-combined element. Diatomic nitrogen is bonded end-to-end by 6 b-bonds that each are only 48 pm long, which results in an extremely strong bond which is the strongest bond in any diatomic molecule after carbon monoxide. The centre-to-centre bond distance for N_2 is 119.4 pm.

Conventional Science considers that diatomic nitrogen is formed by a pair of nitrogen atoms that are triple-bonded ($N \equiv N$), which involves 6 covalent electrons. The 6 b-bonds of the STEM N_2 model contain 6 bitrons or electron-equivalents: in this aspect both models are quite similar.

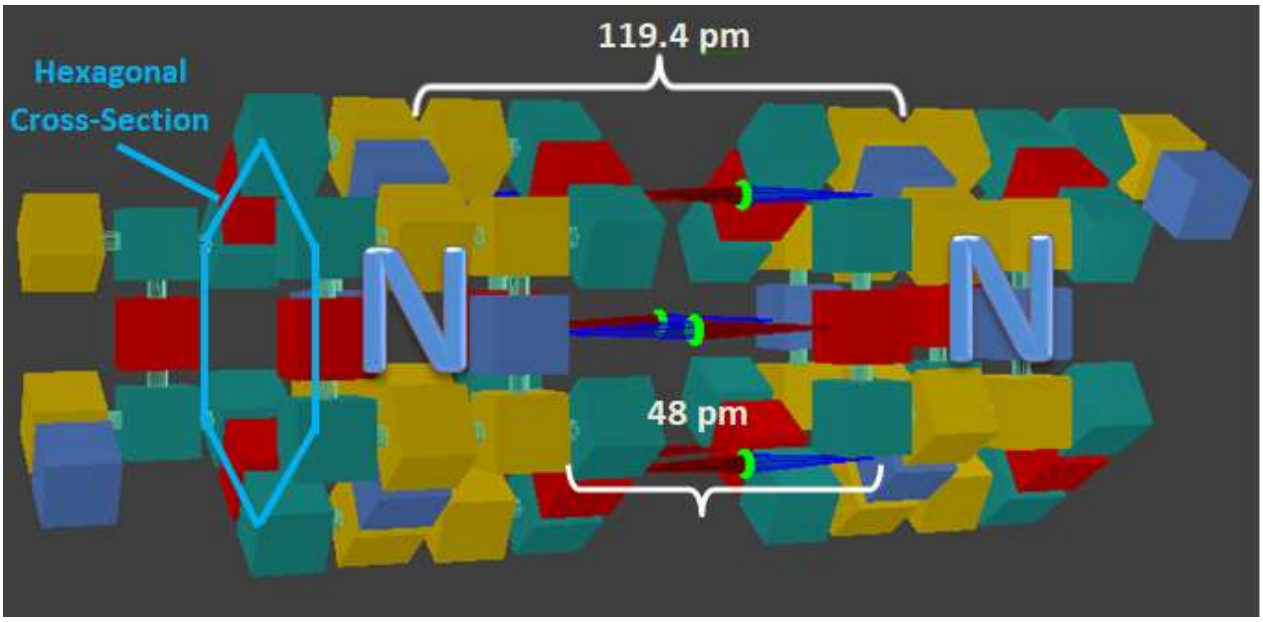

Figure 45: The Diatomic Nitrogen (N_2) Structure

Nitrogen is a common element in the universe, being about seventh in abundance in the Milky Way and the Solar System. Nitrogen occurs in all organisms, primarily in amino acids (and thus proteins), in the nucleic acids (DNA and RNA) and is thus genetically most important to life. The Nitrogen Cycle (figure 46) is important to Earth's ecosystem.

Although nitrogen occurs in mineral deposits of saltpetre (potassium nitrate, KNO_3) and Chile saltpetre (sodium nitrate, $NaNO_3$), commercial production is largely by fractional distillation of liquefied air.

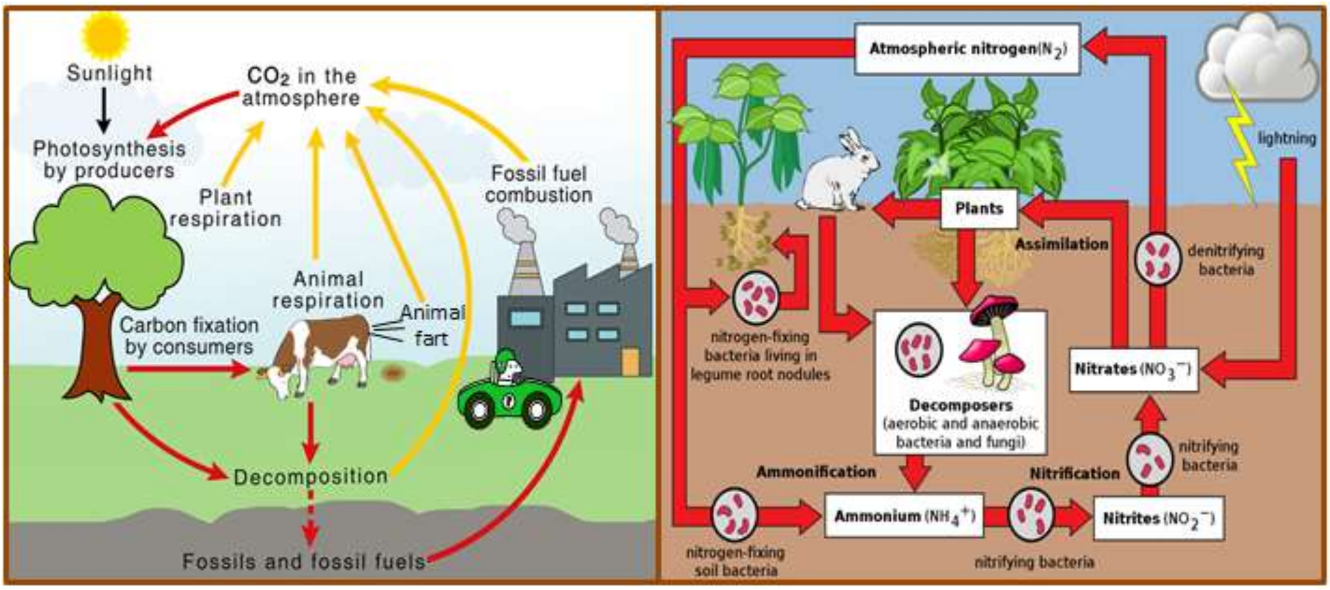

Figure 46: The Carbon and Nitrogen Eco-Cycles

Atomic Structure: Oxygen and Water

The **eighth element** of the Periodic Table is the **Oxygen** atom which consists of 8 protons and 8 neutrons arranged as 4 complete octagonal-shaped nucleon layers. The width of an oxygen atom is 84.4 pm and its height is 57 pm (the same as the hexagonal graphite C-12 atom).

Oxygen is a highly reactive non-metal and oxidizing agent that, by mass, is the third-most abundant element in the universe after hydrogen and helium, and is totally essential for all known forms of life.

The oxygen gas molecule **Dioxygen** (**O_2**) consists of two oxygen atoms linearly joined by 2 b-bonds of length 36.4 pm, as shown in figure 47, to produce a centre-to-centre bond-width of 120.8 pm. Should the upper and lower nucleon layers be the same (e.g. both be neutron layers as shown in figure 47), then the atoms are rotated 45^O to each other around the vertical (z-axis), and there is an offset height of 15 pm. Should one atom have upper and lower neutron layers and the other upper and lower proton layers, then no rotation is required and there is no height offset.

Dioxygen (usually simply called 'oxygen') is a major component (about 21% by volume) of Earth's atmosphere, although early in Earth's history the atmosphere contained almost no oxygen. Microbes that produce their food via photosynthesis generate oxygen as a by-product which, combined with photosynthesis by plants, built up in Earth's atmosphere, drastically changing the environment and the history of life on Earth in the process.

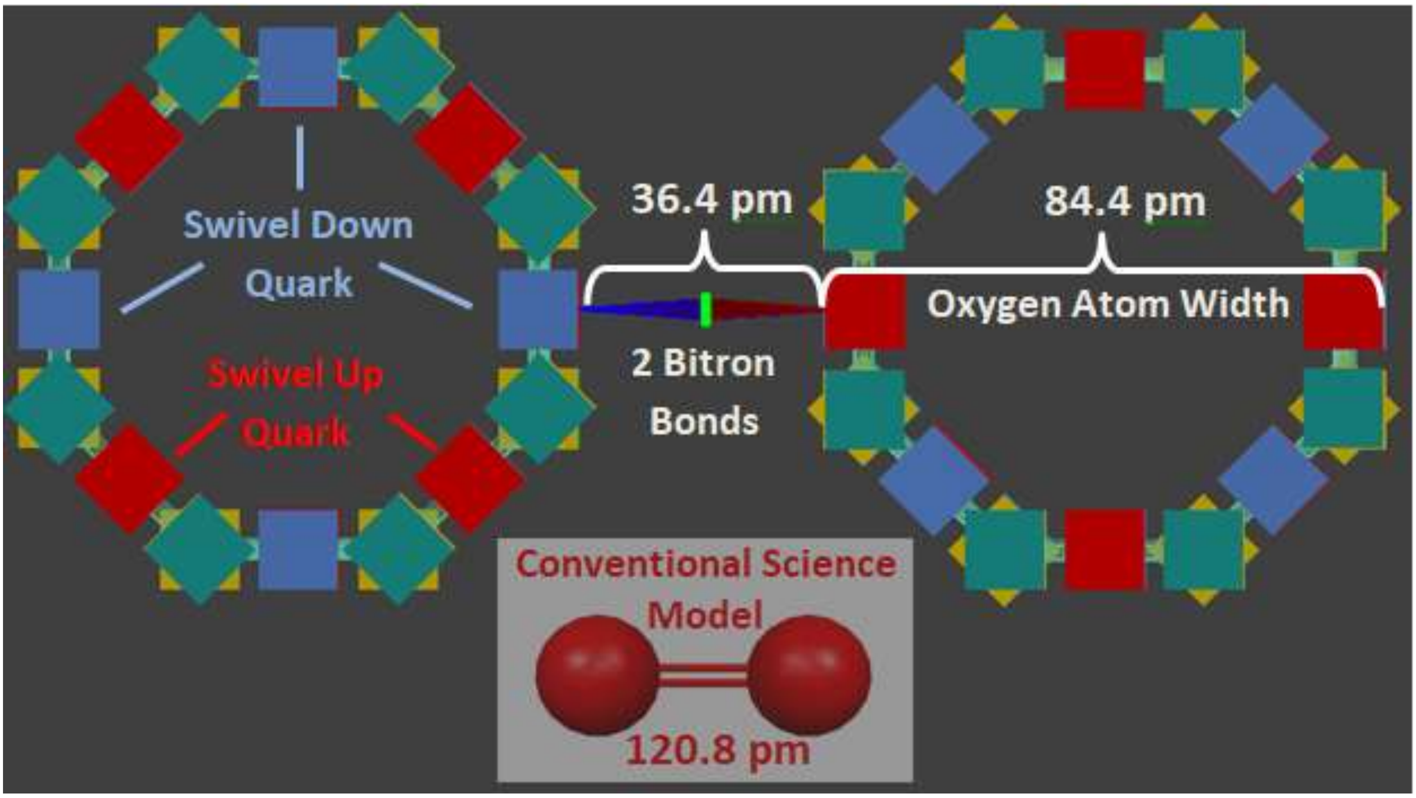

Figure 47: Bar Model of Dioxygen (O_2) Molecule

Ozone (**O_3** or **tri-oxygen**) is an allotrope of oxygen that is much less stable than the dioxygen. About 90% of ozone in the atmosphere is **stratospheric ozone**, which is concentrated between 15 and 30 kilometres above the earth's surface. **Tropospheric ozone** is found in lower concentrations at ground level where it is a key component of smog over major cities. Stratospheric ozone covers the entire planet (the Earth's ozone layer) and protects life on earth by absorbing harmful ultraviolet-B (UV-B) radiation from the sun: prolonged exposure to UV-B radiation is linked to skin cancer, cataracts, genetic damage and immune system suppression in living organisms, and reduced productivity in agricultural crops and the food chain.

The process of ozone creation and destruction is called the **Chapman Cycle**. It starts with the photolysis of molecular dioxygen molecules, which releases a pair of oxygen atoms, each of which attach to separate dioxygen molecules to create ozone. Then the ozone starts to react with newly photolysis-generated oxygen atoms to create dioxygen atoms to complete the cycle.

When a third oxygen atom becomes attached to a linear dioxygen molecule, the 2 end-atoms start to flap about as they are buffeted by other molecules, but quickly find a stable equilibrium point at an angle of 116.8^O to each other on opposite sides of the central oxygen atom as in figure 48.

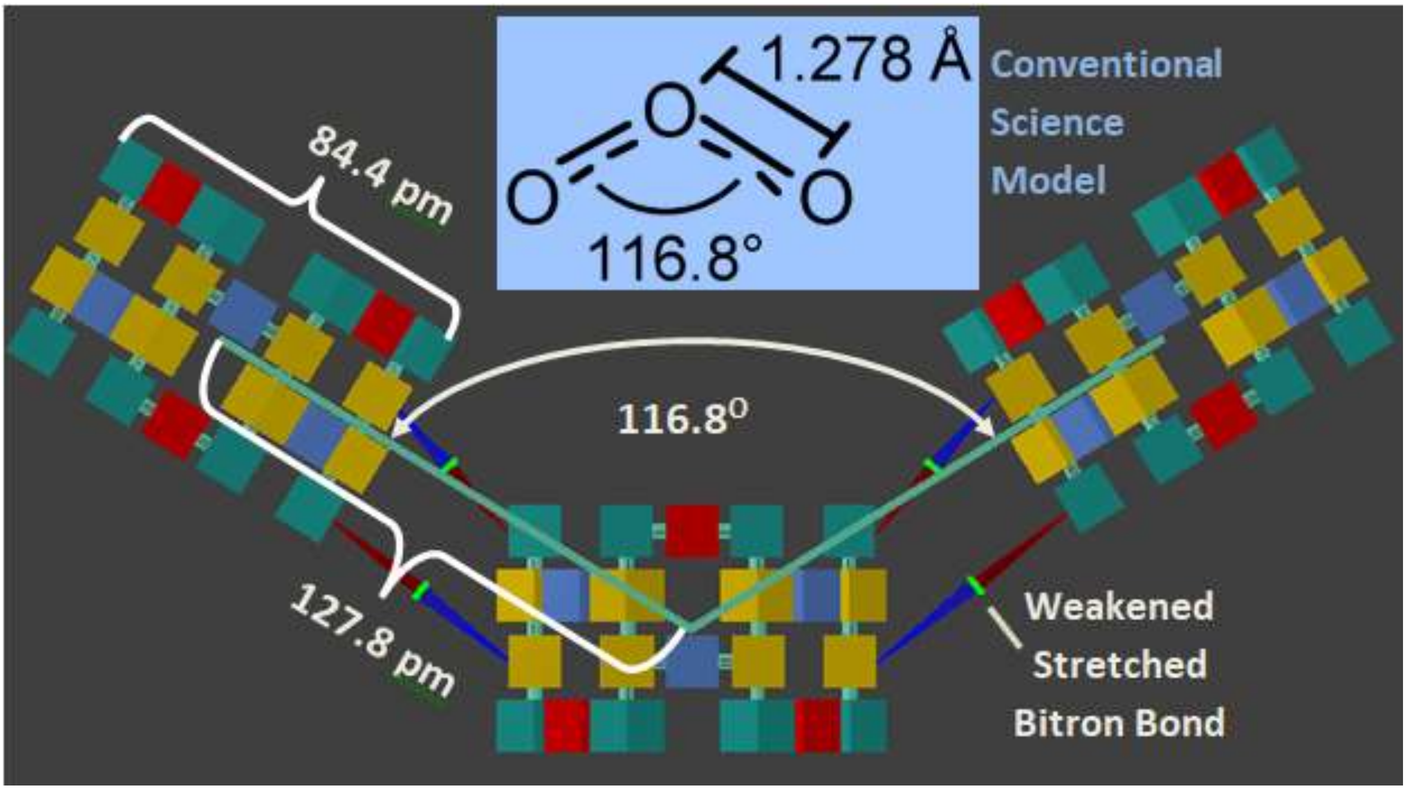

Figure 48: Bar Model of Ozone (O_3) Molecule

When in the equilibrium position, one of the b-bonds on each side is stretched wider than the other b-bond, thus providing a weaker link. Conventional Science uses a dashed line to indicate weak-link b-bonds as in the insert graphic of figure 48; or, in a less satisfactory way, by resonance bond diagrams involving single and double links.

The stretched b-bonds are a point of weakness in an O_3 molecule, and either one of the end oxygen atoms can relatively easily be dislodged to produce O_2 and a free oxygen atom ($O_3 \rightarrow O_2 + O$); or an untenable fourth single oxygen atom attach to one of ozone's end atoms, causing it to split into 2 O_2 molecules ($O_3 + O \rightarrow 2O_2$). Either of these 2 alternatives completes the Chapman Cycle.

Water (**H_2O**) is a transparent, almost colourless simple molecular compound with complicated characteristics. It exists in gaseous, liquid, and solid states, and it is the main constituent of Earth's hydrosphere. At room temperature it is a tasteless and odourless liquid with the ability to dissolve many other substances and, even though it provides no calories or organic nutrients, it represents a solvent that is vital for all known forms of life. Up to 60% of the human adult body consists of water: 73% for the brain and heart, 83% for the lungs, 64% for skin, 79% for muscles and kidneys, and 31% for bones.

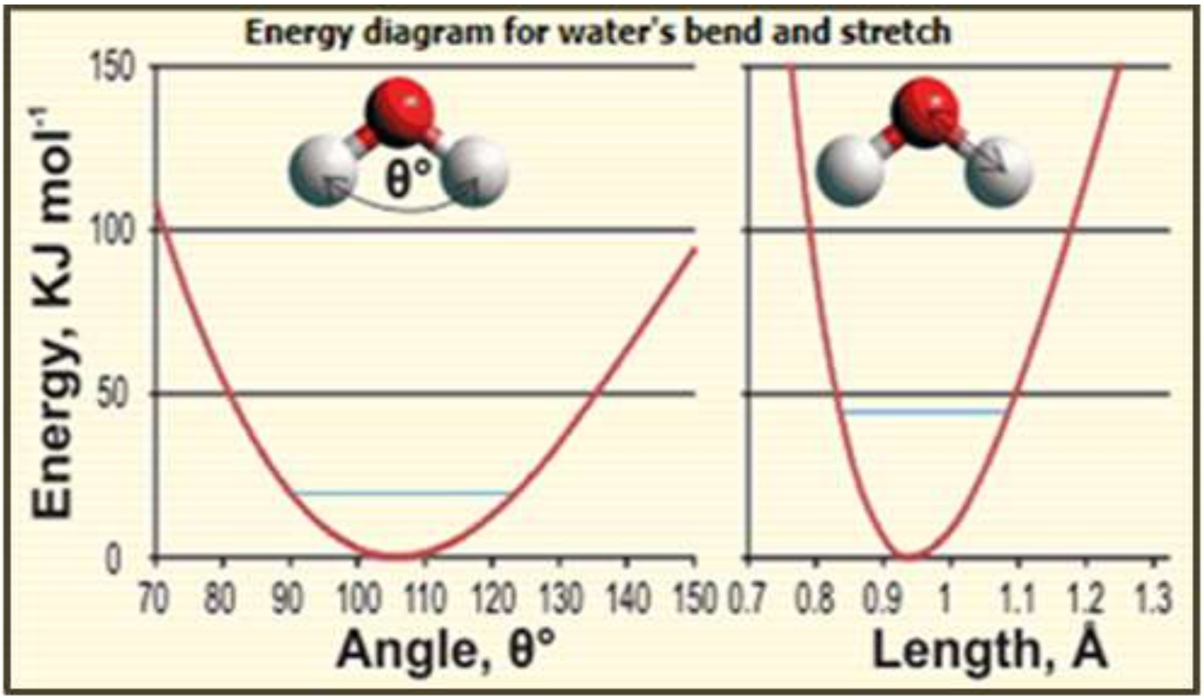

Figure 49: Energy-Induced Bond Bend and Stretch Variation for Gaseous Water (Steam)

The nominal H-O-H bond angle of water is 104.5^{O} and centre-to-centre O-H bond length is 95.4 pm. However, inter-molecular buffeting causes the hydrogen atoms within water molecules to vibrate because, as water hydrogen pairs are bumped inwards towards each other, mutual repulsion causes them to immediately recoil outwards. In steam, this process causes water molecules to reach a **resonant vibration frequency** for a given level of thermal energy, with the H-O-H angle (called '**bend**') reducing and then over-correcting to produce a variance around the mean bond angle of 104.5^{O}, as shown by measured angles Θ in figure 49 (sourced from M Chaplin). Paralleling the vibrational variation in Θ is an apparent change in the length of the O-H bond (called '**stretch**'), as shown in the rightmost graph of figure 49.

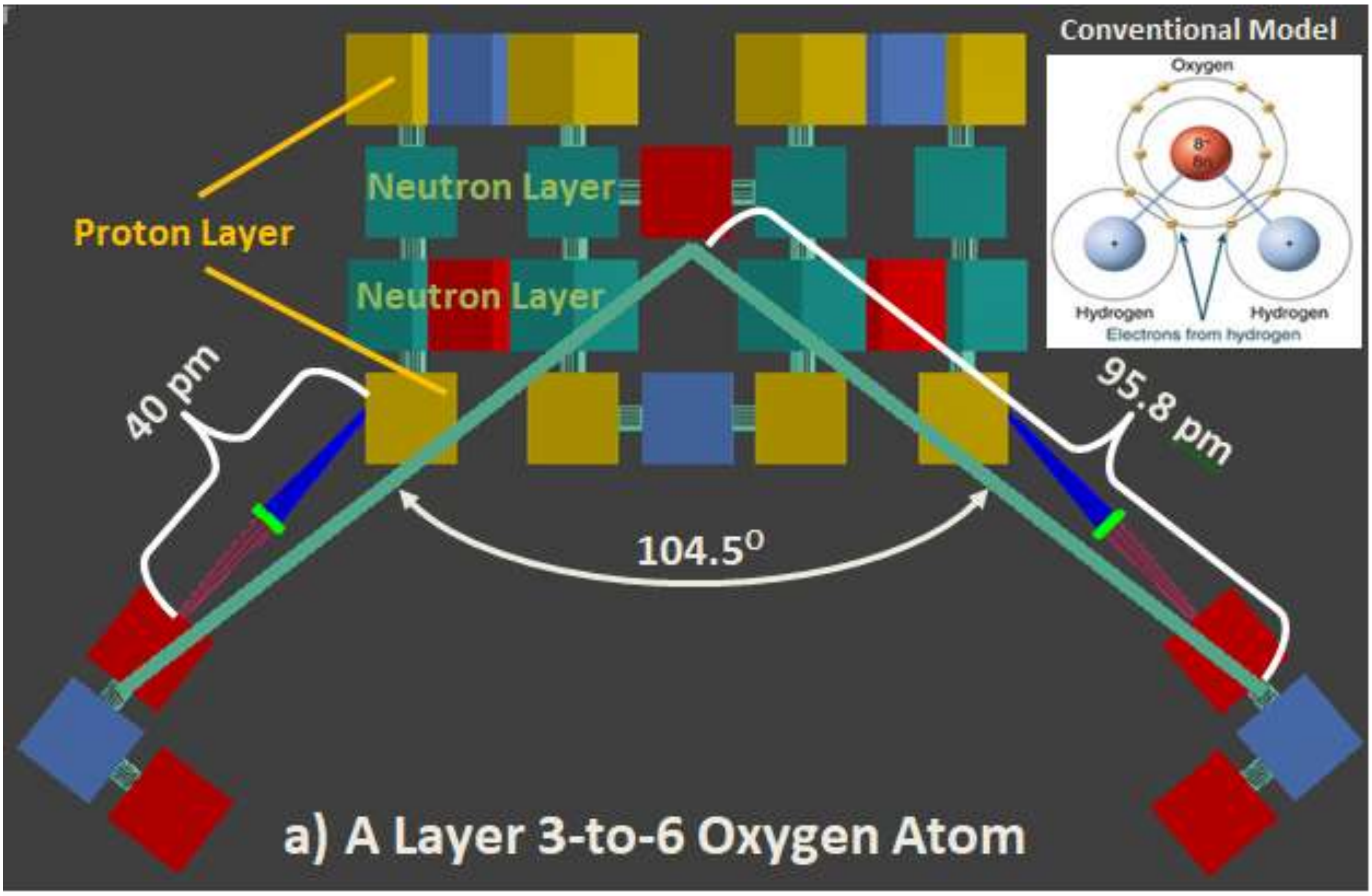

a) A Layer 3-to-6 Oxygen Atom

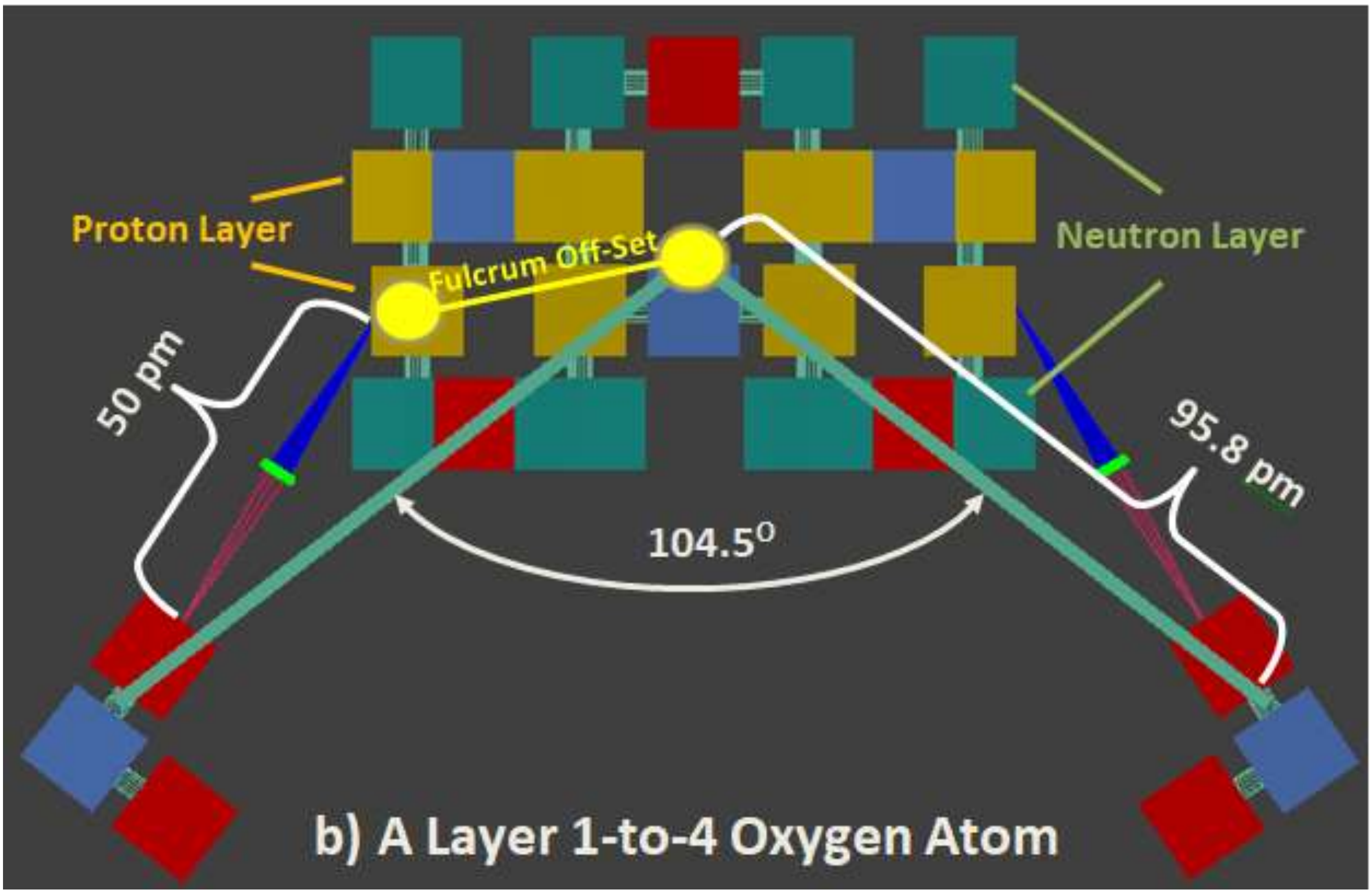

b) A Layer 1-to-4 Oxygen Atom

Figure 50: Alternative Forms for the Water Molecule

Figure 50 shows bar models for two forms of the water molecule: one (figure 50a) is based upon an oxygen atom with top-and-bottom proton layers (corresponding to layers 3-to-6 of figure 8) and the other for an oxygen atom with top-and-bottom neutron layers. For a nominal 95.4 pm centre-to-centre O-H bond length, the corresponding average O-H b-bond length is 45 pm (40 pm for the figure 50a configuration and 50 pm for the figure 50b configuration).

While conventional Science can accommodate vibrational bend due to thermal buffeting, it struggles to explain or justify bond-stretch (a typical ONAM model for water is shown as an insert graphic in figure 50a). However, for STEM, an explanation for bend and stretch is quite straight-forward: due to the **off-set** between the O-H b-bond fulcrum point (a swivel down quark) and the centre of the oxygen atom (as clearly labelled in figure 50b), with bend-vibration causing a corresponding apparent centre-to-centre O-H bond length change. Thus there is negligible stretch in the O-H b-bond (i.e. b-bonds remain the same length), with the bend-angle changes causing apparent bond length stretch (and shrinkage), with both bend and stretch seeming to occur in unison.

Because originally one cubic centimetre of water was used to define the gram, the density of water is nominally1 g/cc at standard temperature and pressure. However, the density of water varies non-linearly with temperature and, as can be seen in the magnified section of the figure 51 graph. As the temperature increases from 0^{O}C, the density rises to peak at 3.98°C, and then decreases. This initial increase of density of water from 0^{O}C to a maximum at 4^{O}C is most unusual because the density of all other liquids consistently decreases as they are heated from their frozen form.

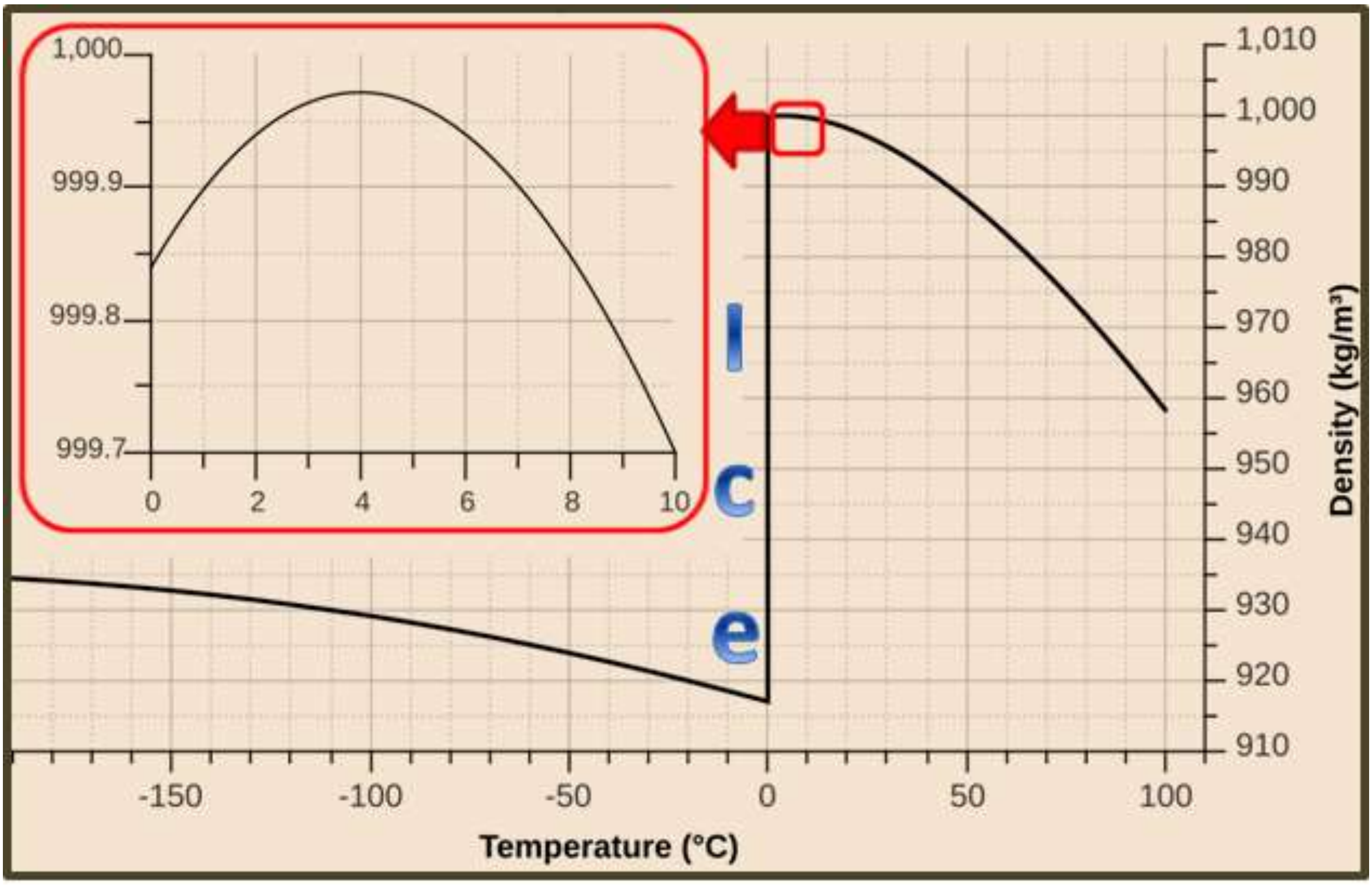

Figure 51: Density of Water (Solid and Liquid) by Temperature

There is no widely accepted explanation for the anomalous change in water's density between 0^{O}C and 4^{O}C, but one of the strong contenders is the two-state model of liquid water based on computer simulations in the 1990's. STEM suggests that slight differences in b-bond length and angle between the layer 3-to-6 and layer 1-to-4 forms of the oxygen atom within water molecules (as evident in figure 50) represents two populations of water molecules, each with slightly different physical characteristics that would be supportive of a 2-state explanation.

In its solid phase as ice, particularly in snowflake form, the dominant form of water molecules becomes hexagonal. As thermal energy reduces as the freezing point is approached, the positive charge of the water molecules' spinning hydrogen atoms attempt to maximise their separation which in turn causes the water molecules to form into hexagonal groupings (see figure 52) with pairs of water atoms facing each other becoming rotated 45^{O} to each other axially, an angle which is locked in by the formation of four p-bonds (bitron-free).

The hexagonal groupings of 6 water molecules repeats horizontally and become locked in by similar layers above and below, via more p-bonds. With a preferential growth pattern in the radii defined by the end-on-end connected arms produces the symmetry of snowflakes, and the randomness of new growth centres provides the almost limitless variety of snowflake patterns. With the space at the centre and apices of the hexagonal groupings of water molecules, when water freezes to form ice, its crystal structure its density reduces by about 9%,. This means that ice floats on water not yet frozen rather than sinking.

Depending on impurities and/or air bubbles, ice can appear transparent transitioning into a translucent to opaque bluish-white solid; and, depending on temperature, pressure and freeze-time, ice exhibits at least eighteen phases or packing geometries.

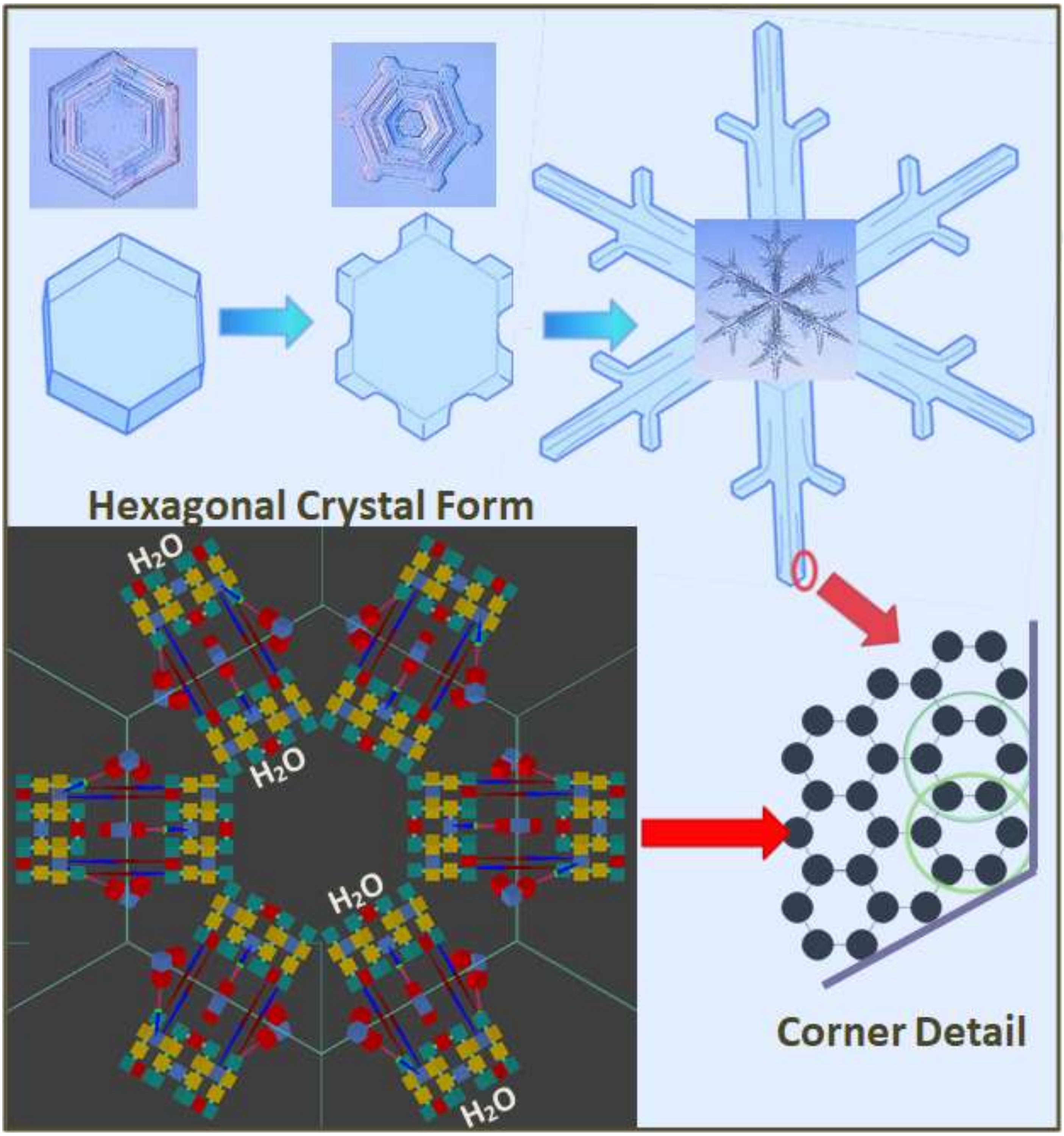

Figure 52: Ice Crystal Formation

Another remarkable property of pure water is **auto-ionisation** (or **self-ionisation**), wherein water dissociates to form hydronium (H_3O^+) and hydroxide (OH^-) ions. The two-way process is shown schematically in figure 53 and represented in animated form by Manuel Rivas's animated gif. Auto-ionisation results from a combination of endothermic molecular buffeting and electric field fluctuations between neighbouring molecules. It is most likely a two-step process that first releases a free proton that has a lifetime averaging about 70 microseconds (10^{-6} seconds) before it manages to attach itself to another molecule or anion.

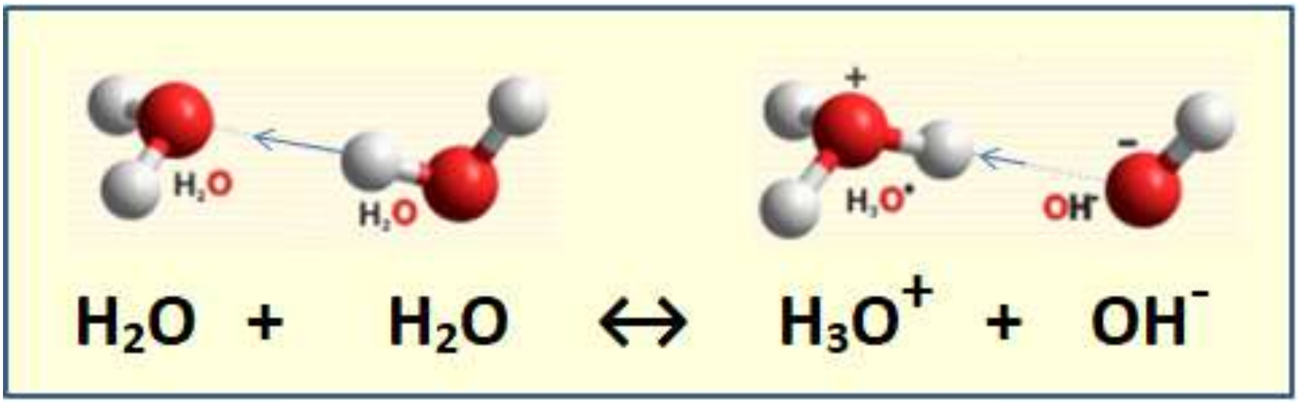

Figure 53: Water Auto-Ionisation and Ionic Hydration

When the process reverses it is often referred to as **ionic hydration**, which is also most likely to be a two-step proton-transfer process, but with the removed hydrogen atom (proton) attaching to a close-by hydroxide anion.

At 25 °C (77 °F) pure water has an equal number of hydroxide and hydronium ions, so it is a neutral solution with a pH of 7 and a pOH of 7, but this can vary dependent upon water temperature. A pH value less than 7 indicates an acidic solution, and a pH value more than 7 indicates a basic solution, with various chemicals added to adjust pH artificially (e.g. swimming pool chemicals).

The water molecule losing a hydrogen atom in the auto-ionisation process is most likely to have a an oxygen atom with top-and-bottom neutron layers (i.e. one that has a pair of positive outer surfaces corresponding to nucleon layers 1 to 4 in figure 8), and thus a slightly weaker hydrogen bond. Similarly, the newly released hydrogen atom (proton) is then most likely to attach to a close-by water molecule consisting of a water molecule centred upon an oxygen atom with top-and-bottom proton layers (i.e. one that has a pair of negative outer surfaces corresponding to nucleon layers 3 to 6) to form a hydronium cation such as shown in figure 54. Alternatively it may attach to a hydroxyl anion to form another water molecule to participate in the ionic hydration process.

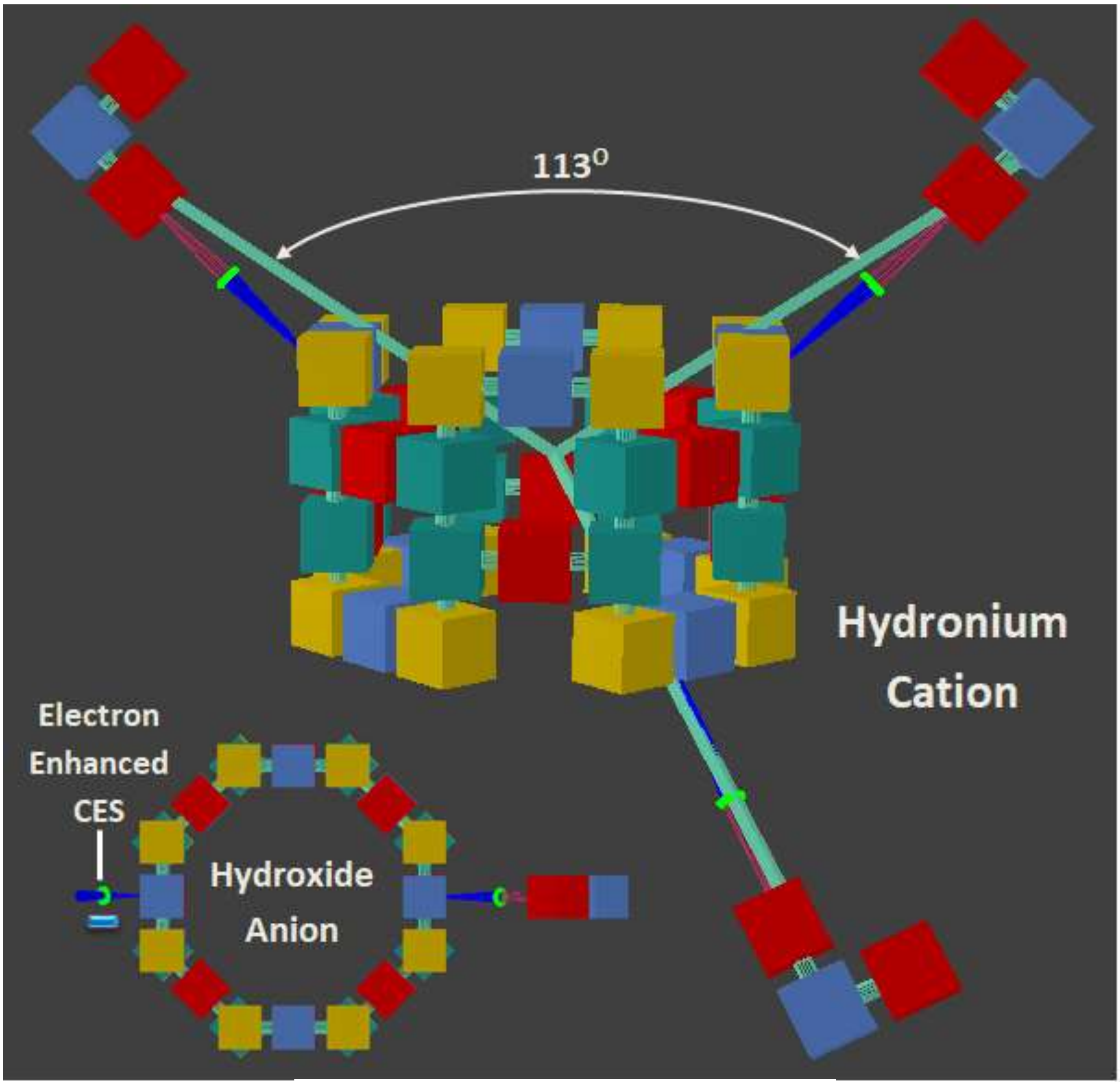

Figure 54: Hydronium and Hydroxide Ions

When a hydrogen atom is severed from its water molecule, the bitron tends to stay attached to the swivel down quark of the hydroxide anion, enhancing the e-CES field and thus making the swivel down quark more negatively energised (**CES enhancement** is covered in more detail in the Chemical Compounds: Ionisation and Redox chapter).

Water and alcohols have similar properties because they both contain hydroxyl groups that can form hydrogen bonds with other water molecules and with alcohol molecules; and thus they are reasonably soluble in water. The hydroxyl group is referred to as a hydrophilic ("water-loving") group, because it forms hydrogen bonds with water that enhance the solubility of an alcohol in water.

Hydroxyl radicals (**.OH**) are produced from the decomposition of hydro-peroxides (ROOH) or by the reaction of excited atomic oxygen with water. The hydroxyl radicals are very stable as a dilute gas, but are highly reactive and undergo chemical reactions to rapidly decay, making them short-lived. Hydroxyl radicals attack essential cell components and are therefore lethal to pathogenic viruses and bacteria.

Polymorphism, Embedding and Natural Variation

The geometric form and charge distribution of elements, and the location and energy level of swivel-quarks in particular, are major factors in the formation of chemical bonds between elements and compounds. Polymorphism and polymorph distribution serves to complicate the chemical bonding process and patterns, with polymorph mixing resulting in significant natural variation in the end-product compounds. Particularly within the hydrocarbon chemical production industry, procedures are designed to maximise the likelihood of the creation of particular chemical combinations and polymorphic forms.

Swivel-quarks are the main operatives responsible for manoeuvring atoms and complexes, either bringing them closer together and orientating them in a preferred docking position or pushing them away from each other, with the distribution of swivel-quarks around an atom being most important to the formation of chemical compounds. For an even-number of proton/neutron layer pairs (e.g. layers 1 to 4 of figure 8, which represents 2 proton/neutron layer pairs), the positive and negative swivel-quarks are evenly matched in strength and distribution on each polygonal side of the atom, whereas for odd number of proton/neutron layer pairs above 1, positive and negative swivel-quarks are dominant on adjacent sides (for a 6 layer atom positive to negative ratio is 2:1 and 1:2 on adjacent sides).

For complete polygonal layers (rightmost column in the stepped Periodic Table of figure 55a), the top and bottom layers are either positive or negative swivel-quark dominant. For an even-number of proton/neutron layer pairs, both top and bottom layers are either negative (as for non-metals) or positive (as for alkali and alkaline earth metals). For an odd-number of proton/neutron layer pairs (including a single layer pair), positive and negative swivel-quarks are dominant on the top and bottom layers. And for all elements with partial layers, the partial layer nucleon pattern changes the nominal full-layer pattern. (Note that the stepped Periodic Table of figure 55a is based upon the appearance of anther power-of-2 polygon. It inter-mixes traditional groupings such as Noble Gasses, Halogens etc.)

Another factor that affects the geometry and behavioural characteristics of atoms is the **embedding** of one atomic structure within another. Embedding, as shown in the generalised graphic of figure 55b, occurs when one or more polygonal forms become encapsulated within another larger diameter form, being held firmly by short, strong b-bonds internal to the outer structure(s). Embedding starts with fluorine (atomic number 9), becoming much more pronounced and structurally significant as atomic number increases from Period 3 onwards as shown in figure 55a.

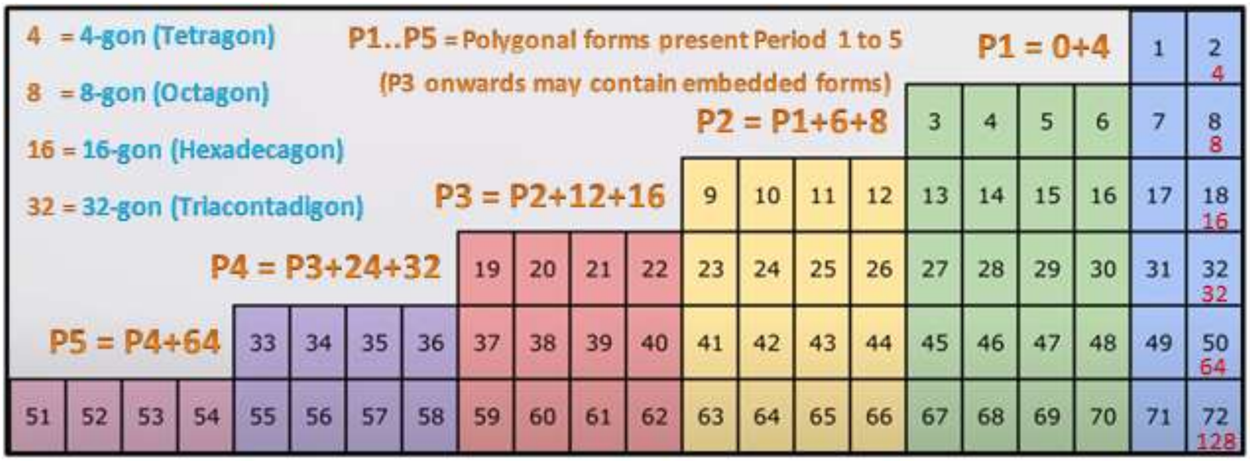

4 = 4-gon (Tetragon)
8 = 8-gon (Octagon)
16 = 16-gon (Hexadecagon)
32 = 32-gon (Triacontadigon)

P1..P5 = Polygonal forms present Period 1 to 5
(P3 onwards may contain embedded forms)

P1 = 0+4
P2 = P1+6+8
P3 = P2+12+16
P4 = P3+24+32
P5 = P4+64

																				1	2 4
																3	4	5	6	7	8 8
												9	10	11	12	13	14	15	16	17	18 16
								19	20	21	22	23	24	25	26	27	28	29	30	31	32 32
				33	34	35	36	37	38	39	40	41	42	43	44	45	46	47	48	49	50 64
51	52	53	54	55	56	57	58	59	60	61	62	63	64	65	66	67	68	69	70	71	72 128

Figure 55a: Stepped Periodic Table Showing Polygonal Form Development

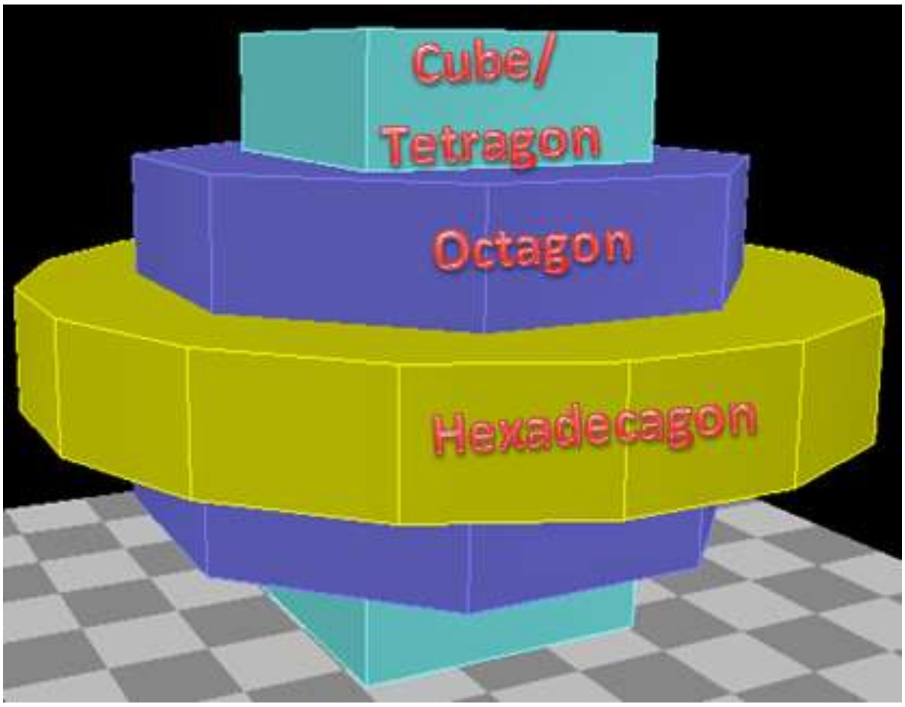

Figure 55b: Common Nuclear Polygonal Embedding Patterns

The tetragonal (diamond-style) and hexagonal (graphite-style) forms of the Carbon-12 atom provide an example of **polymorphism** at the nuclear level. Polymorphism is common in elements beyond carbon in the Periodic table, which contributes to the diversity in the chemical characteristics (e.g. valency, allotropic forms etc.) of many elements. Other polymorphs are fluorine-19, which could have a hexagonal form consisting of 3 complete proton/neutron layer pairs that contains no embedded forms; or a single hexagonal proton/neutron layer pair with an embedded boron-11 structure, as shown as figure 56.

As a third example of polymorphism, neon-20 could consist of a 5 complete cubic proton/neutron layer pairs; 2 8-gon chains (2 layer) and an embedded He-4; 2 complete pentagonal proton/neutron layer pairs; or be an embedded form consisting of a helium-4 structure (single layer pair cubic) embedded within an oxygen atom (a 2-layer pair octagonal structure). The 5 layer cubic form of neon-20 would seem unrealistically high (177 pm), and with no evidence indicating that it exists on Earth, it is discounted. The other 3 possible neon atomic structures will be discussed in more detail in the next chapter.

As well as the natural variations within elements as mentioned above, multiple isotopic forms of elements can be created by the attachment of L-form neutrons. Such attached neutrons can randomly **nucleon-type convert** into protons, as discussed in the Nucleon Type Conversion chapter. Like barnacles attaching to the bottom of a boat or a submerged object, surplus-to-needs neutrons can randomly attach to the top and bottom sides of atoms, with some not being able to type convert because they are connected via a flip-quark, whereas others foot-in attached to proton layers are able to randomly β-decay to a proton (and possibly back again) because they are connected via an invariant quark. Although attached nucleons can change the atomic and mass number of atoms, they do not significantly change either the atom’s basic polygonal geometry or its lateral bonding characteristics that are so important to the formation of chemical bonds.

Random nucleon attachment and type-conversion presents problems to ONAM because it classifies elements purely on the basis of the number of contained protons without any consideration of the geometry that might underpin the atom’s structure. One issue is that to remove or gain any surplus-to-needs neutrons, they need to pass though the atom’s electron haze without disrupting or causing discernible damage to the orbital electron clusters, and magically be plucked from or attached to the existing amorphous collection of nucleons that form the atom’s nucleus.

A second issue is that, although the β^- decay conversion process and associated by-products are well described, the cause and mechanics of the neutron-to-proton conversion process remains totally unexplained, except in terms of possible colour charge change. A third issue is that, the neutron-to-proton conversion must be accompanied by either the ionisation of the atom (creating a cation), or by an outer orbital simultaneously gaining an electron of the appropriate spin to keep the atom electrically neutral. A forth issue is that by having acquired a higher atomic number, the bonding and physical characteristics of the ‘new’ atom would also simultaneously change to those of the ‘new’ element. Similar issues apply to the reverse process associated with proton to a neutron conversion via β^+ decay.

With STEM, there are many variables related to the structure and size of atoms and their preferred bonding patterns, but due to natural variation, no rigid rules can be applied across the range of elements and their associated molecules and compounds. However, most observed physical characteristics and interactions can be readily modelled and explained using the STEM approach. On the other hand, ONAM struggles to explain the range of observed bonding patterns, and has to invoke the concept of hybrid orbitals. So, let's have a closer look at electron orbitals.

Until recent qubit research involving phosphorus anions, orbital electrons are neither observable nor trappable: such research deals only with an outer conduction band electron and provides no evidence of lower level electron orbitals. For bonding purposes orbital electrons are represented probabilistically by the 'spdf' orbitals, which have been derived from quantum mechanical wave equations. However, because of the complexity of the wave equation functions related to multi-electron inter-atom bonds, an exact analytic solution is not feasible, and thus first-level approximations are used, which are collectively referred to as orbital hybridisation. The practice of **orbital hybridisation** involves the selection of groups of electron 'spdf' orbitals which are then subjectively allocated pro-rata, superimposed and combined to form the required hybrid orbitals with different calculated energies (which have not been verified by observation) that have a directional orientation better aligned to observed chemical bond directions and geometries than the raw 'spdf' orbitals.

A hybrid bond thus represents a work-around solution that consists of using a number of electron equivalents from selected 'spdf' orbitals on a pro-rata basis to generate a **pseudo-bond**. For instance, in a carbon-12 atom the s-shell orbital is combined with 3 p-shell orbitals to form four equivalent **sp^3** hybrid orbitals, which are arranged in a tetrahedral pattern around the carbon atom to bond to four different atoms (e.g. CH_4). There are many carefully crafted hybrid forms (sp^x, sd^x and sp^xd^y), which combined with bond resonance, are required to accommodate bonding patterns observed between atoms.

Neither 'spdf' orbitals, hybrid orbitals nor resonance are required by STEM because bond angles are fully explained in terms of nucleus geometry, the degrees of freedom afforded by swivel quarks, and the availability of ionic orbital electrons. B-bonds (and, in some cases involving large bond-lengths, weaker bitron-free p-bonds) and/or covalent bonds involving the sharing of same-type ionic electrons, are considered to be the main forms of bonding, with ionic bonds being considered a special case of covalent bonding. These topics will be expanded upon in the next chapter.

Both STEM and ONAM models of atoms involve electrons with different spin patterns. For ONAM, an increase in atomic number (the number of nuclear protons) means that an atom gains another orbital electron, increasing to an unwieldly 100+ orbital electrons for group 7 elements. With only one pair of opposite spin electrons able to occupy the same orbital space, added electrons (corresponding to the number of protons added to the nucleus) are either paired or unpaired within outer orbitals. Similarly, for the STEM approach, up to two same-type ionic electrons can be supported within each ionic orbital, and bitrons within b-bonds can be released as either left-handed or right-handed chiral spin electrons and, as many bonds are double b-bonds, they can be released simultaneously when bonds are broken. Also, whereas for ONAM electrons are mysteriously sourced from some universally available supply of ready-made electrons, STEM considers the chirally-different forms of electrons are a **derived renewable resource**.

Re-capping, central to STEM is the hypothesis that **there is only one type of energy-generating material** (i.e. **energen**), with electrons, positrons, CES and related fundamental particles consisting of toroidal concentrations of energen. Quarks, nucleons and atoms consist of different combinations of these fundamental particles. **Energy** takes on many different forms (typically, about 10 different forms of energy can be identified), but all types of energy are considered to be derived from the field-energy associated with the fundamental particles in a variety of configurations and environments.

Atomic Structure: Fluorine and Neon

Fluorine is the 9th element in the periodic table, and represents the lightest halogen and which is a pale yellow, highly toxic diatomic gas. Fluorine is the most electronegative of all elements, and is thus extremely reactive, reacting with all elements except for argon, neon, and helium. Only one isotope (F-19) of fluorine occurs naturally in abundance, although several short-lived isotopes have been created synthetically.

Fluorine is the first element to have a distinctly embedded form. As can be seen in figure 56, it consists of a single octagonal proton-neutron layer pair with an **embedded boron-11** structure held in place by 4 internal b-bonds.

Whereas other Period 2 non-metals (carbon, nitrogen and oxygen) have a mix of atoms with neutron and proton upper-and-lower layers, the **stable electronegative characteristics** of fluorine suggest that the embedded boron-11 structure might have a preference for an upper-and-lower proton layer as shown in figure 56.

With a centre-to-centre bond length of 140 pm, the single b-bond joining a pair of F-19 atoms together has a length of 87 pm, and thus the bond is relatively weak. Also, the swivel quark on at least one side the connecting b-bond is restrained because it is also shared by an internal b-bond. Although the restrained swivel quark as shown in figure 56 is a down-quark, with the boron-11 structure rotated by 45^{O}, it has equal probability of being a swivel up-quark. Thus diatomic fluorine could be expected to be a mix consisting of about 2/3 diatoms with one side of the connecting b-bond being restrained, possibly having a V-form; and 1/3 linear, having both atoms restrained to a common axis.

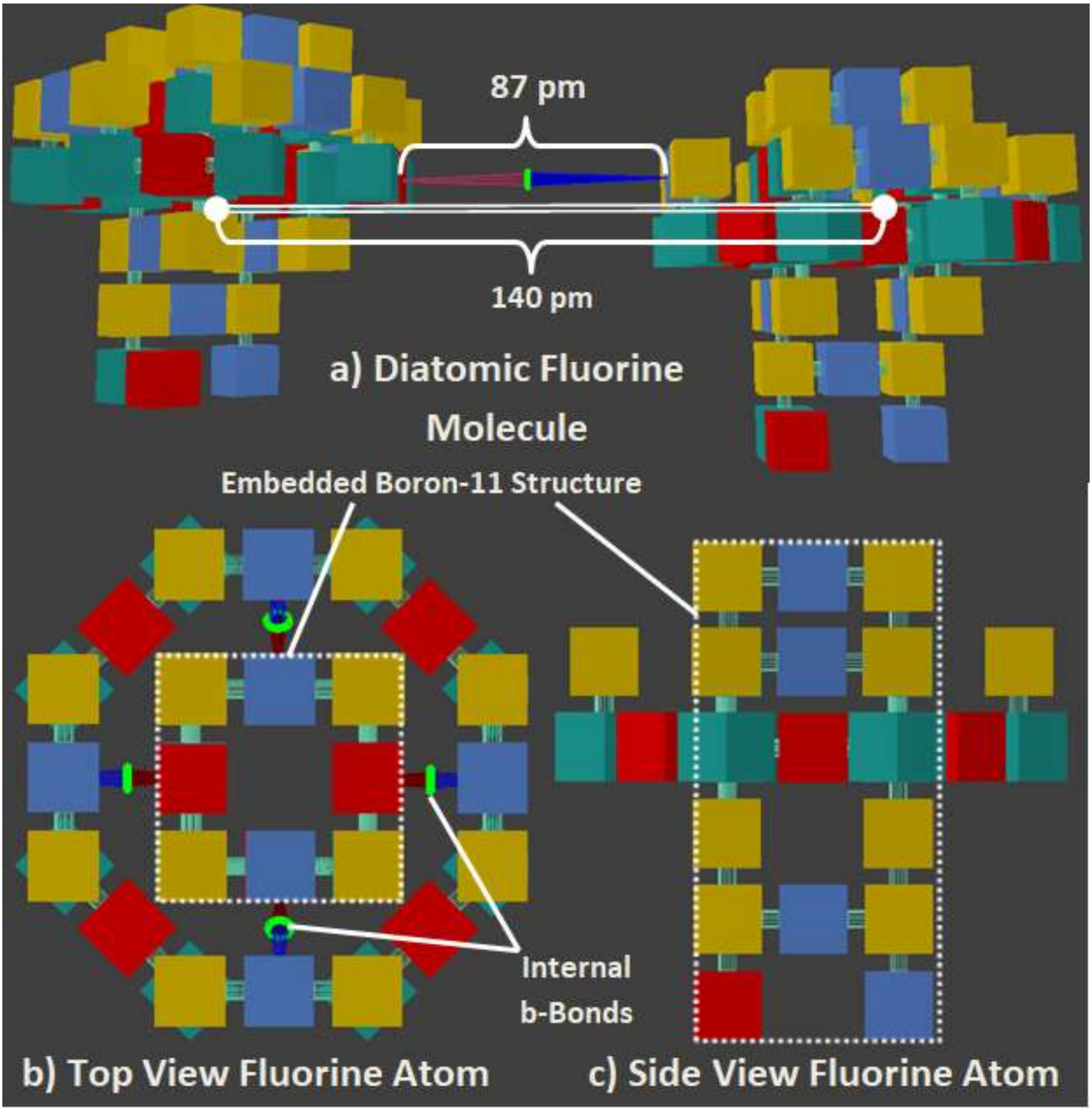

Figure 56: Fluorine Embedded Atomic and Diatomic Molecule Structure

Diatomic fluorine gas crystallizes at −220 °C (−364 °F) to form a transparent and soft a disordered cubic structure (reminiscent of crystallized solid oxygen due to the octagonal proton-neutron layer that is compatible with that of oxygen): it is referred to as **β-fluorine**.

Within the cubic structure of β-fluorine, the orientation of diatomic fluorine molecules at the unit cube apices is random (possibly corresponding to the 1/3 of molecules that are linearly aligned), whereas all other molecules (possibly corresponding to the 2/3 with only one side restrained) are orientated parallel to one of the cube faces due to a combination of their angular V-form and cubic/octagonal forms. G Rech's animation dynamically shows the range and distribution of orientation of β-fluorine's molecules (note that this animation should not be interpreted to infer that molecules continue to tumble and rotate within the β-fluorine crystal structure).

Neon

Neon is the 10th element in the periodic table. It is a colourless, odourless, inert monatomic gas with about two-thirds the density of air under standard temperature and pressure. It is a noble gas and has 3 stable isotopes: Ne-20 (90.48%), Ne-21 (0.27%) and Ne-22 (9.25%).

The reason for neon's relative scarcity on Earth is that it is highly volatile and forms no solid compounds to fix it (only traces of [NeAr]+, [NeH]+, and [HeNe]+ ions have been observed from optical and mass spectrometric studies). Thus, although being the 5th most abundant chemical element in the Universe by mass, neon's relative rarity on Earth is due to its relative lightness, high vapour pressure at very low temperatures, and chemical inertness: all properties that are not dissimilar to those of helium (but helium has the advantage that it can become temporarily embedded within other atoms).

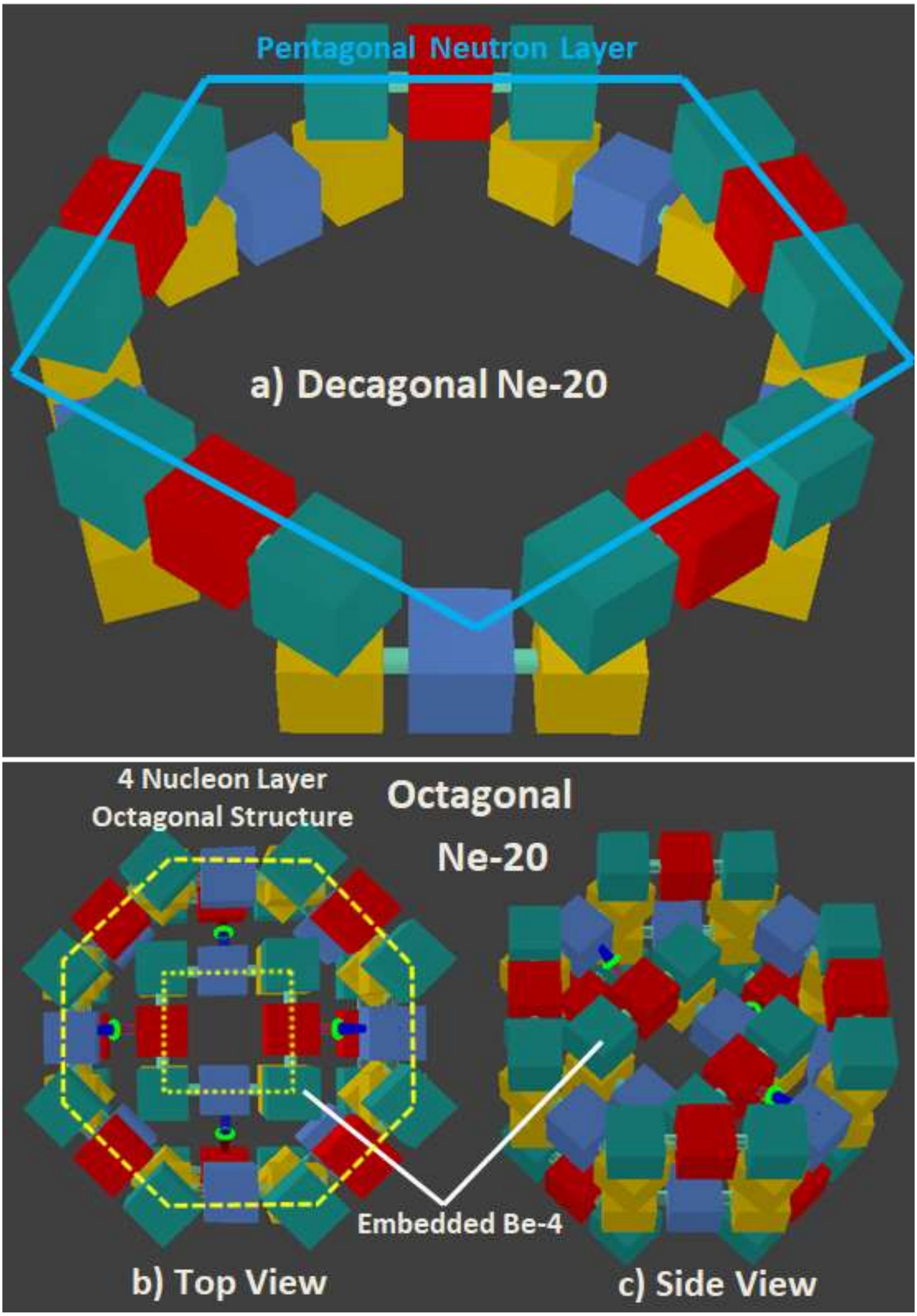

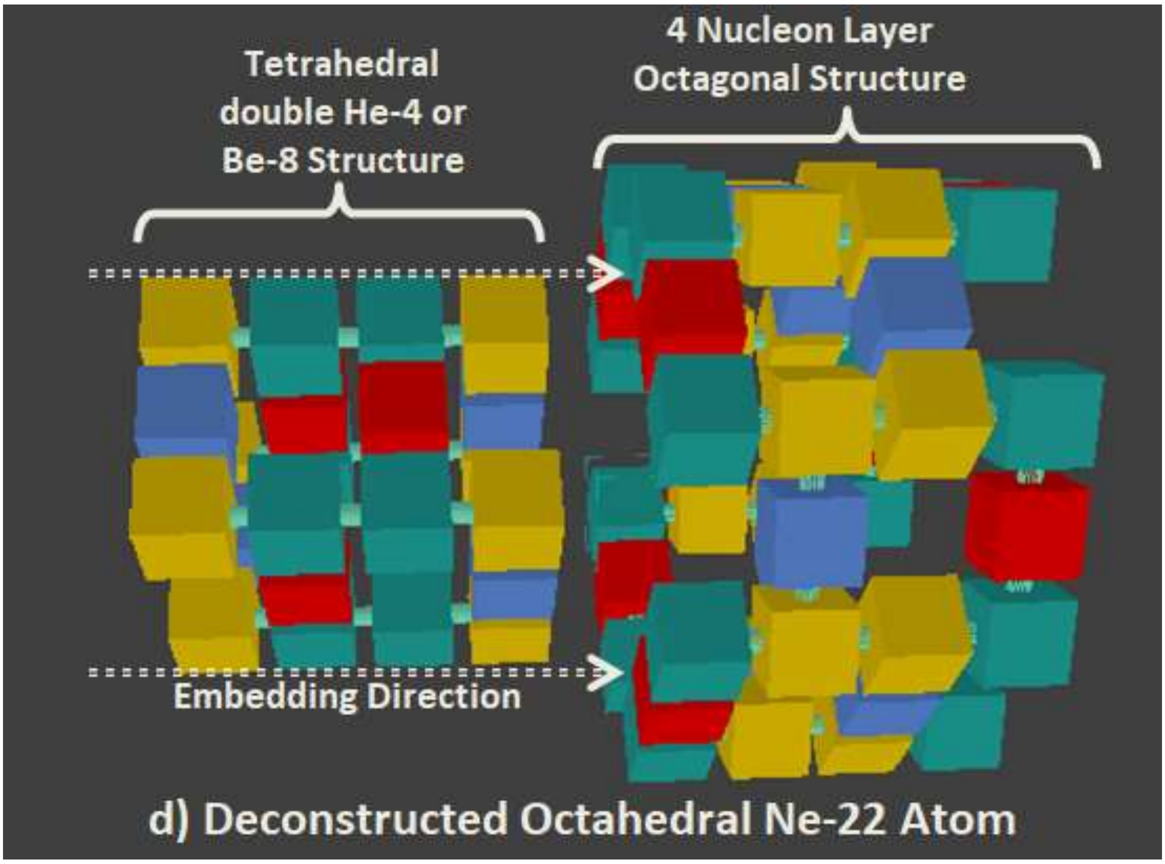

Figure 57: Neon-20 and Embedded Neon-22 Atomic Structures

Neon has 3 isotopic atomic forms, all of which are stable. Neon-20 (Ne-20) is the most abundant at about 90.4%: it consists of a single decagonal (10-sided polygon) structure with only the 1 proton/neutron layer pair, with each layer having a pentagonal shape as highlighted in blue in figure 57a. Ne-22 is the next most abundant form (at about 9.3%) and Ne-21 is the least abundant isotope (at about 0.3%).

Evidence suggests that Neon-20 has been produced in the dense cores of highly evolved stars, wherein helium was consumed by the generation of cubic (diamond form) carbon-12, oxygen-16, neon-20, and magnesium-24. By the time the core of such star was sufficiently massive and reaching temperatures in the order of 700 million K, protons, neutrons, and helium-4 nuclei are considered to have interacted with the newly created nuclei to produce a variety of other elements including fluorine and sodium, and possibly the neon isotopes Ne-21 and Ne-22.

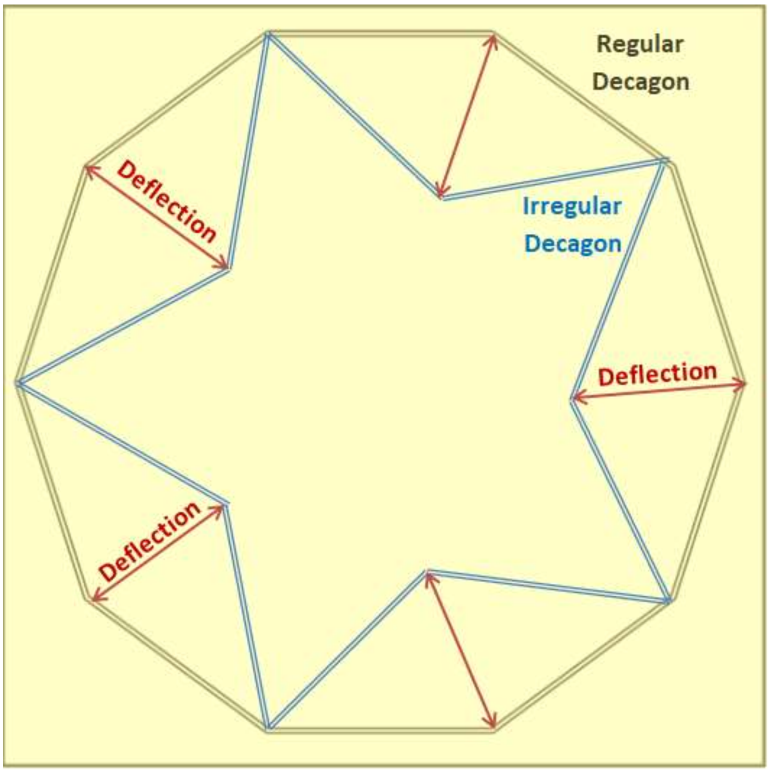

Figure 58: Potential Flexing and Distortion of Neon-20 Structure

The 2 minor isotopes have possibly been derived nucleogenically from magnesium sodium, silicon, and/or aluminium as part of the settling out process. Should this be the case, then Ne-21 and Ne-22, and quite likely some Ne-20 atoms as well, would consist of a double octagonal (i.e.4 nucleon layers) structure and various embedded tetragonal He-4 forms: He-4 for Ne-20 (figure 57b and 57c); He-3 for Ne-21; and Be-8 for Ne-22, either as a diatomic He-4 pseudo-molecule or as an inter-quark bonded He-4 pair (as in figure 57d). Note that the embedded Be-8 form within Ne-22 would be held by 8 b-bonds, double that for its Ne-20 and Ne-21 equivalents, which would provide it with increased stability and strength and could account for its higher abundance with respect to Ne-21.

The decagonal structure of Ne-20 is quite pliable and easily be distorted from a regular decagon by movement around the nucleon articulation axes in keeping with the deflection directions such as shown in exaggerated form as figure 58, which accounts to why, as a monatomic gas, it is not readily able (if at all) to bond with other atoms and complexes.

A clathrate is a general term for a compound in which molecules of one substance, commonly a noble gas, are completely enclosed within the crystal structure of another substance. Solid **neon clathrate hydrate** is produced from an admix of water-ice and neon gas at pressures 0.35–0.48 GPa and temperatures about −30 °C. Within neon clathrate, the pentagonal proton and neutron layer shape of individual Ne-20 atoms causes the ice-water molecules to crystallise as dodecahedron igloos (see figure 59: note that the oxygen atoms are not to scale - they should be larger and closer to the size of the neon atoms) with 12 pentagonal faces around individual Ne-20 atoms. Once the dodecahedron igloos are in place, due to their pliable nature, neon atoms can freely move through the material.

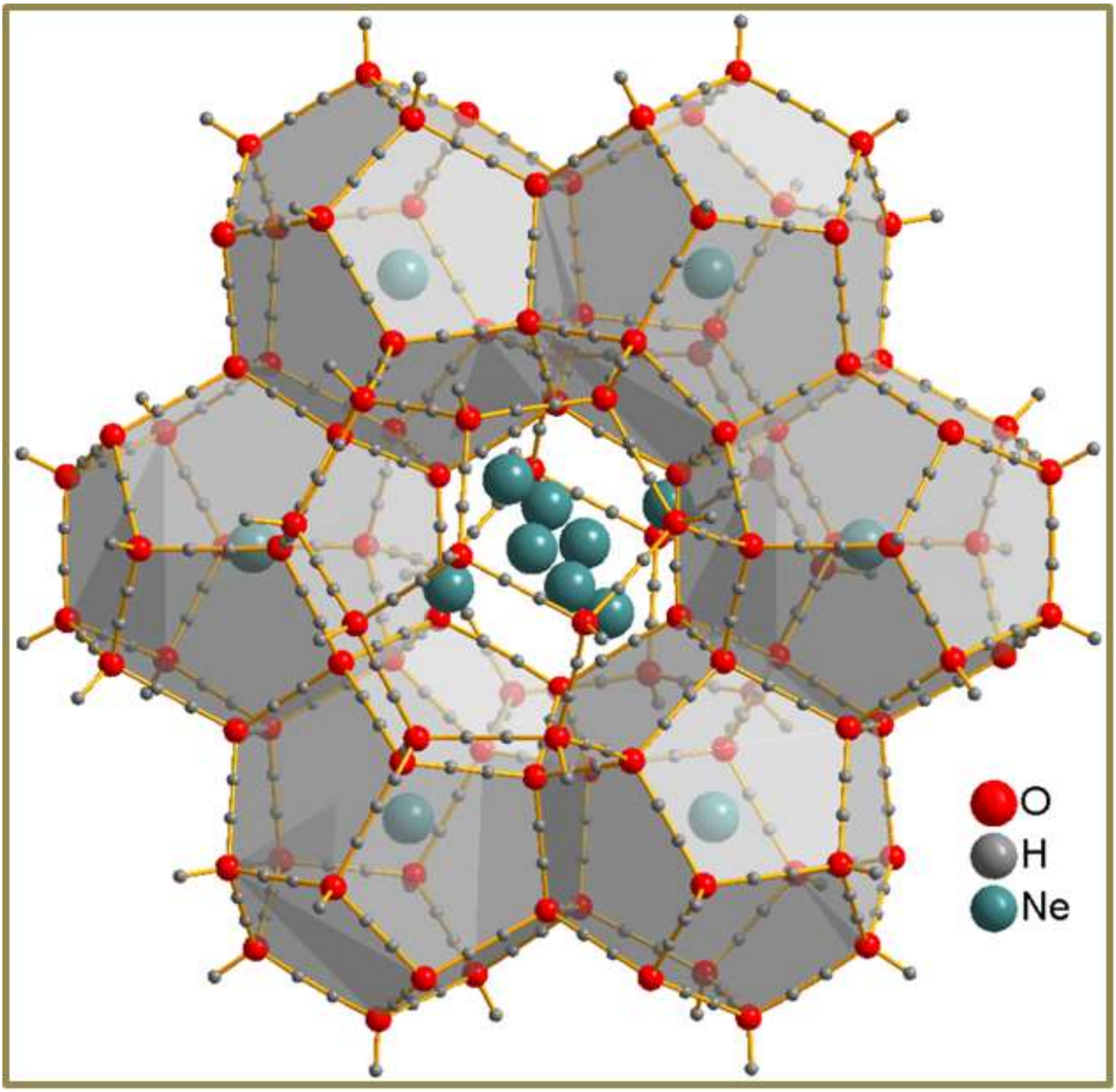

Figure 59: Neon Clathrate Hydrate Structure

Atomic Structure: Period 3 and Onwards

As discussed so far, an element's atoms can present with multiple polymorphic structures, with sub-structure embedding further increasing the possibilities. Particularly as atomic number increases from period 3 onwards, the range of possible polymorphic forms also increases, with the modelling process becoming one of identifying which polymorphic forms are feasible and best match observed bonding geometries for molecules and compounds.

Sodium

Sodium is the 11th element in the periodic table. It is a group-1 alkali metal that is the first element of period-3 of the Periodic table. Similarly to lithium (the period-2 alkali metal), it is a soft, highly reactive metal. Na-23 is sodium's only stable isotope.

As for one of neon's octahedral polymorphic forms, Na-23 consists of a double octahedral layer plus an embedded Li-7 form as shown in figure 60.

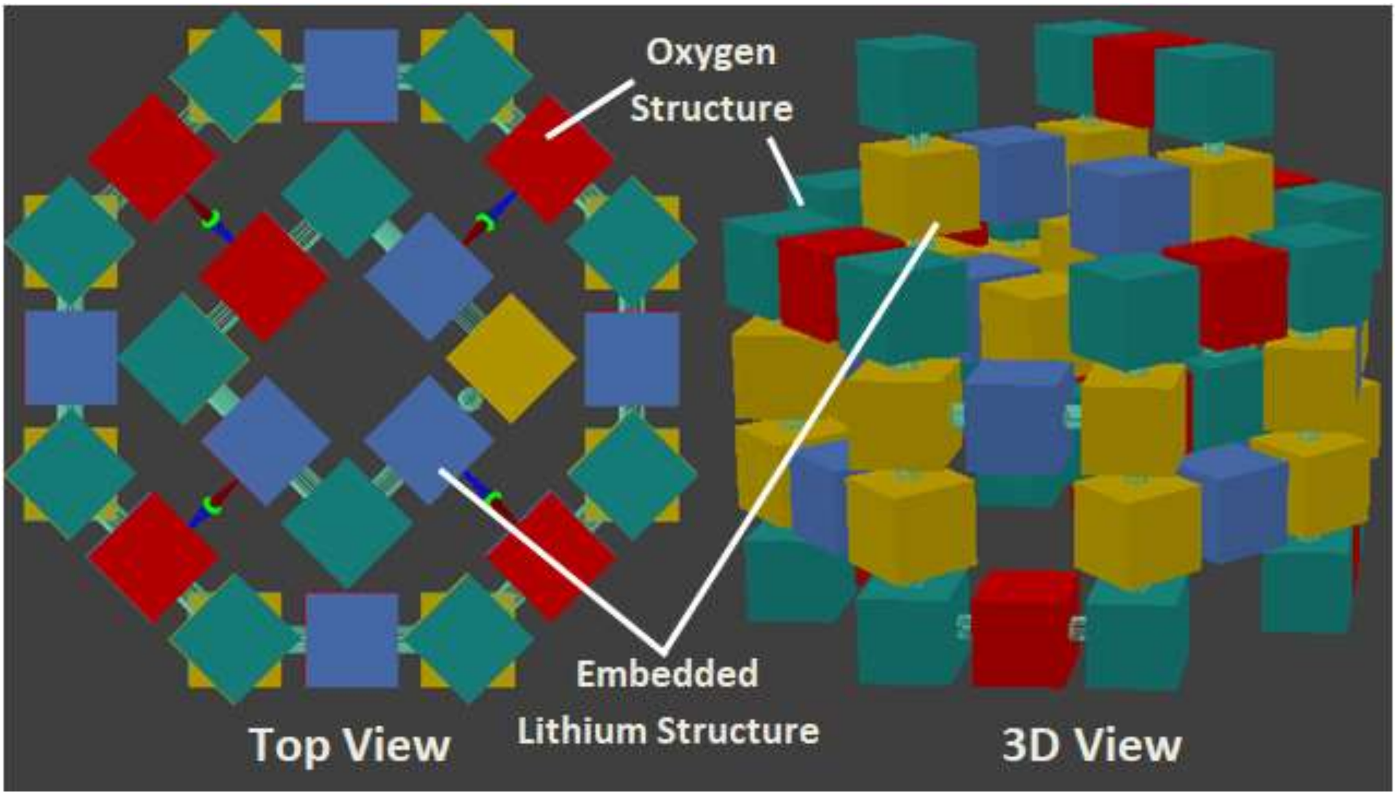

Figure 60: Embedded Structure of Sodium-23 Atom

Whereas diatomic oxygen has a fairly equal mix of atoms with proton and neutron upper-and-lower layers, the low electronegativity of Na-23 suggests that it has a preponderance of upper and lower neutron layers as shown. Also, the upper (as shown in figure 60) unrestrained swivel up quark would account for reactive nature of sodium metal.

Magnesium

Magnesium, the 12th element in the periodic table, and has 5 possible polymorphic forms: a tetragonal consisting of 6 proton/neutron layer pairs; a hexagonal consisting of 4 proton/neutron layer pairs; an octagonal consisting of 3 proton/neutron layer pairs; a one duodecagonal (12-gon) proton/neutron layer pair; or an outer octagonal proton-neutron layer pair plus an embedded Be-8 form.

Although magnesium falls within the beryllium-group (group-2), a 12 nucleon-layer high tetragonal seems unreasonable and unsupported by chemical evidence, as does the duodecagonal form. However, the octagonal form with an embedded Be-8 structure and the hexagonal forms are distinct possibilities. Because, in solid metal form, magnesium has a hexagonal close-packed (HCP) structure, Mg-24 with 79% abundance would most likely consist predominantly of the hexagonal polymorph, and the other 2 isotopes, Mg-25 (10% abundance) and Mg-26 (11%), are possibly a combination of the two octagonal forms (the 6 nucleon layer octagonal or the 4 layer embedded octagonal polymorph). As can be seen, there are many possibilities and much more targeted research is needed to determine which polymorphic and isotopic forms are at play, and to determine their distribution and mix within compounds.

Aluminium

Aluminium is the 13th element in the periodic table. It has one stable isotope, Al-27 (100% abundance), which is a soft, ductile, silver-coloured, non-magnetic metal. Because the crystal form of aluminium metal is face-centred cubic (fcc), the octagonal form consisting of 3 proton/neutron layer pairs (as for the non-embedded magnesium octagonal form) plus a part layer consisting of 2 neutrons and 1 proton (see figure 61b).

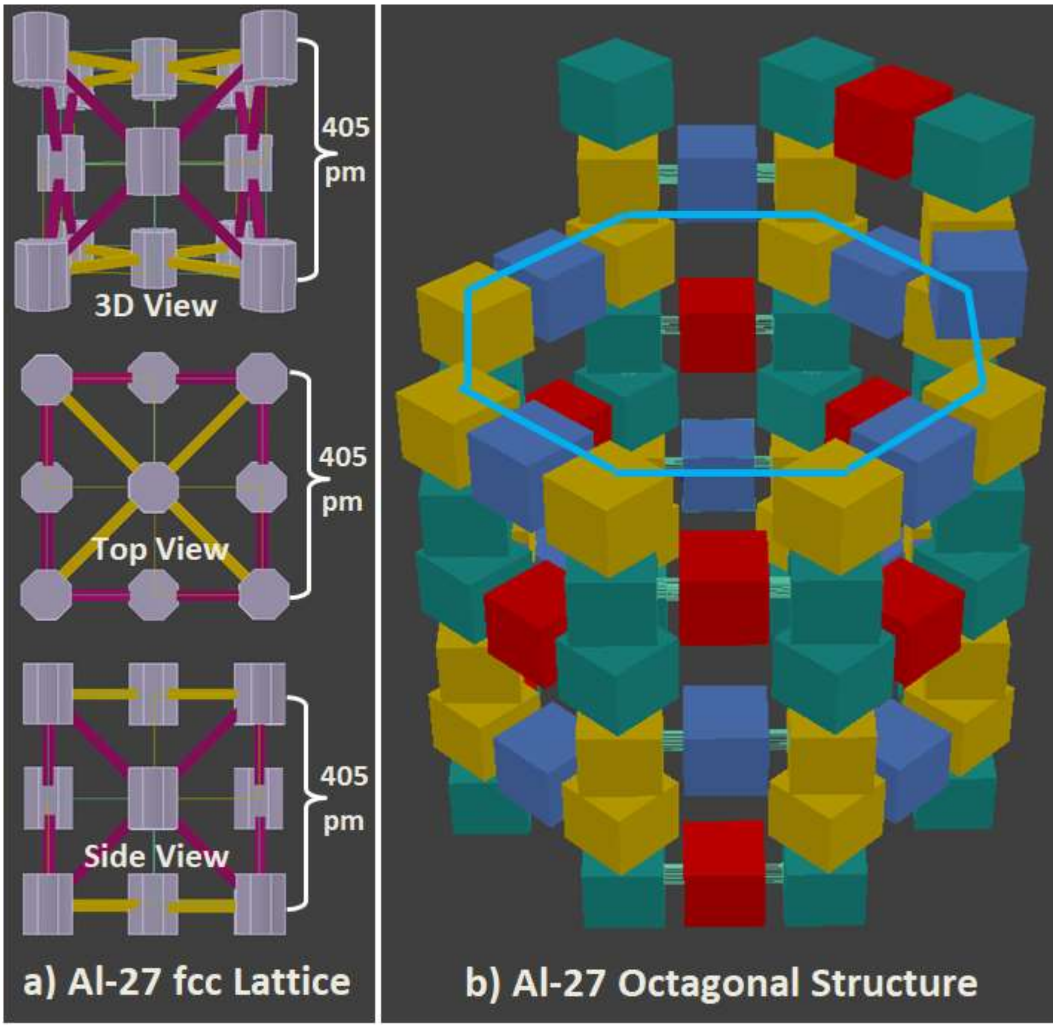

a) Al-27 fcc Lattice

b) Al-27 Octagonal Structure

Figure 61: Structure of Aluminium-27 Atom and Face-Centred-Cubic Crystal Structure

Figure 61a is to scale and shows the main bonding related to the fcc crystal form of aluminium metal related to a unit cube of side length 405 pm: in order to not over-complicate the diagram, bonding between the face-central atoms that form a central square prism have not been shown. Horizontal and vertical bonds (e.g. between unit cube's vertices) are 304 pm and are thus quite weak p-bonds. Diagonal bonds (purple and yellow in figure 61a) are all approximately 100 pm, and would be weak b-bonds, which accounts for why aluminium metal is a soft metal and is such a good electrical conductor.

Silicon

Silicon is the 14th element in the periodic table, and is a hard, brittle crystalline solid. It is a tetravalent metalloid and is relatively unreactive and which, in pure form, is an insulator: however by the addition of dopants it becomes a semiconductor material that can conduct electricity, and is widely used as such within semiconductor technologies. With an abundance of 92%, Si-28 is its main isotope.

Si-28 represents a step back from the 6 nucleon layer octagonal Al-27 atom, and consists of a 4 nucleon layer octagonal structure and an embedded cubic diamond C-12 atom structure. Thus, both silicon and diamond C-12 atom heights are identical, but the silicon atom diagonal width is 101 pm compared with 42 pm for diamond atoms.

Not only does Si-28 have a tight, strong diamond-like crystal structure producing a unit cube of side length of 543 pm, compared with 357 pm for cubic diamond. Inter-atom bonds for both diamond and silicon are p-bonds, and thus both are poor electrical conductors (i.e. they are insulators), but because the silicon p-bonds are longer, the bonds are weaker and silicon is far less hard than diamond and, fortunately, it can be easily doped and machined into thin slices for the creation of a wide range of semiconductor devices.

and Beyond Silicon…

To keep this paper to a manageable length, and because of limited resources, silicon is the last of the atom structures to be detailed. Structures have been developed for many of the elements omitted from this paper, and there is no sign that the remaining elements of the Periodic table will not be amenable to the STEM analysis.

The top section of figure 62 shows a typical ONAM representation for copper, silver and gold. The simplicity of such conventional models belies the complexities, subtlety and variability of the underlying atomic structure. They also emphasise the absurd number of electrons (79 for gold) in '**spdf**' orbitals (but usually shown as circular Bohr orbitals), with a matching number of protons intermingled with even more abundant neutrons within a structure-less spherical nucleus. And despite their large number of orbital electrons, elements like copper, silver and gold are stable.

The figure 62 table provides a comparison of feasible STEM structures for the elements copper, silver and gold. Gold has three levels of embedding within a double 32-gon structure as defined by the **signature** of ***4-3; 8-4; 16-3; 32-2*** using STEM's **P-#** (or **P-hash**) notation, wherein **P** is the number of sides per polygon (each polygon consists of P/2 I-form protons and P/2 neutrons), and # is the number of polygons. For elements that are subject to alpha decay, the 4-sided polygons (such as the **4-3** within Au-197's ***4-3; 8-4; 16-3; 32-2***) are more likely to consist of helium atoms connected by a combination of b- and w-bonds (see figure 27c) rather than inter-quark bonded helium atoms.

A gold atom (Au-197) consists of 79 protons and 118 neutrons, but the ***4-3; 8-4; 16-3; 32-2*** configuration contains 78 protons and 119 neutrons as shown in the '**Totals**' row of the figure 62 table. Thus, on paper at least, there are 1 too few protons and 1 too many neutrons. However, at any point in time, any L-form neutron that is attached via an invariant CES can type-convert into a proton and, possibly later be type-converted back into a neutron. Thus the **full P-# signature** becomes **Au-197/78+1=** ***4-3; 8-4; 16-3; 32-2***, indicating that of the 79 protons, at least 1 is an attached neutron has been type-converted from an L-form proton. This means that some atoms might consist of 80 protons and 117 neutrons, or 78 protons and 119 neutrons; but stochastically, on average, gold contains 79 protons and 118 neutrons. Many other elements may, due to natural variation related to beta decay, similarly display a statistical spread of nucleon counts around the average proton/neutron count without a change in their nuclear geometry.

To add to the complexity, a particular isotropic form of an atom may have several subtly different structures. For instance, some gold atoms could have a full P-# signature of ***Au-197/74+5=4-3; 8-3; 16-3; 32-2*** rather than the figure 62 signature of **Au-197/78+1=** ***4-3; 8-4; 16-3; 32-2***. For this alternative structure of Au-197, the **74+5** indicates that 74 of its 79 protons are within complete proton layers with 5, on average, being attached type-converted L-form neutrons. Some gold atoms with this alternative signature might contain only 74 protons and 123 neutrons while some might contain 83 protons and 114 neutrons; but, on average, would contain 79 protons and 118 neutrons, which represents a broader potential spread of ±5 compared with ±1 for the **Au-197/78+1** structure.

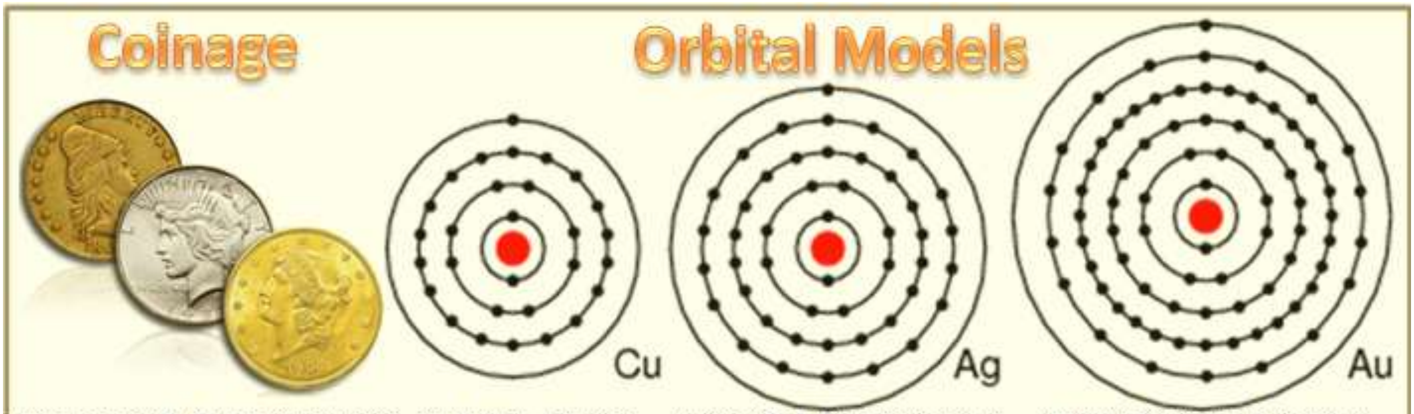

Equivalent STEM Atomic Signature >>> Cu-63/28+1=8-1; 16-3 Ag-107/46+1=4-1; 8-1; 16-3; 32-1 Au-197/78+1=4-3; 8-4; 16-3; 32-2

Polygonal Layers	Nucleons per Layer	Cu-63 (69%)			Cu-65 (31%)			Ag-107 (52%)			Ag-109 (48%)			Au-197 (100%)		
		#	Neutron	Proton	#	Neutron	Proton	#	Neutron	Proton	#	Neutron	Proton	#	Neutron	Proton
Tetrahedral (4-gon)	2	0	0	0	0	0	0	1	2	2	1	2	2	3	6	6
L-form neutrons ...			0	-		0	-		0	-		0	-		0	-
Octagon (8-gon)	4	1	4	4	1	4	4	1	4	4	1	4	4	4	16	16
L-form neutrons ...			0	-		0	-		0	-		0	-		0	-
Hexadecagon (16-gon)	8	3	24	24	3	24	24	3	24	24	3	24	24	3	24	24
L-form neutrons ...			7	-		9	-		0	-		0	-		15	-
Triacontadigon (32-gon)	16	0	0	0	0	0	0	1	16	16	1	16	16	2	32	32
L-form neutrons ...			0	-		0	-		15	-		17	-		26	-
	Totals		35	28		37	28		61	46		63	46		119	78
	Required		34	29		36	29		60	47		62	47		118	79
	Difference		+1	-1		+1	-1		+1	-1		+1	-1		+1	-1

Figure 62: Structure and Nucleon Statistics for Copper, Silver and Gold

Natural variation is thus considered to be an important aspect of atom structure, with the neutron-to-proton ratio needing to be expressed stochastically. STEM's full signature notation is compact and detailed, and represents a suggested step in that direction. At this stage, the signatures for many elements are speculative, with more research and modelling needed to identify the best-fit configurations, particularly for atoms with higher atomic numbers.

However, in spite of the uncertainties, distinct patterns in the structure of elements are apparent both within families of elements, and between element groups and periods within the Periodic table. For instance, the structural similarity the precious element family of gold, silver and copper is apparent in figure 62's table, with the 3 16-gons (***16-3***) being common, but with gold having 2 32-gons, silver isotopes have1 32-gon and copper isotopes has none.

Although not considered to be in the same family, helium, lithium, beryllium, boron and carbon-12 diamond, as discussed earlier in this paper, provide an example of structural similarity the between atoms close together within the Periodic table. Similarly, for the element palladium, which has a physical appearance similar to silver and is adjacent to it in the Periodic table, has a signature of ***Pd-106/44+2=8-1;16-3;32-1*** for Pd-106, which is a structure not far removed from that of silver ***(Ag-107/46+1=4-1;8-1;16-3;32-1***). Adding to the complexity, palladium can also contain between 20 and 30 attached L-form neutrons, with 6 of its 7 isotopes (Pd-100 to Pd-110) being stable.

Importantly, the physical characteristics of elements are dependent upon both the structure of the nucleus and the natural variation, **with a change of proton count not necessarily implying a change of element**. And although some elements can be structurally similar, it would seem that differences in their physical characteristics is more related to their development and modification environments that lead to different patterns of attached nucleons, embedded structures, different statistical variations of their nucleon counts, and different swivel-quark orientation and constraint.

As an interesting aside, as palladium hydride, a palladium atom can absorb and store up to about 900 times its own volume of hydrogen gas at STP (standard temperature and pressure). One possible explanation for this phenomenon is the amount of space present within a palladium atom. Pd-106 is considered to contain no embedded helium atoms (i.e. 4-gon structures), which would make available a significant cavity having a width of about 75 pm, which is the inside of the 8-gon. Should the signature of Pd-106 be ***Pd-106/40+6=16-3; 32-1*** then the cavity width would be about 150 pm. With a long-axial dimension of about 100 pm and width varying between 12 and 27 pm, it is quite feasible that many H_2 molecules could be held internally by each atom. Silver atoms, on the other hand, have embedded 4-gon and 8-gon forms, which results in very little internal space in comparison, and thus far less ability to absorb hydrogen gas.

Chemical Bonds and Compounds

Most molecules and chemical compounds consist of multiple atoms held together by a combination of **b-bonds** and/or **covalent bonds** involving **ionic electrons**. Within some chemicals (and hydrocarbons in particular), atom shape and charge distribution can prevent a swivel up and down quark pair from getting within 100 pm to each other so as to be able to form a bitron-bond: instead, a weaker bitron-less **polar-bond** (or **p-bond**) can be formed.

The other main type of bond is the **inter-quark** bond that binds up and down quarks together to form nucleons, and binds nucleons together to form the polygonal framework of atoms. Inter-quark are **strong-force** bonds that are formed by the inflow vortex of one CES drawing in the outflow vortex field-energy of another same-type CES as shown in figure 6 and as the insert graphic of figure 63. Referring to the schematic graph of figure 63, the inter-quark bond length is considered to lie in the 2 to 3 pm range, which corresponds to the distance between the pair of CES at which the force of attraction increases asymptotically.

The area of repulsive force region (the **work barrier** highlighted in **red** in the graph of figure 63) occurs because each CES resists having part of its field-energy flow being hijacked by the other, resulting in their field-energy becoming compressed between the 2 CES. The significant mutual repulsion between the 2 CES in this region is represents a resistive force that must be overcome to allow them to approach each other and form an inter-quark bond. This work barrier is called the Coulomb Barrier. A high-temperature, high-pressure energised environment is required to overcome the Coulomb Barrier, minimally that of a kimberlite pipe for diamonds, or within a fusion reactor or the core of a star. Inter-quark bond creation does not seem to occur in moderate temperature and pressure environments.

With separation of about 15 pm or greater, the common toroidal spin of a pair of CES generates slight attraction between them. Thus, with 15 to 100 plus pm separation, the pair of CES form weak-attraction bonds of similar strength (and possibly similar in nature) to Van der Waals force bonds. Such bonds are called **weak-bonds** (or **w-bonds**), and are considered to be the weakest of the inter-atomic bonds, but can be supplementary to b-bond attraction between adjacent swivel quarks.

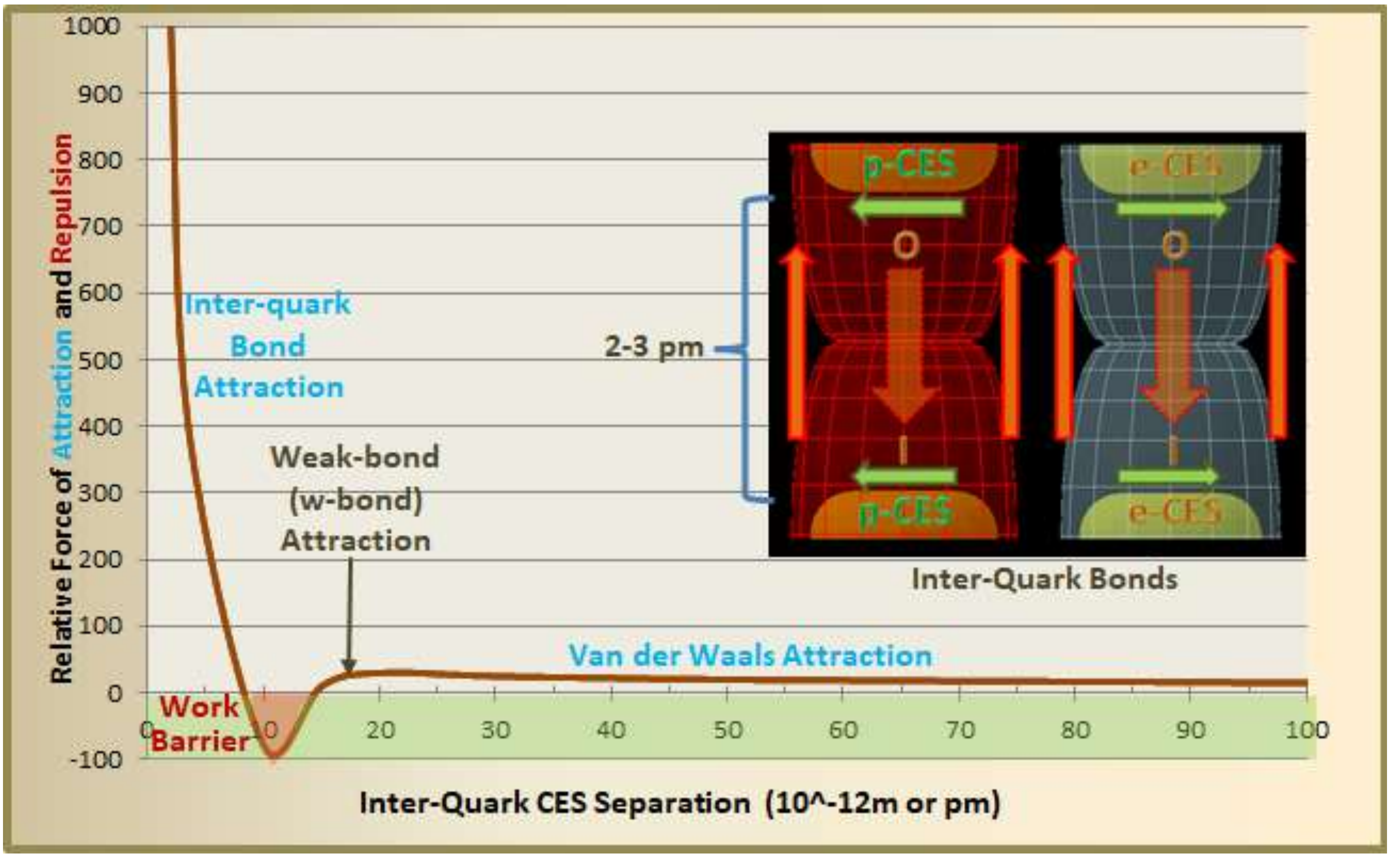

Figure 63: Inter-Quark Bond Attraction/Repulsion by Separation Distance (pm)

For separation less than 15 pm and greater than about 5 pm, two potential inter-quark bond CES are within the work barrier zone and repel each other. Should the work function barrier be forcedly overcome so that they move closer (within the 2 to 3 pm range), a strong-force inter-quark bond is created.

Generalising, inter-quark bonds are by far the strongest bonds, followed by bitron bonds (b-bonds), with polar bonds (p-bonds) and weak (w-bonds or Van der Waals force bonds) vying for the weakest dependent upon bond length.

Conventionally, the process of p-bond (possibly in conjunction with w-bond) formation is called **chemical adsorption** (or **chemisorption**), which may be homogeneous or heterogeneous. An example of chemical adsorption is the hydrogenation of alkenes and alkynes by H_2 molecules, which is enabled by the presence of palladium or nickel:

$$CH \equiv CH + 2(H_2) \xrightarrow{\text{Pd/Raney Ni}} CH_3 - CH_3$$

Other examples of chemical adsorption is the attachment of water molecules to gold nanoparticles; some chromatography processes used for the refining of metals; and the creation of Metal-Organic Frameworks (**MOF**s). MOFs are molecular systems consisting of a metal oxide centre surrounded by organic molecules p-bonded to form a highly porous three-dimensional crystal framework. MOFs are an interesting and fairly new area of research.

Of note, L Yarris from Berkeley Lab suggests that the porous sponge-like capacity of Mg-MOF-74, as shown right, represents a promising compound for the capture of greenhouse gases (carbon capture). Figure 64a shows other examples of MOFs, highlighting the component sub-structures.

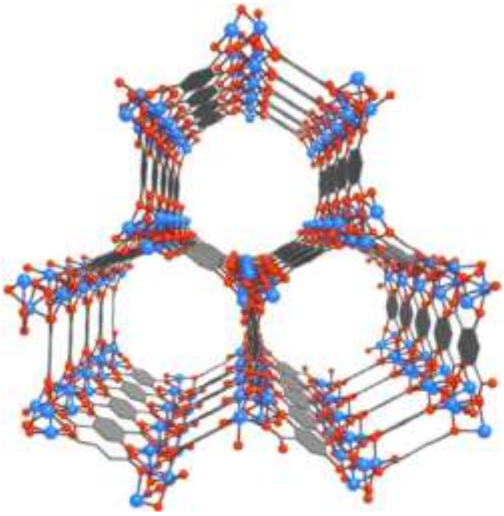

Chemical compounds are categorised by the manner in which the atoms involved are connected, with some compounds involving several different forms of bonding. The four main types of chemical compounds are Molecules, Ionic Compounds, Intermetallic Compounds and Coordination Complexes. The tabulation of figure 64b provides a comparison between the conventional Science and STEM descriptions for the characteristics of these four chemical compound classifications.

B-bonds can form at preferred bond locations between two opposite-chirality inflow CES that are in close proximity. When b-bonds are forcibly broken, multiple cetron and aptron electrons are released, many of which can end up as ionic orbital electrons to create ions (anions and cations respectively) in a process called **ionisation**, which is often accompanied by the release of thermal energy. The ionisation process is described in more detail in the next chapter.

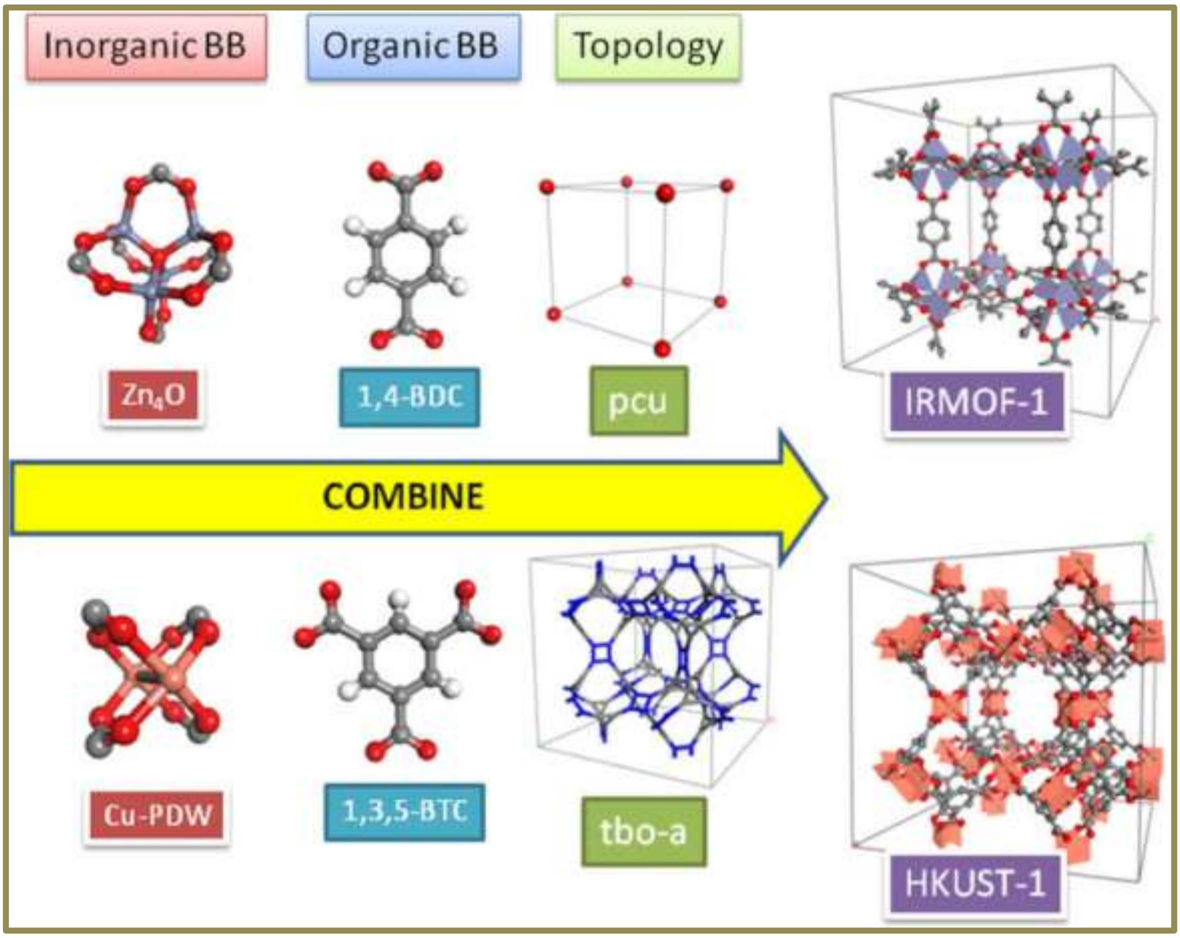

Figure 64a: Metal-Organic Framework (MOF) Examples

Compound Type	Conventional Description	STEM Description
Molecules 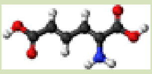	An electrically neutral group of two or more atoms held together by chemical bonds (electron transfer or covalent sharing of outer conduction band electrons).	An electrically neutral group of two or more atoms held together by b-bonds and/or covalent bonds involving ionic electron sharing and, in some more complex molecules and ligands, by p-bonds.
Ionic Compounds 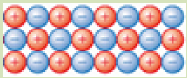	An electrically neutral chemical compound composed of ions held together by electrostatic forces between positively charged ions (cations) and negatively charged ions (anions).	An electrically neutral group of two or more oppositely charged ions (atoms or compounds) variously held together by a combination of b-bonds, p-bonds and ionic covalent bonds.
Intermetallics 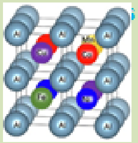	Consist of particular proportions of two or more elemental metals wherein electrons form what may be termed an "electron sea" in which valence electrons are free to move from one atom to another to create a bonding effect.	Composed of definite proportions of two or more elemental metals, which pack due to the size and geometry compatibility of their nuclei that allows their atoms to inter-lock, possibly with a combination of p-bond, w-bond (weak-bond) and multiple loosely-formed covalent ionic bonds.
Coordination Complexes 	Consists of a central atom or ion (often a metal) called the coordination centre, and a surrounding group of ligands (bound molecules or ions).	Consists of a central atom or ion (often a metal) called the coordination centre, and a surrounding group of ligands (bound molecules or ions) held by a combination of p-bonds and w-bonds.

Figure 64b: Chemical Compound Descriptions (Conventional Science and STEM)

The **bonding patterns** within chemical compounds are closely related to the alignment of swivel quarks that allow the formation of b- and b2-bonds. The lateral bond angles are dictated by the polygonal nucleon layer shape and nucleon layer pattern, whereas the top and bottom nucleon layer landscapes dictate most vertical b-bonding more common with the halogens. All bonded groupings adjust their 3-D position in space in according to the net electromagnetic field generated by all attached atoms, with the most common compound geometries being classified as linear, trigonal-planar, tetrahedral, trigonal-pyramidal and octahedral, examples of which are shown in figure 65.

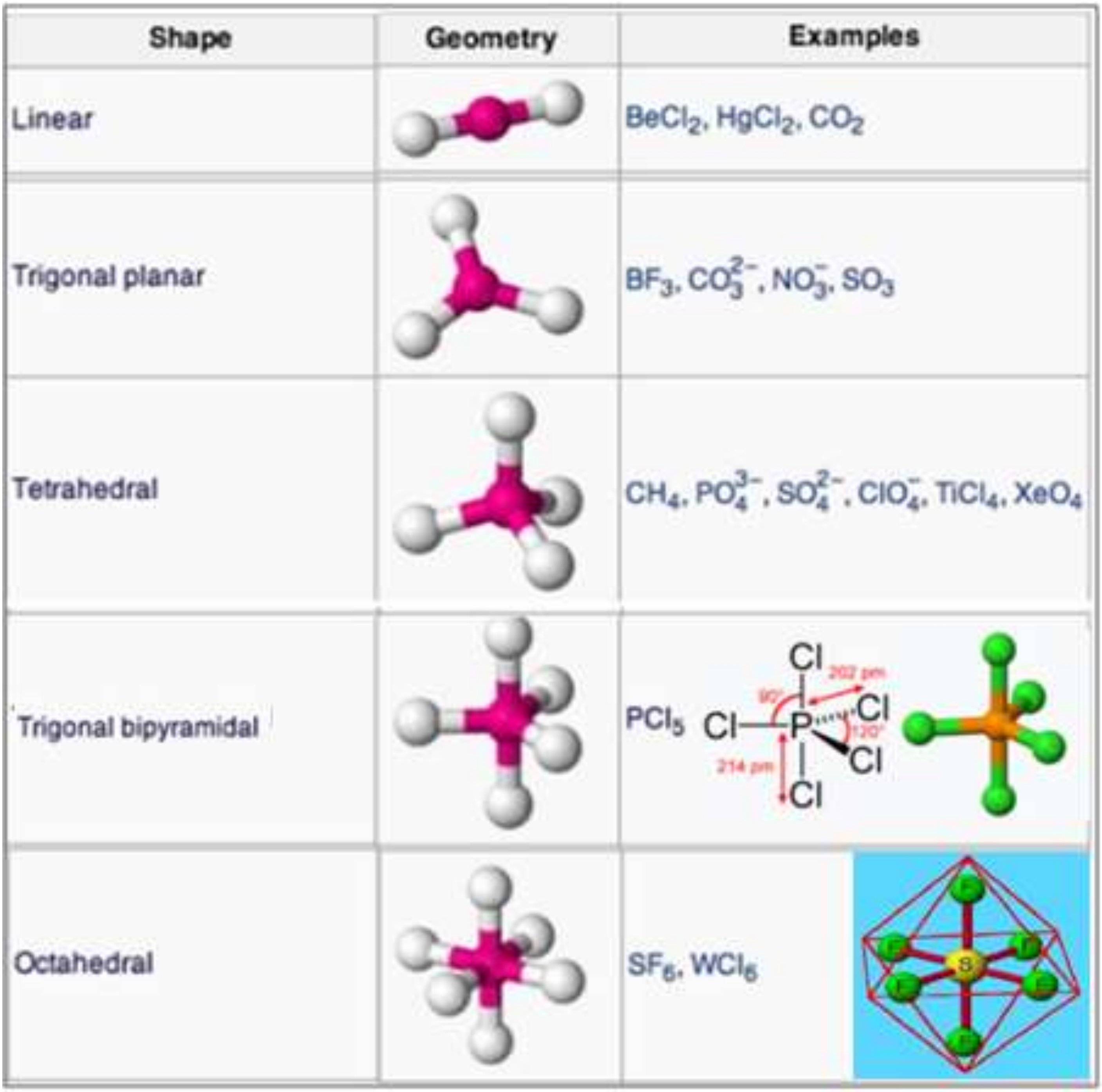

Shape	Geometry	Examples
Linear		$BeCl_2$, $HgCl_2$, CO_2
Trigonal planar		BF_3, CO_3^{2-}, NO_3^-, SO_3
Tetrahedral		CH_4, PO_4^{3-}, SO_4^{2-}, ClO_4^-, $TiCl_4$, XeO_4
Trigonal bipyramidal		PCl_5
Octahedral		SF_6, WCl_6

Figure 65: Common Bonding Geometries

When two molecules collide, they usually deflect each other and/or simply bounce apart, exchanging kinetic energy in the process. As the environment becomes more energised, such as with increased temperature, even mild collisions between atoms and molecules caused by the bumping of vibrating energised particles can result in molecule damage and the formation of ions. An increase of thermal energy can be a pre-requisite and/or an accelerant for many chemical reactions.

STEM contends that chemical reactions and bond geometries are dependent upon the outer polygonal shape and size of the atoms and complexes involved; the field-energy capacitances of each nucleon layer of atoms, including any embedded structures; the distribution, availability, polarity and energisation-level of swivel quarks; and environmental factors (ionisation levels, gas/water molecular activity, catalyst availability etc.). It is thus most difficult to predict chemical reactions, with reaction metrics needing to be established by experimentation and observation.

Catalysis is sometimes a necessary pre-cursor for many chemical reactions. Catalysis involves increasing the rate of a chemical reaction by adding a **catalyst** or an **enabler** to promote the start of the main chemical reaction. Catalysts and enablers create a reversible starter chemical reaction or, even more indirectly, create intermediate/transitional compounds to get other reactions going. The free electrons created by these processes also serve as CES-enhancers for the preferred bond locations and thus be conducive to targeted chemical reactions.

Ionisation and Redox

Ionisation is the process by which an atom or a molecule acquires a negative or positive charge. It can occur in a variety of ways, one being **ionisation-by-dissociation** within an **aqueous solution**. A range of acids and salts can dissolve easily in water because of the structure of the water molecule (see figure 50), which consists of an oxygen atom and two b-bonded L-form protons (i.e. the hydrogen atoms). The unrestrained arms of a water molecule's L-form protons spin rapidly around their b-bond, acting like an electric-whisk or mini jack-hammer, beating and unceremoniously dislodging bitrons and/or breaking the external b-bonds between atoms within other chemical compounds.

Using the example of **hydrogen chloride gas** (HCl), due to the extremely small size of the hydrogen atom and the wedge-like 'V' shape of the water molecule, the arm of one of a water molecule's spinning L-form protons can work its way between a b-bonded hydrogen and chlorine atoms and break the b-bond, with the freed electron(s) being captured as anionic orbital electron by the chlorine atom to create a chlorine **anion**.

The conventional Science view is that a negative ion (an **anion**) is created by a neutral atom acquiring additional electron(s), and that a positive ion (a **cation**) is when it loses one or more electrons. For the STEM approach, an anion is an atom that acquires extra cetron electrons or loses aptrons to provide it with a near-field negative charge. A cation is an atom that acquires extra aptron electrons or loses cetron electrons to provide it with a near-field positive charge. The ionisation process would appear to be a two-stage process involving bond breaking and released electron attachment to create ions.

For ionisation-by-dissociation within an aqueous solution, one of the water molecule's destructive protons quite often becomes a casualty of the ionisation-by-dissociation process, breaking away from its oxygen atom to create a hydrogen cation (a single proton) and a hydroxide anion (OH^-). The released hydrogen cation almost immediately attaches to another water molecule to create a hydronium cation (H_3O^+), which is the **auto-ionisation** process as described in more detail in the Atomic Structure: Oxygen and Water chapter.

Ionisation can also take place when solid ionic compounds are melted or when molecules form a gaseous state. As the crystal form of a solid phase melts, the increase in mobility and energy within the mix cause atoms and molecules to batter each other to the extent that many inter-atomic b-bonds break and ions separate, accompanied by many bitrons being released as electrons (cetrons and aptrons). In gaseous phases ionization is also by collision, and can occur at low pressures when an electric current is passed through them; without such electrical assistance ionisation tends to occur at high temperatures.

Ionisation also occurs whenever sufficiently energetic charged particles or radiant energy travel through gases, liquids, or solids. Energised charged particles, such as cosmic rays, alpha particles (energised helium atoms), positrons and electrons from radioactive materials, and electromagnetic radiation (EMR) can cause extensive ionization along their paths by directly bump-releasing bitrons from their bonds or indirectly by the collision with other kinetically energised molecules or chemical compounds. Cosmic rays and high temperature ionisation are addressed in the Plasma and Cosmic Radiation chapter.

Most information about the ionisation process related to chemical reactions is empirically derived from bulk chemical reactions, with little information relating to the mechanics involved at the atomic level. However this is changing with the development of femtochemistry spectroscopy and quantum computing related nano-technologies.

Femtochemistry came into prominence in 1999 when Professor Ahmed H. Zewail (deceased, 2016) received the Nobel Prize in Chemistry for studies of atoms and molecules during a reaction. Using a super-fast camera that uses femtosecond (1 fs = 10^{-15} seconds) laser flashes, he produced measurements backed up by "slow motion" visuals of chemical bond breaks and formation. One study involved the dissociation of sodium iodide:

$$NaI \rightarrow Na^+ + I^-$$

Although the experiment refers to NaI as being a covalent molecule, it is usually considered to be an ionic solid with a centre-to-centre bond length of 271 pm (2.71 Å) which, based upon the diameter of a sodium atom of 84 pm and 316 pm for iodine, means that the b2-bond length is 71 pm. The bursts of energy from a laser pulse camera were used to excite the 'molecule', causing it to vibrate. Referring to the upper graph of figure 66, when the oscillatory vibrations cause a nucleus centre-to-centre separation of 3.27 Å, the b2-bond would have been stretched to 127 pm, well beyond its ability to hold its bitron pair, with one bitron remaining attached to the swivel down quark of the sodium atom and the other to the swivel up quark of the iodine atom, which corresponds to the minimum potential energy point.

For separation in the range 3.27 to 5 Å, there would be bitron-less p-bond attraction between the now separated ions which, in combination with the vibratory movement displacement, can bring the ions to within 100 pm of each other and so allow a bitron bond to be re-formed. With separation growing beyond 3.27 Å (the grey zone of the figure 66 graph), the kinetic vibratory energy of the individual ions increases, and by the time that nucleus separation reaches 6.9 Å, the p-bond width would be 490 pm, with the ions now being too far apart for their electromagnetic fields to influence each other, and the bond can be considered to be completely broken (i.e. separation is complete). By this stage the aptron and cetron electron orbitals in each ion is established and kinetic energy of each stabilises, and the process is complete although the Brownian motion of the ions continues.

Zewail's femtochemistry endeavours also confirmed that the breaking of two bonds within the ring molecule for Cyclobutane, yielding two Ethylene molecules, is possibly a two-stage mechanism (lower graph of figure 66). The first bond break creates an intermediate tetramethylene molecule about 700 fs before the second bond is broken to form two Ethylene molecules. As can be seen in the lower graph, the activation barrier to each bond breakage was essentially the same, with a slight energy input required before the second barrier could be breached.

Femtochemistry technologies continue to improve, with laser pulse times reducing from the femtosecond (1 fs = 10^{-15} seconds) to the zeptosecond (10^{-21} second) range, so that the type of research pioneered by Professor Zewail should continue to improve and expand.

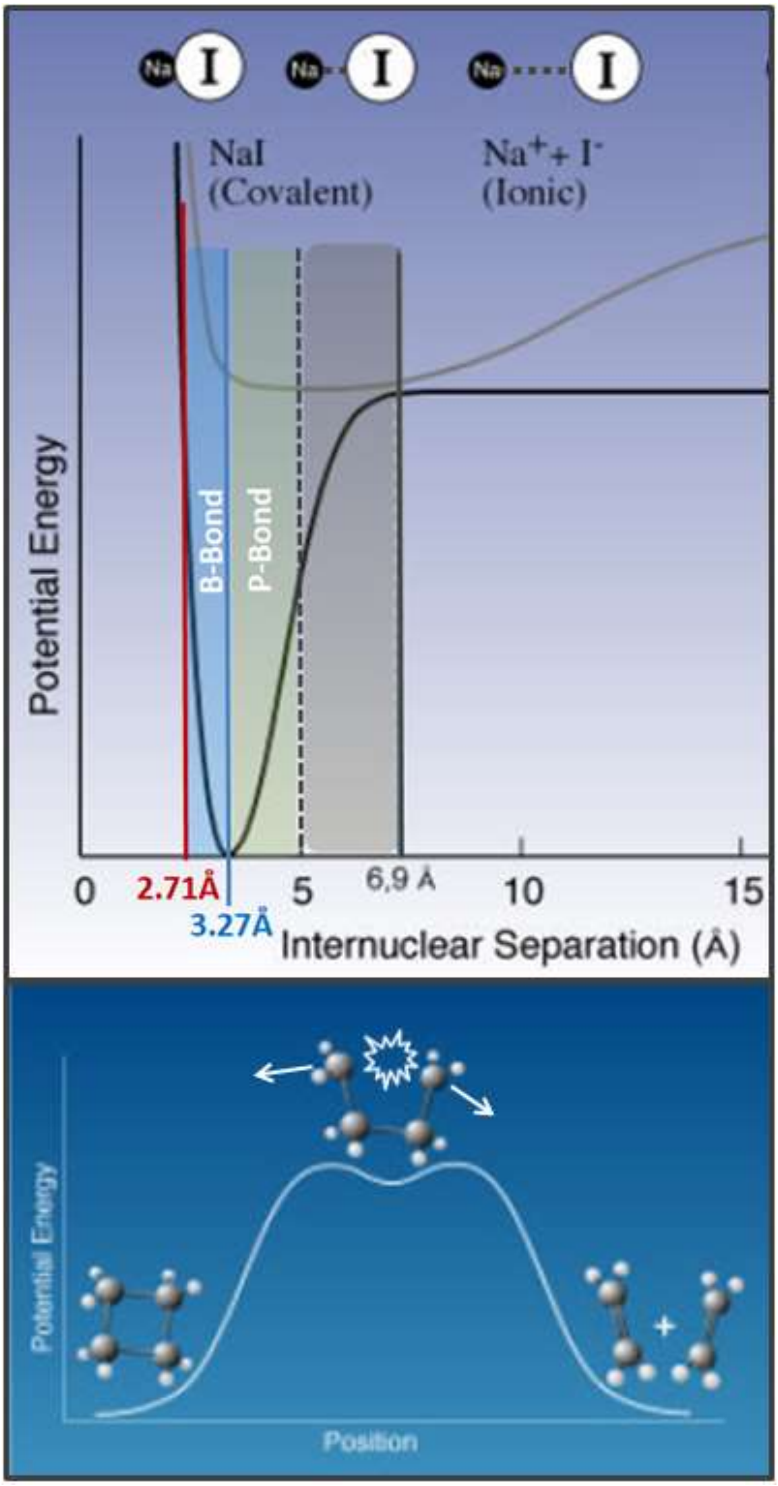

Figure 66: Femtochemistry Sequence of Chemical Bond Breakage

Up to the beginning of 2022, the STEM Development Group considered that the **CES enhancement** of **swivel quarks** were responsible for the creation of **ions**. However, early in 2022, an University of New South Wales (UNSW) research group article titled Quantum computing in silicon hits 99 per cent accuracy, which, when combined with Zewail's femtochemistry research, led to the development of a **two stage ionisation process** involving the attachment of an **ionic electron** to a **flat orbital** (which is distinctly different to the ONAM 'spdf' and Bohr orbitals).

Rather than using an electron dot approach (left in figure 67a), the UNSW research group represents a qubit (quantum bit) as a single phosphorous atom (or more accurately, an anion) implanted within an electrically stable ultra-pure silicon substrate as shown right in figure 67a. The group has managed to control and manipulate the quantum spin of the atom, and the orbit and quantum spin of the ionic electron. The 2018 video lecture by M Simmons titled 'The Einstein Lecture: The Quantum Computing Revolution' describes how phosphorus atoms are injected and manipulated, and the 2022 high fidelity qubits video by A Morello describes the development of a qubit logic gate.

According to the 'spdf' model, a phosphorus atom has 15 orbital electrons: $1s^2$ $2s^2$ $2p^6$ $3s^2$ $3p^3$ with the outer 3 electrons having a common quantum spin direction; or according to the Bohr model it has [2, 8, 5] electrons in the [K, L, M] shells. The single phosphorous atoms used for the UNSW qubits are actually phosphorous anions (P^-), but rather than pairing with one of the $3p^3$ electrons or joining the other five M-orbital electrons, the ionic electron is apparently unaffected by the other orbital electrons, and can be readily manipulated as if the underlying orbital electrons do not exist. And furthermore, should 'spdf' and/or Bohr electron orbitals exist, they do not contribute to, and are unaffected by, the applied external energy regimes used to set up and test the single atom qubits. All this suggests that these inner orbitals, in fact, do not exist; which is the STEM view.

Also, at temperatures near to absolute zero, apart from slight vibrational movement, the ionic electron would seem to be stationary rather than energetically orbiting around the P-31 atom. It stands to reason that if the ionic electron reduces to a stationary state at close to absolute zero, that the 15 inner orbital electrons would also be reduced to a similar stationary state and, due to attraction, they would become irreversibly attached to the positive nucleus. There is, however, no evidence for any such low temperature orbital collapse or subsequent orbital recovery, which further supports the opinion that ONAM 'spdf' and Bohr orbitals do not exist.

The UNSW group used a microwave signal corresponding to its resonance frequency to induce the stationary ionic electron to move and assume an orbital around the nucleus, with its quantum spin direction reversing upon each alternating oscillation of the applied microwave signal. The Bohr model protagonists would consider that the ionic electron's orbital would be planar and equatorial around the nucleus; the 'spdf' model protagonists would consider it to be a spherical 's' type orbital; and STEM considers that, due to the structure of the P-31 atom, it would assume a circular planar (and thus Bohr-like) orbital positioned above (or below) the nucleus without actually passing around the nucleus. So what is the structure of the phosphorous-31that might support such an electron orbital?

The STEM atomic model for phosphorous-31 consists of six full octagonal nucleon layers made up of three double pairs of I-form proton/neutron layers, and containing an embedded lithium-7 form, as shown in the quark model of figure 67b. With no attached L-form nucleons, it has a **P-# signature** of *P-31=4-1; 8-3*. Note that this does not preclude the existence of P-31 with an embedded He-4 form and attached L-form nucleons: this form of P-31; with a P# signature of *P-31+1=4-1; 8-3*, this form of P-31 has an extremely low probability of occurring naturally because it would readily beta-decay into silicon-31.

Of particular interest is the upper (as shown in figure 67b) full neutron layer of the P-31 nucleus: it contains four swivel up quarks that can swivel upwards so that their energy fields combine to generate a positive electromagnetic field above the top outer neutron layer that can support the planar circular orbital of the ionic electron, which would be in an anti-clockwise direction as viewed from above. The magnetic component of the combined swivel quark field would be downwards (as shown), but can be manipulated using **nuclear magnetic resonance** (**NMR**) techniques because, isolated within the silicon bed and at close to absolute zero, the nucleus is free to rotate and acts somewhat like an unrestrained gas molecule. On the other hand, the magnetic orientation and quantum spin of the ionic orbital electron is dictated by the phase of the microwave applied to it.

So, how does this relate to the hydrogen chloride (HCl) ionisation by water example? The hydrogen bond is a single b-bond involving a swivel up quark of the chlorine atom. The **first stage** of its ionisation is that the single b-bond is broken by a water molecule with the bitron remaining attached to the inflow p-CES of the chlorine atom's up quark.

The **second stage** of the ionisation process is that the up quark recoils and swivels upwards to immediately release the bitron as a cetron electron, which is a negative **charge carrier** (**CC**). However, rather than flying off at speed, the cetron electron is captured the combined electromagnetic field of the swivel up quarks within the outer neutron layer, confining it to **a planar circular orbital** above the outer neutron layer to become a chlorine anion (**Cl^-**). In this case the lone hydrogen atom (i.e. proton) is in effect the cation that, as described in the Atomic Structure: Oxygen and Water chapter, almost immediately attach to a water molecule to create a H_3O^+ hydronium molecule, which can also be viewed as another two stage process. Here the positive cation charge is due to the extra proton b-bonded to the oxygen atom rather than from an extra ionic aptron.

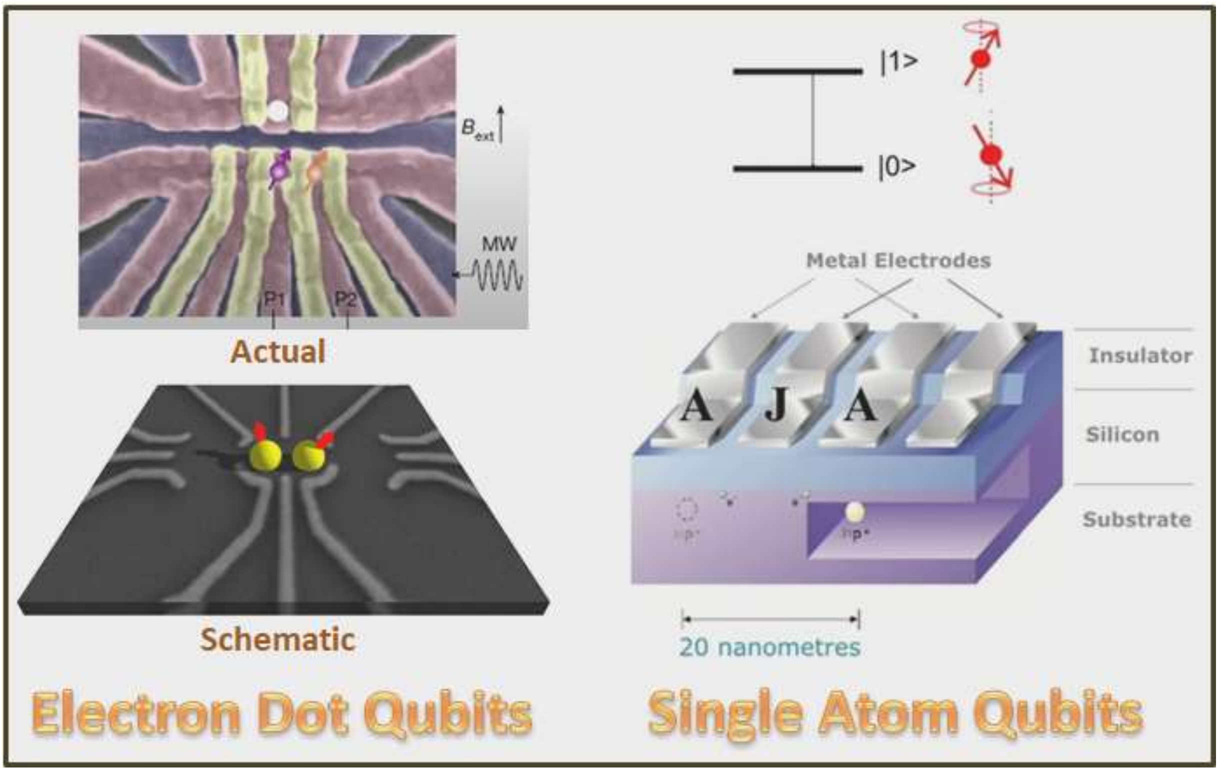

Figure 67a: Electron Dot and Single Phosphorous-31 Atom Schematics

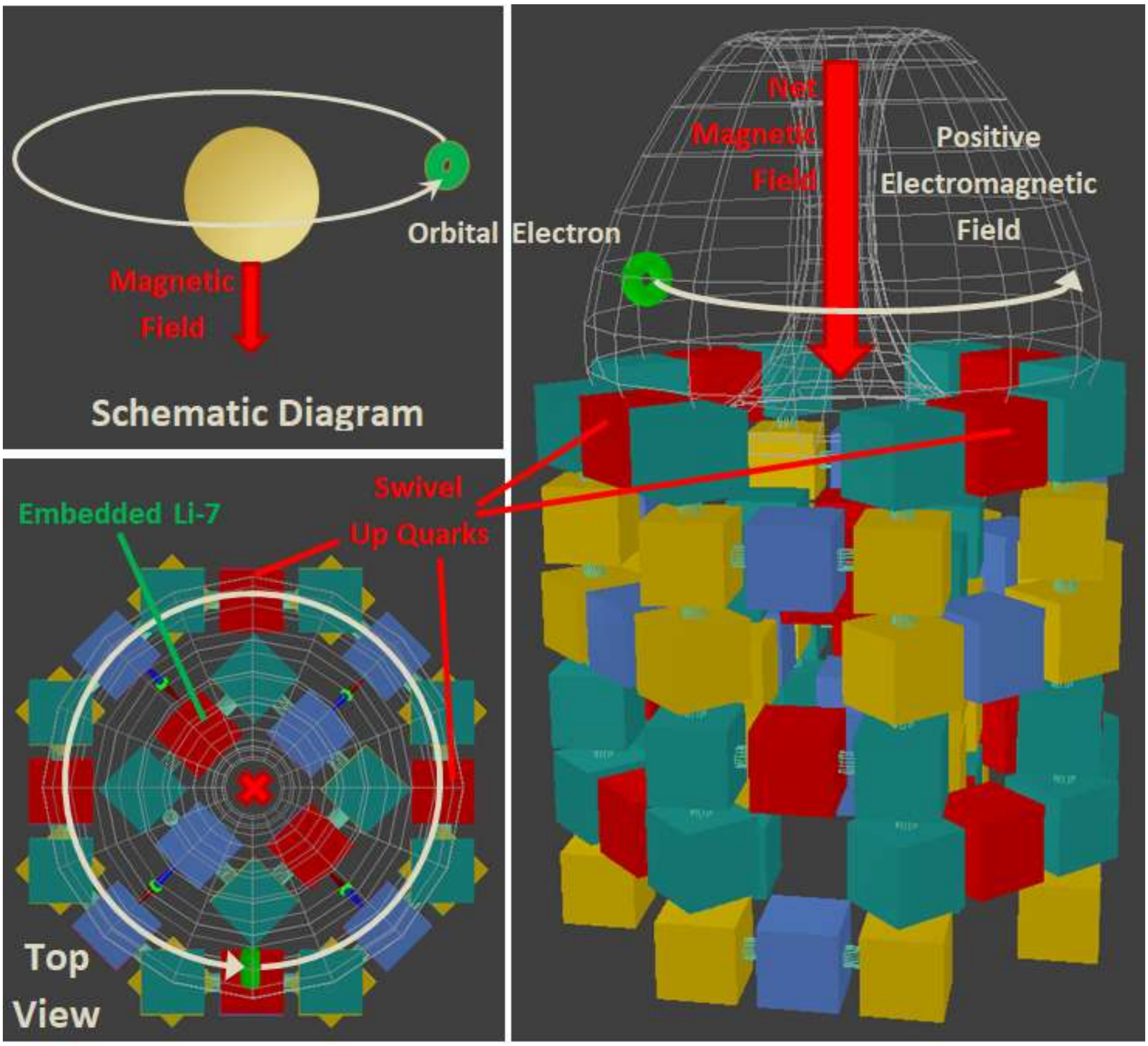

Figure 67b: Quark Model of Phosphorous-31 Anion with Orbital Electron

Whereas a hydrogen atom can only form one b-bond with another atom, single bonds between most other atoms take the form of **double b-bonds** (**b2-bonds** in shorthand notation). For example, for **sodium chloride**, the sodium-to-chlorine b-bond is a b2-bond. When a b2-bond breaks, the bitron of one b-bond briefly remains attached to the inflow p-CES of the swivel up quark to be launched as a cetron in orbit above an outermost neutron layer of the chlorine nucleus to create the anion Cl^-. Simultaneously, the bitron from the other b-bond briefly remains attached to the inflow e-CES to be launched as an **aptron electron** (positive CC) in orbit above (or below) the outermost proton layer of the sodium nucleus to create the cation Na^+.

Apart from the single hydrogen bond situation, the scenario that emerges from this explanation is that, when **ionisation** takes place by the **breaking of a b2-bond**, one bitron remains attached to the swivel up quark but is swung upwards (or downwards) to be launched into a planar circular orbital as a cetron electron (negative CC): it is supported by the combined electromagnetic positive field of the swivel up quarks of the upper neutron layer to create an **anion**. In parallel, the other bitron from the b2-bond remains attached to the swivel down quark and is swung upwards (or downwards) to form an aptron electron orbital supported by the negative electromagnetic field of the swivel down quarks, to create a **cation**. The anion thus has an orbital negative CC and the cation has an orbital positive CC, which is most relevant to the **redox process** and the creation of an electric current by a chemical battery.

Oxidation is considered to occur to an element or complex participating in a chemical reaction should it lose one or more electrons; and **reduction** occurs when electrons are gained. Oxidation is simply the opposite of reduction, and they work in tandem with the electron released by the oxidation process being consumed by the reduction process: in combination they are referred to as the **redox** process The redox process most commonly is associated with chemical interactions between metals, which form positive ions in an ionic chemical, and non-metals, which form negative ions. A simple example is the reaction between sodium metal and chlorine gas, wherein the sodium metal is considered to be oxidised and the chlorine gas reduced:

$$2Na_{(s)} + Cl_{2(g)} \rightarrow 2Na^+Cl^-_{(s)}$$

In this example, the conventional Science view is that the sodium atom donates an outer valence electron making it a positive ion, and a chlorine atom accept an electron to become a negative ion, and the charge difference between the ions bind them together as the ionic solid NaCl. The STEM view is that the sodium atoms single b-bond to the chlorine atoms.

The measurement of **reduction potential** (in volts, with oxidation potential equalling minus the reduction potential) relates to measurements of electrical potential of metal electrodes immersed within aqueous solutions of ions. In general, those transition metals those towards the right-hand end of the transition metal block of the Periodic table (e.g. copper, silver and gold), are reasonably electronegative and thus have high reduction potentials. Alkali metals (on the very left edge of the Periodic table such as potassium or caesium), on the other hand, have lower electronegativity and thus have negative reduction potentials.

Redox reactions, involving metal electrodes immersed within aqueous solutions, lead to the operation of galvanic (or voltaic) and electrolytic cells. Figure 68 shows a galvanic cell setup involving copper and zinc electrodes; the two electrolytes are 1M aqueous solutions of copper sulphate and zinc sulphate respectively; and a salt bridge containing sodium sulphate.

The copper undergoes reduction, which defines the **cathode**; and the zinc is oxidised, which defines the **anode**. Only the copper and zinc cations are involved in the redox reaction, with the anions being spectator ions and can thus be left out of the full equation (bottom of figure 68), which are usually being broken down into 2 **half-equations** (as shown below) to highlight the electron transfers involved with redox reactions.

$$\text{Reduction: } Cu^{2+}_{(a)} + 2e^-_{(f)} \rightarrow Cu_{(s)} \qquad \text{Oxidation: } Zn_{(s)} \rightarrow Zn^{2+}_{(a)} + 2e^-_{(f)}$$

Whereas conventional Science provides only one source/sink pair for electrons, STEM provides for two source/sink pairs and two half-equations for each reduction and oxidation reaction as shown in the table below:

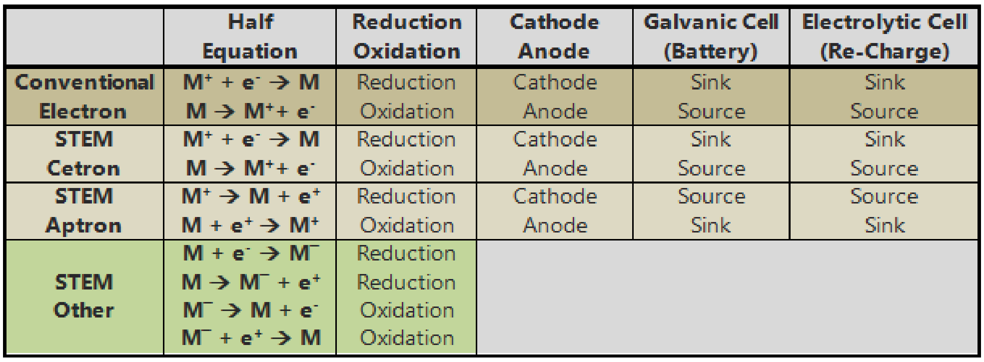

	Half Equation	Reduction Oxidation	Cathode Anode	Galvanic Cell (Battery)	Electrolytic Cell (Re-Charge)
Conventional Electron	$M^+ + e^- \rightarrow M$ $M \rightarrow M^+ + e^-$	Reduction Oxidation	Cathode Anode	Sink Source	Sink Source
STEM Cetron	$M^+ + e^- \rightarrow M$ $M \rightarrow M^+ + e^-$	Reduction Oxidation	Cathode Anode	Sink Source	Sink Source
STEM Aptron	$M^+ \rightarrow M + e^+$ $M + e^+ \rightarrow M^+$	Reduction Oxidation	Cathode Anode	Source Sink	Source Sink
STEM Other	$M + e^- \rightarrow M^-$ $M \rightarrow M^- + e^+$ $M^- \rightarrow M + e^-$ $M^- + e^+ \rightarrow M$	Reduction Reduction Oxidation Oxidation			

The STEM half-equations involve both cetron (**e^-**) and aptron (**e^+**) electron source/sinks as shown below (note that the cetron source/sink equations are the same as those for the conventional Science half equations).

Reduction: $Cu^{2+}_{(a)} \rightarrow Cu_{(s)} + 2e^{+}_{(f)}$ = Aptron Source **$Cu^{2+}_{(a)} + 2e^{-}_{(f)} \rightarrow Cu_{(s)}$ = Cetron Sink**

Oxidation: $Zn_{(s)} + 2e^{+}_{(f)} \rightarrow Zn^{2+}_{(a)}$ = Aptron Sink **$Zn_{(s)} \rightarrow Zn^{2+}_{(a)} + 2e^{-}_{(f)}$ = Cetron Source**

Copper and zinc atoms each have three hexadecagon (16-gon) outer layers, which means that both have a complete upper outer neutron layer and a complete lower outer neutron layer (or vice versa). As a neutral atom with no orbital ionic electrons, they can acquire one or, more often, two orbital aptrons supported by the outer proton layer: when this happens they act as an **aptron sink**. Similarly, the cations Cu^{2+} and Zn^{2+} can become neutral atoms by losing their two attached orbital aptrons, so acting as an **aptron source**; or, by acquiring two orbital cetrons supported by the outer neutron layer, they can act as a **cetron sink**. In the latter case, the neutral atoms have two orbital cetrons and two orbital aptrons, and the propensity to release the two cetrons to convert into a cation, so acting as a **cetron source**.

When copper cations in solution come in contact with the copper cathode, some convert into a neutral copper atom by shedding aptrons, so creating an **aptron source**; others in the same ionic mix take up cetrons so as to create a **cetron sink**. Both processes, acting in unison, result in the deposition of copper metal on the copper cathode, so generating an emf of approximately 0.34 volt.

On the **zinc anode** side, neutral zinc atoms on the outer surface of the anode consist of a mix of those with two orbital cetrons and two orbital aptrons, which shed cetrons to create a **cetron source**; and those with no orbital electrons which take up aptrons to create an **aptron sink**. Both processes acting, in unison, result in the etching of metallic zinc from the outer surface of the anode, an increase of zinc cations in the electrolytic solution and the generation of an emf of approximately -0.76 volt. The net voltage for this galvanic cell is thus 1.10 volt (calculated as 0.34 - (-0.76)).

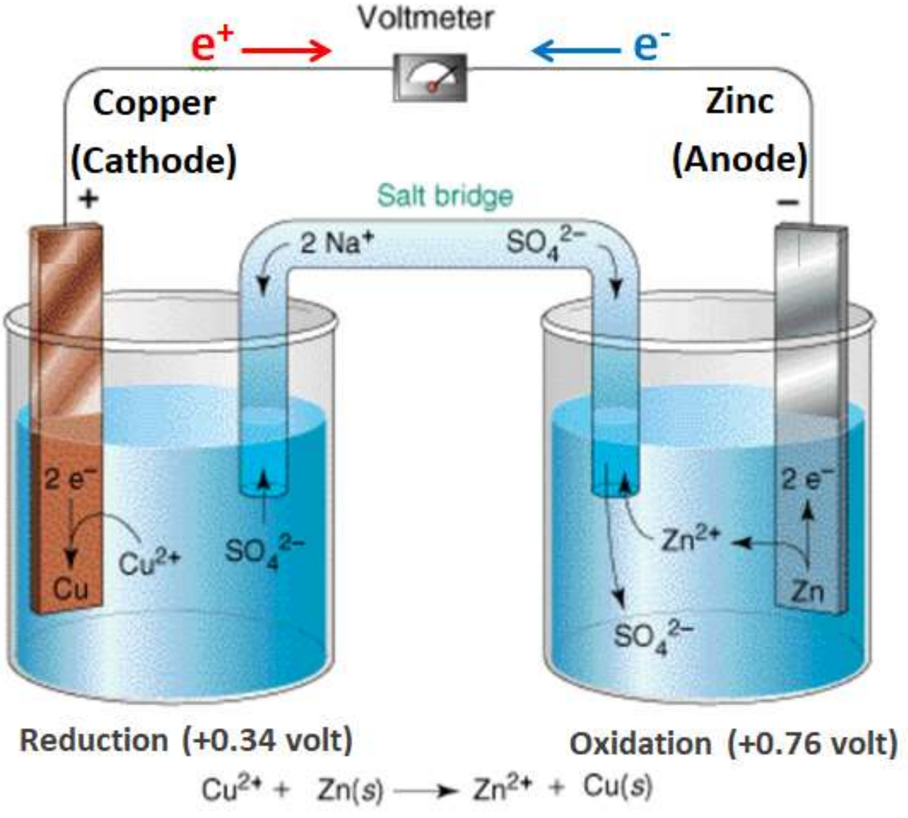

Figure 68: Copper-Zinc Galvanic Cell

The two-way movement of aptrons and cetrons serves to balance the chemically-induced charge imbalance between the electrodes, but not the chemical imbalance in the aqueous solutions; the latter results in a reduction of cations on the cathode side and build-up cations on the anode side. The salt bridge offsets ionic charge imbalance by allowing excess anions on the cathode side to move to the anode side and, conversely, excess cations on the anode side to the cathode side (albeit via a proxy of sodium sulphate electrolytic solution) to maintain the ionic balances of each cell.

With the STEM approach, positive and negative CC (aptron and cetron electrons) are generated by CC source electrode reactions, and removed by the sink electrode reactions: it is a self-sustaining system without any need for positive and negative charge to travel between electrodes via the electrolyte. The salt bridge simply provides the means for the ionic balance of the electrolyte to remain neutral and stable, rather than to repatriate electrons back to the anode from the cathode to complete the circuit.

The conventional Science model for a galvanic cell is not a balanced system. It involves the one-way movement of electrons (or cetrons) from anode to cathode, but a two-way exchange of positive and negative ions via the salt bridge. To be balanced and totally conform with the **law of conservation of energy**, only a one-way movement of negative charge (in the form of sulphate anions in figure 68) from the cathode to the anode side via the salt bridge would be required to compensate for the one-way movement of negative charge through the connecting wire; or, **alternatively**, the electric current could consist of a two-way movement of positive and negative CC (which is the STEM approach) and a matching two-way movement of ionic charge in the other direction. In terms of energy transfer, the STEM approach has a distinct advantage.

The electric circuit imbalance problem came to a head in the 1940's, when the one-way movement of electrons alone was unable to explain the characteristics of current flow in a sparse electron environment of newly discovered semiconductor diode devices, which involved the movement of both negative and positive charge. Electron movement via drift and diffusion accounted for negative charge movement, but conventional Science had no positive charge particle that could similarly move within a semiconductor substrate. The work-around overcome this problem was to introduce the concept of **temporal cations**, which are referred to as **positive-holes**, or simply as '**holes**'.

Positive-holes can be dynamically created by electron loss and then extinguished acquiring another electron. But, unlike cations within an electrolytic solution, cations formed in this manner within a semiconductor substrate cannot physically move. Clever animations can show electrons hole-hopping from neutral atom to a positive-hole, leaving behind a newly formed positive-hole. Using devices such as a fictional moving plus sign, these animations provide an **illusion** of positive charge movement in the opposite direction to that of the electrons. However, neither the holes nor their positive charge physically move: it is simply a sleight-of-hand involving synchronised on-and-off sequencing plus visual prompts to suggest positive-hole movement. Temporal cation creation is a valid process in its own right, but to suggest that 'hole'-hopping electrons can generate a physical movement of positive charge that is analogous to that of electrons subjected to drift and diffusion processes, is a distinct fallacy.

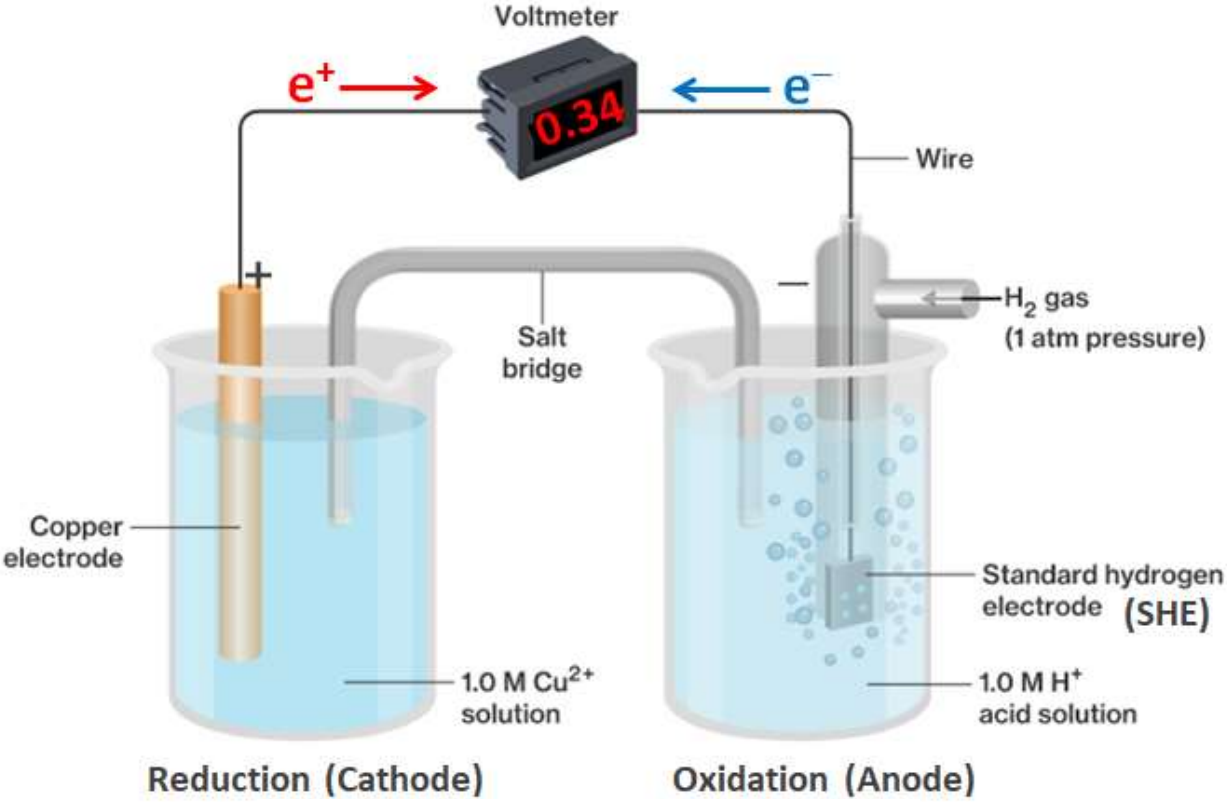

Figure 69: Standard Reduction Potential (E^0) Cell

The STEM approach does not require positive-holes, because positive CC (aptron electrons) fulfil that role, with DC electricity being formed by the **simultaneous two-way movement** of cetron and aptron electrons in opposite direction. More details related to these topics and to electromagnetic field formation can be found in the STEM paper The Duplicit Electron.

A **standard hydrogen electrode** (**SHE**) is used to determine the **standard reduction potential** (**E^0**) of other elements. A SHE consists of a chemically **inert electrode**, typically a standard size and grade of platinum (Pt) plate, immersed in a 1M hydrochloric acid (HCl) solution with H_2 gas is bubbled in at a pressure of one atmosphere and a temperature of 25^{O}C. Because the SHE electrode is inert, it does not participate chemically in the redox process, but the chemical reaction between the hydronium (H_3O^+) of the acid electrolyte and the hydrogen gas provides a ready supply of positive and negative CC.

The positive charge of hydronium results from the single b-bond attachment of a proton (H^+) to a water molecule, as opposed to the attachment of an aptron electron. When one of the three hydrogen atoms attached to the oxygen atom of a hydronium molecule is released to convert hydronium back into water, the b-bond breakage has an equal probability of releasing the bitron as a cetron or an aptron: the process thus acts as both a cetron source and an aptron source, as reflected in the half equation below:

$$2H_3O^+_{(a)} \ (\rightarrow 2H^+_{(a)} + 2H_2O_{(a)} + e^+_{(f)} + e^-_{(f)}) \rightarrow H_{2(g)} + 2H_2O_{(a)} + e^-_{(f)} + e^+_{(f)}$$

In order to maintain the chemical equilibrium of the electrolyte, the b-bond of hydrogen gas molecules (H_2) break to release two protons (H^+), with the b-bond breakage also having an equal probability of releasing the bitron as a cetron or an aptron, as reflected in the half equation:

$$2H_{2(g)} + 4H_2O_{(a)} \ (\rightarrow 4H^+_{(a)} + 4H_2O_{(a)} + e^-_{(f)} + e^+_{(f)}) \rightarrow 4H_3O^+_{(a)} + e^-_{(f)} + e^+_{(f)}$$

The reactions represented by these two inverse processes provide a ready supply of both positive and negative CC for the SHE cell, but generates no electrical potential because there is no provision of a positive or negative CC sink. Thus, when connected to a cell with an electrode made from a different material, the only emf generated is that of the attached cell. For a copper electrode cell such as shown for figure 69, the copper electrode acts as an aptron (i.e. positive CC) source and a cetron sink, it generates a **positive voltage** of +0.34 volt that indicates that it is a **reduction** process. For a zinc electrode the current direction is reversed, with the zinc electrode acting as a cetron (i.e. negative CC) source and an aptron sink: it generates a **negative voltage** of -0.76 volt which is indicative of an **oxidation** process. Wikipedia provides a list of the standard reduction potentials for an extensive range of materials.

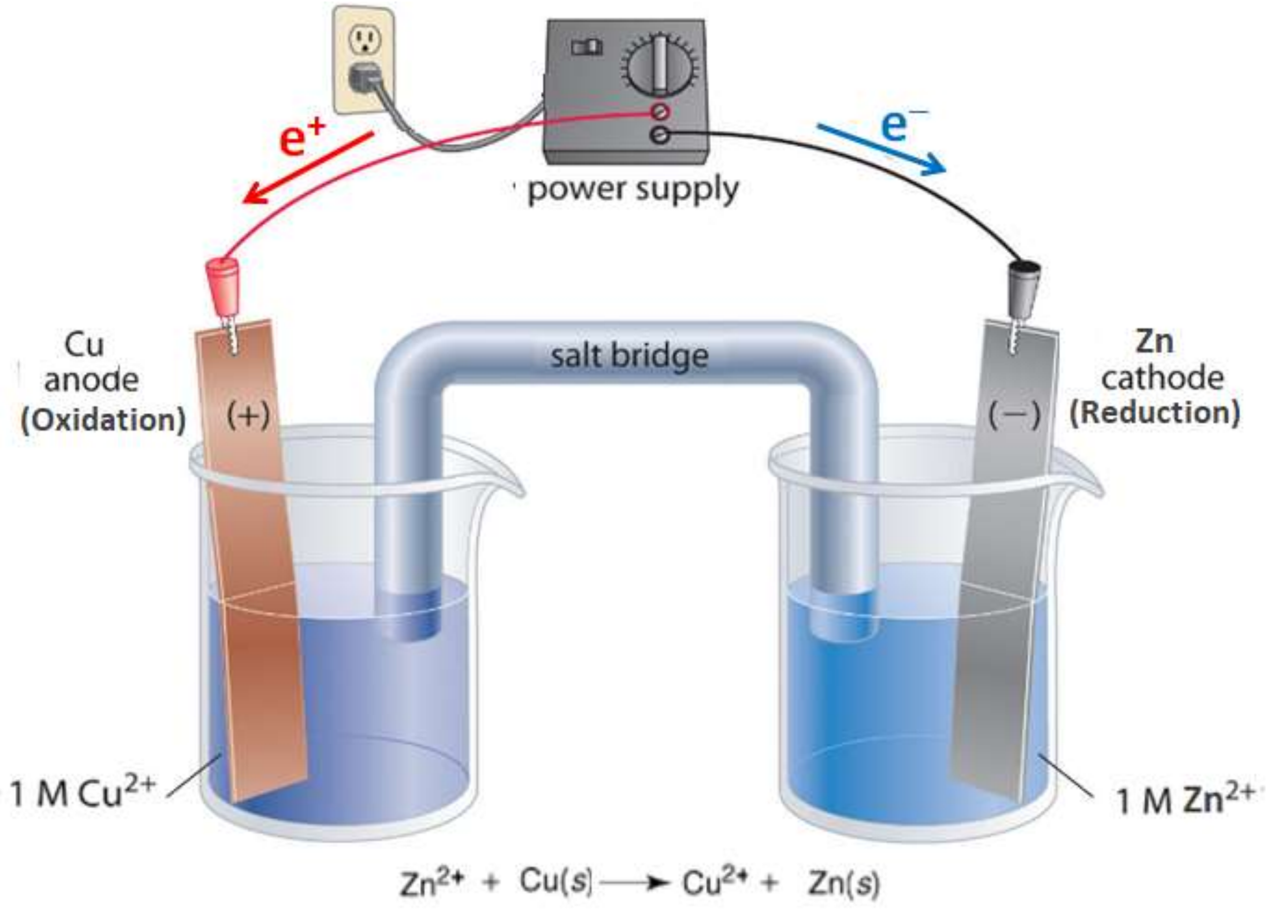

Figure 70: Copper-Zinc Electrolytic Cell

Redox reactions are reversible, which allows (partially) exhausted chemical reactions of a galvanic cell to be revived by applying an appropriate voltage across the cells to generate a current in the opposite direction, effectively re-charging a galvanic battery cell. Thus, although chemical imbalance and crusting can reduce their effectiveness, galvanic cell based batteries can be re-charged using an Electrolytic Cell setup such as that shown in figure 70, which can be used to refresh the galvanic cell setup of figure 68.

The electrolytic cell also involves cetron (**e**⁻) and aptron (**e**⁺) sources and sinks, as shown in the equations below:

Reduction: $Zn^{2+}_{(a)} \rightarrow Zn_{(s)} + 2e^+_{(f)}$ = Aptron Source $Zn^{2+}_{(a)} + 2e^-_{(f)} \rightarrow Zn_{(s)}$ = Cetron Sink

Oxidation: $Cu_{(s)} + 2e^+_{(f)} \rightarrow Cu^{2+}_{(a)}$ = Aptron Sink $Cu_{(s)} \rightarrow Cu^{2+}_{(a)} + 2e^-_{(f)}$ = Cetron Source

Plasma and Cosmic Radiation

Plasma is formed by super-heating matter, which causes electrons to be stripped from the atomic structure to yield a mixture that is rich in electrons and ions. Over 99% of the matter in the visible universe is believed to be plasma. An important source of plasma formation in space is **photoionization**, wherein photons from stellar EMR are absorbed by an existing gas mixture, causing electrons to be emitted.

Closer to Earth, lightning, naked flames, welding arcs, neon/fluorescent tubes, neon signs, plasma (some TV and computer screens), plasma lamps and globes involve the generation of plasmas; and the Earth is surrounded by a dense plasma called the **ionosphere** and impacted by the Sun's solar wind plasma. Plasma can also be created in the laboratory by super-heating a neutral gas and/or subjecting it to a strong electromagnetic field to the point that it is ionised. Also, low-temperature strongly coupled plasma-like electrons and ions, such as complex plasmas and ultracold (100 mK to 10μK) neutral plasma (created by photoionization of laser-cooled xenon atoms), have only been developed and researched since 2007.

For the higher temperature plasmas, as the temperature and the amount of chaotic buffeting within a gaseous mix increases, the atoms' energisation levels increase, with bitrons being released from external bitron bonds as energised cetron electrons and positrons (aptron electrons), which greatly increase the electrical conductivity of the mix. Such early stage ionisation is accompanied with the generation of extensive long-range electromagnetic fields and production of gamma radiation from electron-positron annihilation collisions, which further contributes towards the mix's energisation level.

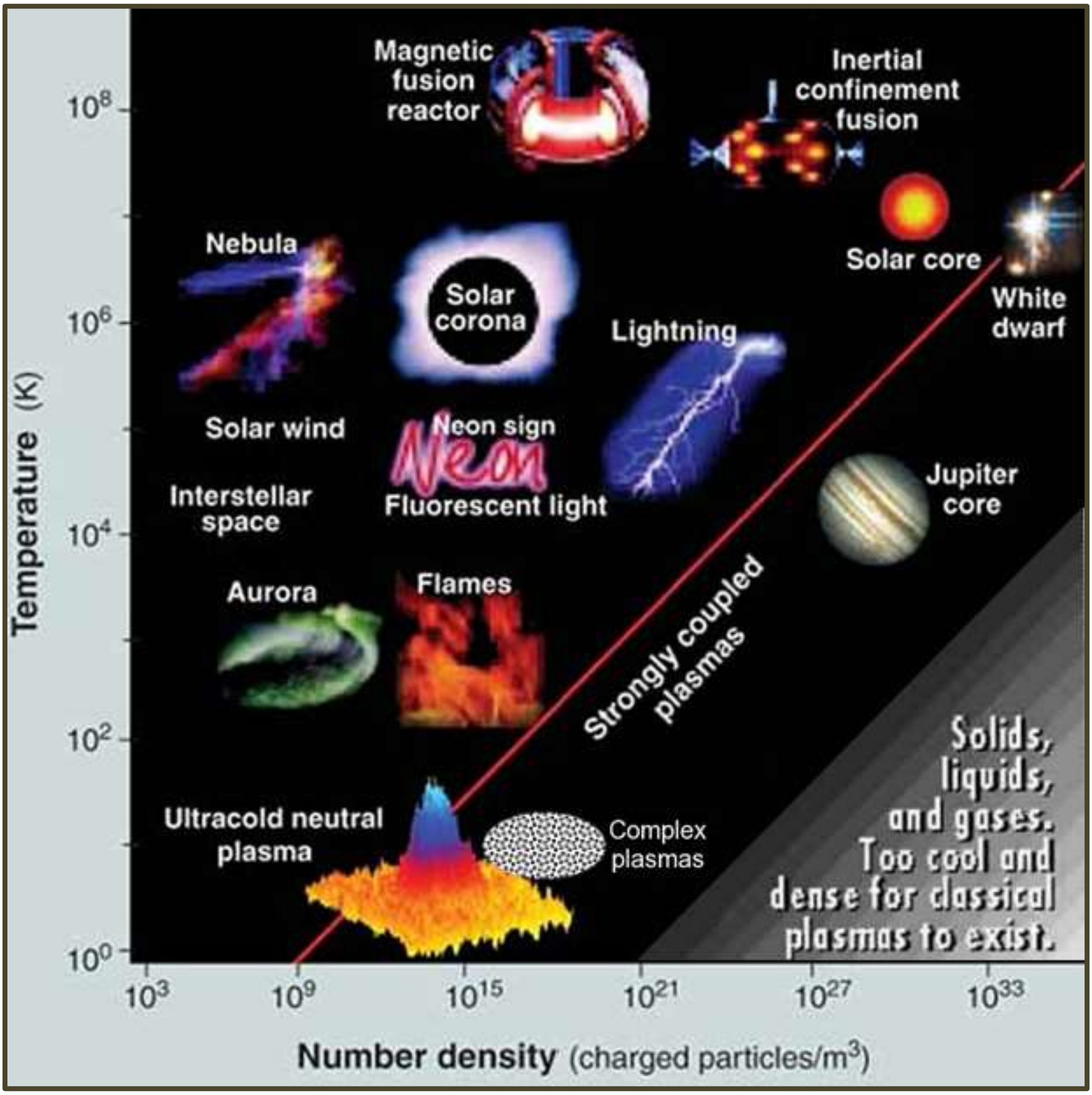

Figure 71: Plasma Temperature/Density Distribution

With increasing energisation levels, more external bitron bonding fails and the plasma mix becomes strongly ionized. Hydrogen is the most elementary and widespread form of plasma in the universe, which at about 7,000^{o} K, and by around 10,000^{o} K hydrogen is completely ionized. For hydrogen ionisation the bitron bonds of hydrogen molecules is stripped away, creating a mix rich in electrons, positrons and protons (hydrogen nuclei), which causes some interesting phenomena to happen:

- Firstly, the destruction of hydrogen molecule bitron bonds means that hydrogen becomes reduced to L-form protons, and thus hydrogen drops out of emission spectra for the plasma mix, with any spectral lines being attributable to contaminant remnants of previously larger atoms.
- Secondly, because highly energised free electrons and positrons abound, protons are nucleon-type converted into neutrons via **β+ decay**, and then back again into protons via **β- decay**. This ongoing circular process generates large numbers of beta rays, neutrinos and anti-neutrinos.
- Thirdly, the ongoing nucleon-conversion process generates a mix of energised free protons and neutrons in close proximity, which allows them to combine and so create new atoms, principally helium, which, in such a highly energised environment, presents as **alpha radiation**.

Cosmic radiation, the high-energy particles arriving from outer space from distant galaxies, consists mainly of protons (89%), Helium (10%) and a mix of heavier nuclei (about 1%), plus abundant levels of high-energy neutrinos, anti-neutrinos and gamma radiation: a content compatible with that of a completely ionized hydrogen plasma mix. When cosmic radiation encounters molecules in the Earth's outer atmosphere, **muons** are generated. The most likely sources of the muons (**CES pairs**) are the quarks of collision-destroyed inbound protons and damaged molecules.

When temperatures rise to **well above the 10^{4} K range**, such as achieved by active stars, the bitron bonds supporting embedded atomic forms within larger atoms fail, creating fission products of lower atomic number. The very fabric of any original atomic material has thus been compromised and beginning to break down, with any semblance to the original atomic structures being lost. Cooling of the plasma cloud at this stage would result in a completely different mix of atoms and compounds.

Should energisation continue even further, nucleon layers of atoms would begin to break down, with their polygonal forms being compromised and reduced to a mix of fragmented nucleon chains, nucleons and/or compromised nucleon fragments. Such utter destruction and decomposition most likely only occurs in the crush within the bowels of collapsing and merging/colliding neutron stars.

Fission, Fusion and the Creation of the Elements

The origins of elements can be attributed to **Big Bang** fusion; **cosmic ray spallation** related fission; **merging neutron stars**; **exploding massive stars**; **dying low mass stars**; and **exploding white dwarfs**. Apart from cosmic ray spallation and radioactive decay series (currently active on Earth and assumedly elsewhere in the Universe), which involve fission, most elements result from fusion processes.

Science's understanding of the creation of the elements is incomplete and far from being exact. The inter-mixing and re-cycling of material between different processes complicates matters, as does the induced and natural fission-related decay of elements. The elements resulting from the Big Bang consist mainly of elements with atomic numbers less than or equal to three (i.e. lithium and below), with elements with a larger than 3 atomic number are generated by star-related processes.

For most of their lives, stars steadily churn concentrations of hydrogen into helium within their cores. When stars larger than about half the mass of the Earth's Sun run out of hydrogen within their core, they begin to collapse under their own gravity, which creates additional pressure in their core to produce by-products such as carbon and oxygen. For stars more than twice the mass of the Sun can also generate nitrogen as well. Once the bulk of a star becomes depleted of hydrogen due to the fusion process, they become **red giants** (see figures 72a and 72b).

Stars with up to about eight times the mass of the Earth's Sun are categorised as **low-mass stars**. Collapsing, dying low-mass stars begin a slow neutron-capture process (the s-process) to create heavier elements like strontium, lead, mercury and the like (those elements highlighted with green in figure 72c).

As the collapse of a low-mass star continues, the outer gaseous layers of helium and hydrogen expand around the carbon and related heavier elements, and can no longer be contained by gravity. These gases are ejected into space to create a **planetary nebula**, leaving behind an essentially carbon core known as a **white dwarf**. A planetary nebula represents the release of elemental material into interstellar space, where it can be recombined and recycled into new stars and planetary systems. Along similar lines, sometimes a white dwarf acquires elemental material from a nearby companion star to become unstable and to subsequently explode as a **type 1a supernova**, which produces the range of elements highlighted with grey in figure 72c.

High-mass or massive stars are those greater than about eight times the mass of the Sun. When a massive star reaches the end of its life, it can explode as a **core-collapse supernova** (or exploding massive star) that produces elements highlighted with yellow in figure 72c, and can result in a **neutron star**.

When neutron stars collide or merge, they create heavier elements via rapid neutron-capture (the r-process) to produce a mix of stable (e.g. silver, gold and lead) and radioactive heavy elements (e.g. uranium and thorium): these elements are highlighted with purple in figure 72c). The radioactive elements produced by merged neutron stars are represented in the fission-related **radioactive decay series**.

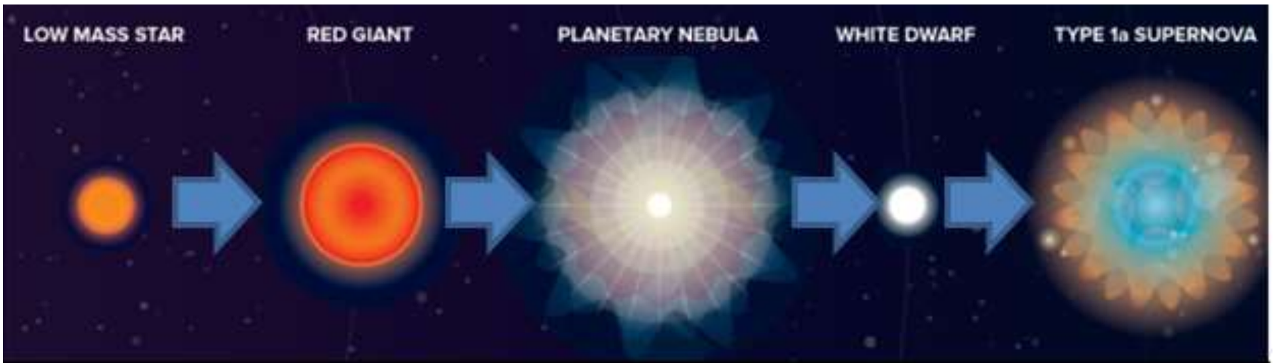

Figure 72a: Evolution of Low-Mass Stars

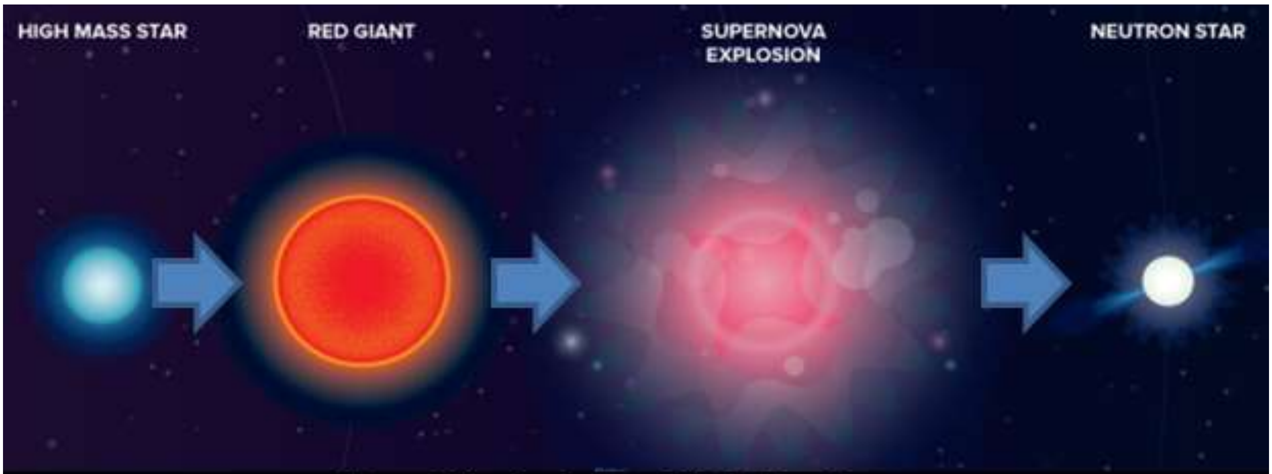

Figure 72b: Evolution of High-Mass Stars

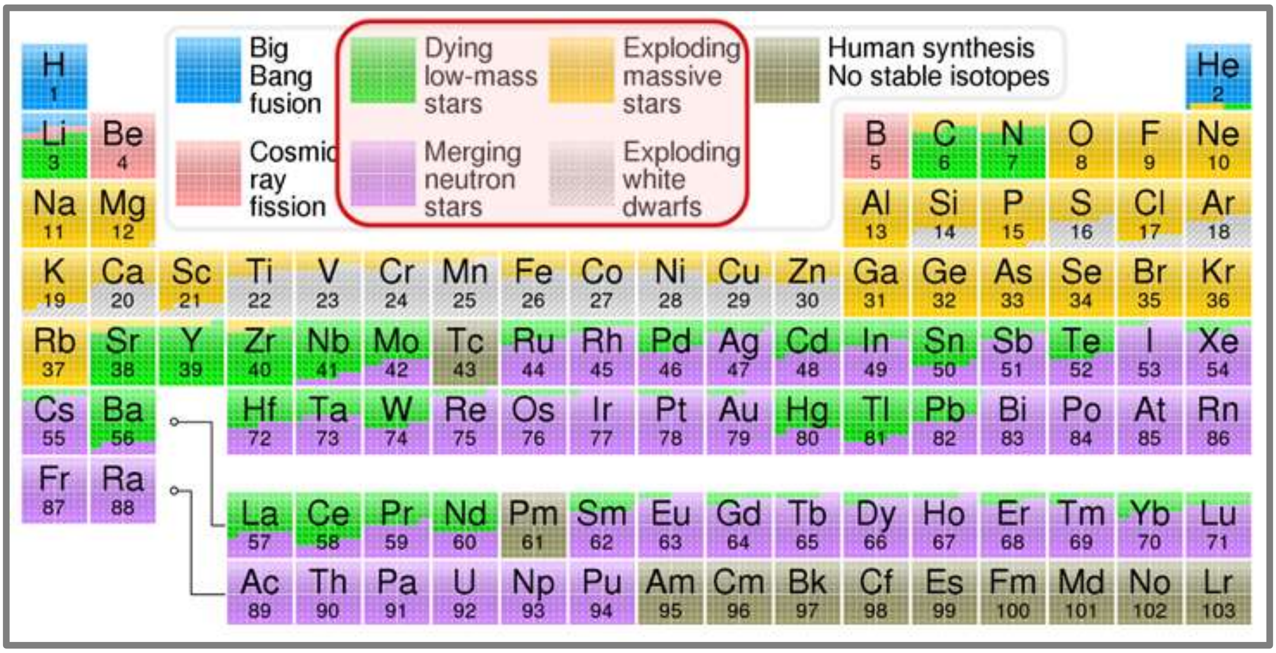

Figure 72c: Cosmological Origins of the Elements in the Periodic Table

The crystal structure of elements created in energetic fusion environments, as provided by exploding massive stars and white dwarfs, tend to have far less externally attached helium atoms and form more uniform crystal structures, and are consequently more stable radioactively. The more uniform crystal structures of these elements tend to keep the planar electron and positron orbitals above and below the atomic nuclei well separated, which minimises the chance of planar orbital electrons and positrons colliding and annihilating each other

The structure of elements created by the r-process (i.e. related to merged or colliding neutron stars), tend to be significantly different to those formed by other means. In such a high temperature and high pressure violent chaotic environments, many larger and unstable atoms are formed. These elements have many helium atoms attached externally by a single inter-quark bond as well as those embedded internally, which contributes to the formation of crystal structures that are far from uniform, The lack of uniform crystal structure results in poor separation of their planar electron and positron orbitals, which produces random electron-positron annihilation events that generate gamma radiation, which in turn initiates a range of other forms of radioactive emissions such as alpha radiation, beta radiation, neutrinos and more gamma radiation (via Bremsstrahlung).

A prime example of the radioactive decay process is the Uranium-238, Actinium-227, Thorium-232 and Neptunium-237 decay series: all involve the change in atomic number and weight by the loss of Helium-4 as alpha particles and the occasional conversion of a neutron into a proton via beta minus (β-) decay, which increases the atomic number (i.e. the proton count) of the atom by 1. The result of these series is a set of daughter products with half-lives from minutes to thousands of years.

In general, the more complex an atom is, the less abundant that it is, and the more natural variation it has in terms of its structure and isotropic forms. Nuclei with even number of protons appear to be more abundant than odd ones and, more generally, even–even nuclei (with even number of protons and even number of neutrons) are more frequent than even–odd elements that are in turn more common than odd–odd ones. Also, up to period-3 of the Periodic table, a different polymorphic form of an element tends to be associated with a change in the polygonal form (e.g. the hexagonal and tetragonal allotropic forms of C-12) of the atom, and beyond period 3, the randomness and variation in atomic structure increases, as does the extent of embedding and the number of attached L-form neutrons.

For the conventional Orbital Nuclear Atomic Model (ONAM), an atom's nucleus consists of a conglomerate of protons and neutrons held together by strong force bonds so as to create an approximately spherical shaped nucleus that is surrounded by high-speed electrons or their wave-form equivalents. Although mathematical models define the patterns and order for orbital electrons, nucleons are considered to be spherical in shape, bound together by strong force bonds but without any specific structure for the nucleus. Elements are defined by the number of protons (= the number of electrons if element is in a neutral state) in the nucleus. Every acquisition or loss of a neutron is considered to change the isotropic form of the element, with alpha and beta decay being considered to instantly change the element and all its associated physical properties, by changing the number of nucleonic protons.

From the STEM perspective, the **structure** of the atomic nucleus is paramount, and that structure is determined by the environment in which an element, or its parent, was created. The removal of attached or embedded helium atoms by the impact of fast-moving (and thus energetic) decay particles creates child-products that retain the essential geometry but not the nucleon count of the parent. This radioactive decay process has been erroneously referred to as 'atom splitting' when it is more akin to 'atom separation': atomic bombs and fission power generators are thus examples of atom separation rather than atom splitting.

Also, STEM contends that elements have much more natural variation in terms of structural variation than is suggested by the simplistic categorisation of elements by atomic number, and their representation by period and group within the Periodic Table. Important aspects of the natural variation are the structure of elements, their embedded forms and the nucleon distribution around their atomic nucleus, all of which is related to the atom's structural genealogy (the way it was created and/or evolved from its ancestors). The P-# signature suggested for elements provides a compact means to define the underlying nuclear structure of an atom and suggest the statistical spread attached β-decay derived protons for the element. As an attempt to quantify the structure, composition and statistical variability within a physical sample of an element, it represents a start rather than an end-point technique.

Much of the research associated with the development of the Standard Model involves the high-energy bombardment of a range of materials by high-speed electrons and/or protons. Such high-energy impact studies have identified two basic groups—quarks and leptons, with each group containing six particles, segregated into three pairs or "generations" according to their mass and stability, with the first-generation quarks and leptons making up all stable matter and the others only existing very briefly before decaying. STEM contends that all basic fundamental particles consist of the toroidal energen concentrations typified by CES, electron, positrons and neutrinos, with CES building into nucleon-based nuclei. Also, STEM does not require the existence of theoretical force-carrying boson or gluon particles, and it is suggested that second and third generation leptons and quarks, as well as antiprotons and antineutrons, all represent abnormal debris fragments derived from impact-destroyed nuclei.

The Force of Gravity

Any energy source which spreads equally in all directions in three dimensions will obey **the inverse square law** due to geometrical considerations, with the intensity of the energy at any given distance ‘**d**’ from the energy source being proportional to the source strength divided by $\mathbf{d^2}$. The inverse square law applies to many other energy-related situations such as electric and magnet fields, gravity, sound, and EMR radiation (e.g. light). The equations for electric (attraction or repulsion) force between 2 electric charges and the gravitational attraction force between 2 masses are:

$F_e = K\frac{q_1 q_2}{d^2}$	$F_g = G\frac{m_1 m_2}{d^2}$
F_e = Electric Force	**F_g = Gravitational force**
q_1, q_2 = electric charge (Coulombs)	**m_1, m_2 = mass in Kg**
$K = 68.9876 \times 10^9\ Nm^2\ C^{-2}$	**$G = 6.67300 \times 10^{-11}\ m^3\ Kg^{-1}\ s^{-2}$**

These 2 equations serve to show that gravitational force is by far the weaker of the two by a factor of about 10^{-36}; and, although not evident in these equations, **strong force** is about 100 times as strong as electric charge force.

With the STEM approach, field-energy is continually being circulated both through and around atoms. Internally, field-energy is balanced between quarks, nucleons and interconnected nucleon layering via strong force inter-quark bonds, providing the essential function of energy distribution and sharing within an atom. Externally, CES within nucleons continually loose small amounts of field-energy to the outside world, although their inflow capacity exceeds those loss levels, with CES with **central inflow vortices** being more effective at retrieving field-energy than those relying upon **outer inflow** of **central outflow** CES.

However, in spite of being potentially able to recoup the field-energy escaping to the outside world, small quantities of field-energy are continually being lost by matter. As well as field-energy loses from the swirling electromagnetic energy-fields of CES, all forms of concentrated field-energy (e.g. cetron and aptron electron charge carriers, photonic and non-photonic EMR) lose and contribute very small amounts of field-energy. Most of this ‘lost’ field-energy accumulates in low concentrations in an atmosphere-like fashion: as such, it is called an ‘**enersphere**’. Enersphere energen forms around all normal matter, and has no discernible flow pattern except that its concentration decreases radially away, most likely inversely to the square of the radial distance from the host object from which it escaped.

Despite CES having enough capacity to retrieve all lost field-energy, probably due to the low concentration and inert nature of enersphere energen, enerspheres tend to grow, possibly eventually stabilising, but never disappearing. With the suction-like action of CES continually trying to retrieve energen from the surrounding enersphere, all atoms exert a small positive pull-force on the enersphere immediately surrounding their host object. The resulting small inwardly-directed forces are cumulative which, when summed over billions of nucleons (1 litre of water contains approximately 2×10^{27} or 2 octillion$_{\text{[USA]}}$ nucleons), the net resultant force vector, STEM suggests, is the force of **Gravity**.

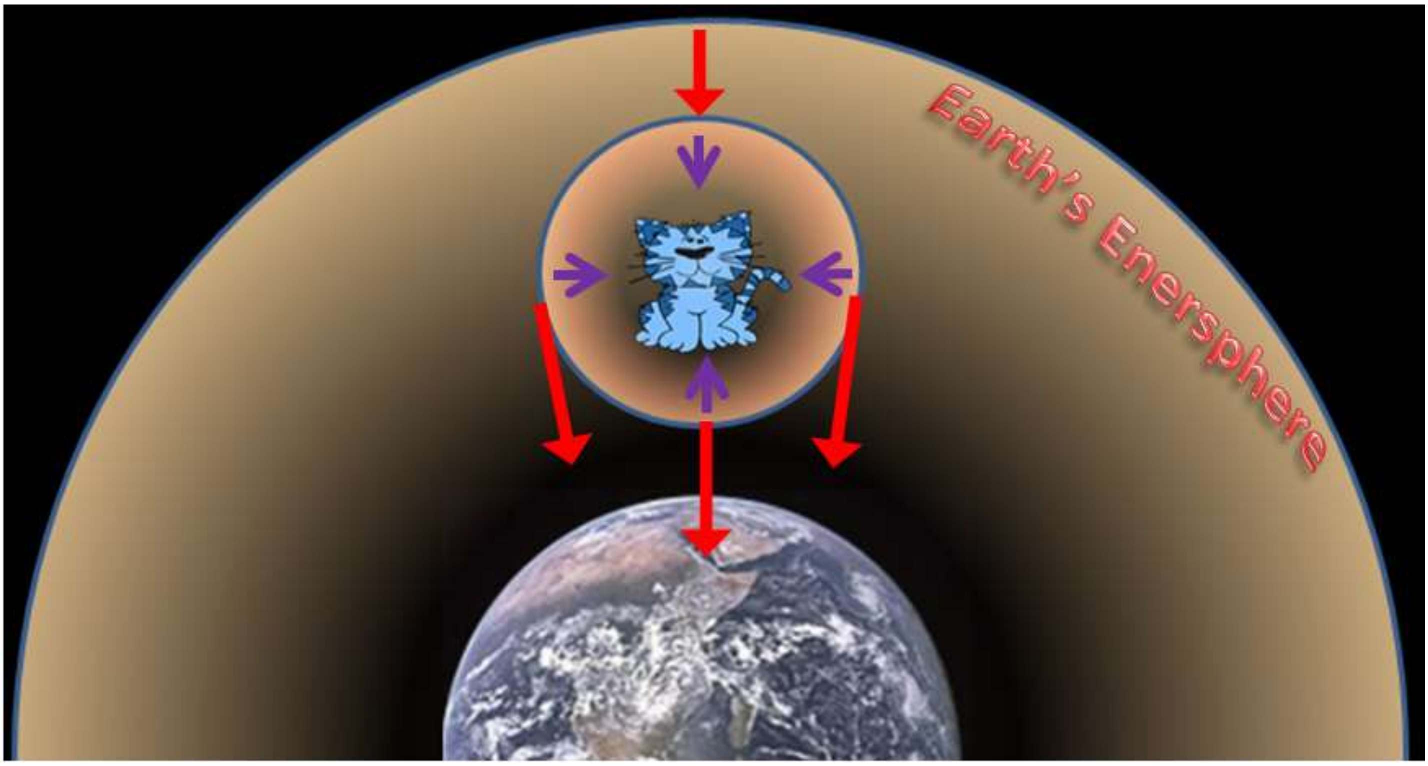

Figure 73: Model for Earth's Gravity

When the enerspheres of two objects overlap, the increased energen concentration between them marginally increases, producing a commensurate increase in the strength of the small inwardly-directed forces on the sides if the objects facing each other, which has the effect of drawing them closer together. The larger the object, the larger is its enersphere and its force of Gravity. Smaller objects (such as a cat, a book or a brick) unrestrained near the surface of a larger object (such as Earth) will move towards the large object.

Figure 73 represents a hypothetical cat sitting with its enersphere fully within the Earth's far larger enersphere. The purple arrows show the direction of the forces pulling the cat's enersphere towards the cat, and the red arrows represent the considerably greater forces resulting from the vast number of Earth atoms pulling the cat and its enersphere towards the surface of the Earth. Due to the overlapping enerspheres, the increase in energen between the cat and Earth adjacent to the cat means that the cat is heading earthwards, free falling under the influence of Gravity.

The depiction of figure 73 is idealised because the shown bubble boundary surfaces do not exist because when one object's enersphere overlaps another's the energen concentrations increase between and around them. The suction-like pull of the inflow CES within each object (here the cat and Earth) would continue to pull energen from the resource-in-common, their merged enerspheres, with Earth's significantly larger pulling power and inertial mass drawing the cat towards it, with the nett forces acting on the cat being similar to those shown, as would be their nett effect. (Note that no cats were injured directly or indirectly in STEM research).

At the macro level, the enerspheres of large bodies extend well into space (e.g. the Moon, Earth, the Sun, the stars and galaxies), with competition for their shared energen resource creating gravitational pull between systems. The huge, far reaching enerspheres of large objects in space suggests that their enerspheres overlap and could possibly be in expansion mode, albeit slowly. It is difficult to imagine any region of space that would be devoid of enersphere energen except possibly at the outer regions of an expanding Universe.

Ignoring the effect of Sun's enersphere, let's consider the simple example of the Moon moving around Earth. Due to its spin, Earth's enersphere would most likely be ellipsoidal rather than spherical, whereas that of the Moon, which orbits without spinning, would be spherical. The over-lap pattern of their enerspheres would mix and blend seamlessly to generate an asymmetrical **energen concentration profile** (labelled '**Typical Space-Density Profile**' in figure 74b) that would move around in a circular annular path.

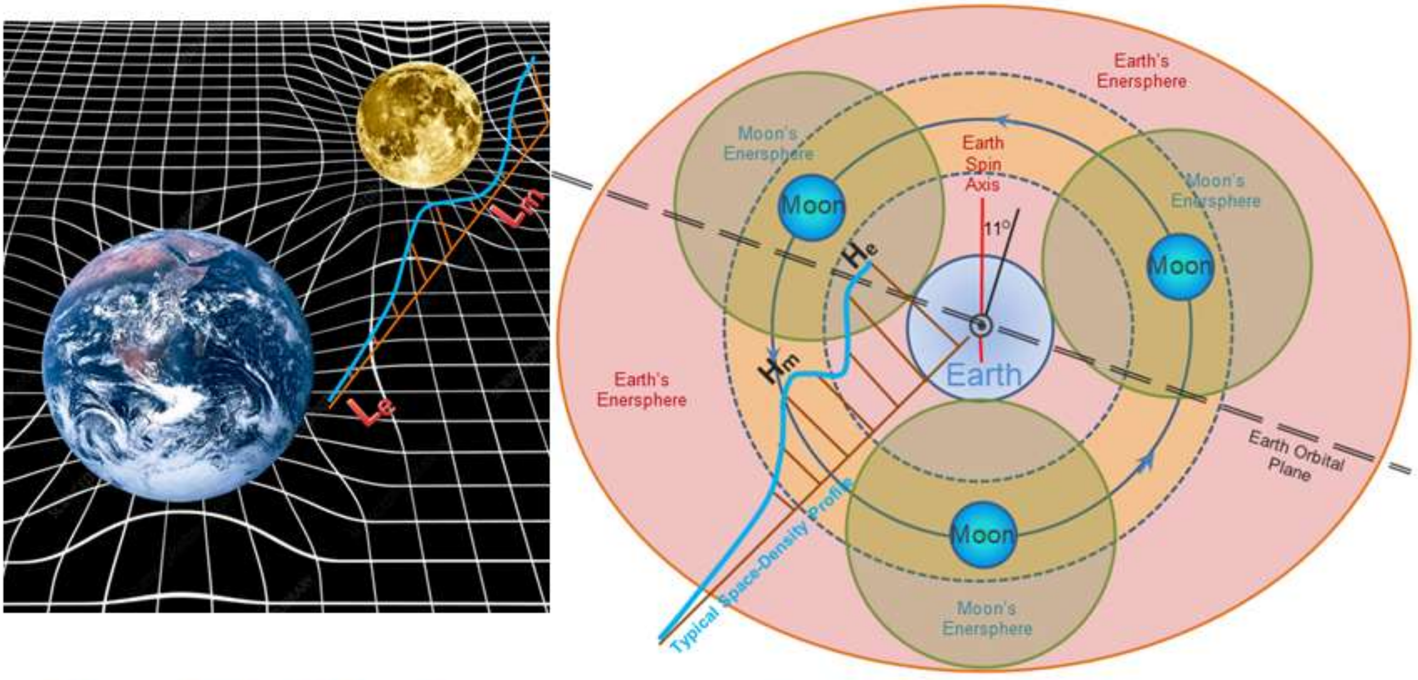

a) Space-Time Distortion   b) Space-Density Distribution

Figure 74: General Relativity and Enersphere Energen Explanations for Gravity

Figure 74a shows a typical contour plot showing the broad indentation that the Earth makes in the fabric of General Relativity's hypothetical **space-time** and the smaller sharper indentation made by the Moon as it orbits around the Earth. The cross-sectional indentation lows, L_e for Earth and L_m for the moon in space-time correspond quite well to the highs H_e and H_m in the space-density profiles of figure 74b, which suggests that space-time surface defined by General Relativity is the inverse of the space-density surface defined by enersphere energen. Or put another way, should the space-time surface plot of figure 74a be viewed looking up from below the page (rather than the normal above-page view), then it would have contours remarkably similar to those for the space-density plots.

Space-density is based upon a physical model predicated by the existence of enerspheres, whereas space-time is an **abstract concept** that has implications related to gravitational **time dilation**. As there is motion and force involved in the space-density approach, time (t) still is an important factor in the space-density approach, but it is simply not combined with 3D-space as a product to create the counter-intuitive mathematical quantity called space-time. Both approaches relate Gravity to the **mass** of the objects involved: for General Relativity, mass causes the warping of space-time; and for STEM the increase of energen between objects, as reflected in space-density plots, increases the net inward pull by atoms within matter, which is related to the number of atoms, and thus to the mass of the objects.

It could be argued that the enersphere energen represents luminiferous aether, the medium postulated to support the propagation of light as electromagnetic waves in Space. However, although enersphere energen has no discernible flow pattern, its concentration decreases radially away from associated matter so that it is not evenly distributed throughout Space, as required for luminiferous aether; a matter made worse by macro object movement and orbitals. Due to its uneven distribution throughout Space, the speed and strength of electromagnetic light waves would vary accordingly, and thus enersphere energen cannot be considered to represent the much sought after luminiferous aether.

Also, as explained in the ‘Photons and EMR Generation’ chapter of the STEM Nature of Light paper, FER-based photonic EMR does not need enersphere energen or luminiferous aether to support or sustain it in Space.

Looking beyond our own Solar system, as **large scale cosmological systems** approach each other, their enerspheres merge causing an increase in enersphere bulk and thus the gravitational pull of each towards the other. For merging systems such as **neutron stars** or **black holes**, a spin embrace results which climaxes in a rapid compression of their combined enerspheres, ultimately leading to a massive explosion of compressed energen and consequential generation of **gravity waves**.

Enerspheres are a remarkable bi-product of the way energen concentrates and combines to make atoms, and of atoms to make matter, with the force of Gravity being due to the retrieval of energen from the enersphere rather than a mysterious external force or a result from the warping of **space-time**. The STEM approach to gravity applies equally as well at the micro-scale (e.g. for small and large objects on Earth and everything in between) as it does at the macro-scale (e.g. large cosmological objects): can the same be said of the space-time approach of General Relativity?

Historical Note. **René Descartes**, famous for his philosophical assertion ***cogito ergo sum*** ("***I think, therefore I am***"), in 1644 proposed that **aether**, the medium then considered to separate objects and matter (cf. space), is filled with vortices whose **inward pressure** is ‘*nothing else than Gravity*’.

Equate **Descartes’s vortices** to in-flow CES vortices within nucleons, and consider the **aether** to be the enersphere energy surrounding matter, then, **philosophically speaking, Descartes’s 377 year-old explanation for Gravity was not far removed from that of STEM.**

(It should also be noted that STEM does subscribe to the notion that aether is the substance or medium in space that supports the propagation of EMR in a wave form.)

Overview of the STEM Approach

The STEM approach introduces many new concepts that are quite different to the conventional Science approach to atomic theory. With STEM the electron model, electric currents, electromagnetic fields, the atomic nucleus structure, ionic orbitals, and the generation of photonic EMR are all inter-related as indicated in the overview chart below.

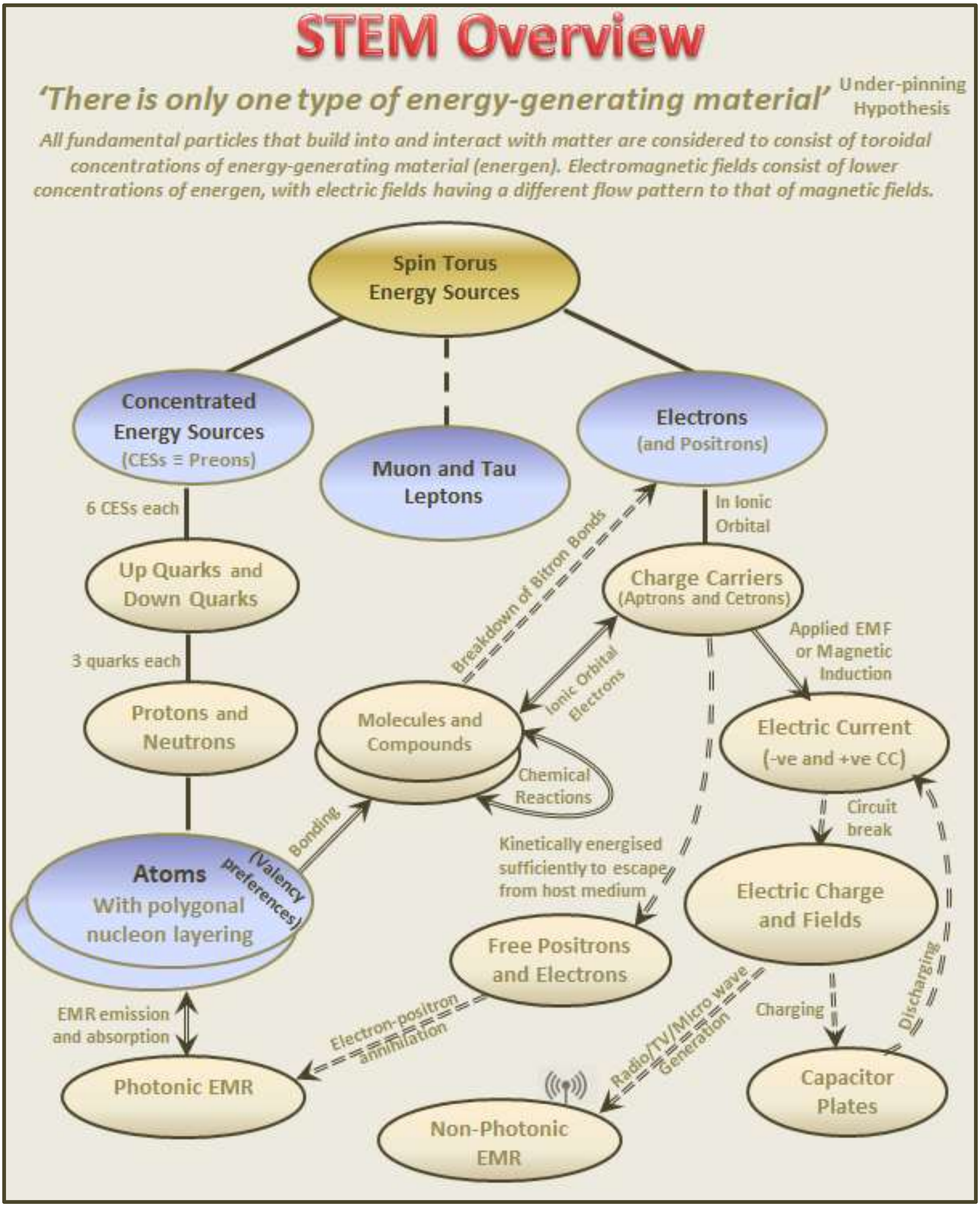

The STEM electron model and its use to explain electric currents and electromagnetic fields can be found in the position paper titled '**Electricity and the Duplicit Electron**', and the creation, composition and behaviour of all known forms of EMR, including light rays and beams, light refraction, reflection and polarisation, is covered in the position paper, titled '**The Nature of Light Based Upon a Physical Model for EMR**'. A summary of the key differences and similarities between the STEM approach and the conventional Science view is provided in the tabulation below.

Aspect		STEM	Conventional Science (CS)	
Electron (or Cetron Electron or **Negative** CC)	Structure	Toroidal energy core surrounded by a chiral electromagnetic field	Point-form definition (no structure or spatial extent) or spherical (unsupported).	
	Size	Energy core R=$2.4x10^{-13}$m; r =$1.6 x10^{-13}$m	QM = Nil (point-form definition); CS radius= 10^{-20} to $7x10^{-13}$m (spherical model)	
	Spin	Newtonian angular momentum = $5.24 x 10^{-35}$ Js	Intrinsic, derived from reduced plank constant = ħ/2 = $5.27 x 10^{-35}$ Js	
	g-factor	g = 2.012 using Newtonian angular momentum (above)	g = 2.00232 using reduced plank constant estimate for spin (above).	
	Charge	negative charge (-1e) due to the left-handed chirality of EM field	Intrinsic negative charge (-1e)	Considered to consist of different material
Positron (Aptron Electron or **Positive** CC)		Positive charge (+1e) due to the right-handed chirality of EM field	Intrinsic positive charge (+1e)	
Electricity	Electric current	Duplex movement of cetron and aptron electrons in opposite directions.	One-way movement of electrons from the negative terminal towards the positive terminal.	
	Circular magnetic field	Due to net toroidal component of cetron and aptron EM fields. Maxwell's RH Fist Rule applies.	No explanation, but Maxwell's RH (right-hand) Fist Rule used to determine direction with respect to current flow	
Electric Fields		Combined field energy of CC that are axially aligned (moving or static). Field Chirality determines whether negative or positive.	No real explanation. Negative and positive fields are generated by particles/materials that intrinsically have either a positive or negative electric charge property.	
Magnetic Fields		Generated by the toroidal component of the field energy of cetron and aptron electrons moving as an electric current.	No real explanation for why they are generated by electron movement as an electric current.	
Up/Down Quarks		Composite particles formed by octahedron array of e-CES and p-CES (large electron/positron like fundamental particles).	Fundamental particles. No real explanation. Up and down quark electric assumed to have a charge of +2/3 e and -1/3 e respectively.	
Nucleons		L-shaped, with a central quark strong-force bonded to 2 other quarks (a neutron = DUD and a proton = UDU).	Composite particles; triangular form consisting of three quarks (a neutron = DUD and a proton = UDU). Each quark is bound to the others by 2 strong force bonds or gluons.	
Atomic nucleus		Nucleons strong-force bonded to form linear nucleons to produce a lattice-like polygonal structure.	An amorphous aggregation of protons and neutrons. No specific structure or explanation of why protons don't forcedly repel each other.	
Orbital Electrons		Zero to four planar ionic orbitals (unrelated to the number of nucleons in the nucleus).	Neutral atoms have same number of orbital electrons as protons. Orbitals pattern undecided: shell-like (CS) or spdf (QM).	
Chemical and Ligand Bonding		**Covalent** (ionic orbital overlap) **b-bond** (pre-electron bond) **p-bond** (more than 100pm long).	**Covalent** (electron sharing via cross-overs) **Ionic** (involving +ve and -ve ions) Requires use of hybridised spdf orbitals.	
Gravity		Due to the retrieval of low-level concentrations of background energen by atomic nuclei.	An abstract explanation, being due to the hypothetical displacement (or warping) of General Relativity's distribution of space-time.	
EMR	Unpolarised Photonic	Consists of solenoidal-like ringlets of energen (FER) in a double helix structure generated by ionic electrons moving to a lower energy level. Particle-like.	Electromagnetic waveforms generated by orbit electrons jumping from a higher to a lower energy level. Require Aether to travel though outer Space. Photons are considered to have sufficient energy to act particle-like.	
	Plane Polarised Photonic	Ringlets (FER) re-orientated with their toroidal spin axes in a plane containing their travel direction.	The electric field of light is confined to a single plane along the direction of travel. The magnetic field is orthogonal to the electric field	
	Non-Photonic	Expanding waves of field energy, with the circular magnetic field of adjacent waves being in opposite directions.	No provision for non-photonic EMR. Man-made micro/radio/TV waves are considered to have the same electromagnetic waveform as all other unpolarised photonic EMR.	

The main differences between the STEM approach and the conventional Science view are that:

- Electrons and positrons have spatial extent and thus their angular momentum (spin) is not intrinsic.
- Electric charge and associated fields are due to chiral energen flow patterns rather being intrinsic properties.
- Electric current is due to the two-way (duplex) movement of negative and positive charge carriers (CC) rather than the one-way movement of electrons.
- Circular magnetic fields around electric current carrying wires are due to the toroidal flow components of cetron (negative CC) and aptron (positive CC) electrons rather than being intrinsic.
- Atomic nuclei have a polygonal lattice-like structure that is reflected by their physical properties and chemical bond characteristics rather than simply being a ball-like amorphous aggregation of nucleons.
- Orbital electrons occupy planar (or ionic) orbitals above and/or below the nucleus rather than in shell-like (CS) or spdf (QM hybrid) orbitals that encompass the whole nucleus.
- An atom has one or two ionic orbitals, each supporting up to 2 cetron or 2 aptron electrons, rather than the number of orbitals of a neutral atom being determined by the number of protons in its nucleus.
- CS has no equivalent to bitron bonds (b-bonds). Bitrons are pre-electron concentrations of energen that form as chemical bonds for bond lengths less than 100pm long.
- Photonic EMR (e.g. visible light) consists of **F**ield-**E**nergy **R**ings (**FER**), that are particle-like ringlets of energen whose combined electromagnetic footprint presents as that of a CS electromagnetic wave.
- Non-photonic EMR (e.g. man-made radio and micro waves) structure is different to photonic EMR.

Key aspects about which conventional Science and STEM both agree upon include:

- All aspects of Newtonian Physics.
- Electron and positron behaviour is well described by the QM wave equations.
- Atoms consist of a nucleus and orbital electrons; and the nucleus consists of protons and neutrons.
- Neutrons can convert into protons and vice versa.
- Charge movement (electric current) generates a circular magnetic field and wire movement through (or of) magnetic fields can generate electric current.

In the early stages of development, the claim that electric current consists of the duplex movement of negative and positive charge carriers (CC) in opposite directions represented a major deviation from conventional Science wisdom and quite difficult to justify. However, recently, two non-science related phenomena have been identified: fractal wood burning and DCPE (Direct Current Positive Electrode) welding. As discussed in STEM's **Electricity and the Duplicit Electron** position paper (pages 16-17), these phenomena can only be explained should positive charge carriers (aptron electrons) be involved. If not proof of concept, these two phenomena represent quite strong supportive evidence.

Two other aspects of STEM that are distinctly different to conventional Science wisdom relate to the structure of atomic nuclei and the nature of atomic orbitals. The latter are planar, and support either cetron or aptron electron orbits above and/or below the nucleus. The hollow polygonal lattice-like structure of nuclei accommodates the embedding of helium nuclei within larger nuclei, which can in turn be released as alpha radiation. Also, STEM's hexagonal and tetragonal nuclear models for carbon-12 explain the different characteristics of graphite and diamond quite well (right down to bond lengths and pattern, the unit cell size and their density estimates): they also explain the subtle differences between cubic and hexagonal diamond.

Conventional Science considers that all EMR consists of electromagnetic waves formed by a pair of synchronised orthogonal electric and magnetic field components. STEM, on the other hand, makes a distinction between photonic and non-photonic EMR. **Photonic EMR** is considered to consist of ringlets of energen called **F**ield-**E**nergy **R**ings (**FER**) that, for a single monochromatic ray in the visible light range, move in a double helix formation. **Non-photonic EMR**, such as man-made micro/radio/TV waves, consists of the same type of field energy (i.e. energen) as for photonic EMR, but its structure is different. It is generated from an antenna by rapidly alternating electric current, which generates outwardly moving waves of field energy, with each successive wave being characterised by a reversal of circular magnetic field direction.

STEM is an energy-centric approach that is predicated by the hypothesis there is only one type of energy-generating material (energen). Energen varies from very low concentrations without any flow movement that forms around and is attached to matter as an enersphere, through to high-concentration torus-shaped forms (e.g. the energy-core of a CES), wherein energen circulates at a speed close to that of light and is associated with a less concentrated form of energen that creates an energy-field with left or right-handed chirality. The characteristics of energen, and the manner in which it interacts with other energen-based fields, particles and materials, are concentration dependent as summarised in the tabulation below.

Energen Form	Characteristics	Interactions	Comments
Enersphere *Very low energen concentration*	A very low concentration of energen accumulates around all matter to form an atmosphere-like **enersphere**. Enersphere energen has no discernible flow pattern and its concentration decreases radially away from associated matter, with overlapping enersphere energen mixing and blending seamlessly.	**Photons** and **electromagnetic fields** can pass through enersphere energen intact. **Inflow CES** within atomic nuclei draw enersphere energy inwards, with the net resultant force vector being the force of **Gravity**.	A mapping of **enersphere density** (ξ) associated with large moving cosmological objects produces **Space-Density** surfaces analogous to those for warped **Space-Time**.
Light Rays and Beams (and all other Photonic EMR) *Low energen concentration*	Light rays and non-visible **photonic EMR** (frequency **10^{10} to 10^{25+} Hz**) consists of **Field Energy Rings (FER)**. FER are low energen concentrations with a toroidal form that has both toroidal and poloidal flow components. Unlike electrons or CES, FER do not have a central core of concentrated energen. **Unpolarised** light rays move in a **double-helix** formation consisting of an intertwined pair of positive and negative FER-based helices.	FER can move through enersphere energen and other FER **intact**. An overlap of FER from intercepting light rays can result in the **constructive** and **destructive interference** of their electric field components. Light rays can readily be polarised (PPL, CPL, EPL) or converted to a **vortex** form.	Photonic EMR is generated by CES in **excited atoms**. It travels at a constant speed (c) within enerspheres or a vacuum, but travels at a slower speed in transparent media due to atomic near-field resistance.
Electromagnetic Fields *Low to Medium energen concentration*	**Electric fields** have a circular twist to their flow pattern and are thus **chiral**. **Magnetic fields** are **non-chiral** because they have no net circular component to their flow. Like poles/charges of electromagnetic field sources **repel**; and opposite poles/charges **attract**.	A **motor** (or **Lorentz**) **force** acts upon a current-carrying wire placed within a magnetic field. Conversely, the movement of magnetic fields can **induce an electric current** to flow within a wire conductor.	The chiral nature of electric fields generates a circular magnetic field across a capacitor (which Maxwell erroneously attributed to a **displacement current**)
Radio and Micro Waves (Non-Photonic EMR) *Low to Medium energen concentration*	Non-photonic EMR is derived from natural sources (mainly from Space) or man-made. For the **man-made** form, an electric field is generated across a **dipole antenna** by an AC current of the desired frequency. Each successive current reversal summarily cuts off the electric field-energy to generate a corresponding wave of positive or negative field-energy with the characteristics of an expanding rolling **circular magnetic field**.	Unlike photonic EMR which can be reflected, refracted and/or scattered by particles within Earth's atmosphere, non-photonic EMR can only be disrupted by significant electromagnetic disturbances. Also, man-made radio waves can be frequency and/or amplitude **encoded for data transmission**.	Radar, microwave, television and radio wave frequencies fall in the **10 to 10^{12} Hz** range. The **circular magnetic field** of their wave crests can induce an electric current in a signal pickup **aerial** (a copper wire tangential to the magnetic field.
Electrons (CC = Charge Carriers) *Medium to High energen concentration*	Consist of a torus-shaped **energy-core** of concentrated energen, and an outer torus of less concentrated **field-energy** which has both toroidal and poloidal flow components. The field-energy has either **left-handed chirality** for a **cetron** electron, which is a **negative charge carrier** (CC); or **right-handed chirality for** an **aptron** electron, which is a **positive CC**.	An **electric current** is the movement of **ionic cetron** and aptron electrons (positive and negative CC) streaming simultaneously in **opposite directions**. The combined field-energy of the aligned CC energises the electric circuit and generates a **circular magnetic field** around the circuit's components.	Good electricity conductors have well aligned ionic orbital electrons. Negative CC escape a host more readily from a positively charged nucleus than positive CC, which require high energy impact to escape as **positrons**.
CES (within Quarks and Nucleons) *High energen concentration*	A **Concentrated Energen Source** (CES) has a similar structure to an electron, but its energy-core is more concentrated and contains about 100 times more energen. An **e-CES** has left-handed chirality and a **p-CES** is right-handed. CES are the basic building-block (i.e. is a **preon**) of the sub-atomic world. It builds into **up-quarks** and **down-quarks** (6 CES/quark); quarks build into **nucleons** (3 quarks/nucleon); and nucleons build into **atomic nuclei**.	Within nucleon layers of an atom's nucleus, the field-energy of CES mediates matter-to-matter encounters. CES are also responsible for **bond formation**: strong-force **inter-quark bonds**; **bitron-bonds** (b-bonds); **polar-bonds** (p-bonds); and **weak-bonds** (w-bonds).	CES, and particularly those that form **swivel quarks** within an atom's nucleon layering, combined with the polygonal shape and size of the nucleus itself, are responsible for the **bonding preferences** of atoms.

Summary and Conclusions

A **Concentrated Energen Source** (**CES**) is STEM **energen**-based version of a **preon**. As f**undamental particles**, both electrons and CES are considered to have a **compact torus** structure similar to that of spheromak which, due to balanced magnetohydrodynamic forces, are stable structures observed in a laboratory environment within plasma. A **muon** is considered to be a CES-pair.

Up and **down-quarks** consist of a face-centred cubic (or octahedral) cluster of 6 CES-style preons or 3 muon-like CES-pairs. **Nucleons** (i.e. protons and neutrons) consist a pair of same-charge quarks each attached by a **strong-force inter-quark** bond to a shared central quark of opposite charge. For early atom-building environments, **L-form** nucleons would be dominant but, within **nucleon chains**, separate **I-form nucleon layers** develop. There are 2 types of L-form nucleons, with the CES flow directions of type-2 being the reverse type-1 flows.

Should nucleon chains end-join, they create **polygonal structures** that have offset pairs of I-form proton and neutron layers: these provide structural frameworks that underpin all atomic nuclei except for hydrogen (which is a single L-form proton).

Swivel-quarks are the main operatives responsible for manoeuvring atoms and complexes appropriately to allow chemical reactions to take place, either by bringing them closer together and drawing them into a preferred bonding position, or pushing them away from each other. The distribution and strength of swivel-quarks around an atom is quite important to the formation of chemical compounds. Within each full nucleon layer, a **swivel up-quark** (positive charge) is central to each I-form neutron, and a **swivel down-quark** (negative charge) central to each I-form proton.

A **bitron-bond** (**b-bond**) forms between a swivel up-quark and a swivel down-quark that are sufficiently close to each other (a distance in the order of 100 pm or less) to allow a pair of opposite **chirality** (or helicity) CES lock onto each other. Should both CES be **inflow CES**, then **attraction** exists between the CES so as to hold molecules and compounds together; should they be **outflow CES**, they **repel** each other, with the b-bond becoming an offset strut.

A **bitron** is a torus-shaped concentration of field-energy that quickly builds up mid-way within a bitron bond. It has an optimal (or quantum) energy level of 0.511 MeV/c^2, which corresponds to the energy of an electron. Strictly speaking, a bitron is not an electron: it is a **pre-electron**. However, if a bitron is forcedly removed from a b-bond by any means (e.g. a sufficiently high applied emf; or is bump-released by the impact of another excited free electron or EMR of sufficient energy), it is released as a **free electron** with an equal probability of being a **cetron** (with left-handed chirality) or a **aptron** (with right-handed chirality), dependent upon which side of the bond's energy-field it exits. In terms of electric currents, cetrons act as **negative charge carriers** (**CC**) and aptrons as **positive CC**.

In an energised environment, should a bitron be released from its b-bond and the CES bond pair remains otherwise unaffected, then a new bitron will quickly form: thus **electrons** can be considered to be a **renewable resource**, with b-bonds representing potential **electron breeders**. Bitron formation and release; ionic orbital electron capture and release; EMR emission and absorption; and the gain and loss of kinetic energy, are all part of a complex and dynamic energy management and transfer system within and between atoms, and thus for matter.

For the STEM approach, neither 'spdf' electron orbitals nor the Bohr electron shells are required. Instead, electron orbitals are considered to be planar and circular, being maintained by the combined electromagnetic field of swivel quarks of an outer nucleon layer, and are called **ionic orbitals**. The combined energy fields of **swivel up quarks** within an outer **neutron layer** of an atomic nucleus support **orbital cetron electrons** (potential negative CCs) and, similarly, an outer **proton layer** can support **orbital aptron electrons** (positrons or potential positive CCs). The **ionisation state** of an atom is thus determined by the relative numbers of cetron and aptron ionic electrons, with negative ions (anions) having more cetron than aptron electrons and positive ions (cations) being the other way round. Neutral atoms either have equal numbers of cetron and aptron electrons or no ionic electrons at all.

STEM contends that most molecules and chemical compounds consist of multiple atoms held together by a combination of ionic **covalent bonds** and/or **b-bonds**, with paired **double bonds** (**b2-bonds**) being the most common type of b-bond with the exception of hydrogen bonds. The **bond pattern** within chemical compounds is closely related to the polygonal shape of nucleon layers of participating atoms and the possible availability of ionic electrons. The geometric form and charge distribution of elements and, in particular, the location and energisation level of swivel-quarks, are major factors in the formation of chemical bonds between elements and compounds. External lateral b-bond geometry is dictated by the shape of the polygonal nucleon layer, whereas top and bottom layer b-bonds, more common with the halogens, depend upon the outer complete and partial nucleon layers. Covalent bonds depend upon the availability of ionic cetron and aptron electrons and relative juxtaposition of the nuclei involved.

Within some chemicals (and hydrocarbons in particular), atom shape, charge distribution and internal restraints can prevent a pair of swivel quarks from getting close enough to form a b-bond: instead, a weaker bitron-less **polar-bond** (or **p-bond**) can be formed. **Intermetallic compounds** and **coordination complexes** contain a combination of p-bonds and **weak-bonds (w-bonds** are weak would-be inter-quark bonds, with CES separation of 15 pm or more).

Covalent bonds involve the sharing of ionic orbital electrons, with **ionic bonds** involving ionic electron sharing and, in some more complex molecules and ligands, by p-bonds. ONAM, on the other hand, needs a work-around in terms of **hybrid orbitals**, **resonance** and **molecular orbitals** that are all tailor-made from '**spdf**' **orbitals** to explain chemical bonds, which are classified as being either **covalent** or **ionic**.

An important aspect of many chemical reactions is **ionisation-by-dissociation** within an **aqueous solution** and associated **redox** reactions. Although the half-equation for the oxidation of hydrogen is quite similar for both approaches, their half-equations for other **redox** reactions can be quite different. For ONAM, **oxidation** is by electron loss (**OIL**) and **reduction** is by electron gain (**RIG**). The OIL/RIG acronym also applies to STEM, except that the negative electron remains a negative CC (cetron), with the redox half-equations being extended to include positive CC (aptrons). Specifically, **oxidation** becomes defined by aptron gain and/or **cetron loss** (OIL), creating an aptron sink and a cetron source. Similarly, **reduction** becomes aptron loss and/or **cetron gain** (RIG), creating an aptron source and a cetron sink. Thus STEM provides a source and a sink for both positive and negative CC, whereas ONAM provides a source and sink only for negative CC. With no provision for positive CC, conventional Science has had to introduce the flawed concept of static-cation based **positive holes** to act as positive CC in order to explain electric currents within semiconductors.

The nucleus of some elements can have different polygonal form, and are thus **polymorphic**. Nuclear polymorphs of atoms can create different **allotropic** forms of elements. For example, the tetragonal and hexagonal polymorphs of carbon-12 can result in the cubic diamond and graphite allotropes respectively, each of which has vastly different physical characteristics. Other allotropes, such as dioxygen and ozone or the various allotropic forms of phosphorus-31, can result from a modification of inter-atomic bonds rather than from different nuclear polymorphs.

For chemical compound formation, b-bonds are external to atoms, but they can also be internal to an atom, where they serve to secure smaller polygonal forms to create **embedded atomic structures**. Such internal b-bonds are far shorter and stronger than external b-bonds, but still considerably weaker than inter-quark bonds. Embedding starts with fluorine and becomes much more pronounced and structurally significant as atomic number increases from Period 3 onwards. Embedded atoms can have several subtly different embedded patterns which represent different embedded polymorphic forms, each of which can be uniquely identified by its **P-# signature** (see below).

As an environment becomes more energised, swivel-quarks and any ionic orbital electrons become more energised and chemical reactions tend to take place more readily, with an increase of thermal energy often being a pre-requisite, and/or an accelerant, for many chemical reactions. **Catalysis** is sometimes a necessary pre-cursor for some chemical reactions and, particularly within the hydrocarbon chemical production industry, procedures have been established by trial-and-error experimentation to maximise the likelihood of the creation of required chemical and polymorphic forms. Polymorphism and polymorph distribution can also complicate the chemical bonding process and patterns, with polymorph mixing resulting in significant natural variation in chemical reactions and the end-product compounds.

Each CES within up/down quarks can be flipped from being a p-CES into an e-CES (or vice versa) by the reversal of its poloidal field energy flow direction, with the exception of 1 p-CES per quark that is referred to as the **invariant CES**. Each nucleon consists of 3 quarks an so contain 18 CES, of which 15 CES are **flippable CES** and 3 (1 per quark) are invariant p-CES that cannot be flipped. Should all 15 flippable CES be unrestrained, should one flippable outflow CES be impact-converted (or flipped), the other 14 respond by flipping in unison to produce an instantaneous **nucleon type-conversion**. Such nucleon-type conversion presents as **beta (β+ and β-) decay** and, to a lesser extent, as **electron capture**. However, a nucleon cannot be type-converted should any one of its 15 flippable CES be restrained by participating in a b-bond or an inter-quark bond

STEM contends that a proportion of an atom's protons in any concentrated sample of a particular element can be randomly derived from β-decayed neutrons, which can result in a natural variation in the proton count of individual atoms within the sample, but without necessarily changing its polygonal structural form or element type. This concept conflicts with the more simplistic conventional Science view that the proton count uniquely defines the element.An element's **full P-# signature** provides an indication of such β-decay related natural variation in terms of an estimate of the number of protons that can, on average, be expected to be β-decay protons derived from appropriately attached (foot-in) neutrons. For example, should the full signature of palladium-106 be ***Pd-106/44+2=8-116-3; 32-1;*** then the ***44+2*** part indicates that, on average, 2 of its 46 protons can be expected to be β-decay protons. However, within a palladium mix, there is a statistical variability that is heavily skewed by atoms containing 46 protons, so that, although some individual atoms might be 46 ± one or two protons, the nucleus of all the atoms within the sample would have the same structural form and can still be considered to be Pd-106.

β-decay (and electron capture) inversely changes the proton and neutron count of an atom by 1 without its nuclear structure (i.e. its P-# signature) being changed and, in some cases, the process can be reversed over time, whereas . **alpha decay**, which is associated the nucleon bombardment of susceptible elements (e.g. the **radioactive series** decay of unstable heavy atoms), is an irreversible process. It reduces both the proton and neutron count by 2 and modifies the structure of the nucleus, which results in a distinctly different atom type with a different P-# signature.

For radioactively-stable elements (e.g. copper), ionic orbitals are considered to keep cetron and aptron electrons (or positrons) well separated on opposite sides of the atomic nucleus. Such separation, combined with a regular atomic lattice, prevents mutual **electron-positron annihilation.** On the other hand, for **radioactive elements** and compounds, it is claimed that the separation of electrons and positrons via ionic orbitals is poor, which results in frequent and ongoing random electron-positron annihilation events that produce gamma radiation, which in turn initiate a range of radioactive decay processes such as alpha radiation, beta radiation, more gamma radiation (via Bremsstrahlung), and neutrinos. STEM thus claims that it is random electron-positron annihilation events that release gamma rays, which in turn leads to a range of other forms of radioactive emissions.

All atomic particles (CES, nucleons, electrons etc.) lose minor amounts of field-energy and, although some of this ‘lost’ energen is absorbed by other matter, STEM hypothesises that much of it accumulates around the host object to create an **enersphere**, which is an atmosphere-like low concentration of ‘stagnant’ energen. The energy field of out-facing CES within a nucleon generate the external electromagnetic fields of an atom, and the **central vortex** of each such CES is either an **inflow** or an **outflow** vortex. Although there are equal numbers of central inflow and outflow vortices within an atom, the central suction-like action of inflow CES vortices is considered to be marginally more efficient than that of their outflow counterparts, which creates a small positive pull on the enersphere immediately surrounding an atom’s host object. STEM suggests that these minute inwardly-directed forces associated with each atom, when summed over the billions of atoms within ‘normal’ matter, is the pull of **Gravity**.

Central to STEM is the hypothesis that **there is only one type of energy-generating material** (i.e. **energen**), with electrons, positrons, CES and related fundamental particles consisting of toroidal concentrations of energen. Quarks, nucleons and atoms consist of different combinations of these fundamental particles. Electromagnetic fields and electromagnetic radiation (EMR) consist of **field-energy**, which ultimately was derived from the fundamental particles in a variety of configurations and environments, with **Gravity** being considered to be due to the retrieval of accumulated lost or leaked field-energy. Conventional Science, on the other hand, implies that positive and negative charge, magnetic fields, Gravity fields, protons, neutrons, electrons, gluons and a range of other exotic particles represent distinctly different energy forms and/or are possibly adaptions of several different types of energy sources.

Energy/mass and size estimates for the **fundamental particles** (i.e. electrons, up/down quarks, preons and the nucleons) vary and are often disputed. However, STEM’s estimates have been successfully applied to create true-to-scale models of atoms and simple bonded molecules and compounds, which is something no other approach can match. STEM also has the potential to align the mathematics of Atomic Physics and Chemistry more closely with Newtonian Physics (possibly seen as a retrograde step by some parties), and to provide a framework for improved future modelling and for better predictive tools (which can hardly be seen as retrograde). STEM is still in its infancy, and needs much more research and development support but, even in its current state of development, it introduces new concepts and explanations that carry significant implications for all theoretical and applied Science areas.

STEM Development expects that, as demonstrated by quantum computing and femtochemistry/alto-frequency laser research, nano-technologies, DNA-related biological research and newer related spin-off technologies will lead to more detailed pictures of nuclear structure and geometry in the near future. They have a practical emphasis related to Applied Physics and Chemistry, and most likely will become the technologies of the future, with the brute-force methodologies of Quantum Mechanics and the Standard Model, which have produced many overly complicated, esoteric, conflicted, incomplete and possibly flawed explanations, become less relevant.

Contact: David.Johnson.Pivot@gmail.com